the Energy to Lead

QUARTERLY REPORT

GTI PROJECT NUMBER 20916

Modeling of Microbial Induced Corrosion on Metallic Pipelines Resulting from Biomethane and the Integrity Impact of Biomethane on Non-Metallic Pipelines

DOT Prj# 293

Contract Number: DTPH56-09-T-000002

Reporting Period:
4th Project Quarter

Report Issued (Period Ending):
September 27, 2010

Prepared For:
U.S. Department of Transportation Pipeline and Hazardous Materials Safety Administration
Anthony Rallis
Technical Manager
Office of Pipeline Safety/Southwest Region
713-272-2835
Anthony.rallis@dot.gov

Prepared By:

GTI Project Team:
Karen Crippen, Daniel Ersoy, Monica Ferrer, Zhongquan Zhou, Xiangyang Zhu

Kristine Cruz, *Team Project Manager*
Kristine.cruz@gastechnology.org
847-768-0910

Gas Technology Institute
1700 S. Mount Prospect Rd.
Des Plaines, Illinois 60018
www.gastechnology.org

Legal Notice

This information was prepared by Gas Technology Institute ("GTI") for DOT/PHMSA (Contract Number: DTPH56-09-T-000002.

Neither GTI, the members of GTI, the Sponsor(s), nor any person acting on behalf of any of them:

a. Makes any warranty or representation, express or implied with respect to the accuracy, completeness, or usefulness of the information contained in this report, or that the use of any information, apparatus, method, or process disclosed in this report may not infringe privately-owned rights. Inasmuch as this project is experimental in nature, the technical information, results, or conclusions cannot be predicted. Conclusions and analysis of results by GTI represent GTI's opinion based on inferences from measurements and empirical relationships, which inferences and assumptions are not infallible, and with respect to which competent specialists may differ.

b. Assumes any liability with respect to the use of, or for any and all damages resulting from the use of, any information, apparatus, method, or process disclosed in this report; any other use of, or reliance on, this report by any third party is at the third party's sole risk.

c. The results within this report relate only to the items tested.

Table of Contents

Page

Table of Tables

Page

Table of Figures

Page

Project Objective

The objective of this project is to understand key elements related to promoting the successful delivery of biomethane into natural gas pipeline networks. This project focuses on two key areas of concern: [1] the effect of microbial induced corrosion on metallic pipes and [2] the impacts of biogas/biomethane on a non-metallic gathering network from sustained biogas feedstock exposure. This report summarizes the work that has been conducted through the third quarter of 2010. Results from Tasks 1, 2, 3, 4, 6, 7 and 8 are discussed in detail within this report.

List Activities/Deliverables Completed During Reporting Period

		SCH Date	CMPL Date
Task #6:	Conduct Literature Search (Gap Analysis)	9/30/2010	9/30/2010
Task #7:	Develop Baseline and Comparative Testing Protocols	9/30/2010	9/30/2010

Technical Status

Task 1 - Literature Review of Internal Microbial Corrosion

Microbiologically influenced corrosion (MIC) is a complex and aggressive mode of corrosion [1-19]. A comprehensive literature review of publications, standard documents, research reports, and publications in scientific journals was conducted on the topic of internal MIC over a nine-month period. The literature review is focused on information about MIC detection and limitation, MIC mitigation and prevention, and their relationship to overall pipeline corrosion, as well as those major factors or mechanisms which control the internal MIC process on metallic pipelines. The second focus of the literature review is to incorporate the data from Task 2 (conditions in raw biogas gathering line) and discuss its implications for potential microbial corrosion. The literature review will identify a set of major parameters for the construction of a preliminary MIC model in Task 3.

Background

Corrosion is mainly the consequence of electrochemical reactions on the surface of a metal. Its kinetics is determined by the physico-chemical environment at the metal surface, such as concentration of oxygen, salts, pH, reduction-oxidation (redox) potential, and conductivity (Figure 1). Microbiologically influenced corrosion (MIC) is corrosion influenced by the presence or activities of microorganisms including bacteria and fungi [20-23]. Microorganisms growing at the metal surface form a biofilm and the release of chemicals or the deposition of electrochemically active minerals from biofilms alters the rates and types of electrochemical reactions at the biofilm-metal surface interface and produces a broad range of outcomes such as pitting, crevice corrosion, under-deposit corrosion, selective dealloying, enhanced erosion, and galvanic corrosion [22, 24-29] (Figure 2). The accurate diagnosis of MIC requires combination of microbiological, surface analytical and electrochemical techniques.

Figure 1. Internal Microbial Corrosion.

Despite the tremendous advances made in recent years to improve knowledge of the mechanisms of microbial corrosion, and development of better monitoring techniques, biocides, and other control measures, it is still not known with certainty how many species of microorganisms contribute to corrosion, how to reliably detect their presence prior to corrosion events, or how to rapidly assess the efficacy of mitigation procedures [2, 5-7, 23, 30-33].

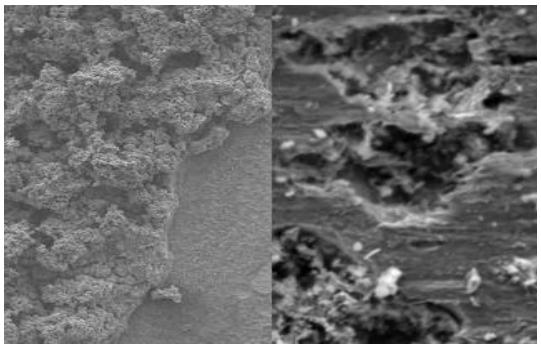

Figure 2. SEM Micrograph of Biofilm and Microbial Corrosion.

MIC can occur in unexpected places. It tends to occur repeatedly at certain locations (Table 1) [34]. In general, MIC "problem areas" for many industries occur more often in welds and heat-affected zones, separators, drips, under the deposits, after hydrotesting, and when cooling systems are not passivated after "turnarounds" are complete.

MIC-Related Microorganisms and MIC Mechanisms

Many bacteria occurring naturally in waters and soils are considered corrosion-causing bacteria, including but not limited to, sulfate-reducing bacteria (SRB), acid-producing bacteria (APB), metal-oxidizing bacteria (MOB), metal-reducing bacteria (MRB), sulfur/sulfide oxidizing bacteria, nitrate-reducing bacteria, and slime-forming bacteria. Each of these physiological groups of microorganisms may contain hundreds or thousands of individual species. Each group of bacteria or an individual species of bacteria alone can cause metal corrosion; however in a natural environment, it is always microbial communities containing many different types of microbes that cause the MIC, and the resulting corrosion is always far more severe compared to the data generated under single strain laboratory conditions [3]. However, the mere presence of given classes of organisms associated with MIC (e.g., SRB) does not necessarily indicate that MIC is occurring. Nor does the showing that a given type of microorganisms is present establish a cause-and-effect relationship between the bacteria and metal dissolution [11, 35].

Many MIC mechanisms have been proposed since von Wolzgen Kuhr and Van Der Vlugt in 1934 [36]; most of them are focused on SRB corrosion [14, 17-19, 37-40]. A general mechanistic MIC model proposed by Pope includes three phases [28, 41] (Figure 3) . In Phase I, microbes attach to metal surface and start forming a biofilm. The attachment colonization of microbes in this phase is affected by many conditions such as preexisting corrosion on the metal surface, metal surface condition (roughness, welds, inclusions, etc.), and local chemical-electrochemical environments. The further development of biofilm on metal surface in Phase II creates an occluded area (inside and under the biofilms) that is relatively anodic to the surrounding area. In this phase, the occluded area becomes more acidic, attracting chloride and other anions and starts forming deposits on the metal surface (nodules or tubercles). Phase III involves the formation of a mature nodule over a well-defined pit. The low pH (<4.0) in the active pit region shifts the corrosion process to chemically-driven underdeposit acid attack. In this phase, the corrosion process would continue even in the absence of microbes [41].

Table 1. Where MIC is most likely to occur [34].

Industry/Application	Potential Problem Sites for MIC	Organisms Responsible
Pipelines-oil, gas, water, wastewater	Internal corrosion primarily at the bottom position Dead ends and stagnant areas Low points in long-distance pipes	Aerobic and anaerobic acid producers, SRB, manganese and iron-oxidizing bacteria, sulfur oxidizing bacteria
Chemical process industry	Heat exchangers, condensers, and storage tanks-especially at the bottom where there is sludge build-up Water distribution systems	Aerobic and anaerobic acid producers, SRB, manganese, and iron-oxidizing bacteria In oil storage tanks also methanogens, oil-hydrolyzing bacteria
Cooling water systems	Cooling towers Heat exchangers-in tubes and welded areas-on shell where water is on shell side	Algae, fungi, and other microorganisms in cooling towers Slime-forming bacteria, aerobic and anaerobic bacteria, metal-oxidizing bacteria, and other microorganisms and invertebrates
Fire protection systems	Dead ends and stagnant areas	Anaerobic bacteria, including SRB
Docks, piers, oil platforms, and other aquatic structures	Just below the low-tide line Splash zone	SRB below barnacles, mussels, and other areas sequestered from oxygen
Pulp and paper	Rotating cylinder machines Whitewater clarifiers	Slime-forming bacteria and fungi on paper-making machines Iron-oxidizing bacteria SRB in waste
Power generation plants	Heat exchangers and condensers Firewater distribution systems Intakes	As above for heat exchangers and fire protection systems Under mussels and other fouling organisms on intakes
Desalonation	Biofilm development on reverse osmosis membranes	Slime-forming bacteria

However, in a complex environment, a consortium of different types of microorganisms often work synergistically, resulting in far more severe corrosion compared to the data generated under single strain laboratory conditions [3]. For instance, APB produce low molecular weight organic acids (short chain fatty acids such as acetic, butyric, formic, lactic, succinic, and propionic acids) and inorganic acids (e.g., HCl, H_2CO_3, and H_2SO_4). While both types of acids can cause metal corrosion by either direct reaction with metal or disrupting the protective surface oxides films and calcium scales [11, 22, 42-47], the organic acids provide the environment and nutrients for the growth of other bacteria such as SRB [48] (Figure 4). In addition, biogenic acids increase the concentration of protons (H^+), which can then become reduced at the cathode, generating hydrogen, an electron source for SRB and other hydrogen-consuming organisms [11]. Activities of aerobic microbes deplete oxygen in the biofilm, create an environment for growth of anaerobic bacteria, and form an oxygen gradient within the biofilm. This causes a potential change beneath the film, resulting in the development of an anodic region surrounded by a large cathodic area and galvanic corrosion. In addition, if the protective oxide film is breached beneath a biofilm, then the metal cannot be reoxidize or self-heal. Oxygen gradients and breached oxide film result in metal pitting beneath biofilms. Therefore MIC is the consequence of collective effects of microbial consortia on metal surfaces.

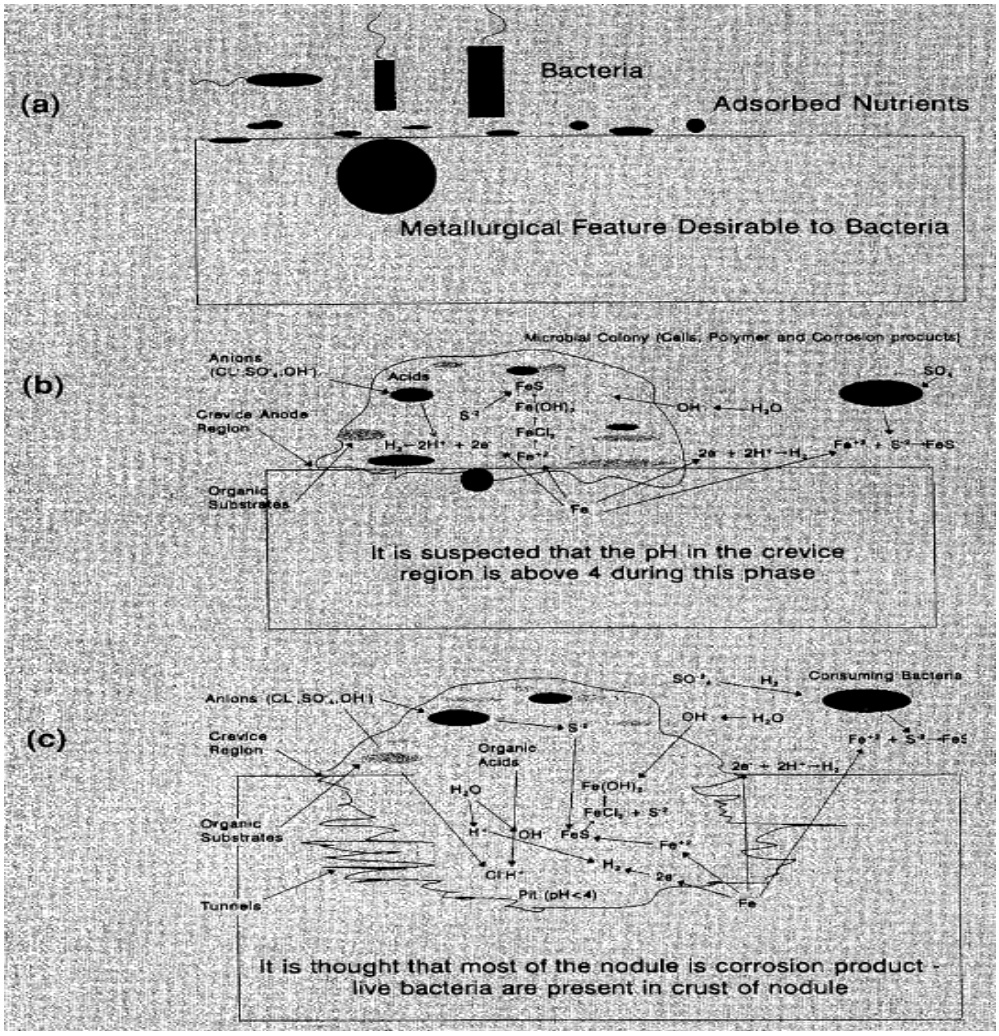

Figure 3. MIC Development Model [41]. (a) Recognition of Desirable Sites. (b) Colony Formation and Crevice Corrosion Begins and Anode is Fixed. (c) Nodule is Formed over "Mature" Pit.

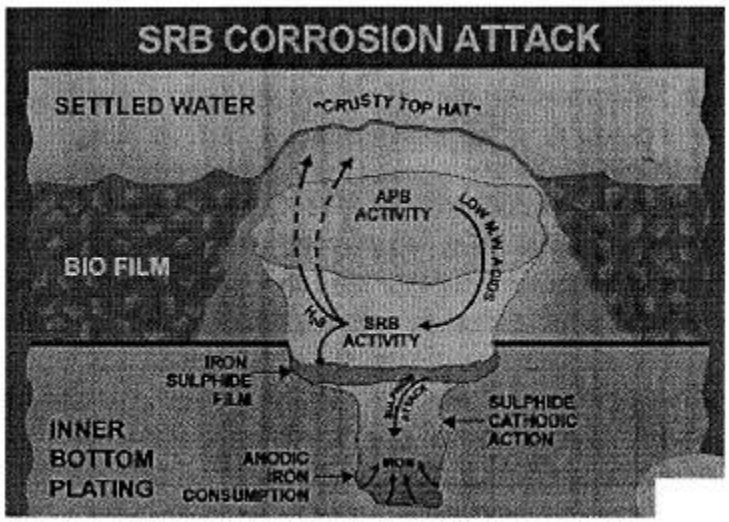

Figure 4. Interaction of SRB and APB on Metal Corrosion [49].

SRB-induced corrosion

Sulfate-reducing bacteria (SRB) constitute a physiologically diverse group of obligate anaerobic, heterotrophic, and mixotrophic bacteria that are responsible for dissimilatory sulfate reduction. They are present in a variety of environments, including oil- and gas-bearing formations, seawater, freshwater, soils, and domestic, industrial, and mining wastewaters [50]. Though SRB are anaerobic bacteria, SRB can survive and quickly recover from brief oxygen exposure [13, 39, 49]. SRB use hydrogen, organic acids (lactic, acetic, propionic, succinic, pyruvic, etc.), and variety of other low molecular weight organic compounds (ethanol, aliphatic acids, sugars, amino acids, indole, nicotinic acid, etc.) as electron donors and also as carbon and energy sources. Sulfate can be used as an electron acceptor for anaerobic respiration [51-53]. Previous microbiological studies have suggested that SRB play a key role in microbial corrosion [3, 30] and other problems of great economic impact in oil and gas industries [30]. For instance, oil reservoir souring is a well known phenomenon after seawater injection into reservoirs for oil extraction, i.e., the reservoir formation water provides volatile fatty acids (VFAs) as electron donors and the seawater provides the sulfate (~2,700 mg/L) as electron acceptor for SRB's anaerobic respiration.

It has been reported by many researchers that the corrosion rates caused by SRB under laboratory conditions are much lower than the rates under field conditions [10, 13-18, 38, 54], and the rates under laboratory conditions usually cannot be maintained at high level for long periods of time. The existence and activity of SRB causes the average corrosion rate of steel exposed to anaerobic soil to be more than 20 times higher than that of the control case, the maximum corrosion rate of steel and iron being reported by SRB to be 7.4 mm/y [14, 24, 55]. Pitting corrosion is characteristic of the action of SRBs on steel, with pits being open and filled with soft black corrosion products in the form of iron sulfides [10]. When the corrosion products are removed, the metal underneath is bright but rapidly rusts on exposure to air.

Various mechanisms have been proposed to explain the accelerated corrosion rate observed in the presence of SRB. The most classic among them is cathodic depolarization, proposed by Von Wolzogen Kühr and Van Der Vlugt in 1934 [36]. They proposed that cathodic depolarization is achieved by the metabolic oxidation of hydrogen by SRBs.

$4Fe \rightarrow 4Fe^{+2} + 8e^{-}$	(anodic reaction)	(1)
$8H_2O \rightarrow 8H^{+} + 8OH^{-}$	(water dissociation)	(2)
$8H^{+} + 8e^{-} \rightarrow 8H^{0}$	(cathodic reaction)	(3)
$SO_4^{-2} + 8H^{0}$ MIC $\rightarrow S^{-2} + 4H_2O$	(cathodic depolarization)	(4)
$Fe^{2+} + S^{-2} \rightarrow FeS$	(corrosion products)	(5)
$3Fe^{+2} + 6OH^{-} \rightarrow 3Fe(OH)_2$	(corrosion products)	(6)
$4Fe + SO_4^{-2} + 4H_2O \rightarrow 3Fe(OH)_2 + FeS + 2OH^{-}$	(overall reaction)	(7)

The cathodic depolarization theory posits that SRB at the cathode remove the H^0 from a polarized metal surface (through hydrogenase) for anaerobic respiration (to produce energy by reducing sulfate to sulfide), resulting in increased corrosion rate. However, many later researchers found evidence that conflicts with cathodic depolarization hypothesis [10]. It has been reported that the reactions occurring at the anode are at least as important as the cathode's and could be predominant in the case of SRB corrosion [56].

The most severe damage resulting from the corrosion of steel by SRB is most often localized, taking the form of pits, crates or similar clearly delimited areas of corrosion. Pitting corrosion is a process of the nucleation and growth type, and the mechanism of pitting corrosion is generally an autocatalytic stabilization of a galvanic cell between a small corroding area (the anode) and its non-corroding surroundings (the cathode). Thus, the more modern theory of SRB-induced corrosion involves the formation of ferrous sulfide film on metal surface and the formation of galvanic cell between ferrous sulfide film and steel base.

The galvanic corrosion theory states that under anaerobic conditions, SRB uses various electron donors (mainly small molecule organic acids) to reduce inorganic sulfate to sulfide. As a result, hydrogen sulfide accumulates in the biofilm near the metal surface and iron sulfide quickly forms on and covers the carbon steel surface. The iron sulfide film (cathode) and bare steel base (anode) forms a galvanic cell [57]. At the early stage, the film (mainly mackinawite, $FeS_{(1-x)}$, 35% S, dense and protective) is patchy and irregular, and therefore SRB-induced corrosion rates are high due to the galvanic couple between patchy iron sulfide (cathode) and steel base (anode). However, after a uniform mackinawite film is formed, it protects metal from further corrosion, resulting in reduced SRB corrosion [24]. When mackinawite takes up more sulfide and gradually converts to greigite (Fe_3S_4) and pyrite (FeS_2, 52.5% S), the change in film density breaks the iron sulfide film and the resulting ruptured film exposes the bare metal, forms a galvanic corrosion cell again between the steel substrate and an unbroken sulfide film attached to the steel surface, and causes elevated corrosion rate [18, 58]. Pyrite is 12 times more corrosive than mackinawite due to higher potential difference to the iron anode (482 mV vs 610 mV). However, the incubation time for breakdown of mackinawite film, dependant on various factors such as redox potential, solution chemistry, physical properties of films, is not predictable, and may take 2-3 months [14, 17]. A high concentration of ferrous iron in the medium may accelerate the breakdown of dense biogenic FeS film on the metal surface, and accelerate the corrosion rate [17, 19]. High amounts of soluble iron also prevent formation of protective sulfide layers on ferrous metals [16]. Once mackinawite film is ruptured, the corrosion is independent of SRB number and growth rate.

The galvanic corrosion cell is normally short lived because the iron sulfide matrix becomes saturated with electrons derived from the corrosion process. However, anaerobic SRB remove electrons directly from FeS_x matrix (cathode), sustaining a flow of electrons through the galvanic couple from the corroding steel [18]. The microbes use these electrons to reduce sulfate to sulfide, which combines with ferrous ions (Fe^{2+}) derived from corrosion of the steel to precipitate more FeS_x, thus further increasing corrosive action. Other researchers found that the activity of the SRB on the anode (electrochemical or metabolic) might be more important than their activity on the cathode in terms of stabilizing the coupling current between the anode and the cathode, and proposed a theory that the SRB acidify the anode by precipitating ferrous ions into ferrous sulfide and stabilize the pH of the cathode, thus inducing a sustained galvanic coupling [56, 57, 59, 60]. The galvanic couple accounts for ~ 10% of the observed damage. Extension of the life of the corrosion cell through electron transfer to active bacteria is responsible for most of the metal loss [18]. Another classic hypothesis regarding the sustaining galvanic corrosion cell was proposed by King and Miller [17, 24, 61]. They attribute the sustaining life of galvanic cell to the adsorption of atomic hydrogen by the ferrous sulfide

corrosion product. Ferrous sulfide is not, however, a permanent cathode [62] and its regeneration and the maintenance of a high sustained corrosion rate is dependent on the removal of this hydrogen by the action of bacterial hydrogenase.

Other alternative hypotheses also exist, and may contribute to the explanation of SRB-induced corrosion. For instance, some SRB secrete exopolysaccharides (EPS), which facilitates irreversible cell attachment, leading to colonization on the steel surface. EPS can bind metal ions, causing metal ion concentration cells [63]. Hydrogen sulfide acidifies a corrosive medium and catalyzes penetration of hydrogen into steels, a process known as H_2S-induced cracking or sulfide stress cracking [64, 65]. Periodic oxygen incursions and sulfur/sulfide oxidizing bacteria can oxidize FeS_x to more corrosive sulfides such as pyrite (higher sulfur content) and production of elemental sulfur ($2S^{2-} + O_2 + 4H^+ \rightarrow 2S^{(0)} + 2H_2O$). Both products will increase corrosion significantly [13, 19, 39]. Elemental sulfur sustains the galvanic couple between iron and the corrosion product FeS_x by accepting electrons from the FeS_x. High local acidity generated on particles of solid sulfur reacting with water could also be responsible for high corrosion rates of iron and steel.

APB-induced corrosion

Acid-producing bacteria (APB) are present in a variety of environments, including oi1- and gas-bearing formations, soils, and domestic, industrial and mining wastewaters. Acid-producing bacteria produce organic acids (e.g., acetic, butyric, formic, lactic, succinic, and propionic acids) and inorganic acids (e.g., HCl, H_2CO_3, H_2SO_4), causing metal corrosion by either direct reaction with metal or disrupting the protective surface oxides films and calcium scales [11, 22, 42-47]. In addition, biogenic acids increase the concentration of protons (H^+), which can then become reduced at the cathode, generating hydrogen, an electron source for SRB and other hydrogen-consuming organisms [11, 57]. Short chain organic acids provide the nutrients for other bacteria growth such as SRB and can lead to general attack, pitting attack, and stress corrosion cracking [48]. Acetic acid-producing bacteria and butyric acid-producing bacteria have been found to be present in environmental samples and in particular, samples from gas and oil production operations [4, 66, 67]. Consumption of hydrogen by SRB through formation of H_2S allows the APB to continue acid production. Some fungi also produce organic acids and other byproducts which support the growth of various other bacteria such as SRB [22].

MOB- induced corrosion

Metal-oxidizing bacteria (MOB), mainly iron-oxidizing bacteria and manganese-oxidizing bacteria, are generally filamentous, are typically found in fresh and marine water, and are frequently surrounded by a sheath usually encrusted with iron, manganese, or both. Iron-oxidizing bacteria such as *Gallionella, Sphaerotilus, Leptothrix, Siderocapsa, Thiobacillus, Crenothrix,* and *Clonothrix* oxidize the soluble ferrous (Fe^{2+}) and produce orange-red tubercles of iron oxides and hydroxides by oxidizing ferrous ions (electron donors) from the bulk medium or the substratum [68, 69]. They are commonly associated with tubercle formation and corrosion of water distribution pipelines. The small area under the deposit, deprived of oxygen, forms a galvanic cell with surrounding metal with large cathode to anode ratio, resulting in under-deposit corrosion, pitting, and crevice corrosion [22, 70], sometimes with assistance from sulfate-reducing bacteria [71]. *Gallionella* spp. contributes to the generation of conditions favorable to

colonization by SRB [20]. Manganese-oxidizing bacteria oxidize the soluble manganese (Mn^{2+}) to insoluble manganese oxide (Mn_2O_3, MnOOH, Mn_3O_4, and MnO_2). The oxides are formed extracellularly and encrust the polymeric material (bacterial capsules) that surrounds individual cells or cell aggregates. *Leptothrix* and *Siderocapsa* are particularly associated with formation of highly enriched manganese oxide deposits. Manganese oxide can elevate corrosion current, and can also serve as a cathode to support corrosion at an oxygen depleted anode (metal surface) within the deposit, resulting in similar under-deposit corrosion, pitting, and crevice corrosion [22, 70].

The detection of iron- and manganese-oxidizing bacteria is usually dependent on diagnostic liquid cultures, which is very difficult even for experienced microbiologists. Microscopic identification of iron-oxidizing bacteria is also quite difficult for an experienced analyst. Several direct and indirect tests for the presence of corrosion-causing bacteria are summarized in NACE Standard TM0101-2006 [22]. However, these techniques are not capable of quantifying metal-oxidizing bacteria. A new technique called quantitative polymerase chain reaction (qPCR) is now available for quick detection and quantification by targeting 16S rRNA gene of *Leptothrix*, *Sphaerotilus*, and *Gallionella* [72, 73]. The presence of iron-oxidizing bacteria within tubercles associated with localized corrosion is considered a positive indication of MIC.

MRB-induced corrosion

Under oxic conditions, the metal surface becomes oxidized, causing the formation of metal oxides and hydroxides, which protect the metal surface from further corrosion. Some metal-reducing bacteria (MRB) are capable of using metal oxides or hydroxides (Fe^{3+} and Mn^{4+}) as electron acceptors efficiently (i.e., redox potential is similar to nitrate) and out-compete low potential electron acceptors such as sulfate or carbon dioxide [74]. When MRB is in direct contact with solid iron (Fe^{3+}) and manganese (Mn^{4+}) oxides, the dissimilatory reduction produces soluble ions (Fe^{2+} and Mn^{2+}), resulting in dissolution of surface oxides. This destabilizes the passivating protective film (oxide film) and allows further corrosion (localized corrosion) to take place [11, 48]. Medium containing ferric citrate ($FeC_6H_5O_7 \cdot 3H_2O$) as the terminal electron acceptor and acetate as the sole carbon source can be used to detect the presence of IOB. A positive indication of growth and iron reduction is a color change in the medium from brown to green [22].

Other bacteria-induced corrosion

Acidophilic sulfur/sulfide-oxidizing bacteria oxidize sulfide or elemental sulfur to sulfate or sulfuric acid. For example, *Thiobacillus* bacteria are the most common sulfur-oxidizing bacteria, and are almost always accompanied by SRB. Sulfur/sulfide-oxidizing bacteria obtain the carbon required for the synthesis of new cell material by fixation of CO_2 from the atmosphere and energy from oxidation and reduction reactions [64, 75]. Ferrous iron from reduced sulfur compounds serve as the electron donor, and oxygen is the preferred electron acceptor. In the absence of oxygen, organisms grow on reduced inorganic sulfur compounds using ferric iron as an alternative electron acceptor. The specific oxidation reactions leading to production of sulfuric acid (H_2SO_4) varies with the initial reduced sulfur species (H_2S, $S_2O_3^{2-}$, $S_3O_6^{2-}$, $S_4O_6^{2-}$, S^0). Elemental sulfur, thiosulfates, metal sulfides, H_2S, and tetrathionates can be oxidized to H_2SO_4 [76].

Methanogens and some strains of SRB frequently co-exist in a symbiotic relationship. They remove hydrogen from the surface of metals catalyzed by a reversible hydrogenase, enhance the cathodic reduction of proton (cathodic depolarization), and thereby accelerate anodic metal dissolution [11, 77]. Culturing of methanogens is very difficult due to the strictly anaerobic nature of methanogens. Genetic techniques are now available for quick detection and quantification of methanogens by targeting a specific functional gene [72].

Nitrate- and nitrite-reducing bacteria use nitrogen oxides as alternative electron acceptors under anoxic conditions [78]. In the presence of nitrate, denitrifying bacteria are reported to cause metal corrosion [31, 79].

Hydrogen embrittlement of metals occurs when molecular hydrogen invades the metal lattice, filling interstitial regions and thereby distorting the lattice structure and weakening the metal-metal bond [11]. Bacterial production of hydrogen can directly promote hydrogen embrittlement of metals. Indirectly, the generation of acids, which can be reduced to hydrogen at cathodic sites, as well as the generation of sulfide, which promotes the adsorption of hydrogen into metal matrices may also promote hydrogen embrittlement.

MIC Indicators

Water is required for microbial metabolism and growth and corrosion processes. Water quality parameters that are considered important to understanding internal corrosion and MIC for a particular industrial system include temperature, pH, alkalinity, sulfide, nitrite, dissolved gases (CO_2, H_2S, O_2, NH_3, etc.), total dissolved solid (TDS), chemical oxygen demand (COD), microorganisms (bacteria, algae, and fungi), etc. Raw biogas contains up to 40% CO_2 and 0.66% of H_2S (Table 2). Dissolved CO_2 and H_2S in water form carbonic acid and weak acidic hydrogen sulfide which attack metal. Dissolved oxygen might not be indicative as to the oxygen content within the biofilm. A better measurement is COD which measures the concentration of electron donors available for sulfate or metal reduction; hence a low COD means a low risk of finding SRB and iron-reducing bacteria in the system. Chloride (Cl^-) ions are very aggressive and participate in many forms of corrosion, including MIC. Chloride ions from the electrolyte migrate to the anode to neutralize any buildup of charge, forming heavy metal chlorides that are extremely corrosive to metal surface, particularly stainless steels.

Pope and Pope [3] listed a series of chemical and metallurgical indicators for diagnosis of MIC in natural gas pipeline.

Chemical MIC indicators include:

1) Sulfide: a strong positive indication. SRB reduce sulfate to sulfide, which combines with Fe and forms FeS.
2) Sulfate: a positive indication that SRB-induced MIC may occur. The $FeSO_4$ corrosion product is soluble but less aggressive than the chloride iron for steel corrosion.
3) Chlorides: a positive indication. Chlorides are known to breakdown protective oxide layers and are a cathodic depolarizer. Iron chloride is soluble and its formation promotes anodic dissolution of iron and steel.
4) Short-chain volatile fatty acids: a positive indication for growth of APB.
5) pH: a positive indication that MIC may occur at the site if pH is less than approx. 5.5.

6) Ferrous iron: a positive indication that MIC may have occurred at the site. This is especially true if iron sulfide(s) is present.
7) Ferric iron: a positive indication that corrosion may have occurred at the site. Can also be an indication that the sample was exposed to oxygen in the pipeline, or after the sample was collected. The information is of little value in distinguishing between MIC and other forms of corrosion.
8) Hardness: an indication that scaling can occur (if pH is above about 8.0 and carbonates are present) and, therefore, generalized corrosion may be less likely. However, this has little influence on the possibility that MIC may occur at the site.
9) Carbonate: a neutral indicator of the possibility of MIC but could be important in choices of mitigation measures. Carbonate can form scales which can prevent the successful application of inhibitors or biocides.

Metallurgical MIC indicators include:

1) Discrete deposits: a positive indication that MIC may occur at the site.
2) Deposit color: a black or gray deposit is a strong positive indication that MIC has occurred at the site. Black or gray deposits almost always suggest ferrous iron (a reduced form of iron often associated with MIC).
3) Under deposit pit: a strongly positive indication that MIC has occurred at the site
4) Shiny pit: a strongly positive indication of high acidity at the site and it indicates that MIC may be active.
5) Larger pits composed of smaller pits: a positive indication that MIC has occurred at the site.

MIC Detection and Monitoring

Internal MIC is a significant problem affecting the oil and gas and other industries. Routine monitoring of water quality may identify potential problem organisms and the factors that may promote bacterial growth and attack. Water quality parameters that are considered important to understanding internal corrosion and MIC for a particular industrial system include temperature, pH, alkalinity, sulfide, nitrite, dissolved gases (CO_2, H_2S, O_2, NH_3, etc.), total dissolved solid (TDS), chemical oxygen demand (COD), microorganisms (bacteria, algae, and fungi), etc. COD measures the concentration of electron donors available for sulfate or metal reduction; hence a low COD means a low risk of finding SRB and iron-reducing bacteria in the system. On the other hand, dissolved oxygen might not be indicative as to the oxygen content within the biofilm. Nevertheless, changes in these parameters, especially long-term trends in one direction or large anomalies, indicate a need for further investigation. Online monitors are commercially available for monitoring temperature, pH, conductivity, and TDS, and portable or laboratory spectrophotometers and kits are available for the other tests. MIC investigations require microbiological, chemical, and metallurgical testing for proper diagnosis.

Free-floating planktonic bacteria are often the focus of monitoring for MIC since system fluids are generally easier to sample than metallic surface. However, the results of planktonic bacteria can sometimes be misleading as to whether MIC will occur or, if so, to what extent [80, 81]. Many bacteria such as *Pseudomonas*, *Serratia*, and SRB secrete EPS, which improves the adherence capacity to a metal surface and promotes further trapping of microorganisms in the substratum. The environmental conditions at biofilm/surface interfaces are often radically

different from the bulk medium in terms of pH, dissolved oxygen, and other organic and inorganic species. Oxygen consumption by aerobic bacteria living in the surface region of the biofilm leads to the creation of an anaerobic space for the growth of anaerobic bacteria, which, in turn, results in the formation of oxygen concentration gradients and differential aeration cell on a metal surface [60]. The most devastating MIC takes place in the presence of microbial consortia in which many physiological types of bacteria, including SRB, APB, MOB and MRB, interact in a complex way within the structure of biofilms [3, 54, 82]. Compared to planktonic bacterial counts, sessile bacteria (e.g., biofilm) are more relevant to microbial corrosion [83]. However, monitoring sessile bacteria or biofilm is more complicated, requiring either that the pipeline be excavated or halted for internal sampling or that accommodations be made in the system design to allow for regular collection or on-line tracking of attached organisms during operation.

The most commonly used means of monitoring MIC is to quantify the number of bacteria capable of growing in various microbial growth media (solid or liquid) after inoculation with water samples (serial dilution) obtained from pipelines and other locations [81, 84]. Solid samples such as internal deposits, corrosion products, and surface swabs should be suspended in a sterile phosphate buffer to release viable microbes for inoculation. After incubation at a certain temperature for a pre-determined period of time (days to weeks), the result is expressed as the number of colony forming units (CFU) for solid medium or the most probable number (MPN) for liquid medium. Many bacteria growth media are commercially available or can be made in the laboratory to selectively grow and detect certain type of microbes – aerobic bacteria, anaerobic bacteria, APB, SRB, sulfur-oxidizing bacteria, iron-related bacteria, low nutrient bacteria, nitrite/nitrate-reducing bacteria, and slime-forming bacteria, fungi, algae, etc. General aerobic or anaerobic bacteria counts are normally always included in a MIC monitoring program to gauge the environmental conditions for microbial growth. Some microorganisms such as sulfur-oxidizing bacteria, iron-oxidizing bacteria, and iron-reducing bacteria are very difficult to grow in culture, and the indicators for active growth sometimes are not always appropriate or easy to identify. It is also important to note that the bacterial growth media that are intended to support the growth of a particular type of bacteria are not completely selective, and the vast majority (90-99%) of microbial species cannot currently be grown in the laboratory [85-88], thus underestimating the size and misrepresenting the true composition of microbial communities in the sample [73, 89, 90].

Correct and consistent procedures are crucial for the success of growth methods in MIC monitoring. Sample collection may expose microorganisms to abrupt changes in pressure, temperature, atmosphere, and light, causing redistribution in numbers and types of microorganisms in the original samples. Therefore, the sample collection method, sample transportation, culturing techniques and growth medium, incubation temperature and time should be kept strictly controlled in order to reveal trends in bacteria number over long periods of time. This information is far more important and useful than a single data point when detecting and monitoring the microbial corrosion in a particular system. NACE Standard TM0194-2004 details the sampling procedures for planktonic bacteria, culturing techniques, growth medium and growth indicator for general heterotrophic bacteria and SRB, and provides the guidelines for the assessment of sessile bacteria [81].

To circumvent problems associated with cultivation-based methods, many culture-independent genetic techniques have been developed in the past decade [91, 92], and are beginning to be used in the oil and gas industry for problems related to MIC. One such method is called reverse sample genome probing (RSGP), which allows determination of up to 30 SRB species on an environmental sample in a single DNA hybridization assay [93-95]. Another genetic method example is quantitative polymerase chain reaction (qPCR) [72, 96-98]. qPCR can be designed to target and quantify a specific gene which only exists in a specific species or specific group of bacteria, such as SRB, APB and IOB. qPCR has also been used to determine microorganism abundance in many different types of complex environmental samples such as sediments, water, wastewater, feces, and marine samples, from domain down to genus and species levels [97-101]. The results are more accurate and can be obtained in a few hours instead of days or weeks required for traditional growth methods [72, 73]. Unlike traditional culturing method, qPCR detects and quantifies the target microorganisms in the samples without cultivation, thus, it does not alter the composition of the microbial community in the original sample. In addition, qPCR also works for dry and old samples without live bacteria, a huge advantage over traditional growth methods.

Bacteria in the water sample can also be directly counted under a microscope with or without staining. With proper staining (e.g., fluorescent dye), it is even possible to distinguish the live and dead bacteria under microscope. If bacteria are stained with fluorescently labeled oligonucleotides, it is possible to identify the genera or species of microbes in microbial communities, helping understand how biofilms develop and influence corrosion processes. However, direct counting with a microscope is difficult, time consuming, and sometimes impossible when the sample is turbid or colored, and requires a well-trained observer to gain useful information. Hydrocarbons, deposits, and other contaminants in the sample occasionally fluoresce under ultraviolet light thereby preventing the use of fluorescent dye. Other enumeration methods involve the measurement of molecules peculiar to microbes (e.g., antibody-based SRB enumeration), or biochemical activities (e.g., hydrogenase-based SRB enumeration, adenosine triphosphate or ATP assay). These methods are generally difficult to calibrate against "real world" microbes and have high detection limits.

Chemical characterization of corrosion products and bulk fluids collected from corrosion sites is also important in the diagnosis of MIC. Inductively coupled plasma atomic emission spectroscopy (ICP-AES), ion chromatography (IC), and other traditional colorimetric and spectrophotometric assays are commonly used to measure elemental concentrations in water or pipeline deposit samples. Metallurgical testing includes energy-dispersive X-ray (EDX), X-ray diffraction (XRD), and Raman spectroscopy. These are used to analyze corrosion morphology (pitting depth, shape, coverage, etc.) and corrosion products (chemical composition, compounds, etc.). Other techniques such as scanning electron microscope (SEM), environmental SEM (ESEM), and confocal scanning laser microscope can also be used to qualitatively evaluate the biofilm and/or corrosion products [11]. The integrated consideration of chemical and metallurgical data, microbial data and operational conditions is needed for proper detection and diagnosis of MIC [11].

The choice of internal corrosion (including MIC) monitoring is based on variety of factors, such as leak history, product quality, presence of corrosion indicators detected in previous

samples (e.g., dew point and/or free water levels, acid gas pressures, iron, and bacteria counts, etc.), as well as other operational and economic factors. In many oil and gas operations, monitoring has often combined with the use of corrosion detection devices with sampling and analysis of gas, liquids, and solids obtained from the system. Under some conditions, microbial corrosion and overall internal corrosion may be monitored using corrosion coupons or probes. The coupons are made from an alloy similar to the metal in the system, and typically installed in the bottom quadrant of gas lines so they would be exposed to any liquids that condensed or are inadvertently put into the system, or in a "side-stream" which offers the additional advantage of allowing one to experimentally alter biocide levels and process conditions, giving reasonably fast and reliable information on their affects on the system. The presence of biofilm and microbial activities on a coupon surface changes the local chemistry, possibly modifying the local anodic and cathodic processes and initiating or dramatically altering corrosion process such as pitting. Extensive microscopic analysis of coupons can yield important evidence with regard to pit initiation mechanisms, identify the severity of localized attack through the measurement of pitting (pit densities, depths, and diameters), calculate pitting rates by bacteria or other corrosive components, and determine the severity of attack.

The drawback of corrosion (including MIC) monitoring with metal coupons or probes is that it is destructive and requires time-consuming analysis of numerous coupons sequentially placed in the pipeline in order to obtain information on long-term buildup of biofilms and corrosion initiation. Various electrochemical techniques have been developed for nondestructive and long-term monitoring of the formation and activity of biofilm and possibly detection of an early MIC problem [83, 102, 103]. Such electrochemical techniques include electrical resistance (ER) probes, linear polarization resistance (LPR) probes, galvanic probes, hydrogen probes, electrochemical impedance spectroscopy (EIS), electrochemical noise (ECN), etc. ER probes are used to determine metal loss by measuring the increase in resistance of a metal specimen as its cross-sectional area is reduced by corrosion. LPR probes measure instantaneous corrosion rates and qualitative pitting tendency of metals in electrolytes. ECN measures the fluctuations of the potential, current and resistance over time and then determines the overall corrosion rates and rapid sustained pitting (RSP). For example, Hernández-Gayosso and colleagues successfully detected the formation of biofilm, increased corrosion rate and initiation of localized corrosion on electrodes using EIS technology [83].

One drawback to most electrochemical techniques is the need for electrolytes in the area of the measuring device. Another weakness of most electrochemical techniques is the failure to quantify the localized corrosion, especially RSP [104, 105]. These techniques give average readings for the surface of a test electrode, and it is not clear whether a measured corrosion current corresponds to uniform corrosion of the entire surface or to localized corrosion of just a few sites on the surface. In the latter case, corrosion rates will be severely underestimated if the measured corrosion loss is not normalized to the area at which localized corrosion occurs. This general disadvantage of electrochemical techniques is especially bothersome in the case of MIC, where most corrosion processes are of an extremely localized nature [11, 48].

MIC Prevention and Mitigation

Once internal MIC has been established in a pipeline, complete mitigation is neither practical nor possible. Therefore, the prevention of internal MIC from being initially established should be

a top priority. One of the first defense systems against internal corrosion is to ensure that the product being transported is free of moisture. For corrosion to occur, there must be moisture, CO_2, O_2, or some other reduction reactant, such as one produced by microbes. Gathering lines in production fields have a much more significant problem with internal corrosion than the typical transmission pipeline. MIC after hydrotesting is a common problem when the system was not completely dried after testing. Water used in hydrotesting should be as clean as possible by removing particulates, contaminants and nutrients such as oils, iron, phosphate, and nitrate. When necessary, water should be treated to reduce hardness, remove oxygen, or alter pH.

Although coatings/linings have been used on the internal aspects of natural gas pipelines principally to improve flow characteristics, some internal linings also appear to protect against at least some forms of corrosion, including MIC, by effectively isolating the pipeline from the impact of surrounding environment [106]. However, due to its feasibility and cost, internal coatings are generally limited to new installations or areas easily accessible to "in situ" lining and areas in which pigging would not destroy the integrity of the lining. It should be noted that the target area must be completely lined. Failure to coat weld regions or other features in contact with lined portions of the system could focus corrosion on the unlined areas, thereby accelerating corrosion in these areas. In addition, coating performance can be compromised by microbial degradation of coatings or components in the coating system, leading to water permeation and disbondment of coating. MIC regularly takes place on pipe surfaces under the disbonded coatings, where water and nutrients promote the growth of microorganisms, resulting in the formation of corrosion cells. The severity of corrosion under the disbonded coating strongly depends on the conductivity of the water trapped in the pocket under the separated coating.

System design, maintenance, and water quality are the keys to MIC prevention and control [34, 107]. Materials selection, accessibility for cleaning and water treatment, provision for drains, traps, recycle circuits, and monitoring equipment, control of water velocity and elimination of stagnant, low-flow areas and dead legs, and minimization of crevices and welds are the key considerations in system design. Regular cleaning, including chemical and mechanical cleaning, should be part of the operating routine to remove sludge, deposits, and foulants from the system.

The mitigation measures of internal MIC consist primarily of mechanical cleaning (pigging) and chemical treatment (biocides and corrosion inhibitors). Chemical treatments usually involve the use (in batch or continuously) of biocides, corrosion inhibitors or both to control microbes in the system. A successful MIC control program requires assessment of the MIC potential in a system, screening tests of chemical treatments, and aggressive monitoring of actual systems after treatment. It is worth noting that most laboratory studies of biocide efficiency in man-made system often fail to duplicate their successful results when they are applied in industrial systems. Organisms embedded within the biofilm are protected from biocides, largely due to the diffusion barriers generated by the EPS matrix that hinders the chemical penetration of the entire thickness of the deposits [23, 108]. Moreover, bacteria within the biofilm are probably physiologically altered and may develop resistance to a particular biocide if it is used repeatedly [2, 109]. Therefore, before the biocide treatment, a “time-kill” study is often needed to identify what chemical agent(s) is (are) the most effective in killing the bacteria in a particular system.

The resistance of bacteria to biocides depends on the nature of the chemicals used. Biocides can be classified as either oxidizing or non-oxidizing. Apart from ozone and hydrogen peroxide, all the oxidizing agents used as biocides contain halogens. The non-oxidizers are relatively non-reactive chemicals and, therefore, compatible with strong reducing agents in water treatment application [110]. Examples of typical non-oxidizing biocides are formaldehyde, glutaraldehyde, methanol, isothiazolones, quaternary amines, and tetrakishydroxymethylphosphonium sulfate (THPS). Non-oxidizing biocides are often used in combination with dispersants and surfactants to stimulate full biocides penetration into the biofilm. Whether biocides can be used continuously or in a batch mode, or periodically depends on the system. In the case of continuous treatment, it is necessary to alternate several biocides to prevent biocide resistant bacteria strain from being developed. Batch treatment is usually applied to the system after hydrotesting and pigging operation. The effectiveness of biocide treatments depend on proper treatment schedule, effective doses, and appropriate locations, and combination with other control technologies (e.g., pigging) [106]. For instance, an additional pigging run using a sphere or ball pig to push a slug of a biocide solution (1% cocodiamine and quaternary in methanol) was reported to be very effective to keep the pipe free of bacteria after hydrotesting [2]. The mixture biocide solution in this treatment also acts as a corrosion inhibitor against carbon dioxide and hydrogen sulfide attack.

Batch or continuous injection of corrosion inhibitors is also commonly employed to treat/prevent many types of corrosion including MIC. Most corrosion inhibitors used in the natural gas industry are more effective in preventing and treating generalized-type corrosion than the focused, RSP corrosion usually associated with MIC, due to the difficulty in penetrating existing biofilms and corrosion products and to the fact that bacteria may degrade some corrosion inhibitors [4, 111]. The concentrations of biocides and corrosion inhibitors have to be closely monitored in the system during treatment since the treatment chemicals can be degraded or used up faster by factors such as pH, TDS, chlorides, temperature, oxygen, etc. Spore-forming microorganisms such as species in genus *Bacillus* and *Clostridium* can usually survive biocide treatment, and re-generate in the pipeline system when biocide concentration becomes lower and other conditions become favorable. *Bacillus* has been isolated frequently from tubercles formed on metals and associated with microfouling [20]. These organisms are copious producers of organic acids.

“Pigs” are the most common device used for the mechanical cleaning of the pipeline interior, and pigging is one of the most effective means of controlling microbes on metal surfaces and, therefore, internal MIC. Pigs are inserted into the pipelines and pushed through the pipe using gas pressure. The frequency of pigging and types of pigs utilized are determined, at least in part, by the results of the pigging itself, such as the amount and types of materials removed from the line. The objectives of mechanical cleaning are to remove materials capable of inhibiting gas flow and/or promoting corrosion (including MIC) from the pipeline. These materials include fluids (including water) and solids (e.g., sand, corrosion products, nodules, and biofilms/slimes). Water is required for microbial metabolism and growth and corrosion processes; solids provide shelter for microorganisms and water, reduce the efficiency of treatment chemicals (e.g., biocides and corrosion inhibitors), and allow the formation of concentration cells.

In addition to viable microbes in the removed materials, pH, iron, chloride, and sulfide should also be measured in the monitoring program. Chloride (Cl^-) ions are very aggressive and participate in many forms of corrosion, including MIC. Chloride ions from the electrolyte migrate to the anode to neutralize any buildup of charge, forming heavy metal chlorides that are extremely corrosive to metal surface, particularly stainless steels. Under these circumstances, pitting involves the conventional features of differential aeration, a large cathode-to-anode surface area, and the development of acidity and metallic chlorides [22]. Webster and Newman examined the impact of media constituents on localized corrosion and concluded that localized corrosion would not readily occur unless chloride ion was the predominant anion in the medium [112]. Sulfide levels in the corrosion products and fluids can serve as an indication of MIC-type corrosion.

A very different approach which has been proposed as a potential alternative to protect pipeline from internal corrosion is to use beneficial biofilm on metal surface as a corrosion inhibition mechanism [113]. Biofilms have been reported to be effective on inhibition of general corrosion in some circumstance for mild steel, copper, aluminum, and stainless steels [114-119]. The mechanisms most frequently cited for the inhibition are:

1) formation of a diffusion barrier to corrosion products that stifles metal dissolution,
2) removal of corrosive agents (e.g., oxygen) from metal surface by bacteria physiological activities (e.g., aerobic respiration) [120, 121],
3) growth inhibition of corrosion-causing bacteria by antimicrobials generated within biofilm (e.g., SRB corrosion inhibition by gramicidin S-producing *Bacillus brevis* biofilm [115, 117, 118],
4) generation of protective layer by biofilms (e.g., *Bacillus licheniformis* biofilm produces on aluminum surface a sticky protective layer of gamma-polyglutamate) [120],
5) formation of passive layers (e.g. magnetite film) [120], and
6) production of metabolic products that act as corrosion inhibitors (e.g., siderophores) [122, 123].

However, biofilm formation on metal surface is unpredictable and uncontrollable, and is often not uniform. Bacteria tend to colonize preferentially on rough surfaces and are more attracted to anodic sites [124]. Biofilm growth rate depends on substratum, available nutrients, temperature, and electron acceptors. Biofilm composition is affected by small perturbations in the environment (e.g., temperature, nutrient concentration, and flow). A little-understood phenomenon – biofilm sloughing – creates a discontinuity of biofilm on metal surface (patchiness), which results in local differences in metabolic products, pH, dissolved oxygen, and gradients of nutrients and ions within the biofilm. Patchy biofilms create differential aeration cells which can lead to intensification of localized corrosion rates under the biofilms [125, 126]. Biofilm formation is an extremely complex biological/chemical process, and its impact on corrosion processes is difficult to predict and control. Therefore, more research is needed before biofilms can be used as corrosion inhibition mechanisms in the field.

Task 2 – Microbial/Chemical Profile in Raw Biogas Pipeline

Twelve raw biogas samples from 10 dairy farms in the mid-western, eastern and western regions of the U.S. were collected in the previous Dairy Farm Biogas project for determination of major raw biogas components and corrosion-related bacteria population carried over from anaerobic digestion processes. In addition, a condensate sample was collected in this project for determination of microbial and chemical profiles in raw biogas pipelines. The data will be used to formulate a synthetic condensate and bacteria consortium for Task 3 experiments to determine the corrosion effect of microbes on metal pipelines and collect data for MIC modeling in Task 4.

Major gas compositions in raw biogas

All twelve raw biogas samples were analyzed for major components such as methane, carbon dioxide, oxygen, and a handful of other compounds. This analysis was performed using ASTM D1946. Table 2 includes only the compounds that had observed concentrations above the method detection limit. For example, of the 12 raw biogas samples tested, only 11 raw biogas samples contained hydrogen sulfide above the method detection limit with an average concentration of 0.31% ± 0.15%.

Table 2. Results from Major Components Analysis for 12 Raw Biogas Samples

Compound	Detection Limit (Mol%)	Samples Above Detection Limit	Average (Mol%)	Standard Deviation	Min (Mol%)	Max (Mol%)
Carbon Dioxide	0.03	12	35.5	4.17	28.57	40.39
Oxygen/Argon	0.03	12	0.74	0.82	0.22	2.94
Nitrogen	0.03	12	3.08	3.46	0.64	12.67
Methane	0.002	12	60.42	5.40	49.03	68.58
Hexane Plus	0.0001	7	0.0002	0.0001	0.0001	0.0004
Ammonia	0.001	1	0.004	NA	0.004	0.004
Hydrogen Sulfide	0.000005	11	0.3085	0.1473	0.148	0.6570
Carbonyl Sulfide	0.000005	12	0.000154	0.0001	0.000034	0.000409

As indicated in Table 2, hydrogen sulfide is a significant component in raw biogas and a thorough speciation analysis using ASTM D6228 was performed on the 12 raw biogas samples to identify the species of sulfur compounds as shown in Table 3. The raw biogas samples tested had an average total sulfur concentration of 2830 ppmv (168 grains/100 scf) with a range from 0.34 ppmv (0.02 grains/100scf) to 6580 ppmv (390 grains/100 scf). While the major sulfur species is hydrogen sulfide for almost all of samples analyzed, most of samples also contain other sulfur compounds in various quantities such as sulfur dioxide, carbonyl sulfide, mercaptan, etc. It should be noted that one raw biogas sample collected from one of the dairy farms contained an unusually low amount of total sulfur, 0.02 grains/100scf. No explanation for this low concentration has been confirmed but the weather conditions on that day were very unfavorable for sample collection. The recorded ambient temperature during this specific sampling event was -8°C, therefore it is possible that the integrity of the sample was

compromised. If this sample is removed from the raw biogas data set, then the new calculated average for total sulfur concentration would be 182 grains/100 scf. Unlike the average total sulfur concentration observed from the raw biogas samples, the total sulfur concentration typically found in pipeline tariffs are much lower and range from 0.5-20 grains/100 scf [127].

Table 3. Results from Sulfur Analysis for 12 Raw Biogas Samples.

Compound	Detection Limit (ppmv)	Samples Above the Detection Limit	Average (ppmv)	Standard Deviation	Min (ppmv)	Max (ppmv)
Hydrogen Sulfide	0.05	11	3090	1470	1480	6570
Sulfur Dioxide	0.05	10	1.31	2.36	0.07	7.73
Carbonyl Sulfide	0.05	12	1.54	1.05	0.34	4.09
Carbon Disulfide	0.05	3	0.09	0.072	0.03	0.17
Methyl Mercaptan	0.05	11	2.00	2.01	0.25	6.12
Ethyl Mercaptan	0.05	11	0.20	0.072	0.07	0.30
i-Propyl Mercaptan	0.05	11	0.55	0.39	0.09	1.35
n-Propyl Mercaptan	0.05	4	0.08	0.012	0.06	0.09
t-Butyl Mercaptan	0.05	4	0.27	0.242	0.05	0.60
Dimethyl Sulfide	0.05	9	0.30	0.321	0.09	0.32
Dimethyl Disulfide	0.05	1	0.32	NA	0.32	0.32
Diethyl Disulfide	0.05	1	0.15	NA	0.15	0.15
Thiophene	0.05	7	0.15	0.068	0.25	0.26
Total Sulfur (ppm)	NA	12	2830	1670	0.34	6580
Total Sulfur (As Grains/100 SCF @ 14.73 psia, 60°F)	NA	12	168	98	0.02	390

Major microbial compositions in raw biogas

Microbiological analyses were performed in 10 raw biogas samples to determine 1) the number of total (live and dead) heterotrophic bacteria and various corrosion causing bacteria (APB, IOB, and SRB), 2) the number and identity of live bacteria, and 3) the number and identity of bacterial spores. The number of total bacteria and total corrosion-causing bacteria including both dead and live bacteria on the filter was determined by a genetic method (qPCR) by targeting specific genes present in the target microorganisms, and the data was reported as numbers per 100 scf of gas sample. The number of live bacteria and spore was determined by inoculating samples (phosphate buffer saline suspension of filter) to appropriate bacteria medium and incubated at 37 ºC for a pre-determined time, and the data was reported as colony-forming unit (CFU) per 100 scf of gas sample.

The filter sample was placed in a 50-ml tube with 30 ml of sterile phosphate buffered saline (PBS, pH 7.2 ± 0.1), vortexed for 5-10 sec, and sonicated for 2 min ± 5 sec in waterbath sonicator filled with fresh aqueous solution of 0.3% vol/vol Tween 80. After sonication, the filter suspension was used for Most Probable Number (MPN) test, Spore Enumeration, and DNA extraction. The MPN test determines the number of live heterotrophic bacteria in the filter samples carried over from anaerobic digestion process. MPN tests were performed in thioglycolate medium (TG media) in triplicate with serial dilutions of filter suspension samples. After 7 days incubation at 37 ºC aerobically and anaerobically, the positive culture bottles were scored and the number of heterotrophic bacteria determined using a statistically derived table (Most Probable Number from Serial Dilution, Bacteriological Analytical Manual, FDA, February 2006). The positive MPN culture then was used for DNA extraction. A second part of the filter suspension sample was used for Spore Enumeration using a Pour Plate Procedure modified from NASA standard assay NHB 5340.1D. The sample suspension is heat-shocked at 80 ± 2 ºC water bath for 15 min to kill vegetative cells, inoculated onto Tryptic Soy Agar (TSA) medium, incubated at 37 ºC aerobically and anaerobically for 3 days before colony counts to determine the number of live spores in the filter sample. The spore colonies were used for DNA extraction.

DNA extraction for filter suspension samples without prior growth and positive MPN culture in TG media and spore colonies on TSA plate after growth was performed using FastDNA SPIN Kit for Soil (MP Biomedicals LLC). DNA from filter suspension samples was used for determination of bacterial identity and qPCR quantification of total bacteria, total APB, total SRB, and total IOB. DNA from MPN culture and spore colonies was used for determination of identities of live bacteria and spores. qPCR quantification of specific groups of bacteria was achieved by targeting bacterial 16S rRNA, *ackA* and *buk*, *dsrAB*, and IOB 16S rRNA genes, respectively, following the instructions of the Rotor-Gene 3000 4 Channel Multiplexing System and QuantiTect PCR kits (Qiagen Inc., Valencia, California).

The extracted DNA was amplified with polymerase chain reaction (PCR) using various primers specific to the target bacteria groups and the PCR products were used for determination of bacteria identities in the samples. For heterotrophic bacteria, universal primer pair BA8F/UN1492R was used to target 16S rRNA gene, and if it failed due to low quantity of target DNA in the samples, a second universal primer pair BA338F/BA1392R was used for a nested PCR to amplify target 16S rRNA gene from the samples. For acid-producing bacteria (APB),

two pairs of primers were used to amplify *ackA* (ackA-3F and ackA-4R) and *buk* (buk-5F and buk-6R) genes, respectively. Two pairs of primers (IOB-F486 and IOB-R1132, and Gall-F704 and IOB-R1000) were also used to amplify 16S rRNA gene from iron-oxidizing bacteria (IOB).

The PCR products were purified using QIAquick PCR Purification Kit, and the purified PCR products were inserted into pGEM-T Easy Vector System I (Promega Corp., Madison, Wisconsin). The vectors were then transformed into DH5α Subcloning Efficiency Chemically Competent Cells purchased from Invitrogen (Carlsbad, California), and the cells were inoculated onto LB agar medium for screening of white colonies after overnight incubation at 37 ºC. The white colonies were picked and their DNA prepared for sequencing. The sequences were analyzed with the Blast program in GenBank database and identities of heterotrophic bacteria, APB, and IOB were determined.

The results from genetic quantification (qPCR) on filter samples indicates how many heterotrophic bacteria are generated by anaerobic digestion and have remained in the raw biogas stream, whether or not they are dead or still alive. APB, IOB, and SRB are major corrosion-causing bacteria, and the genetic tests indicate if the anaerobic digestion process might pose a pipeline corrosion risk if the raw gas is not treated. However, many microbes may not be able to survive the adverse environment during anaerobic digestion, and the number of microbes which are still alive in the raw biogas stream is supposed to be much smaller. In addition, downstream clean-up processes may also kill some of live microbes carried over from the raw biogas. The number of live bacteria is more relevant to the risk the microbes pose to the integrity of pipelines. It is worth noting, though, that some bacteria may be killed during sampling process (filtration); as a result, the number of live bacteria retrieved from MPN testing might be underestimated to a certain degree. Bacterial spores may survive very adverse environment such as clean-up process and sampling process, and may pose higher risks to pipeline integrity and human health.

The results in Table 4 indicated that most raw biogas samples carried an average of 2.72E+06 heterotrophic bacteria per 100 scf with a range of 5.81E+05 to 3.8E+07 per 100 scf from anaerobic digestion. In terms of more specific groups of bacteria, most raw biogas samples contained two major types of corrosion-causing bacteria - APB and IOB, with an average of 1.82E+04 and 2.52E+03 per 100 scf, respectively. SRB was detected only in 1 raw biogas sample, indicating that SRB are not a significant group of bacteria in anaerobic digestion process during biogas production.

The bacteria leaving the digester may be dead already due to the unfavorable environment in the digester, or may die after they were caught by a filter during the sampling process due to desiccation. Therefore, the live bacteria or spores detected by MPN test and Pour Plate method may only represent a portion of microbes which could survive the whole process, and might be more relevant to the pipeline integrity and health risk of consumers if the filter would fail for some reasons. Live aerobic bacteria were detected in all 10 raw biogas samples, and anaerobic bacteria in 8 samples, with a mean 4.04E+02 and 1.45E+02 per 100 scf, respectively. Only four of the 10 raw biogas samples tested positive for bacteria spores, containing an average number of 537 spores per 100 scf.

Table 4. Results from Biological Testing for 10 Raw Biogas Samples

Method	qPCR				MPN		Pour Plate
	Total Bacteria	Total APB	Total IOB	Total SRB	Live Aerobic Bacteria	Live Anaerobic Bacteria	Live Spores
	CFU/100 scf or #/100 scf						
Mean	2.72E+06	1.82E+04	2.52E+03	1.10E+02	4.04E+02	1.45E+02	5.37E+02
Standard Deviation	3.14	3.3	1.66	NA	2.75E+00	1.86E+00	1.74E+00
Minimum	5.81E+05	1.23E+03	1.02E+03	1.10E+02	9.82E+01	8.75E+01	2.48E+02
Maximum	3.80E+07	6.03E+04	5.09E+03	1.10E+02	2.11E+03	5.95E+02	8.51E+02
Samples above Detection Limit	10	9	8	1	10	8	4

Identities of major microbial species in raw biogas

DNA samples collected from the previous Dairy Farm Biogas project were used in this project to determine the microbial profile in raw biogas samples. There are four sources from which DNA was isolated: 1) directly from the biogas filter, 2) from positive MPN cultures incubated under aerobic condition, 3) from positive MPN cultures incubated under anaerobic condition, and 4) from positive bacterial spore cultures. The DNA from the above sources was used to determine the identities of heterotrophic bacteria, bacterial spores, and corrosion-related APB and IOB by targeting 16S rRNA genes or specific functional genes such as *ackA* and *buk* genes.

All 24 heterotrophic bacteria sequences isolated from three filter samples without growing in the culture medium were closely related to *Paenibacillus* sp. (Table 5). However, after the filter suspension samples were grown in culture medium aerobically, various *Bacillus* sp. were enriched and became the dominant heterotrophic bacteria (Table 6). They accounted for 58% of 24 sequences isolated, and with a majority of them being *B. licheniformis* (38%). When filter suspension samples were grown in culture medium anaerobically, all 16 sequences isolated were closely related to *Paenibacillus* sp., though these were different species from those directly obtained from filter samples without growth (Table 7).

Table 5. The Closest Relatives of Heterotrophic Bacteria Sequences Isolated Directly from 3 Filter Samples without Growth using Universal Primers Targeting 16S rRNA Gene

Closest relative in Genbank	Genbank accession No.	% Identity	Frequency
Paenibacillus glucanolyticus	AB073189	99	3
Paenibacillus glucanolyticus strain FR1_105	EU373524	99	1
Paenibacillus sp. isolate P14-7	AJ297712	96	1
Paenibacillus sp. JAM-FM32	AB526335	99-100	19

The identities of bacterial spores isolated from 4 positive culture samples were also determined (Table 8). Of 56 bacterial spore sequences retrieved, the majority of them were identified as *Bacillus licheniformis* (48%), and various other *Bacillus* species (43%).

Table 6. The Closest Relatives of Heterotrophic Bacteria Sequences Isolated from 3 Positive Aerobic MPN Cultures using Universal Primers Targeting 16S rRNA Gene

Closest relative in Genbank	Genbank accession No.	% Identity	Frequency
Bacillus licheniformis isolate CCM28B	FN433039	100	1
Bacillus licheniformis strain CICC 10087	GQ375232	100	1
Bacillus licheniformis strain CICC 10181	GQ375235	100	2
Bacillus licheniformis strain NBST2	GU011947	99	1
Bacillus licheniformis strain nju-1411-1	FJ915147	99-100	3
Bacillus licheniformis strain YP1A	EF105377	100	1
Bacillus sp. strain R-30915	AM910273	99	3
Bacillus sp. FE-1	EU271855	99	1
Bacillus sphaericus strain 601	DQ350820	98	1
Bordetella avium 197N	AM167904	98	2
Sporosarcina ginsengisoli	AB245381	96-99	2
Sporosarcina luteola	AB473560	100	1
Uncultured bacterium clone 101-68	EF157238	98	3
Uncultured bacterium clone 2G4-89	EU160423	98	1
Uncultured bacterium clone B1	FJ868757	96	1

Table 7. The Closest Relatives of Heterotrophic Bacteria Sequences Isolated from 2 Positive Anaerobic MPN Cultures using Universal Primers Targeting 16S rRNA Gene

Closest relative in Genbank	Genbank accession No.	% Identity	Frequency
Paenibacillus barengoltzii strain THWCS9	GQ284356	98-99	2
Paenibacillus barengoltzii strain THWCSN47	GQ284370	98	1
Paenibacillus sp. strain HanTHS1	AM283040	98	2
Paenibacillus sp. 5T01	AM162346	99	4
Paenibacillus sp. enrichment culture clone 9	FJ930068	99-100	7

The results indicate that the dominant heterotrophic bacteria or bacterial spores in raw biogas derived from dairy biomass belong to two genera, i.e. *Paenibacillus* and *Bacillus*. *Bacillus* is large and diverse genus of bacteria in the Family Bacillaceae. *Paenibacillus* is a genus split off from genus *Bacillus* in 1997 based on ssRNA analysis. Both belong to Class *Bacilli* and Order *Bacillales*. They are Gram-positive aerobic or facultative endospore-forming bacteria. Collectively, the aerobic spore-formers are versatile chemoheterotrophs capable of respiration of most all substrates derived from plant and animal sources, including cellulose, starch, pectin, proteins, agar, hydrocarbons, and others, although simple organic compounds such as sugars, amino acids, organic acids are preferred. In some cases, they also ferment carbohydrates in a mixed reaction that typically produces glycerol and butanediol. Endospore forming bacteria play a significant role in the biological cycles of carbon and nitrogen. The majority of these are mesophiles, with temperature optima between 30 ºC and 45 ºC, but some are thermophiles with optima as high as 65 ºC. They are found growing over a range of pH from 2 to 11. In the laboratory, under optimal conditions of growth, *Bacillus* species exhibit generation times of about 25 minutes.

P. glucanolyticus is rod-shaped, motile, facultative anaerobic endospore-forming bacteria that hydrolyze various β-blucans, including carboxymethyl cellulose and pustulan [128]. Cells of

P. glucanolyticus are long (usually >3.0 µm) and thin (<0.9 µm), and produce oval terminal spores that markedly distend the sporangium. Colonies are flat, smooth, and opaque and are motile during growth on dry nutrient agar plates. *P. glucanolyticus* degrades cellobiose, D-fructose, D-galactose, D-glucose, lactose, maltose, D-mannose, raffinose, salicin, sucrose, trehalose, and D-xylose, and produces acids.

Table 8. The Closest Relatives of Bacterial Spore Sequences Isolated from 4 Positive Spore Cultures using Universal Primers Targeting 16S rRNA Gene

Closest relative in Genbank	Genbank accession No.	% Identity	Frequency
Bacillus anthracis str. 'Ames Ancestor'	AE017334	100	1
Bacillus bataviensis strain MSU1210	AY647284	99	1
Bacillus licheniformis ATCC 14580	CP000002	99-100	7
Bacillus licheniformis strain B8	EU117278	97	1
Bacillus licheniformis strain CICC10094	AY842873	99	4
Bacillus licheniformis strain MML2501	EU344793	99-100	4
Bacillus licheniformis strain MZ-14	EU586786	100	1
Bacillus licheniformis strain TCCC11009	EU231623	99	2
Bacillus licheniformis strain YP1A	EF105377	99-100	2
Bacillus licheniformis strain YRL03	EU373408	99-100	6
Bacillus sp. BT97	DQ358737	97	1
Bacillus sp. By137(B)Ydz-ss	EU070408	100	1
Bacillus sp. CBD 118	DQ374636	99	1
Bacillus sp. CSS-4	DQ084465	99-100	3
Bacillus sp. DCA-5	DQ238044	100	2
Bacillus sp. MO15	AY553108	97	1
Bacillus sp. N6	AB043854	99-100	8
Bacillus thuringiensis serovar konkukian strain I	EU438936	100	3
Bacillus thuringiensis strain KR19-22	EU414475	100	1
Clostridium beijerinckii NCIMB 8052	CP000721	99-100	2
Clostridium puniceum	X71857	99	1
Paenibacillus sp. MB 2039	AY257871	99	1
Uncultured Bacillus sp. clone ACf137	AM489497	99	2

B. licheniformis is Gram-positive, rod-shaped, motile, aerobic endospore-forming thermophilic bacteria (with a diameter < 0.9 µm) that hydrolyze sugars fermentatively. Colonies of *B. licheniformis* are round, surface smooth, flat, margin irregular and 2-4 mm in diameter. Ellipsoidal spores are produced in not swollen sporangia and placed centrally [129]. *Bacillus licheniformis* has been associated with a range of clinical conditions, food spoilage and incidents of food-borne gastro-enteritis. *B. licheniformis* has also been associated with septicaemia, peritonitis, ophthalmitis, and food poisoning in humans, as well as with bovine toxaemia and abortions. Food-borne *B. licheniformis* outbreaks are predominantly associated with cooked meats and vegetables [130]. *B. licheniformis* is a common contaminant of dairy products; it is the most common aerobic spore-forming bacteria isolated from dairy farm [131]. The optimal growth temperature is around 50°C, though it can survive at much higher temperatures. Optimal temperature for enzyme secretion is 37°C. It can exist in spore form under harsh environments or in a vegetative state when conditions are good.

Since the results from qPCR analysis (Table 4) indicated the widespread existence of two major types of corrosion-related bacteria (APB and IOB), the identities of dominant APB and IOB species were determined by targeting *ackA* and *buk* genes for APB, and 16S rRNA genes for IOB. The attempt to directly amplify *ackA* and *buk* genes from filter suspension samples without prior growth in the medium failed; therefore the dominant profile of APB was derived from samples after they were inoculated to, and grown in, the culture medium (Table 9 and Table 10). *Bacillus sp.* (e.g. B. licheniformis and B. cereus), *Geobacillus sp*., and *Clostridium sp*. were the dominant acid-producing species in raw biogas derived from dairy biomass.

Table 9. The Closest Relatives of APB Sequences Isolated from 3 Positive Aerobic MPN Cultures using Primers Targeting *ackA* and *buk* Genes

Closest relative in Genbank	Genbank accession No.	% Identity	Frequency
Bacillus licheniformis ATCC 14580	CP000002	93-100	34
Clostridium acetobutylicum ATCC 824	AE001437	74-75	2
Geobacillus sp. WCH70	CP001638	75-76	3
Geobacillus sp. Y412MC10	CP001793	76	1
Methanosarcina mazei strain Goe1	AE008384	73	1

Table 10. The Closest Relatives of APB Sequences Isolated from 2 Positive Anaerobic MPN Cultures using Primers Targeting *ackA* and *buk* Genes

Closest relative in Genbank	Genbank accession No.	% Identity	Frequency
Bacillus anthracis str. A0248	CP001598	79-82	9
Bacillus cereus E33L	CP000001	98-100	7
Bacillus pumilus SAFR-032	CP000813	90-92	3
Clostridium acetobutylicum ATCC 824	AE001437	73-77	5
Geobacillus sp. Y412MC10	CP001793	74-75	8
Methanosarcina acetivorans str. C2A	AE010299	75	1
Vibrio fischeri MJ11 chromosome I	CP001139	74	1

The IOB sequences derived from filter suspension samples were very diverse (Table 11). The majority of sequences (18 out of 27) isolated were closely related to sequences of bacteria which have not been cultured successfully. Four sequences were closely related to *Acidovorax* species. A well-known IOB *Gallionella ferruginea* was only detected once. After filter suspension samples were grown under aerobic or anaerobic conditions, *Bacillus* and *Paenibacillus* were found to be the dominant species (11 out of 25 and 35 sequences, respectively) (Table 12 and Table 13). The well-known IOB *Sphaerotilus* and *Gallionella* were only detected once, respectively. Fifteen sequences (out of 35) isolated after anaerobic growth were closely related to uncultured bacterial sequences. *Gallionella*, *Leptothrix*, and *Sphaerotilus* are the three major genera of iron-oxidizing bacteria. Only a few species within these genera have been isolated from the environment and successfully cultured in the laboratory. The primers designed based on limited number of sequences deposited in Genbank database might not be optimal, and may amplify some non-target DNA sequences from other bacteria. The identity results appeared to confirm this assumption since many *Bacillus* and *Paenibacillus* sequences had been isolated from the samples. In summary, IOB might not be a significant corrosion-related population in raw biogas samples.

Table 11. The Closest Relatives of IOB Sequences Isolated Directly from 2 Filter Samples without Growth using Primers Targeting IOB 16S rRNA Gene

Closest relative in Genbank	Genbank accession No.	% Identity	Frequency
Acidovorax facilis strain TSWCSN46	GQ284412	100	1
Acidovorax sp. PPs-5	FJ605421	99	2
Acidovorax temperans strain 2R3-13	GU169008	100	1
Beta proteobacterium ASRB1	AY612302	99	1
Gallionella ferruginea	L07897	100	1
Paenibacillus barengoltzii strain THWCSN14	GQ284362	99	1
Paenibacillus sp. 5M01	AM162347	99	1
Paenibacillus sp. D273a	FJ430033	100	1
Uncultured bacterium clone MRA3016	FN428762	99-100	2
Uncultured bacterium clone nbw217a04c1	GQ074849	100	1
Uncultured bacterium clone nbw335c11c1	GQ090536	100	2
Uncultured bacterium clone nbw390c06c1	GQ096609	99	1
Uncultured bacterium clone nbw403b10c1	GQ098239	99	1
Uncultured bacterium clone nbw518g07c1	GQ104363	100	1
Uncultured bacterium clone nbw520b12c1	GQ104478	99	1
Uncultured bacterium clone nbw530e12c1	GQ105704	100	1
Uncultured bacterium clone nbw534f08c1	GQ106415	100	1
Uncultured bacterium clone nbw579c08c1	GQ106258	100	1
Uncultured bacterium clone nbw638f09c1	GQ114515	100	1
Uncultured bacterium clone nbw639h01c1	GQ114609	100	1
Uncultured bacterium clone nbw680e07c1	GQ114021	100	1
Uncultured bacterium clone nbw906h06c1	GQ032518	99	1
Uncultured beta proteobacterium clone R64LS	FM863753	100	1
Uncultured Ralstonia sp. clone 1P-1-G07	EU704794	99	1

Table 12. The Closest Relatives of IOB Sequences Isolated from 3 Positive Aerobic MPN Cultures using Primers Targeting IOB 16S rRNA Gene

Closest relative in Genbank	Genbank accession No.	% Identity	Frequency
Bacillus boroniphilus strain PL69	GU001903	99	1
Bacillus licheniformis strain 3EC7A1	EU304968	99	1
Bacillus licheniformis strain ES_MS4c	EU888508	99	1
Bacillus sp. BCL23-1	EF026994	100	1
Bacillus sp. HB1	FM208185	99	1
Bacillus sp. JJM-1	GU132507	99-100	5
Bacillus sp. MB66	AB518978	99	1
Pigmentiphaga sp. Zn-d-2	EU170477	98-99	9
Ralstonia sp. RS2	AB503703	100	1
Salmonella enterica strain st8r	FJ544366	100	1
Sphaerotilus sp. HS	EU636006	99	1
Uncultured Bacillus sp. clone QNSW24	FJ384500	99	1
Uncultured bacterium clone NCH1312/73f	EU560864	96	1

Table 13. The Closest Relatives of IOB Sequences Isolated from 2 Positive Anaerobic MPN Cultures using Primers Targeting IOB 16S rRNA Gene

Closest relative in Genbank	Genbank accession No.	% Identity	Frequency
Bacillus sp. JJM-1	GU132507	99	1
Gallionella ferruginea	L07897	99-100	5
Paenibacillus barengoltzii strain SAFN-125	DQ124699	99	1
Paenibacillus barengoltzii strain THWCSN13	GQ284361	99	3
Paenibacillus barengoltzii strain THWCSN14	GQ284362	99	2
Paenibacillus sp. 5M01	AM162347	99	1
Paenibacillus sp. AT5	GU097198	98	2
Paenibacillus sp. D273a	FJ430033	100	1
Paenibacillus sp. oral taxon 786 strain F0064	GQ422747	99	1
Pseudoxanthomonas taiwanensis strain NFC7-12	EU250946	99-100	3
Uncultured bacterium clone AR18	EU008373	99	2
Uncultured bacterium clone EU32	EU008374	99	1
Uncultured bacterium clone EU40	EU008371	99	1
Uncultured bacterium clone EU40A	EU008377	99	1
Uncultured bacterium clone nbw335c11c1	GQ090536	100	5
Uncultured bacterium clone nbw520b12c1	GQ104478	100	2
Uncultured bacterium clone nbw641c05c1	GQ115240	100	1
Uncultured bacterium clone p02_E05	FJ602432	100	1
Uncultured bacterium clone TSBAR002_E10	AB486284	99	1

Major chemical compositions in condensate of raw biogas line

GTI obtained a 5-gallon sample of raw biogas condensate from a waste water treatment plant (WWTP) in the mid-west area of the U.S. This condensate consisted of liquid that dropped out from a stream of untreated digester biogas being used to fuel a turbine combustion engine for a Combined Heat and Power (CHP) application. Chemical and microbiological analyses were conducted to characterize the liquid in order to prepare a simulated condensate recipe for work on subsequent tasks. Table 14 summarizes the analytes and their associated analytical techniques.

Table 14. Analytical Methods Used for Condensate Sample.

Analyte Group	Analysis Technique
Organic and Inorganic Carbon	EPA Method 9060
Alkalinity	Titration (SM 2320 B)
Biochemical Oxygen Demand	5-day (SM 5210 B)
Chemical Oxygen Demand	Closed Reflux, Titrimetric (SM 5220 C)
Suspended , Dissolved, Total Solids	Gravimetric (SM 2540 B, C, D)
pH, as received	SM 4500 H+
Conductivity, µS/cm as received	SM 2510
Dissolved Gases	Headspace Analysis (EPA RSK-175)
Total Ammonia	Distillation / Nesslerization (SM 4500 NH3 C)
Metals	Inductively Coupled Plasma Optical Emission Spectroscopy
Anions	Ion Chromatography
Toxicity	MicrotoxOmni
CHNS	Leco

Aliquots of the larger sample were taken for analysis in appropriate vials. The dissolved gas analysis was conducted from a sealed 40-ml VOA vial to which sample was displaced by a measured amount of helium. The metals ICP analysis was performed after digestion in nitric acid and hydrogen peroxide. All other analyses were done on an as-received basis. A toxicity test was also performed by exposing fibrio fischeri luminescent bacteria to the sample and determining at what concentration one-half of the bacteria are killed (EC50). The analytical results are summarized in Table 15.

Table 15. Analytical Results of Condensate Sample

Analyte	Results
Total Organic Carbon, mg/l	5.9
Total Inorganic Carbon, mg/l	250
Total Ammonia	240
Alkalinity, mg/l	960
BOD, mg/l	< 2
Chemical Oxygen Demand, mg/l	45
Total Suspended Solids, mg/l	< 10
Total Dissolved Solids, mg/l	< 25
Total Solids, mg/l	< 25
pH, as received	7.32
Conductivity, µS/cm	1700
Dissolved Ammonia, mg/l	< 15
Dissolved Carbon Dioxide, mg/l	218
Dissolved Hydrogen Sulfide, mg/l	0.0014
Dissolved Methane, mg/l	0.73
Dissolved Oxygen, mg/l	17.9
Calcium, mg/l	1.8
Iron mg/l	1.2
Potassium, mg/l	8
Magnesium, mg/l	0.3
Molybdenum, mg/l	0.3
Sodium, mg/l	5.9
Phosphorus, mg/l	14.8
Silicon, mg/l	18.3
Tin, mg/l	14.8
Titanium, mg/l	0.2
Zinc, mg/l	0.5
Organic Acid Anion, mg/l (calibrated as acetate)	~5
Sulfate, mg/l	0.4
Anion/Cation Ratio	1.17
Toxicity, EC50 (15 minutes)	49.27%

The condensate was a clear liquid, with no apparent solids, confirmed by the suspended, dissolved, and total solids analysis. Conductivity was also low. The predominant dissolved species present are inorganic carbon and ammonia. The inorganic carbon is likely bicarbonate based on the solution pH, although some dissolved carbon dioxide is present. The ammonia is likely present as ammonium ion due to the lack of dissolved ammonia content. A small amount of organic carbon was found, it is likely present as the acetate ion since it was an early eluter on the ion chromatography analysis, plus some dissolved methane. The presence of organic acids is in agreement with the dominant presence of APB in the biogas and condensate samples. Sulfate ion was present, but surprisingly, no chloride, nitrate, phosphate or other ions were found. The anion/cation balance ratio calculates out to be near unity, once the dissolved carbon dioxide is subtracted, and the silicon converted to silicate ion.

It is expected that nutrient supplement will be needed for the artificial growth medium to support bacteria consortium growth during corrosion experiment. A nutrient broth (DIFCO Cat# 234000) was also analyzed. The typical nutrient broth medium contains 3 g of beef extract and 5 g of peptone per liter. The quantity of nutrient broth added to the recipe in this project will be determined by experiments with a goal to support bacteria consortium growth at the rate that each electrochemical corrosion experiment can be completed in about a week. A typical analysis of nutrient broth is presented in Table 16.

Table 16. The Major Composition of Nutrient Broth.

Analyte	Results
Total Carbon, wt%	41.01
Total Hydrogen, wt%	6.47
Total Nitrogen, wt%	14.07
Total Sulfur, wt%	0.43
Calcium, wt%	0.02
Iron wt%	0.002
Potassium, wt%	3
Magnesium, wt%	0.04
Sodium, wt%	1.83
Phosphorus, wt%	0.81

1.1.2.1. Major microbial compositions in condensate of raw biogas line

Microbiological analyses were performed on condensate sample to determine 1) the number of total (live and dead) heterotrophic bacteria and various corrosion causing bacteria (APB, IOB, and SRB), 2) the number and identity of live bacteria, and 3) the number and identity of bacterial spores. The number of total bacteria and total corrosion-causing bacteria including both dead and live bacteria in the condensate was determined by a genetic method (qPCR) by targeting specific genes present in the target microorganisms, and the data was reported as numbers per 100 ml of condensate sample. The number of live bacteria and spore was determined by inoculating condensate sample to appropriate bacteria medium and incubated at 37 ºC for a pre-determined time, and the data was reported as colony-forming unit (CFU) per 100 ml of condensate sample.

The condensate sample was detected to contain 1.62E+05 heterotrophic bacteria and 1.64E+04 APB per 100 ml of liquid; IOB and SRB were not detected in this sample by qPCR assays. No live bacteria were detected by the MPN test from the condensate sample statistically; however, the sample contained 50 live spores per 100 ml of liquid.

The EC50 toxicity of this sample is 49% at 15 min exposure, meaning that 50% of fibrio fischeri luminescent bacteria would be killed after exposure to condensate at 49% of concentration (assuming the undiluted condensate has concentration of 100%) for 15 min. In the MPN test, the dilution factor is 10 after inoculating 1 ml of condensate sample to 9 ml of TG growth medium. The 10-fold diluted condensate sample is apparently toxic enough and still inhibits the growth of any live bacteria potentially present in the sample. When condensate was inoculated to TG medium at a 20-fold dilution, both cultures under aerobic and anaerobic

conditions turned to turbid after 48 hrs and 72 hrs incubation, respectively. The DNA was then isolated for determination of dominant bacteria species in condensate cultures.

Identities of major microbial species in condensate of raw biogas line

DNA used for the determination of identities of major bacteria species in condensate sample was isolated from 1) condensate liquid directly; 2) positive growth cultures after inoculating condensate (1:20 dilution) to TG medium and incubating under aerobic and anaerobic conditions; and 3) from positive bacterial spore culture.

The attempt to amplify *ackA* and *buk* genes of APB and 16 sRNA gene of IOB from DNA isolated directly from condensate liquid was not successful; therefore the dominant profile of APB and IOB in condensate was not determined. The identities of heterotrophic bacteria and bacterial spores after growth in the medium were determined by targeting 16S rRNA genes.

Sixteen heterotrophic bacteria sequences were retrieved from the condensate sample without growing in the culture medium. Most of them were closely related to various species of *Bacillus* and *P. glucanolyticus* (Table 17). However, after the condensate sample was grown in culture medium aerobically and anaerobically, bacteria profile was changed significantly. Under aerobic condition, endosymbiotic bacteria of *Nilaparvata lugens* and *Herminiimonas saxobsidens* were enriched and became the dominant heterotrophic bacteria (Table 18). When condensate sample was grown in culture medium anaerobically, the most dominant bacteria were *Herminiimonas saxobsidens* (Table 19). *Herminiimonas saxobsidens* are Gram-negative, rod-shaped bacteria. Cells are motile by means of polar flagella, non-sporulating and strictly aerobic. It utilizes acetate, propionate, oxalate, succinate and malate.

The identities of bacterial spores isolated from condensate spore culture were also determined (Table 20). Of 28 bacterial spore sequences retrieved, all of them were identified either as *Bacillus nealsonii* (39%) or various other *Bacillus* species (61%).

Table 17. The Closest Relatives of Heterotrophic Bacteria Sequences Isolated Directly from Condensate Sample without Growth using Universal Primers Targeting 16S rRNA Gene

Closest relative in Genbank	Genbank accession No.	% Identity	Frequency
Bacillus nealsonii strain CT18	EU660368	99	1
Bacillus sp. ADP4II	FJ943257	99	1
Bacillus sp. CBD 118	DQ374636	98	1
Bacillus sp. P307	FJ943260	99	1
Bacillus sp. P308	FJ554672	99	1
Bacillus sp. S209	AB425363	99	1
Bacillus sp. U4A	FJ943261	98	1
Paenibacillus glucanolyticus	AB073189	99	2
Thiomonas intermedia K12	CP002021	99	4
Uncultured Rhodocyclaceae bacterium clone MFC-B162-H11	FJ393146	99-100	3

Table 18. The Closest Relatives of Heterotrophic Bacteria Sequences Isolated from Aerobic Culture using Universal Primers Targeting 16S rRNA Gene

Closest relative in Genbank	Genbank accession No.	% Identity	Frequency
Endosymbiont of Nilaparvata lugens clone M285	GU124500	99-100	6
Herminiimonas saxobsidens	AB512141	99-100	4
Uncultured bacterium clone 13S_1c03	FJ382922	100	1
Uncultured bacterium clone 13S_2c01	FJ382887	99	1
Uncultured bacterium clone L-4	AY625148	100	1

Table 19. The Closest Relatives of Heterotrophic Bacteria Sequences Isolated from Anaerobic Culture using Universal Primers Targeting 16S rRNA Gene

Closest relative in Genbank	Genbank accession No.	% Identity	Frequency
Endosymbiont of Nilaparvata lugens clone M285	GU124500	99	1
Herminiimonas saxobsidens	AB512141	99	10
Uncultured bacterium clone 13S_2c01	FJ382887	99	4
Uncultured bacterium clone L-4	AY625148	99	2
Uncultured proteobacterium clone Hmd24B60	EF196996	99	1

Table 20. The Closest Relatives of Bacterial Spore Sequences Isolated from Condensate Spore Cultures using Universal Primers Targeting 16S rRNA Gene

Closest relative in Genbank	Genbank accession No.	% Identity	Frequency
Bacillus nealsonii strain CT18	EU660368	98-99	10
Bacillus nealsonii strain TSWCSN40	GQ284408	99	1
Bacillus sp. ADP4II	FJ943257	99	5
Bacillus sp. P307	FJ943260	98-99	6
Bacillus sp. P308	FJ554672	97-99	5
Bacillus sp. U4A	FJ943261	98	1

Task 3 - Lab Evaluation of Microbial Corrosion under Simulated Field Conditions

Conditions for Modeling Experiments

Corrosion is mainly the consequence of electrochemical reactions, influenced by the physico-chemical environment at the metal surface, such as oxygen, salts, pH, redox potential, and conductivity, etc. MIC is electrochemical corrosion influenced by the presence or activities of microorganisms. Microorganisms growing at the metal surface form a biofilm and release chemicals or electrochemically active minerals, which alter the rates and types of electrochemical reactions at the biofilm-metal interface and result in various types of corrosions (e.g. pitting, crevice corrosion, under-deposit corrosion, and galvanic corrosion)

Biogas, generated through the anaerobic digestion from a variety of biomass sources, is one of the fastest growing renewable fuels. Within the past few years, there has been enthusiasm and investment in bioconversion of waste products into quality fuel, encouraged by political and public pressure to create and use "green" energy products. Local gas distribution companies (LDCs) are poised to take delivery of (interchange) cleaned biomethane into their existing lines for general distribution. However, based upon its source (dairy waste, landfill, wastewater sludge, agricultural waste, etc.), biogas may contain constituents that may affect pipeline integrity and system operations, and possibly impede pipeline safety. One such known constituent is bacteria associated with microbiologically-induced corrosion (MIC) in the biogas carried over from the anaerobic digestion process. However, the relationship between the numbers of specific MIC bacteria introduced into the pipe, internal pipe conditions, and severity of metallic pipeline corrosion has not been fully understood [12, 132] despite the fact that MIC has been long recognized as one of the major causes of corrosion of metal pipes [7, 23, 30, 31].

Raw biogas, saturated with moisture, contains hundreds of live bacteria (Table 4) including those known to cause MIC (e.g., APB, IOB, and SRB) from the anaerobic digestion process. The properties of condensate formed in gathering pipeline are affected by biogas composition (CO_2 and H_2S, etc) (Table 2), dissolved chemicals and nutrients from the anaerobic digestion process, which in turn, influence the dominant bacterial profile and microbial interactions with the metal surfaces. The potential impact of microbial corrosion on the integrity of metallic gathering pipelines must be addressed.

Consequences of the direct introduction of live microbes to metallic pipeline networks are unknown. A clear understanding of such potential integrity impact is crucial to safe introduction of biogas into metallic natural gas networks. In addition, a predictive tool to foretell MIC severity under field conditions is necessary for the effective management of pipeline integrity, especially for gathering lines containing the raw biogas.

Internal corrosion in raw biogas lines are affected by many factors or combination of factors including CO_2, H_2S, organic acid (mainly acetic acid), microbes, oxygen, chloride, etc. The focus on a single mechanism such as microbial corrosion is therefore not appropriate or practical in an actual pipeline system [133]. The development of the MIC model has to include other factors which may interact with microbial activities and their metabolites, and change electrochemical characteristics at the metal-biofilm interface. Parameters which affect microbial growth and activities will probably affect the onset of microbial corrosion (i.e. pitting), corrosion rate and severity. The parameters which may be included in the MIC model are nutrients (sulfate, fatty

acids, total dissolved solids, utilizable nitrogen), CO_2, H_2S, O_2, pH of condensate, salinity, alkalinity, dissolved iron, sulfide, chlorides, bicarbonates, ferrous and ferric iron, and temperature. The final parameters which were included in our preliminary MIC model were determined based on the results from Task 1 literature review and Task 2 sample analyses.

The major bacterial populations in raw biogas and condensate samples collected from gathering lines have been determined in Task 2, and the results used to formulate a major corrosion-related bacteria consortium to evaluate the microbial corrosion of metallic pipelines. In addition, chemical compositions and properties of typical condensate in raw biogas gathering line were thoroughly analyzed in Task 2. Therefore, the microbial corrosion evaluation was performed in synthetic condensate to mimic the field conditions typically found in raw biogas gathering line.

Microbial consortium

The accurate diagnosis of MIC requires combination of microbiological, chemical, and metallurgical analyses. The microbiological indicators include detection and quantification of various microorganisms on metal-liquid interfaces, especially corrosive bacteria in biofilms formed on metal surfaces.

qPCR assays indicated that most of raw biogas samples contained two types of corrosion-causing bacteria – APB and IOB (Table 4), and the condensate sample mainly contained APB. However, after the raw biogas samples were inoculated in TG media and incubated for 7 days at 37 ºC, qPCR on positive growth cultures indicated the presence of overwhelming number of APB in most of samples (data not shown). The identities of most sequences of heterotrophic bacteria or bacterial spores in raw biogas were closely related to the sequences of two bacteria genera, i.e. *Paenibacillus* and *Bacillus* (Table 5 to Table 8). Species determination of corrosion-related bacteria showed the presence of *Clostridium* and *Acidovorax* species, in addition to dominant *Paenibacillus* and *Bacillus* species (Table 9 to Table 13). IOB such as *Gallionella*, *Leptothrix*, and *Sphaerotilus* might not be a significant corrosion-related population in raw biogas samples. From the condensate sample, the dominant heterotrophic bacteria species were also closely related to *Bacillus* and *Paenibacillus* (Table 17 and Table 20), though after growth in TG medium, the dominant bacteria species changed to *H. saxobsidens*.

The majority of sequences isolated from this project are closely related to the sequences of genus *Bacillus*, followed by *Paenibacillus*, and *Clostridium*. Of all the sequences from these three genera, *Bacillus* sequences accounted for approximately 71.4%, *Paenibacillus* 24.3% and *Clostridium* 4.3%. The most representative *Bacillus* species is *B. licheniformis*. Therefore the proposed bacteria consortium which will be used in the corrosion experiment includes the enriched condensate culture (dominated by *H. saxobsidens*) and spiked *B. licheniformis.*

Artificial growth medium

The artificial growth medium (AGM) for corrosion experiments is based on the results of a thorough chemical analysis of the condensate sample and other nutrient requirements for bacteria growth such as trace elements and vitamins. In addition, nutrient broth will be added to the artificial medium during the corrosion experiment in attempt to support bacteria consortium growth at the rate that each electrochemical corrosion experiment can be completed in a

reasonable time. The quantity of nutrient broth added to the medium will be determined through experiments on growth curves under various conditions. The AGM recipe (minus nutrient broth) is as following (Table 21).

Table 21. Artificial Growth Medium Recipe for Corrosion Experiments

Macronutrients	Milligram per L
NH_4HCO_3	400 mg
$Na_2HPO_4 \cdot H_2O$	30 mg
K_2SO_4	20 mg
$CaCl_2$	9 mg
$FeCl_2 \cdot 4H_2O$	5 mg
$MgSO_4 \cdot 7\ H_2O$	3 mg

100X Trace Elements stock (add 10 ml to 1 L)	Milligram per 100 mL
$MnCl_2 \cdot 4H_2O$	180
$CoCl_2 \cdot 6H_2O$	270
H_3BO_3	50
$CuCl_2 \cdot 2H_2O$	24
$NaMoO_4 \cdot 2H_2O$	23
$ZnCl_2$	19

100X Vitamins stock (add 10 ml to 1 L) *from ATCC Vitamin Supplement Formulation Catalog No: MD-VS	Milligram per 100 mL
Biotin	0.2
Folic Acid	0.2
Pyridoxine Hydrochloride	1.0
Riboflavin	0.5
Thiamin	0.5
Nicotinic Acid	0.5
B_{12}	0.01
p-Aminobenzoic Acid	0.5
Thioctic Acid	0.5
Calcium pantothenate	0.5
Monopotassium phosphate	0.5

Filter-sterilize macronutrients, 100X trace elements stock, and 100X vitamins stock individually. Store at 4 ºC until use.

Preparation of Bacteria Consortium

Based on thorough analysis of biogas and condensate samples, the bacteria consortium for MIC modeling experiment consists of *B. licheniformis* (ATCC 14580) and the baseline bacteria populations enriched from the field condensate sample. The thorough analysis of enrichment culture of condensate sample indicated the dominant presence of *H. saxobsidens*.

Bacillus licheniformis (ATCC 14580) are Gram-positive, rod-shaped, motile, aerobic endospore-forming thermophilic bacteria that hydrolyze sugars fermentatively. Colonies of *B.*

licheniformis are round, surface smooth, flat, margin irregular and 2-4 mm in diameter. Ellipsoidal spores are produced in not swollen sporangia and placed centrally [129]. *B. licheniformis* is a common contaminant of dairy products; it is the most common aerobic spore-forming bacteria isolated from dairy farm [131]. The optimal growth temperature is around 50°C, though it can survive at much higher temperatures. *B. licheniformis* was purchased from American Type Culture Collection (ATCC14580) for this project.

Herminiimonas saxobsidens are Gram-negative, rod-shaped bacteria. Cells are motile by means of polar flagella, non-sporulating and strictly aerobic. It utilizes acetate, propionate, oxalate, succinate and malate ions. The enriched condensate culture will be used to provide baseline bacteria population in corrosion experiments.

Growth of *Bacillus licheniformis* under various conditions

The growth curve of B. licheniformis was first performed in Nutrient Broth (BD Cat# 234000). A 5% volume of overnight culture inoculums was inoculated into NB medium and the culture tubes were incubated aerobically or under 0.7% of O2 in headspace at 30 C with 100 rpm shaking. Absorbance/OD was measured at 600 nm periodically and the OD reading was plotted against time of incubation to generate a growth curve for the bacteria. The growth curves under various conditions are shown in Figure 5 through Figure 7. *B. licheniformis* growth curve in NB medium under aerobic condition showed an exponential growth phase between 5 and 13 hrs after incubation at 30 C (Figure 5).

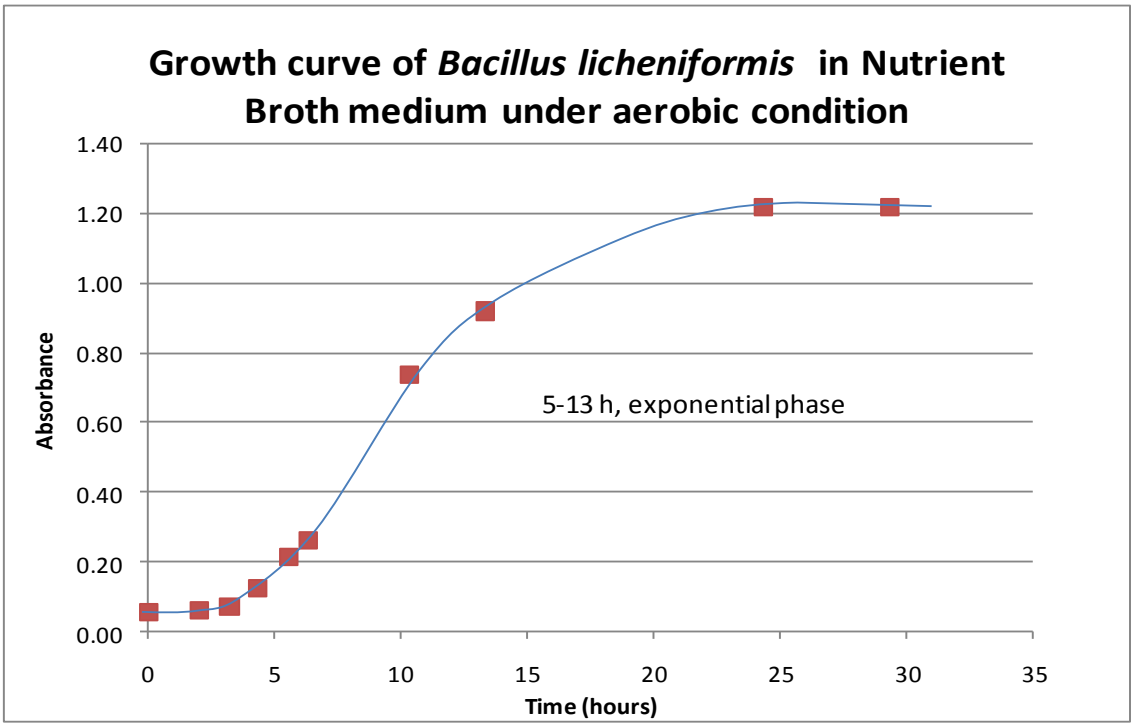

Figure 5. Growth curve of *B. licheniformis* in 0.8% nutrient broth under aerobic conditions.

Typical raw biogas line is not strictly aerobic or anaerobic; it contains an average of 0.7 Mol% of oxygen based on 12 raw biogas samples collected (Table 2). The presence of oxygen in the raw biogas line explains why the dominant bacteria isolated from the samples are aerobic bacteria or facultative anaerobic bacteria, such as *B. licheniformis*, *P. barengoltzii*, *H. saxobsidens* (aerobes), and *P. glucanolyticus* (facultative anaerobe). In order to mimic raw biogas line condition, the growth curve of *B. licheniformis* was repeated under conditions in presence of 0.7% of O_2 in headspace of culture bottles. The medium was purged with gas containing 94.3% N_2-5% H_2-0.7% O_2 to create the growth conditions for the bacteria. The growth curve under 0.7% of oxygen is shown in Figure 6. When aerobic *B. licheniformis* culture was incubated under 0.7% oxygen condition, *B. licheniformis* exhibited a longer lag growth phase (~12 hours), and reached lower OD readings (~0.3) within 24 hours of incubation at 30 ºC in 0.8% NB. The exponential growth phase was between 15 and 23 hours of incubation, about 10 hours later compared to aerobic conditions.

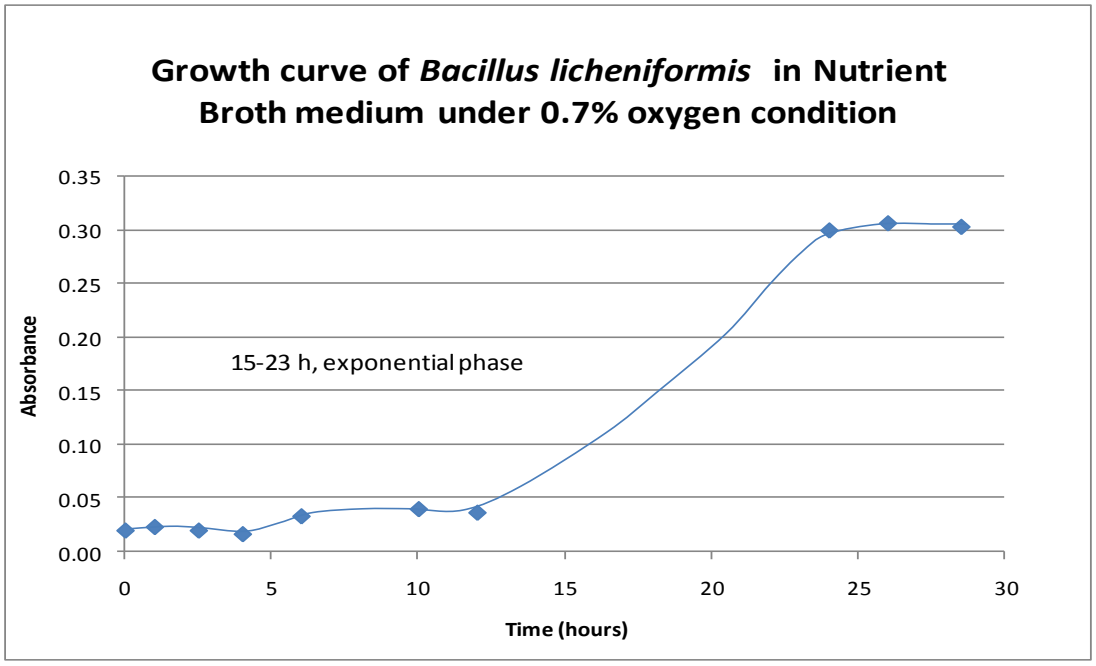

Figure 6. Growth curve of *B. licheniformis* in 0.8% nutrient broth under 0.7% oxygen.

When artificial growth medium (AGM) is used, it is necessary that AGM is supplemented with an appropriate percentage of NB in order to support bacterial consortium growth in corrosion experiments. The quantity of NB supplement required for growth of *B. licheniformis* was determined under 0.7% of headspace oxygen conditions at 30 ºC. The culture OD was monitored periodically to determine the growth potential at various concentrations of NB supplement. Under aerobic conditions, at least 0.3% of NB supplement to AGM was required to support the growth of *B. licheniformis*, with the highest OD (0.45) reached after 45 hours of incubation. However, under 0.7% O_2 condition, the highest OD was only 0.31 after 72 hours of incubation in AGM supplemented with 0.3% NB; the culture pH decreased from 7.6 at the beginning to 7.24 after 168 hours. A more detailed growth curve was determined for *B. licheniformis* in AGM supplemented with 0.3% of NB and under 0.7% O2 at 30 ºC in Figure 7. *B. licheniformis* showed

an exponential growth phase during 15-40 hours of incubation, with the highest OD (0.32) reached after 156 hours of incubation.

Therefore, *B. licheniformis* culture prepared in AGM supplemented with 0.3% of NB under 0.7% of headspace oxygen will be used to prepare bacteria consortium for corrosion experiments.

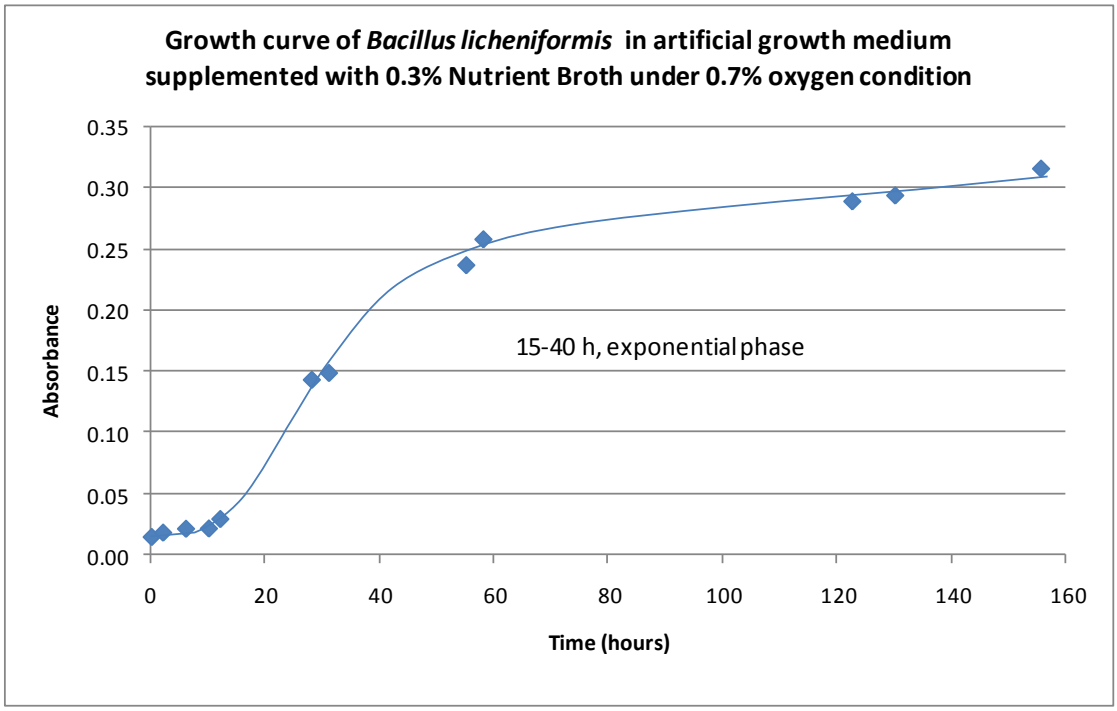

Figure 7. Growth curve of *B. licheniformis* in AGM supplemented with 0.3% nutrient broth under 0.7% oxygen.

1.1.3.2.1. Preparation of baseline bacteria culture from condensate sample

A 5% volume of field condensate sample was inoculated into AGM supplemented with 0.3% of NB and incubated under 0.7% of headspace oxygen at 30 ºC at 100 rpm shaking. Absorbance/OD was measured at 600 nm periodically and the OD reading was plotted with time of incubation to determine the exponential growth phase of the baseline bacteria population from the condensate sample. The field condensate sample showed an exponential growth phase between 15 and 30 hrs of incubation (Figure 8). The highest OD (0.14) was reached at 36 hours of incubation; then OD dropped to 0.12 after 156 hours of incubation.

1.1.3.2.2. Final bacteria consortium and growth medium for corrosion experiments

B. licheniformis and field condensate sample were grown in a large volume of AGM supplemented with 0.3% NB under 0.7% of headspace oxygen at 30 ºC at 100 rpm shaking. The cultures during exponential growth phase were collected and bacteria concentrations determined using the plate count method. The culture was then aliquoted and stored at 4 ºC until use. The bacteria consortium was prepared by mixing the *B. licheniformis* culture and the enrichment culture of field condensate at the ratio of 1:10 (bacteria number). Various concentrations of this bacteria consortium will be used in the electrochemical corrosion experiments.

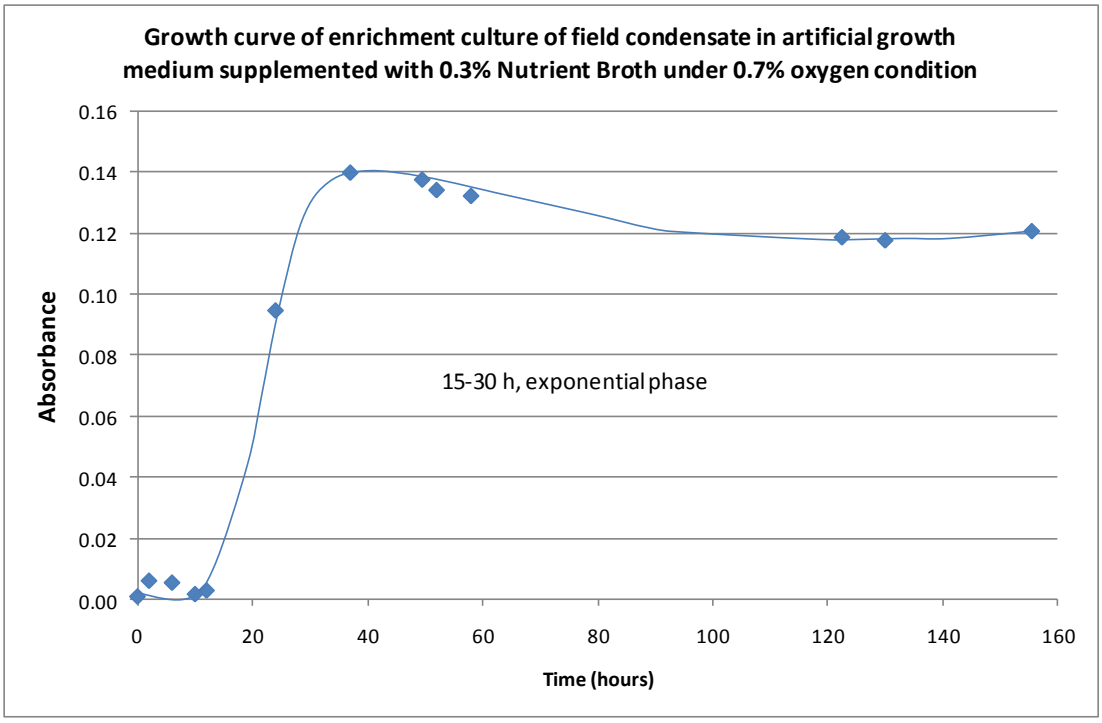

Figure 8. Growth curve of enrichment culture of field condensate in AGM supplemented with 0.3% nutrient broth under 0.7% oxygen.

The recipe of the AGM was shown in Table 21. The AGM was supplemented with 0.3% of NB to support bacteria consortium during electrochemical corrosion experiments. The pH and resistance were summarized in Table 22. Hydrophilic PVDF filter was used in salt bridge to prevent the bacteria consortium in anodic cell from entering cathodic cell.

Table 22. Properties of AMG.

	Resistance (KOhms)	pH
1X AGM	2.741	7.25
1X AGM with PVDF filter (0.1 µm)	2.958	
1X AGM + 0.3% NB	2.386	7.05
1X AGM + 0.3% NB with PVDF filter (0.1 µm)	2.563	

1.1.3.1. Instrumentation for Modeling Data Collection

Microbes are known to induce localized corrosion in deaerated conditions. Generally speaking, localized corrosion can be defined as the stabilization of a galvanic cell between a small anode that corrodes and a large cathodic surrounding area that is protected more or less. For microbiologically induced localized corrosion to occur, microbes such as SRB and APB not only have to initiate localized corrosion but also to stabilize it by sustaining a steady coupling current between small anodes and large cathodes [134]. Differential acidification is known to be one of the most powerful driving forces for localized corrosion [135]. Metabolites from microbial metabolism and the subsequent interaction between metabolites and corrosion products

(e.g., the precipitation of iron sulfides) induce a differential acidification between anodes and cathodes [136]. In addition, in the presence of CO_2 and H_2S, other effects can contribute to further local acidification and, especially, to the possible presence of conductive corrosion products [137, 138].

MIC has been studied mainly by electrochemical techniques that provide surface-averaged measurements. Techniques such as electrochemical impedance spectroscopy (EIS) or linear polarization give results, such as the uniform corrosion rate, that are not applicable to localized corrosion, including MIC [59]. Even electrochemical noise is not directly relevant to localized corrosion [139]. What is "noisy" is the random process of pit nucleation between electrodes of reduced size. However, a pit nucleus is not yet an actual pit. Depending upon repassivation statistics, this initial step of pit nucleation may lead either to stable growth of a few pits or just a grainy surface in overall uniform corrosion [134]. On large electrodes, neither pit growth nor uniform corrosion is noisy because both are related to stable direct currents. The technique applied in this Task uses a multielectrode analyzer, potentiostat/galvanostat, and micro pH probe to measure potential, galvanic current, corrosion rate, and pH at the biofilm/metal interface under the influence of activities of a consortium of microorganisms. The data will be used to develop a preliminary model for prediction of microbiologically-induced corrosion under simulated conditions in raw biogas pipeline.

Electrodes and electrochemical cells

The electrodes are constructed of type C1018 carbon steel wire purchased from California Fine Wire Company. The diameter of the wire is 2 mm, and the chemical composition is (in wt%): C 0.175%, Mn 0.75%, P 0.04%, S 0.05% with the balance Fe. The surface of anode exposed to liquid medium and bacteria is 3.14 mm^2. The cathode is made of coiled wire with exposed surface area being approximately 470 mm^2, resulting in a cathode to anode ratio of 150 to 1. The anode and cathode are insulated from the solution by heat shrink Teflon tubing and epoxy. Before starting an experiment, the electrodes are wet polished using silicon carbide (SiC) paper in sequence from 240-grit to 600-grit.

The electrochemical cell is a polycarbonate reaction vessel (2.5 L) with polycarbonate end plates to seal the vessel. The end plate has assorted ports for various electrochemical electrodes, pH probes, temperature probe, gas inlet and outlet for medium purging and headspace gas replacement, medium inlet and outlet for medium circulation, and inoculation ports [59]. Figure 9 and Figure 10 are top and side view of the anodic cell. The top and side view of the cathodic cell is shown in Figure 11. The anode electrodes are kept horizontal and facing up in the vessel since gravity has significant effect on bacterial attachment, and the horizontal surfaces facilitate bacterial adhesion [140, 141]. Membrane filters (0.2 µm) are placed at the gas inlet and outlet to protect the cell from external contamination. Figure 12 shows an assembled two-cell electrochemical system.

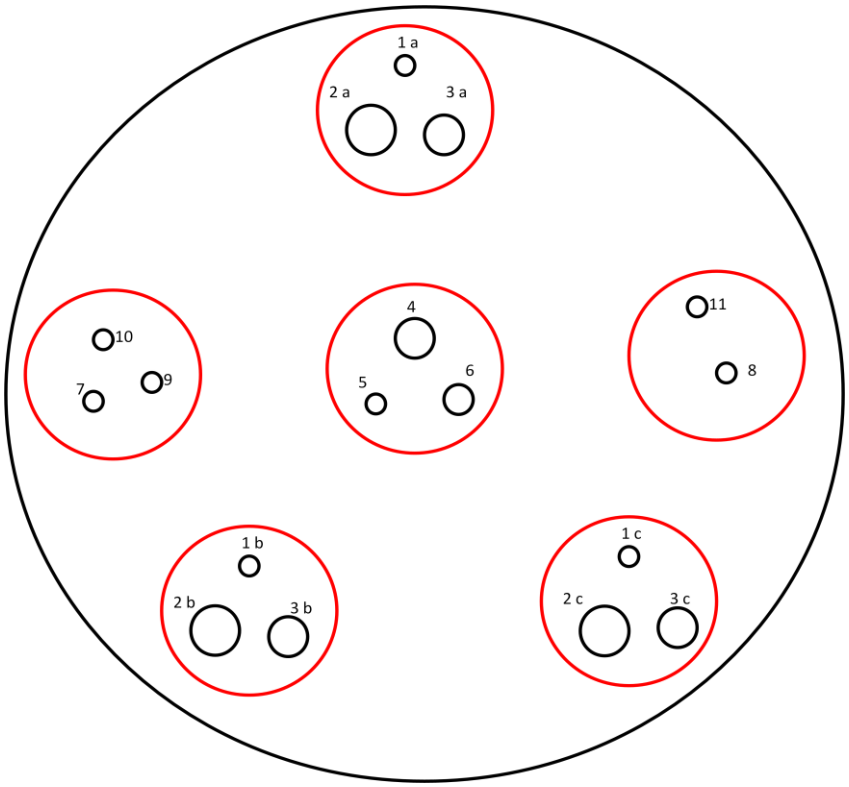

Figure 9. Top view of anodic cell.

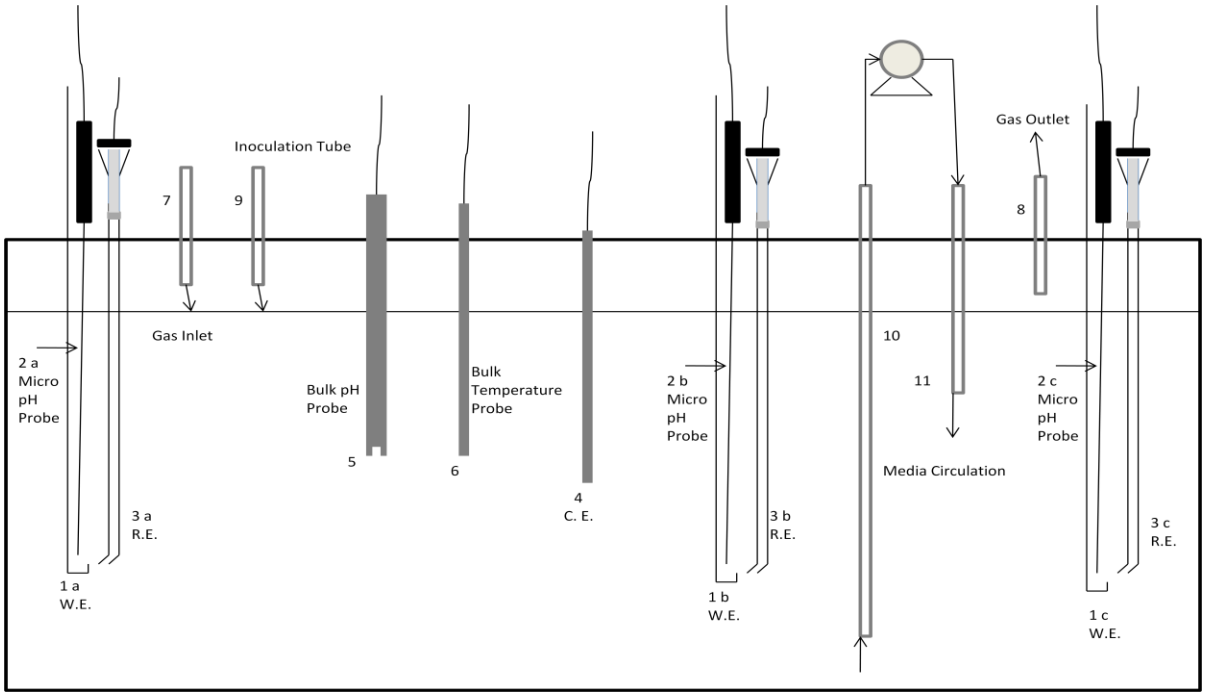

Figure 10. Side view of anodic cell. W.E.: working electrode; C.E.: counter electrode; R.E.: reference electrode.

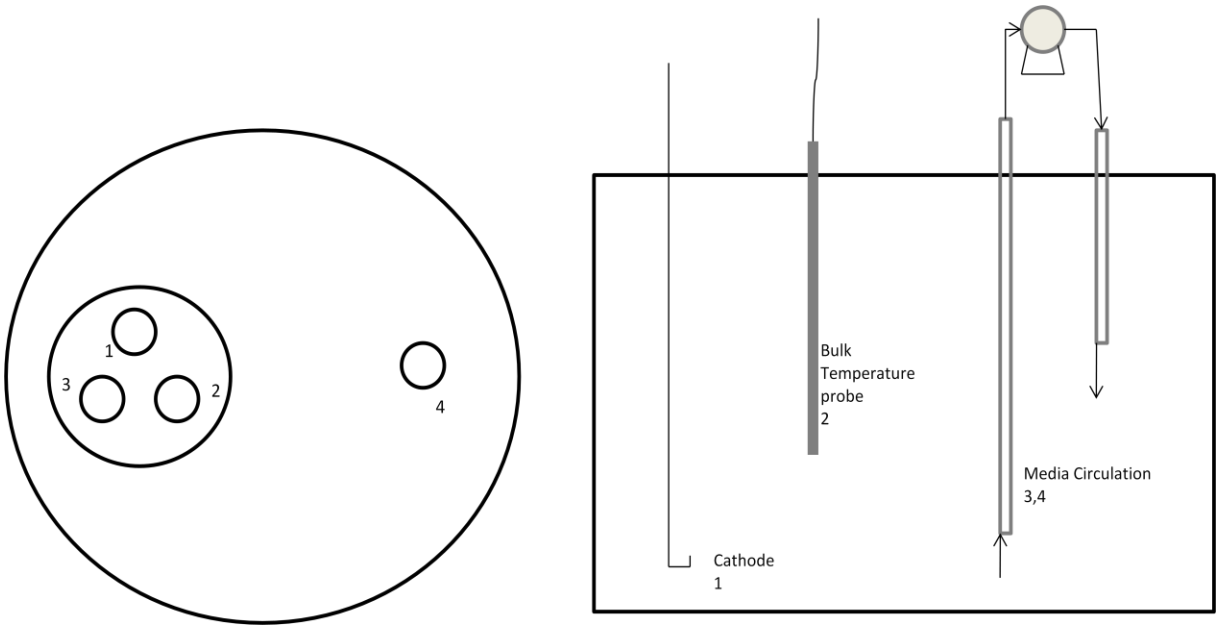

Figure 11. Top and side view of cathodic cell.

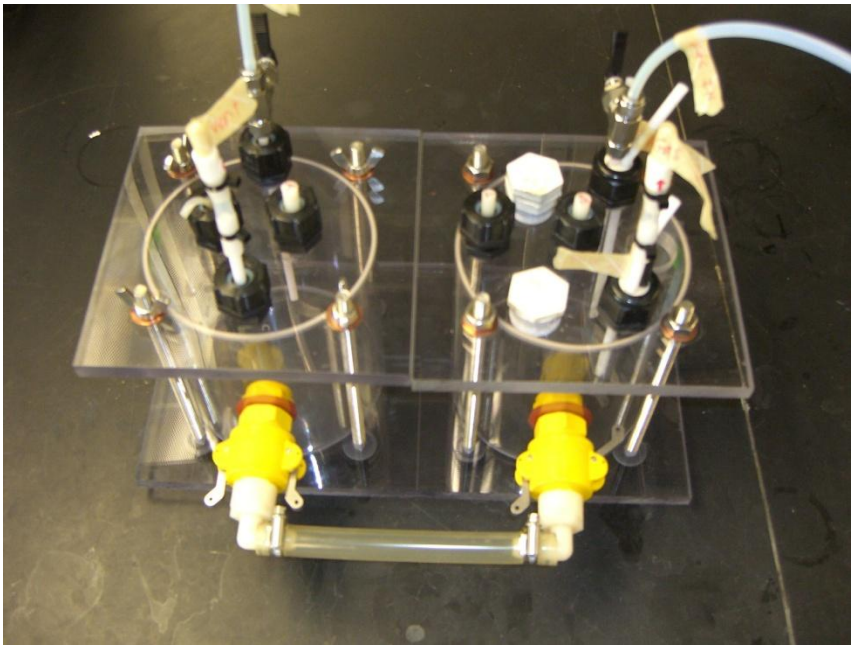

Figure 12. The assembled two-cell electrochemical system.

Electrochemistry and data acquisition

Figure 13 illustrates the setup and connections of electrochemical cells (anodic and cathodic cells) and the design of the electrochemical experiments for data collection. Three working electrodes (WE, anodes A1, A2, and A3) are immersed in AGM and bacteria culture in Cell A. The cathode coil is exposed to growth medium in Cell B without bacteria. An Ultra M micro

Combination pH probe (model PHR-146B, Lazar Res Lab) is placed to the close proximity to the surface of the A1 and A3 anodes to monitor the pH changes in the biofilm/metal interface. In addition, three Calomel reference electrodes (RE) are also placed in close proximity to each working electrode through the Reference Electrodes Bridge Tube. Cell A also contains a Graphite Counter Electrode (CE) and a pH probe for monitoring of pH of the bulk growth medium. Cell A and B are connected with a Salt Bridge filled with artificial growth medium and separated with a hydrophilic PVDF membrane filter (0.1 µm pore size) to prevent the migration of bacteria from Cell A to Cell B.

The small anode and large cathode electrodes are submerged under artificial growth medium in Cell A and B, respectively. Cell A is inoculated with an appropriate quantity of bacteria consortium and Cell B is abiotic. Anodes A1 and A2 are connected to the cathode through a Nano Corr S-18 Coupled Multielectrode Analyzer (Corr Instruments) for measurement of electrode potential and coupling galvanic current between the anode and cathode using CorrVisual software at 1-hour intervals. While A2 is constantly connected, A1 and its corresponding RE will be disconnected from the Analyzer twice a day and connected to CE through a potentiostat/galvanostat/ZRA (Gamry Instruments Reference 600) for measurement of corrosion rate on anodes by linear polarization without the influence of galvanic current (A1-RE-CE connection). The corrosion rate of A3 is measured by potentiostat/galvanostat/ZRA before and after the corrosion rate measurement of A1. Unlike A1, A3 will never be connected to a large cathode; therefore, the corrosion rate of A3 (as control) is expected to be significantly lower than that of A1.

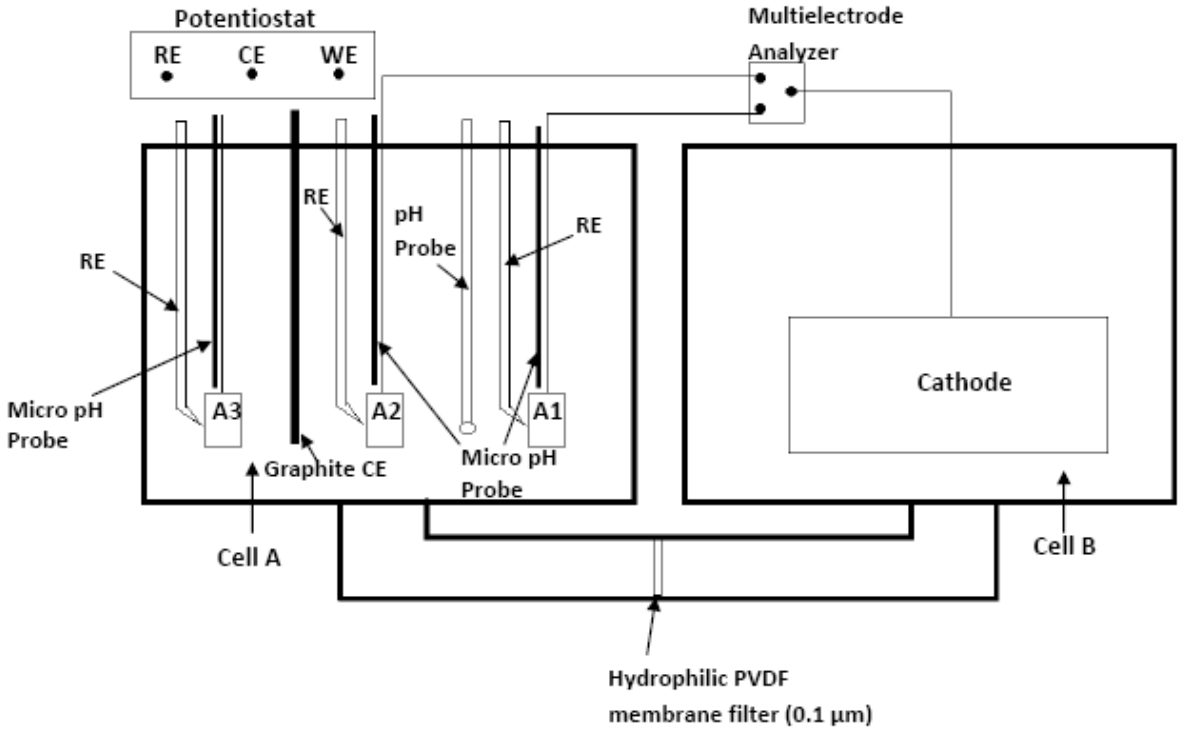

Figure 13. Setup and connections of electrochemical cells.

Electrochemical Measurement for Microbial Corrosion

The electrochemical cells are assembled as completely as possible to minimize the assembly steps after sterilization (autoclave at 121°C for 45 minutes). The cells are assembled first without anode and cathode electrodes, and dried for 2 hrs in an 80ºC oven. After the anode and cathode electrodes are inserted into their corresponding ports on the cell tops, the cells are purged with N_2 gas, sealed, and autoclaved at 121°C for 45 minutes. pH probes cannot be autoclaved, therefore they are sterilized by soaking in Sporicidin® Sterilizing and Disinfecting Solution (SSDS) overnight. Finally the autoclaved cells and pH probes are assembled in a laminar flow hood under ultraviolet (UV) light.

Both Cell A and B contain 2 L of sterile AGM supplemented with 0.3% of NB purged with filtered 94.3% N_2-5% H_2-0.7% O_2 gas mix for 60 minutes. Cell A will be inoculated with bacterial consortium, while Cell B is kept abiotic. A salt bridge filled with same growth medium connects Cell A and B, but a hydrophilic PVDF membrane filter (0.1 µm pore size) in the bridge prevents the migration of bacteria from Cell A to Cell B. The temperatures of Cell A and B are maintained at 30 ºC with heating tape. In addition, the headspace of Cell A is purged with gas mix daily to maintain 0.7% oxygen condition.

After inoculation of bacteria consortium into Cell A, the experiment is operated as a batch cell and a daily culture sample is taken to determine the concentration of planktonic bacteria using the plate count method with serial dilution in triplicate. When the concentration reaches 10^6 cells/ml, medium replacement in Cell A starts. 10% of culture volume in Cell A is replaced daily with fresh growth medium filtered through a 0.2-µm membrane. The medium in Cell A is circulated from bottom to top to avoid stratification. The medium composition in Cell A is analyzed periodically.

The electrochemical data and other data (e.g pH, chemical composition of medium) will be used to develop a preliminary model for prediction of corrosion rate under influence of bacteria consortium. At the end of the experiment, the anode is fixed with 2% glutaraldehyde buffered with 0.2 M sodium phosphate for 12 hours, dehydrated in acetone-distilled water series of 25%, 50%, 80%, and 100% acetone (10 minutes each), dried at 80 ºC for 10 minutes, and placed in a desiccator until inspection. The inspections include scanning electron microscope (SEM) for determination of the biofilm thickness and structure, pit shape and diameter, and EDS/EDX and Raman Spectroscopy for pit chemistry.

Task 4 - Preliminary MIC Model Development

During localized corrosion, a large number of phenomena occur over a large range of length and time scales. In a corrosion system influenced by microbial growth, for example, there are surface (at the metal-liquid interface) and homogeneous (in the liquid) parallel reactions taking place, as well as multiple chemical equilibriums between several species [142]. The situation is complicated by the bacterial metabolism that adds new chemical interactions, like nutrients uptake and products release. Some of these compounds can promote corrosion (e.g. acids, oxygen, and chloride ions); others can inhibit it (e.g. phosphates). Chemical species are transported to the metal/biofilm/liquid system by physical processes like molecular diffusion, convection, and migration of ions. The heterogeneity is three dimensional, with strong concentration gradients making the chemical environment at the metal surface much different from the environment in bulk liquid. There are also important differences between places covered with bacterial colonies and the noncolonized areas. All these localized interactions pose an important challenge for researchers.

Corrosion models can be used to understand the complex relationships among multiple variables and to allow for corrosion rate prediction. Yet, appropriate models applicable to predict MIC damage are not readily available. Risk based models [143, 144] have been developed to predict MIC in pipeline and nuclear systems. However, such models often do not involve *MIC mechanisms* and thus, the time dependent nature of the corrosion rate cannot be predicted. Picioreanu and van Loosdrecht developed a mathematical model was based on reaction/transport principles [142]. The model incorporated system mass balances including diffusion, migration, and reaction terms for all relevant chemical species (O_2, Fe^{2+}, Fe^{3+}, HO^-, H^+, Na^+, and Cl^-), biofilm characteristics (e.g., surface coverage, density, thickness), and the electroneutrality condition to onset of localized corrosion. Mechanistic models [145, 146] developed for oil and gas production systems may not be applicable to the biogas systems due to different microbial populations and MIC mechanisms.

While the use of empirical modeling is often the only practical approach in corrosion modeling development, the goal of Task 4 is to develop a preliminary mechanistic MIC model for application to raw biogas pipelines that is based on well-established physico-chemical and engineering principles. The preliminary model developed under simulated field conditions posed by a consortium of dominant corrosion-causing bacteria from anaerobic digestion will lay a foundation for further improvement by including more complex interactions, allowing futureMIC prediction to be made in broader conditions.

The basic equation to describe the transport process of corrosive species at the biofilm/metal interface is the Nernst-Plank equation:

$$\frac{dc_j}{dt} - \nabla \cdot N_j + \sum R_k = 0 \qquad (1)$$

coupled with the equation of electroneutrality:

$$\sum z_j c_j = 0 \qquad (2)$$

where $N_j = (D_j \nabla c_j) + z_j u_j c_j \nabla \varphi + v c_j$ is flux and z_j, D_j, u_j and c_j are valence, diffusivity, mobility and concentration of the jth species, respectively. φ is electrostatic potential in solution. R_k is k^{th} irreversible reaction rate of the j_{th} species. v is velocity of the solution.

The above differential equations and the corresponding boundary conditions will be solved to determine the changes of the concentrations of each species and the rate of the pipe steel corrosion caused by corrosive species including microbial reactions [147-155].

Experiments for data collection of modeling parameters are being performed under simulated raw biogas gathering line conditions. The artificial condensate liquid was synthesized based on the comprehensive analysis of the field condensate sample to mimic the chemical compositions, major corrosive bacteria species, pH, salinity, conductivity, redox potential, etc. The effect of activities of bacteria consortia on the corrosion rate of steel can be measured from current flows between the small electrodes and the large electrode. The counter and reference electrodes are used to measure linear polarization resistance and thus corrosion rate at each electrode surface. A micro-pH electrode is used to measure pH near the electrode surface.

The prevailing variables that control the microbial reactions and corrosion process such as concentration and composition of bacteria consortium, pH, temperature, and condensate composition and properties are captured in the experimental setup. The variation of these variables against time is measured, and the results used to construct the preliminary mechanistic model to predict the rate of MIC posed by corrosion-causing bacteria in raw biogas on metallic pipelines.

Task 6 – Conduct Literature Search (Gap Analysis) for Material Compatibility Data

Biogas Constituents

The chemical compositions of biogas that have been identified in Task 1 together with their physical and chemical properties have been reviewed A literature search was performed to collect the data relating these compounds to the non-metallic materials that have been selected in Task 5 for further compatibility analysis.

Chemical Compositions of Biogas

The chemical composition of biogas/biomethane was evaluated in Task 1 by tabulating the data from a literature search and previous project sample analysis. The data set of this study is large and comprehensively covers the sources of biogas/bomethane, including those from landfill and dairy farms that will be introduced to the gas industry. Since there are limit data for waste water, it is not included in this study.

The gas compositional impact was performed using the data sets for the raw and processed dairy and landfill gas as presented in the Task 1 report. The data were summarized and basic statistic calculations were made including determining the maximum, minimum, average, median, and 90% mode concentrations, along with the standard deviation and the average deviation from the mean, see Table 23 to Table 26. Each gas constituent was ranked using an equation that took into account the 90% mode concentration, the number of samples analyzed and the number of positive hits, according to the following equation:

$$Rank = (90\%\ Mode\ Concentration) * (\#\ of\ Hits)/(\#\ of\ Sample\ Analyzed)$$

(1)

The equation results were categorized using the scoring scheme shown in Table 27. Constituents with zero hits or only one hit were automatically assigned a rank of "0".

Overview of the Biogas Constituents and the Potential Impacts on the Gathering Network Materials

The components in biogas are categorized into ten subgroups as below:

1. Non-corrosive inorganic gases
2. Corrosive inorganic gases
3. Alkanes
4. Cycloalkanes
5. Alkenes
6. Aromatic hydrocarbons
7. Organosulfur compounds
8. Halocarbons
9. Organosilicones
10. Metals

Non-corrosive Inorganic Gases

Helium, hydrogen and nitrogen are the three non-corrosive inorganic gases that have been identified above detection level in the biogas from landfill and dairy farms. These gases do not react with the plastics or elastomers, but can permeate into them.

Corrosive Inorganic Gases

The corrosive gases that have been identified above detection level in the biogas from landfill and dairy farms include:

1) Carbon dioxide (CO_2)

CO_2 is non-corrosive in the absence of water. It forms carbonic acid (H_2CO_3) when it dissolves in water:

$$CO_2 + H_2O \rightleftharpoons H_2CO_3$$

The majority of the CO_2 is not converted into carbonic acid, it remains as CO_2 molecules. In aqueous solution carbonic acid only exists in equilibrium with carbon dioxide, and the concentration of H_2CO_3 is much lower than the dissolved CO_2 concentration. At a given temperature, the composition of an aqueous solution of CO_2 is determined by the partial pressure of CO_2 (P_{CO_2}) above the solution. The equilibrium species in a CO_2 aqueous solution and the associated CO_2 partial pressure and pH are summarized in Table 28.

Carbonic acid is a weak acid, but it promotes corrosion of steel, especially if hydrogen sulfide and oxygen are present. Most of the common plastics and elastomers are resistant to carbonic acid.

2) Carbon monoxide (CO)

Carbon monoxide (CO), also called carbonic oxide, is a colorless, odorless and tasteless gas which is lighter than air. It is highly toxic to humans and animals in higher quantities.

Carbon monoxide is produced from the partial oxidation of carbon-containing compounds; it forms when there is not enough oxygen to produce carbon dioxide (CO_2), such as when operating a

stove or an internal combustion engine in an enclosed space. With the presence of oxygen, it will be eventually oxidized to carbon dioxide.

3) Oxygen (O_2)

Oxygen is an active gas and reacts with many materials. One of the most detrimental effects of oxygen in biogas is that it promotes the oxidation of some species such as hydrogen sulfide and sulfur dioxide and form sulfur trioxide (SO_3). When water vapor is present in the gas phase, SO_3 reacts with water forming sulfuric acid which can be condensed out from gas phase once the dew point temperature is reached. The concentration of the sulfuric acid in the condensate varies from dilute to highly concentrated depend on the concentration of SO_3 in the gas phase. Sulfuric acid is a strong acid and very corrosive to many metallic and nonmetallic materials. Many plastics and elastomers are not resistant to sulfuric acid, especially the concentrated sulfuric acid which is highly oxidizing and corrosive.

4) Hydrogen sulfide (H_2S)

H_2S is a colorless, very poisonous, flammable gas with the characteristic foul odor of rotten eggs. It often results from the bacterial breakdown of organic matter in the absence of oxygen, such as in swamps and sewers (anaerobic digestion).

H_2S is somewhat soluble in water and acts as a weak acid, and reacts with metal ions to form metal sulfides causing metallic corrosion. The direct impact of H_2S on the non metallic polymer materials is not significant, but forming sulfuric acid from H_2S with the presence of oxygen is more detrimental to most of the plastics and elastomers.

5) Sulfur dioxide (SO_2)

SO_2 is a colorless, toxic gas. It is soluble in water and the aqueous solution of sulfur dioxide is referred to as sulfurous acid:

$$SO_2 + H_2O \rightleftharpoons HSO_3^- + H^+$$

SO_2 can be oxidized within airborne water droplet forming sulfuric acid which is very corrosive.

6) Ammonia (NH_3)

Ammonia is a colorless gas with a characteristic pungent odor. It dissolves in water and form a moderately basic aqueous solution.

Alkanes

In addition to methane which is the major component in biogas, the other alkanes from C2 to C13 are identified at ppm level in biogas. They are saturated organic hydrocarbon compounds, with the atoms linked together exclusively by single bonds without cyclic structure. The general physical properties of C1 to C13 alkanes are summarized in Table 29.

Under ambient conditions, C1 to C4 alkanes are gaseous, and C5 to C13 are liquids. In general, alkanes are relatively low reactive because the saturated C-C single bonds in their molecular chains are stable and cannot be easily broken.

The major impacts from these alkanes on the non-metallic pipeline infrastructure materials include the absorption/desorption of lighter alkane gases; and solvation/dissolution effect by the heavier alkane liquids which have been described in Task 5 discussing the chemical resistance of materials. These impacts are the results of the physical interaction between the alkanes and the pipeline materials, and determined by their structural similarity, i.e. the more similar the two materials are, the larger interaction they have. Solubility parameters are often used to predict the

degree of the interaction between materials, and will be discussed in the next section on the compatibility analysis.

Cycloalkanes

Cyclopentane and cyclohexane are the two cylcoalkanes that have been identified in the landfill gas at ppm level.

Cycloalkanes, are types of alkanes which have a ring chemical structure of their molecules. Cycloalkanes consist of only carbon (C) and hydrogen (H) atoms and are saturated. Cycloalkanes with a single ring are named analogously to their normal alkane counterpart of the same carbon count, e.g., cyclopentane, cyclohexane. The larger cycloalkanes, with greater than 20 carbon atoms are typically called cycloparaffins.

Cyclopentane and cyclohexane are liquids at ambient condition with relatively low boiling point; they are used as nonpolar solvent. Their general physical properties are listed in Table 29. They are chemically very stable like alkanes, and the major impacts on polymers are the solvation effect.

Alkenes

Only ethene and propene are identified in the landfill gas at ppm level. Ethene and propene are the simplest alkene, which are unsaturated hydrocarbon containing C-C double bonds. They are gaseous at ambient conditions, and are more reactive than alkanes but still relatively stable. The general physical properties of ethene and propene are listed in Table 29.

There is not many information in the open literature about the impacts of ethene and propene on plastic materials and elastomers. The potential effect may be on the absorption of ethene or propene by the polymer materials.

Aromatic hydrocarbons

Benzene, toluene, ethylbenzene, xylene (BTEX), styrene and C3-benzene are identified in the landfill gas at ppm level. Benzene is the major BTEX constituent. Tolune, ethylbenzene, xylene, styrene and C3-benzene are substituted benzenes.

They all contain a single benzene ring, and are liquid at ambient conditions and generally used as solvents. Their general physical properties are listed in Table 29. Their major impacts on polymer materials are solvation.

Organosulfur compounds

Many organic sulfur compounds including organic sulfides, mercaptan, thiophene, thiophane, and others have been identified in the biogas at ppm level. Methyl mercaptan and dimethyl sulfide are the major compounds. Table 30 summarizes the general physical properties of the organosulfur compounds that have been identified in the biogas. Except carbonyl sulfide, the above organosulfur compounds are liquid at ambient conditions. There are very limit data in the literature about the impact of organosulfur compounds on the polymer materials.

1) Mercaptans (Thiol)

Mercaptans, also called thiol, are the compounds that contain the functional group composed of a sulfur-hydrogen bond (-SH). Mercaptans and alcohols have similar molecular structure. Due to the small electronegativity difference between sulfur and hydrogen, an S-H bond is less polar than the hydroxyl group.

Many mercaptans have strong odors resembling that of garlic. The odor of mercaptans is often strong and repulsive, particularly for those of low molecular weight. They are used as odorant in natural gas distribution systems.

Mercaptans show little association by hydrogen bonding, with both water molecules and among themselves. Hence, they have lower boiling points and are less soluble in water and other polar solvents than alcohols of similar molecular weight.

Mercaptans are easily oxidized, e.g. in the presence of base, they are oxidized by reagents such as iodine to form an organic disulfide. Oxidation by more powerful reagents yields sulfonic acids. Mercaptans are more acidic compared to the alcohols.

2) Organic sulfides

Organic sulfides, or thioethers, are characterized by C-S-C bonds. They have strong foul odor and are volatile. They are easily oxidized to sulfoxides (R-(S=O)-R) which can be further oxidized to sulfones ($R\text{-}S(=O)_2\text{-}R$)

Disulfides contain C-S-S-C, with a covalent sulfur to sulfur bond which is used in polymer chemistry for the crosslinking of rubber.

3) Thiophene and Thiophane

Thiophene is a heterocyclic compound consisting of a flat five-member ring, it is considered aromatic. It is a colorless liquid at room temperature. Upon hydrogenation, thiophene gives tetrahydrothiophene, which is also called thiophane.

Thiophane is the saturated thiophene. It is a volatile, clear, colorless liquid with strong unpleasant odor. It is occasionally used as an odorant in natural gas.

Halocarbons

Halocarbon compounds are the organic compounds containing covalently bonded fluorine, chlorine, bromine, or iodine. Trace chlorocarbons and chlorofuorocarbons have been identified in the biogas from landfill and dairy farms, and their general physical properties are listed in Table 31.

1) Chlorocarbons

Chlorocarbons are organic compounds containing at least one covalently bonded chlorine atom. They are typically denser than water, and have stronger intermolecular interactions than hydrocarbons resulting in a higher boiling point.

2) Chlorofuorocarbons (CFC)

A chlorofluorocarbon (CFC) is an organic compound that contains carbon, chlorine, and fluorine. Many CFCs have been widely used as refrigerants, propellants (in aerosol applications), and solvents. In general they are volatile, but less so than parent alkane due to stronger intermolecular interactions induced by halides. The densities of CFCs are higher than the corresponding alkanes and correlates with the number of chlorides.

Organosilicones

Organosilicon compounds are organic compounds containing carbon silicon bonds (C-Si). Siloxane is one type of organosilicon compounds consisting of alternating silicon and oxygen bonds (Si-O) with side carbon chains (R) attached to silicon atoms. Siloxanes can be found in products such as cosmetics, deodorant, defoamers, water repelling windshield coatings, food additives and some soaps, and they occur in landfill gas.

Trace organosilicones including Hexamethyldisilane, Octamethylcyclotetrasiloxane, Decamethylpentasiloxane and Decamthyltetrasioxane have been identified in the landfill gas. The general physical properties of these compounds are listed in Table 32.

Metals

Trace metal elements including Antimony, Zinc, Arsenic, Mercury, Copper and Molybdenum have been identified in biogas, and are present as organometallic compounds. Based on the available information in the literature, it is not likely that these compounds will significantly impact the non-metallic pipeline materials, especially at the levels that have been identified in biogas.

Solubility Parameter

Solubility parameter is normally used to predict the interaction between materials and can provide a good indication of the solubility of one material in another. The general theory is the materials with similar values of solubility are likely to be miscible.

The Hildebrand solubility parameter is the square root of the cohesive energy density:

$$\delta = \sqrt{((\Delta H_v - RT)/V_m)} \quad \textbf{(2)}$$

The cohesive energy density is the amount of energy needed to completely remove unit volume of molecules from their neighbors to infinite separation (an ideal gas), which is equal to the heat of vaporization divided by molar volume. In order for a material to dissolve, these same interactions need to be overcome as the molecules are separated from each other and surrounded by the solvent.

The Hildebrand solubility parameter provides useful predictions for non-polar and slightly polar systems without hydrogen bonding, particularly for polymer/solvent interactions to predict the solubility and swelling of polymers by solvents. For polar molecules, Hansen Solubility Parameters which is the dimensional solubility parameters are used.

The solubility parameters of the organic constituents in biogas and the polymers that have been selected in Task 5 for compatibility analysis are collected in order to evaluate the interaction between gas constituents and pipeline materials and assess the impact from these components on the material integrity. The Hilderbrand solubility parameters for biogas and the selected polymers are listed in Table 33 and Table 34 respectively, including the dada published in the handbooks and those calculated using Equation (2). Those chemicals that don't have the solubility parameter or the necessary property data in the handbooks for calculation are given "NA" in the table. The chemicals and their property data used for the calculation by Equation (2) are listed in Table 35 with the calculation results.

Compatibility Analysis

The compatibility of the polymers with each chemical constituent in the biogas is assessed by calculating the difference of the solubility parameter between the polymer and a chemical:

$$\Delta\delta = ABS(\delta_{polymer} - \delta_{chemical}) \quad \textbf{(3)}$$

Since the solubility parameter for a polymer normally is within a range due to the variation of the formulation, $\Delta\delta$ is calculated at the minimum, maximum and average for each polymer. The impact of a chemical on a polymer is determined by the minimum $\Delta\delta$ and categorized into five levels of rating from "1" to "5" as below:

- Severe (5): $0 \le \Delta\delta \le 0.5$
- Moderate to severe (4): $0.5 < \Delta\delta \le 1$
- Moderate (3): $1 < \Delta\delta \le 2$
- Minor to Moderate (2): $2 < \Delta\delta \le 3$

- Minor (1): $\Delta\delta>3$

For chemicals without solubility data, they are given a rating of "5" since the risks from their impact on the pipeline materials are unknown. The results of the compatibility analysis are summarized in Table 36, Table 37, Table 38, Table 39 and Table 40 respectively for the two plastic pipe materials (PE and PA12) and four elastomeric materials (SBR, NBR, CR and SI) with the chemicals in "Group 3" to "Group 9". The rating for the chemicals with unknown solubility data are highlighted with red in the table, which will be further discussed in the gap analysis in this section.

The compatibility of the plastics and elastomers discussed above with the inorganic materials in "Group 1", "Group 2" and "Group 10" is assessed based on their chemical resistance that has been reviewed in Task 5. The impact is also categorized into the above five rating levels. The overall risk is assessed by the impact from each chemical (Rating) and the rank of its concentration level in the gas (Weight). The score of the risk is calculated as:

$$Risk\ Score = Rating * Weight$$

The data (rating, weight and risk score) are summarized in the tables (from Table 41 to Table 48) for the two plastic materials (PE and PA12) and four elastomers (SBR, NBR, CR and SI) in the raw and processed gases (landfill and dairy):

- Table 41: PE and PA12 in Raw Landfill Biogas
- Table 42: PE and PA12 in Processed Landfill Biogas
- Table 43: SBR, NBR, CR and SI in Raw Landfill Biogas
- Table 44: SBR, NBR, CR and SI in Processed Landfill Biogas
- Table 45: PE and PA12 in Raw Dairy Biogas
- Table 46: PE and PA12 in Processed Dairy Biogas
- Table 47: SBR, NBR, CR and SI in Raw Dairy Biogas
- Table 48: SBR, NBR, CR and SI in Processed Dairy Biogas

The compatibility of the chemicals with the six polymers is mapped in Figure 14and Figure 15 for the biogas from landfill and dairy farm respectively. The total risk score of each material is plotted in Figure 16. PA12 has better performance compared to PE. NBR is relatively better compared to the other three elastomers, but its overall risk score is still on the high end. The total risk score is significantly reduced in the processed landfill biogas since many chemicals are removed or their concentrations are lowered by the gas cleaning process, but the risk scores are still considerably high for all the materials.

The total risk score in dairy gas is much lower compared to landfill gas because there are fewer chemicals in it. In raw dairy gas, the overall performance of PE is similar to PA12, and SI is relatively better compared to SBR, NBR and CR. The impact from the processed dairy gas is reduced to a lower level for all the materials due to the removal of the major harmful chemicals.

Compatibility with Raw and Processed Landfill Biogas

The potential risk from each chemical group on the materials is assessed by adding up the risk score of each chemical in this group. Figure 17 shows the risk score of the ten chemical groups in raw and processed landfill biogas for the two plastics (PE and PA12) and four elastomers (SBR, NBR, CR and SI). There is no impact from G1 (non-corrosive inorganic gases) and G10 (metals) on any of the materials. G3 (alkanes), G7 (organosulfur compounds) and G8 (halocarbons) are the top three groups that have important impact on plastic and elastomeric materials. The next two chemical groups having

intermediate impact are G6 (aromatic hydrocarbons) and G9 (organosilicones). The risk score in G2 (Corrosive Inorganic Gases), G4 (Cycloalkanes) and G5 (Alkenes) are relatively low.

1) Corrosive Inorganic Gases (G2)

Carbon dioxide and hydrogen sulfide are the two major corrosive components in raw landfill gas and their concentrations are ranked as severe. Oxygen and sulfur dioxide are at moderate level. As shown in Figure 17, the risk score of this group is relatively low compared to the organic chemicals such as alkanes (G3), organosulfur compounds (G7) or halocarbons (G8). PE has better performance due to its chemical resistance to most of the corrosive species in this group. But hydrogen sulfide and sulfur dioxide have deleterious effects on PA12 and the elastomers, and they are the important corrosive species in this group that impact the material performance except for PE. The concentration of the corrosive species is reduced by the gas cleaning process, but it is still at the moderate level in the processed gas which gives minor to moderate risk to PA12 and the elastomers (SBR, NBR, CR and SI).

2) Alkanes (G3)

Alkanes have significant impact on PE and most elastomers, especially the heavy alkanes with more than six carbons in the molecular chain which have higher concentration in landfill gas and also have a similar cohesive energy (solubility parameter) as the plastics and elastomers. PA12 has a better resistance than PE to alkanes because it has a larger cohesive energy. The gas cleaning process reduces the concentration levels of the chemical constituents in landfill gas and the total risk score in this group is reduced accordingly. However, the total risk score in this group still remains the highest compared to the rest of chemical groups in the processed gas indicating that the cleaning process cannot reduce the heavy alkanes in landfill gas to the levels that their impact on pipeline materials becomes insignificant.

3) Cycloalkanes (G4)

The compounds in this group have larger impact on most of the materials except PA12. But there are only four compounds that have been identified in landfill gas and their concentration levels are moderate, thus the overall risk of this group is relatively low. The concentrations of these compounds are reduced in the processed gas, but the cleaning does not completely eliminate the impacts from this chemical group.

4) Alkenes (G5)

There are three compounds in this group (ethene, propene and pentene) that have been identified in landfill gas, and their concentrations are at the level of “minor to moderate”. The impacts from these chemicals on the polymers are unknown due to lack of the relevant data in literature. In the processed landfill gas, ethene and pentene cannot be reduced below the detectable level.

5) Aromatic Hydrocarbons (G6)

All of the aromatic hydrocarbons in landfill gas have larger impact (4 or 5) on the plastics and elastomers. But their concentration levels are” moderate (3)” or “moderate to severe (4)” in raw landfill gas, therefore the perceived risk in this group is intermediate. The gas cleaning process helps to reduce their concentration levels, but the majority of the chemicals in this group still remain in the processed landfill gas at ppm level.

6) Organosulfur Compounds (G7)

There are many organosulfur compounds in landfill gas. Many of the compounds in this group have larger impact (4 or 5) on the polymer. Some of the other compounds in this group do

not have enough information in literature to evaluate their compatibility with the polymers. The total risk score for this group is high because of the larger impact or uncertainty.

The gas cleaning process removes many chemicals in this group including those with unknown compatibility. The risk score in the processed gas is significantly reduced due to the removal of the compounds with larger impact or uncertainty.

7) Halocarbons (G8)

Similar as G7, there are many halocarbon compounds in landfill gas, and many of them have larger impact or unknown compatibility. The risk score for this group is high in raw gas but it is significantly reduced in processed gas due to the removal of many compounds with larger impact or uncertainty.

8) Organosilicones (G9)

There is no compatibility data for all the chemicals in the organosilicones (Group 9) because of a lack of literature information for this type of chemical. The concentration levels of these chemicals are moderate in raw landfill biogas and they are basically removed after cleaning. The only chemical in this group that remains in the processed gas is Octamethylcyclotetrasiloxane (D4) and its concentration is not significantly changed by the cleaning.

Compatibility with Biogas from Dairy Farm

Biogas from dairy farms has much less chemicals compared to that gas obtained from landfill. Alkenes (G5), halocarbons (G8) and organosilicones (G9) have not been identified in dairy gases. Using the same approach as the compatibility analysis for landfill, the risk score for the compounds in each chemical group in dairy gas are added up and plotted in Figure 18 for the plastics (PE and PA12) and elastomers (SBR, NBR, CR and SI) respectively. It appears that G7 (organosulfur compounds) has the highest risk score for any plastics or elastomers. The compounds in G2 (inorganic corrosive gas), G3 (alkanes) and G6 (aromatic hydrocarbons) also have considerable impact on some of the materials.

1) Corrosive Inorganic Gases (G2)

Ammonia is an additional inorganic species found in the dairy gas, as compared to landfill gas. Its concentration level can be relatively high compared to the majority of the compounds in dairy gas. However, its impact is limited on the specific material, i,e., SBR is not compatible with ammonia. The performance of the other materials with the chemicals of this group in dairy gas is about the same as landfill.

The gas cleaning process reduces the concentrations of hydrogen sulfide, sulfur dioxide, and ammonia below detectable levels. Therefore, the impact from the corrosive compounds in this group is significantly reduced in the processed gas.

2) Alkanes (G3)

The total risk score of this group for each material is lower in dairy than landfill. In the processed dairy gas, all the compounds other than methane in this group are removed.

3) Cycloalkanes (G4)

Cyclopentanes are the only type of compound that has been identified in raw dairy gases, and their concentrations are relatively low. They are removed by the cleaning process.

4) Aromatic Hydrocarbons (G6)

There are small amount of benzene, toluene and C3 benzene in the raw dairy gases. Because of the relatively low concentrations of these chemicals, the overall risk score of this group is low

for all the materials (PE, PA12, SBR, NBR, CR and SI). The chemicals in this group are removed by the gas cleaning process.

9) Organosulfur Compounds (G7)

There are less organosulfur compounds in dairy gas than landfill. But the risk score of this group for dairy gas is relatively high compared to the rest of groups. The concentrations of these chemicals are at level of "minor" to "moderate", but in the processed dairy gas only carbonyl sulfide remains and the other compounds are below detectable level.

Gas and Material Selection for Testing

Three gas samples will be collected from biogas plants for the testing in Task 8. Two raw gases with one landfill and one dairy gas, and one processed landfill gas will be tested for the selected plastic and elastomeric materials. The processed dairy gas is eliminated from the testing because it is much cleaner than the processed landfill gas and does not have the additional chemicals that are not identified in the processed landfill. A standard natural gas will be included in the test as a reference.

The compositions of the sample gases to be used for testing are representative to the gases that have been analyzed. The sites will be selected from the gas sample database at GTI.

One plastic material and two elastomers will be tested in Task 8. PE is selected because its overall risk score is much higher than PA12 in landfill gas based on the compatibility analysis. SBR and NBR are selected as the elastomers for testing because: (a) they are both widely used elastomers in the natural gas industry, (b) SBR has relatively less resistance to many chemicals in both types of biogas, and (c) NBR has relatively better performance in biogas. These three materials will tested with the three sample gases and the standard natural gas to generate an example data set.

Gap Analysis

There are some chemicals in biogas that do not have available data in the literature to evaluate their compatibility. These chemicals are mapped in Figure 19 with their concentration rank and chemical group. The chemicals with unknown compatibility data include some alkenes, organosulfur compounds, halocarbons and organosilicones. Most of these chemicals are at moderate concentration levels. None of the chemicals in alkene and organosilicone group has any available compatibility data, and therefore it is difficult to assess the risk from these groups.

The organosulfur compounds or halocarbons may have similar impact on polymers as other chemicals from the same chemical group, but there is a lack of data. Further investigation of the chemicals with unknown compatibility may be helpful to understand the potential risk on pipeline materials from any of the chemicals present in biogas.

Task 7 - Identify and Develop Baseline and Comparative Testing Protocols

The standard and consensus test methods that have been used to study the material properties of plastics and elastomers were reviewed to identify the testing protocols for evaluating pipeline materials for biogas application. The protocols are separated into the Baseline Testing and Comparative Testing. The identified standard test methods for baseline and comparative testing are summarized in Table 49, and the test methods are described in the below sections.

Baseline Testing

These tests are designed to provide baseline assessment of a material's physical and chemical makeup. The specimens will be prepared from the new materials and tested without gas exposure. Table 50 shows the baseline test matrix.

Density

GTI internal test methods *PP300 (Helium (True) Density Measurement by Micromeritics AccuPycTM 1330 Gas Displacement Pycnometer)* will be used to measure the density of the test materials.

A sample's volume is determined by measuring the pressure change of helium in a previously determined, calibrated volume. The sample's density is then calculated based on the weight of sample taken for the volume analysis.

Three replicates will be tested for each material in this test.

Glass Transition Temperature (Tg)

ASTM D 3418 (Standard Test Method for Transition of Polymers by Differential Scanning Calorimetry) will be used to measure Tg of the test materials.

This test method consists of heating or cooling the test material at a controlled rate in a specified purge gas at a controlled flow rate and continuously monitoring with a suitable sensing device the difference in temperature or the difference in heat input between a reference material and a test material due to energy changes in the material. A transition is marked by adsorption or release of energy by the specimen resulting in a corresponding endothermic or exothermic peak or baseline shift in the heating or cooling curve.

Three replicates will be tested for each material in this test.

Chemical Makeup

ASTM D 3677 (Standard Test Methods for Rubber Identification by Infrared Spectrophotometry) will be used to analyze the chemical makeup of plastics and elastomers to be tested.

This test method provides composition analysis based on infrared examination of pyrolysis products (pyrolyzates) and films using specific peaks as outline in the standard.

Extractable Content (for elastomers)

This test procedure is used to identify elastomers. *ASTM D 297 (Standard Test Methods for Rubber Products-Chemical Analysis)* will be used.

These test methods cover the qualitative and quantitative analyses of the composition of rubber products of the "R" family (Reference ASTM D 1418). The methods are further broken out into Part A and Part B tests.

Part A consists of general test methods for use in the determination of some or all of the major constituents of a rubber product.

Part B covers the determination of specific polymers present in a rubber product.

Comparative Testing

Table 51 shows the comparative testing matrix. The comparative tests will be run on the test specimens with and without gas saturation. These tests will provide the comparative material properties of the concerned materials in the selected gas compositions.

Four gas samples are going to be used for the gas saturation test. The gas samples include one raw biogas from a landfill, one raw biogas from a dairy farm, one processed landfill gas and a standard natural gas as reference. The raw and processed biogas samples will be collected from the biogas plants.

The gas saturation test will be conducted in a stainless steel vessel at a pressure of 60 psi. The test specimens will be loaded into the test vessel and fully exposed to the sample gas which will be continually replenished at a low flow rate. The test vessel will be controlled at 120ºF during the saturation test to simulate the worse scenario in the field where the warm biogas coming out from the digester is delivered into the gathering pipeline.

Table 52 shows the specimen dimensions for the comparative tests. In order to have a good control of the specimen dimensions, PE plaques will be used to machine the plastic test specimens. The plaques will be molded using pipe grade material. The elastomeric test specimens will be machined from selected sheet materials (SBR and NBR) which have similar formulations as the materials used to make the seals for natural gas pipelines.

The comparative tests will be run at room temperature except slow crack growth test which will be run at 176ºF.

Compression Test (only for elastomers)

This test is to determine the compression-deflection characteristic of elastomers. *ASTM D 575 (Standard Test Method for Rubber Properties in Compression)* will be used.

The tests are run at a specified deflection in which the force required for this deflection is measured or by applying a specified force and measuring the amount of deflection.

Six replicates are required for this test.

Dimensional Change

This test is to measure the dimensional change of the test materials after exposure to the tested gases using a thermomechanical analyzer (TMA). A modified *ASTM E831 (Standard Test Method for Linear Thermal Expansion of Solid Materials by Thermomechanical Analysis)* is used as the test procedure.

The tests will be run with the baseline condition first and then the test specimens will be saturated with the selected gas samples. The dimension of the test specimens after saturation will be measured again using this test procedure to calculate the dimensional change from baseline.

Three replicates are required for this test.

Hardness

This test is to measure the hardness of elastomers and thermoplastics. *ASTM D2240 (Standard Test Method for Rubber Property-Durometer Hardness)* will be used.

This test method is based on the penetration of a specific type of indentor when forced into the material under specified conditions. The indentation hardness is inversely related to the penetration and is dependent on the elastic modulus and viscoelastic behavior of the material.

Five replicates are required for this test.

Tensile Strength

ASTM D638 (Standard Test Method for Tensile Properties of Plastics) is used as the test procedure to measure the tensile properties of plastic pipe materials. This test is run with the test specimens in the form of standard dumbbell-shaped (Type I) under defined conditions of pretreatment, temperature, humidity, and testing machine speed.

ASTM D412 (Standard Test Method for Vulcanized Rubber and Thermoplastic elastomers-Tension) is used as the test procedure to measure the tensile properties of elastomers. This test is run with the test specimens in the form of standard dumbbell-shaped (Die C) under defined conditions of pretreatment, temperature, humidity, and testing machine speed.

Six replicates are required for the tensile test.

Slow Crack Growth Resistance (only for plastic pipe materials)

This test is to determine the resistance of polyethylene materials to slow crack growth. *ASTM F1473 (Standard Test Method for Notch Tensile Test to Measure the Resistance to Slow Crack Growth of Polyethylene Pipes and Resins)* will be used.

The test will be performed at 176ºF and at 348 psi, and three replicates are required for this test.

Scanning Electron Microscope-Energy Disperse X-ray Spectroscopy (SEM-EDX)

The tested specimens will be selected for SEM-EDX analysis to determine the interaction between gas constituents and the polymer materials, and the resulting structural and composition change. ASTM E986 is used as a reference for this test.

Task 8 - Perform Bounded Testing to Generate a Strong Example Data Set

The focus of Task 8 in this quarter is to develop a protocol for collecting the raw/processed biogas samples from the plants and design the vessel for gas saturation test. A HazOp analysis has been initiated in this quarter for the safety review on gas sample collection at biogas sites and gas saturation testing. The safety review will be completed in next quarter and the design will be finalized.

Protocol for Biogas Collection

The biogas samples will be collected from biogas plants and compressed into a high pressure cylinder (2000 psi) and returned to GTI in order to supply the gas for the saturation tests. The biogas supplied in the plant near ambient pressure, and it has to be compressed by a compressor so that it can be filled into the high pressure gas cylinder. A portable compressor (FuelMaker FM4) which can be brought to the sample collection sites is being modified for this use at GTI.

The raw biogas is generally saturated with moisture and the liquid water will be condensate from the gas at high pressure when the gas is compressed. Some compounds in the raw gas may dissolve in the water condensate and result in the variation of the gas composition. To avoid this change of gas chemistry during sample collection, the raw gas will be dehydrated before it is compressed.

FuelMaker FM4 Compressor

The specification for the compressor to be used to collect biogas samples have been developed, and it is shown in Table 53. The unit selected for is the FuelMaker FM4 compressor, with a power requirement of 220 Volts, 1 phase AC (at 60 Hz). It draws 6 Amps of current, resulting in an average electrical consumption between 0.9-1.3 kWh.

Considerations for Gas Sampling at Biogas Plants

1) Determine the following site specifications:
    - Electrical power on-site (e.g. 240 Volts)
    - Pipe fittings from site gas outlet
    - Gas pressure from site gas outlet
    - Pipe fittings for processed biomethane (if applicable)
    - Gas pressure for processed biomethane (if applicable)
2) The sampling schematic will be configured as shown in Figure 20.
3) A HazOp analysis will be performed on this process to ensure the safety and quality of our process.
4) Properties to consider when collecting gas are the following:
    - Temperature of gas (50°C-60°C).
    - Density change during compression (for compressibility factor).
    - Impurities that may affect equipment (H_2S, siloxanes, etc.).
    - Liquid condensation by dew-point from components (e.g. CO_2).

Design Pressure Test Vessel

The pressure test vessel has been designed for the gas saturation test. It consists of a three feet long and four inch diameter stainless steel (SS316) pipe. The test samples will be loaded onto a sample cage and inserted into the vessel. The sample cage has been designed, and the construction of one cage has been completed, see Figure 21.

Table 23. Chemical Compositions of the Raw Biogas from Landfill

Component	Max	Min	Median	Avg	Std Dev	Ave Dev	90% Mode	# of Samples Analyzed	# of Samples with Hits	Result	Rank
Helium, mol%	0.10	0.10	0.10	0.10	0.0005	0.0005	0.10	84	3	0.004	1
Hydrogen, mol%	0.96	0.05	0.17	0.27	0.241	0.18	30.44	84	16	5.8	3
Carbon Dioxide, mol%	45.93	0.01	36.23	32.45	11.069	7.51	40.66	114	113	40.3	5
Oxygen/Argon, mol%	15.67	0.12	1.52	2.53	2.877	2.07	6.37	92	67	4.6	3
Nitrogen, mol%	57.07	0.04	9.82	12.37	12.873	8.82	26.99	87	80	24.8	4
Carbon Monoxide, mol%	0.04	0.04	0.04	0.04	NA	NA	NA	84	1	0	0
Methane, mol%	73.53	1.50	52.85	51.80	12.132	8.02	63.42	114	114	63.4	5
Ethane, ppmv	61	16	26	34	16	14	62	84	8	5.9	3
Ethene, ppmv	36	26	31	31	5	5	35	84	2	0.8	2
Ethyne, ppmv	NA	NA	NA	NA	NA	NA	NA	84	0	0	0
Propane, ppmv	59	15	22	25	10	8	36	84	32	13.7	4
Propene, ppmv	59	16	26	32	18	16	52	84	4	2.5	3
Propadiene, ppmv	NA	NA	NA	NA	NA	NA	NA	84	0	0	0
Propyne, ppmv	NA	NA	NA	NA	NA	NA	NA	84	0	0	0
i-Butane, ppmv	22	16	18	19	2	2	22	84	7	1.8	3
n-Butane, ppmv	NA	NA	19	NA	NA	NA	NA	84	1	0	0
1-Butene, ppmv	NA	NA	NA	NA	NA	NA	NA	84	0	0	0
i-Butene, ppmv	NA	NA	NA	NA	NA	NA	NA	84	0	0	0
trans-2-Butene, ppmv	NA	NA	NA	NA	NA	NA	NA	84	0	0	0
cis-2-Butene, ppmv	NA	NA	NA	NA	NA	NA	NA	84	0	0	0
1,3-Butadiene, ppmv	NA	NA	NA	NA	NA	NA	NA	84	0	0	0
i-Pentane, ppmv	36	16	21	23	6	4	28	84	11	3.7	3
n-Pentane, ppmv	24	16	24	21	4	3	24	84	3	0.9	2
neo-Pentane, ppmv	NA	NA	NA	NA	NA	NA	NA	84	0	0	0
Pentenes, ppmv	28	23	25	25	3	3	28	84	2	0.7	2
Hexane Plus, ppmv	558	16	119	147	111	83	326	84	72	279	5
Ammonia, ppmv	NA	NA	NA	NA	NA	NA	NA	15	0	0	0

Table 23. Chemical Compositions of the Raw Biogas from Landfill (Continued)

Component	Max	Min	Median	Avg	Std Dev	Ave Dev	90% Mode	# of Samples Analyzed	# of Samples with Hits	Result	Rank
Cyclopentane, ppmv	4.00	0.69	1.44	1.89	1.08	0.91	4.00	46	35	3.0	3
Methylcyclopentane, ppmv	2.00	0.32	1.00	1.17	0.43	0.32	2.00	46	24	1.0	3
Cyclohexane, ppmv	10.65	0.29	1.00	2.42	2.35	1.74	5.59	61	44	4.0	3
Methylcyclohexane, ppmv	3.42	0.62	2.00	1.71	0.77	0.67	3.00	50	38	2.3	3
Benzene, ppmv	46.17	0.17	2.00	4.22	7.05	4.03	9.39	80	72	8.5	3
Toluene, ppmv	69.77	0.41	10.33	14.07	14.45	9.74	27.49	85	83	26.8	4
Ethylbenzene, ppmv	129.12	0.02	3.36	6.68	16.46	5.82	10.03	62	57	9.2	3
m,p-Xylene, ppmv	92.83	0.84	7.80	12.26	16.66	10.21	27.96	70	63	25.2	4
Styrene, ppmv	81.73	0.78	1.25	9.72	21.71	13.84	25.59	54	12	5.7	3
o-Xylene, ppmv	15.19	0.02	2.00	2.53	2.46	1.65	5.00	54	44	4.1	3
C3 Benzenes, ppmv	62.00	1.00	4.00	10.15	13.05	9.06	24.00	53	48	21.7	4
Naphthalene, ppmv	NA	NA	NA	NA	NA	NA	NA	46	0	0	0
C1 Naphthalenes, ppmv	NA	NA	NA	NA	NA	NA	NA	46	0	0	0
C2 Naphthalenes, ppmv	NA	NA	NA	NA	NA	NA	NA	46	0	0	0
hexane, ppmv	122.23	1.30	11.59	19.93	22.55	16.94	49.22	57	54	46.6	4
Heptanes, ppmv	73.00	1.00	10.50	16.88	15.56	12.52	36.30	46	45	35.5	4
2,2,4-Trimethylpentane, ppmv	2.00	0.00	1.00	1.10	0.53	0.38	2.00	46	17	0.7	2
Octanes, ppmv	51.96	2.00	9.00	14.63	13.19	9.84	34.53	46	45	33.8	4
Nonanes, ppmv	59.06	1.00	11.00	15.24	14.18	10.09	38.58	46	46	38.6	4
Decanes, ppmv	96.00	1.10	23.50	29.68	21.45	15.94	60.79	46	45	59.5	4
Undecanes, ppmv	69.70	2.00	13.00	19.05	17.58	13.20	49.50	46	43	46.3	4
Dodecanes, ppmv	13.00	1.00	2.00	3.88	3.63	2.97	9.60	46	22	4.6	3
Tridecanes, ppmv	2.00	1.00	1.00	1.25	0.43	0.38	1.70	46	3	0.1	2
Tetradecanes, ppmv	NA	NA	NA	NA	NA	NA	NA	46	0	0	0
Pentadecanes, ppmv	NA	NA	NA	NA	NA	NA	NA	46	0	0	0
Hexadecanes, ppmv	NA	NA	NA	NA	NA	NA	NA	46	0	0	0
Heptadecanes, ppmv	NA	NA	NA	NA	NA	NA	NA	46	0	0	0

Table 23. Chemical Compositions of the Raw Biogas from Landfill (Continued)

Component	Max	Min	Median	Avg	Std Dev	Ave Dev	90% Mode	# of Samples Analyzed	# of Samples with Hits	Result	Rank
Octadecanes, ppmv	NA	NA	NA	NA	NA	NA	NA	46	0	0	0
Nonadecanes, ppmv	NA	NA	NA	NA	NA	NA	NA	46	0	0	0
Eicosanes +, ppmv	NA	NA	NA	NA	NA	NA	NA	46	0	0	0
Hydrogen Sulfide, ppmv	1830	0.08	104.50	183.88	261.19	160	400	85	72	339	5
Sulfur Dioxide, ppmv	1.13	0.10	0.25	0.35	0.25	0.19	0.59	73	16	0.1	2
Carbonyl Sulfide, ppmv	5.18	0.05	0.30	0.71	1.13	0.65	1.34	73	60	1.1	3
Carbon Disulfide, ppmv	5.93	0.04	0.12	0.39	0.99	0.44	0.55	73	44	0.3	2
Methyl Mercaptan, ppmv	67.8	0.07	1.98	4.52	10.02	4.76	9.94	73	51	6.9	3
Ethyl Mercaptan, ppmv	1.31	0.06	0.21	0.29	0.24	0.18	0.62	73	48	0.4	2
i-Propyl Mercaptan, ppmv	11.10	0.05	0.78	1.13	1.65	0.89	2.19	73	50	1.5	3
n-Propyl Mercaptan, ppmv	0.46	0.05	0.11	0.13	0.08	0.05	0.21	72	33	0.1	2
t-Butyl Mercaptan, ppmv	1.12	0.05	0.15	0.19	0.17	0.10	0.29	73	49	0.2	2
Dimethyl Sulfide, ppmv	131	0.05	2.45	11.74	25.27	13.86	19.57	73	55	14.7	4
Methyl Ethyl Sulfide, ppmv	1.75	0.05	0.20	0.38	0.47	0.34	1.18	73	20	0.3	2
Diethyl Sulfide, ppmv	0.14	0.02	0.06	0.07	0.03	0.03	0.11	73	9	0.01	1
Di-t-Butyl Sulfide, ppmv	NA	NA	NA	NA	NA	NA	NA	73	0	0	0
Dimethyl Disulfide, ppmv	11.30	0.03	0.08	0.75	2.17	1.09	1.01	73	39	0.5	2
Methyl Ethyl Disulfide, ppmv	0.42	0.06	0.12	0.18	0.14	0.12	0.34	73	4	0.02	1
Methyl i-Propyl Disulfide, ppmv	NA	NA	NA	NA	NA	NA	NA	73	0	0	0
Diethyl Disulfide, ppmv	0.28	0.28	0.28	0.28	NA	NA	NA	73	1	0	0
Methyl n-Propyl Disulfide, ppmv	0.03	0.03	0.03	0.03	0.00	0.00	0.03	73	2	0.001	1
Methyl t-Butyl Disulfide, ppmv	NA	NA	0.04	NA	NA	NA	NA	73	1	0	0
Ethyl i-Propyl Disulfide, ppmv	NA	NA	NA	NA	NA	NA	NA	73	0	0	0
Ethyl n-Propyl Disulfide, ppmv	NA	NA	NA	NA	NA	NA	NA	73	0	0	0
Ethyl t-Butyl Disulfide, ppmv	NA	NA	NA	NA	NA	NA	NA	73	0	0	0
Di-i-Propyl Disulfide, ppmv	NA	NA	NA	NA	NA	NA	NA	73	0	0	0

Table 23. Chemical Compositions of the Raw Biogas from Landfill (Continued)

Component	Max	Min	Med	Avg	Std Dev	Ave Dev	90% Mode	# of Samples	# of Hits	Result	Rank
i-Propyl n-Propyl Disulfide, ppmv	NA	NA	NA	NA	NA	NA	NA	73	0	0	0
Di-n-Propyl Disulfide, ppmv	NA	NA	NA	NA	NA	NA	NA	73	0	0	0
i-Propyl t-Butyl Disulfide, ppmv	0.06	0.03	0.05	0.05	0.02	0.02	0.06	73	2	0.002	1
n-Propyl t-Butyl Disulfide, ppmv	NA	NA	NA	NA	NA	NA	NA	73	0	0	0
Di-t-Butyl Disulfide, ppmv	NA	NA	NA	NA	NA	NA	NA	73	0	0	0
Dimethyl Trisulfide, ppmv	0.29	0.02	0.04	0.07	0.08	0.05	0.18	73	14	0.03	1
Diethyl Trisulfide, ppmv	NA	NA	NA	NA	NA	NA	NA	73	0	0	0
Di-t-Butyl Trisulfide, ppmv	NA	NA	NA	NA	NA	NA	NA	73	0	0	0
Thiophene, ppmv	2.68	0.05	0.24	0.45	0.54	0.38	1.20	73	49	0.8	2
C1-Thiophenes, ppmv	3.06	0.06	0.39	0.72	0.79	0.60	1.85	73	30	0.8	2
C2-Thiophenes, ppmv	0.74	0.06	0.13	0.22	0.20	0.16	0.48	73	12	0.08	1
C3-Thiophenes, ppmv	NA	NA	NA	NA	NA	NA	NA	72	0	0	0
Benzothiophene, ppmv	NA	NA	NA	NA	NA	NA	NA	73	0	0	0
C1-Benzothiophenes, ppmv	NA	NA	NA	NA	NA	NA	NA	73	0	0	0
C2-Benzothiophenes, ppmv	NA	NA	NA	NA	NA	NA	NA	73	0	0	0
Thiophane, ppmv	1.59	0.05	0.18	0.35	0.40	0.30	0.92	72	21	0.3	2
Thiophenol, ppmv	0.18	0.05	0.08	0.10	0.05	0.05	0.16	73	4	0.01	1
Individual Unidentified, ppmv as S	9.91	0.05	0.61	1.03	1.48	0.81	1.97	73	49	1.3	3
Dichlorodifluoromethane (CFC-12), ppmv	112	0.02	0.98	9.54	18.97	12.18	25.01	54	47	21.8	4
1,2-Dichlorotetrafluoroethane (CFC-114), ppmv	1.57	0.10	0.30	0.54	0.49	0.40	1.26	37	8	0.3	2
1,1,2-Trichloro-1,2,2-trifluoroethane , ppmv	0.72	0.12	0.42	0.42	0.20	0.18	0.66	48	6	0.08	1
Trichlorofluoromethane (CFC-11), ppmv	30.17	0.07	0.42	5.95	10.54	8.14	25.54	49	15	7.8	3
Chloromethane, ppmv	0.35	0.14	0.25	0.25	0.10	0.10	0.33	37	2	0.02	1
Dichloromethane (Methylene Chloride), ppmv	116	0.03	2.48	10.17	23.89	12.73	18.20	70	41	10.7	4
Chloroform, ppmv	NA	NA	NA	NA	NA	NA	NA	37	0	0	0
Carbon Tetrachloride, ppmv	NA	NA	NA	NA	NA	NA	NA	37	0	0	0

Table 23. Chemical Compositions of the Raw Biogas from Landfill (Continued)

Component	Max	Min	Med	Avg	Std Dev	Ave Dev	90% Mode	# of Samples	# of Hits	Result	Rank
Chloroethane, ppmv	4.59	0.12	0.43	0.87	0.96	0.64	1.74	47	26	1.0	2
1,1-Dichloroethane, ppmv	13.81	0.11	0.45	1.59	3.32	1.72	1.95	49	15	0.6	2
1,2-Dichloroethane, ppmv	0.22	0.14	0.20	0.18	0.03	0.03	0.22	37	5	0.03	1
1,1,1-Trichloroethane, ppmv	3.02	0.17	0.34	0.79	0.95	0.70	1.81	47	7	0.3	2
1,1,2-Trichloroethane, ppmv	NA	NA	NA	NA	NA	NA	NA	37	0	0	0
1,1,2,2-Tetrachloroethane, ppmv	NA	NA	NA	NA	NA	NA	NA	37	0	0	0
Chloroethene (Vinyl Chloride), ppmv	31.18	0.01	0.53	3.41	7.48	4.50	5.73	53	41	4.4	3
1,1-Dichloroethene, ppmv	1.39	0.23	0.46	0.74	0.45	0.43	1.29	46	5	0.1	2
cis-1,2-Dichloroethene, ppmv	42.05	0.02	0.40	4.32	9.89	6.03	8.87	56	49	7.8	3
Trichloroethene, ppmv	25.91	0.01	0.31	4.99	8.90	7.21	19.78	43	14	6.4	3
Tetrachloroethene, ppmv	34.44	0.04	0.23	5.97	11.28	8.71	22.42	42	17	9.1	3
1,2-Dichloropropane, ppmv	NA	NA	NA	NA	NA	NA	NA	37	0	0	0
3-Chloropropene, ppmv	NA	NA	NA	NA	NA	NA	NA	37	0	0	0
cis-1,3-Dichloropropene, ppmv	NA	NA	NA	NA	NA	NA	NA	37	0	0	0
trans-1,3-Dichloropropene, ppmv	NA	NA	NA	NA	NA	NA	NA	37	0	0	0
Bromomethane, ppmv	NA	NA	NA	NA	NA	NA	NA	37	0	0	0
1,2-Dibromoethane, ppmv	NA	NA	NA	NA	NA	NA	NA	37	0	0	0
Chlorobenzene, ppmv	2.36	0.02	0.16	0.50	0.80	0.60	1.39	45	7	0.2	2
1,2-Dichlorobenzene, ppmv	0.56	0.02	0.12	0.21	0.21	0.18	0.43	44	4	0.04	1
1,3-Dichlorobenzene, ppmv	1.17	0.05	0.31	0.46	0.46	0.41	0.99	44	4	0.09	1
1,4-Dichlorobenzene, ppmv	0.75	0.05	0.19	0.25	0.21	0.16	0.46	44	8	0.08	1
1,2,4-Trichlorobenzene, ppmv	NA	NA	NA	NA	NA	NA	NA	38	0	0	0
Hexachloro-1,3-butadiene, ppmv	NA	NA	NA	NA	NA	NA	NA	37	0	0	0
Mercury, µg/M^3	1.70	0.05	0.60	0.72	0.64	0.58	1.50	7.00	5	1.1	3
Arsenic, µg/M^3	339	59	222	209	92	75	326	9	9	326	5

Table 23. Chemical Compositions of the Raw Biogas from Landfill (Continued)

Component	Max	Min	Med	Avg	Std Dev	Ave Dev	90% Mode	# of Samples	# of Hits	Result	Rank
Barium, µg/M^3	NA	NA	NA	NA	NA	NA	NA	9	0	0	0
Beryllium, µg/M^3	NA	NA	NA	NA	NA	NA	NA	9	0	0	0
Cadmium, µg/M^3	NA	NA	NA	NA	NA	NA	NA	9	0	0	0
Cobalt, µg/M^3	NA	NA	NA	NA	NA	NA	NA	9	0	0	0
Chromium, µg/M^3	NA	NA	NA	NA	NA	NA	NA	9	0	0	0
Copper, µg/M^3	NA	NA	NA	NA	NA	NA	NA	9	0	0	0
Manganese, µg/M^3	NA	NA	NA	NA	NA	NA	NA	9	0	0	0
Molybdenum, µg/M^3	NA	NA	NA	NA	NA	NA	NA	9	0	0	0
Nickel, µg/M^3	NA	NA	NA	NA	NA	NA	NA	9	0	0	0
Lead, µg/M^3	NA	NA	NA	NA	NA	NA	NA	9	0	0	0
Antimony, µg/M^3	417	85	277	268	101	83	393	9	9	393	5
Selenium, µg/M^3	NA	NA	NA	NA	NA	NA	NA	9	0	0	0
Strontium, µg/M^3	NA	NA	NA	NA	NA	NA	NA	9	0	0	0
Thallium, µg/M^3	NA	NA	NA	NA	NA	NA	NA	9	0	0	0
Zinc, µg/M^3	96	29	54	57	23	19	86	9	7	67.2	4
1,1,3,3-Tetramethyldisiloxane, ppmv as Si	NA	NA	NA	NA	NA	NA	NA	24	0	0	0
Pentamethyldisiloxane, ppmv as Si	NA	NA	NA	NA	NA	NA	NA	24	0	0	0
Hexamethyldisilane, ppmv as Si	2	0.50	0.81	1.08	0.55	0.44	1.87	24	15	1.2	3
Hexamethyldisiloxane (L2), ppmv as Si	2	0.03	0.24	0.44	0.51	0.40	1.28	37	13	0.5	2
Octamethyltrisiloxane (L3), ppmv as Si	0	0.01	0.01	0.03	0.03	0.03	0.07	34	4	0.01	1
Octamethylcyclotetrasiloxane , ppmv as Si	12	0.37	3.21	3.68	2.42	1.75	6.57	37	35	6.2	3
Decamethyltetrasiloxane (L4), ppmv as Si	2	2.21	2.21	2.21	0.00	0.00	2.21	33	1	0.07	1
Decamethylcyclopentasiloxane, ppmv as Si	3	0.12	0.85	1.02	0.79	0.65	2.09	37	30	1.7	3
Dodecamethylpentasiloxane , ppmv as Si	0	0.00	NA	NA	NA	NA	NA	25	0	0	0
Trimethyl silanol, ppmv as Si	3	0.60	1.23	1.52	0.89	0.79	2.83	13	8	1.7	3
Hexamathylcyclotrisiloxane , ppmv as Si	0	0.00	0.13	0.12	0.08	0.06	0.25	11	11	0.2	2
Unidentified Si	4	0.74	0.91	1.43	1.13	0.83	2.63	24	7	0.8	2

Table 24. Chemical Compositions of the Processed Biogas from Landfill

Component	Max	Min	Median	Avg	Std Dev	Ave Dev	90% Mode	# of Samples Analyzed	# of Samples with Hits	Result	Rank
Helium, mol%	NA	NA	NA	NA	NA	NA	NA	35	0	0	0
Hydrogen, mol%	1.00	0.06	0.65	0.48	0.38	0.36	0.93	35	7	0.2	2
Carbon Dioxide, mol%	32.32	0.04	0.95	3.74	8.89	5.11	1.68	35	33	1.6	3
Oxygen/Argon, mol%	22.12	0.47	0.82	2.88	4.84	2.88	4.71	35	19	2.6	3
Nitrogen, mol%	77.83	0.55	3.68	8.62	13.80	7.96	24.18	35	35	24.2	4
Carbon Monoxide, mol%	NA	NA	NA	NA	NA	NA	NA	35	0	0	0
Methane, mol%	97.92	38.21	94.07	88.72	16.42	10.36	97.32	35	34	94.5	5
Ethane, ppmv	NA	NA	NA	NA	NA	NA	NA	35	0	0.0	0
Ethene, ppmv	NA	NA	15.59	NA	NA	NA	NA	35	1	0.0	0
Ethyne, ppmv	NA	NA	NA	NA	NA	NA	NA	35	0	0	0
Propane, ppmv	42	15	34	32	7.05	5.5	40	35	30	34.0	4
Propene, ppmv	20	16	17	18	1.39	1.1	19	35	6	3.3	3
Propadiene, ppmv	NA	NA	NA	NA	NA	NA	NA	35	0	0	0
Propyne, ppmv	NA	NA	NA	NA	NA	NA	NA	35	0	0	0
i-Butane, ppmv	20	17	18	18	1.06	1.0	20	35	8	4.5	3
n-Butane, ppmv	NA	NA	NA	NA	NA	NA	NA	35	0	0	0
1-Butene, ppmv	NA	NA	NA	NA	NA	NA	NA	35	0	0	0
i-Butene, ppmv	NA	NA	NA	NA	NA	NA	NA	35	0	0	0
trans-2-Butene, ppmv	NA	NA	NA	NA	NA	NA	NA	35	0	0	0
cis-2-Butene, ppmv	NA	NA	NA	NA	NA	NA	NA	35	0	0	0
1,3-Butadiene, ppmv	NA	NA	NA	NA	NA	NA	NA	35	0	0	0
i-Pentane, ppmv	NA	NA	NA	NA	NA	NA	NA	35	0	0	0
n-Pentane, ppmv	NA	NA	NA	NA	NA	NA	NA	35	0	0	0
neo-Pentane, ppmv	NA	NA	NA	NA	NA	NA	NA	35	0	0	0
Pentenes, ppmv	NA	NA	NA	NA	NA	NA	NA	35	0	0	0
Hexane Plus, ppmv	121	1	16	42	43.97	40	110	35	21	66	4
Ammonia, ppmv	NA	NA	NA	NA	NA	NA	NA	35	0	0	0

Table 24. Chemical Compositions of the Processed Biogas from Landfill (Continued)

Component	Max	Min	Median	Avg	Std Dev	Ave Dev	90% Mode	# of Samples Analyzed	# of Samples with Hits	Result	Rank
Cyclopentane, ppmv	2	1	1	1	0.50	0.49	2	19	9	0.9	2
Methylcyclopentane, ppmv	1	1	1	1	0.00	0.00	1	19	4	0.2	2
Cyclohexane, ppmv	1	1	1	1	0.00	0.00	1	19	7	0.4	2
Methylcyclohexane, ppmv	1	1	1	1	0.00	0.00	1	19	5	0.3	2
Benzene, ppmv	1	1	1	1	0.00	0.00	1	19	4	0.2	2
Toluene, ppmv	7	5	6	6	0.82	0.67	7	19	3	1.1	3
Ethylbenzene, ppmv	2	2	2	2	0.00	0.00	2	19	3	0.3	2
m,p-Xylene, ppmv	3	2	3	3	0.47	0.44	3	19	3	0.5	2
Styrene, ppmv	NA	NA	NA	NA	NA	NA	NA	19	0	0	0
o-Xylene, ppmv	1	1	1	1	0.00	0.00	1	19	3	0.2	2
C3 Benzenes, ppmv	4	3	4	4	0.47	0.44	4	19	3	0.6	2
Naphthalene, ppmv	NA	NA	NA	NA	NA	NA	NA	19	0	0	0
C1 Naphthalenes, ppmv	NA	NA	NA	NA	NA	NA	NA	19	0	0	0
C2 Naphthalenes, ppmv	NA	NA	NA	NA	NA	NA	NA	19	0	0	0
hexane, ppmv	15	1	6	7	5.18	4.60	13	19	10	6.9	3
Heptanes, ppmv	10	1	9	6	4.10	4.00	10	19	5	2.5	3
2,2,4-Trimethylpentane, ppmv	NA	NA	NA	NA	NA	NA	NA	19	0	0	0
Octanes, ppmv	9	7	8	8	0.82	0.67	9	19	3	1.4	3
Nonanes, ppmv	9	7	9	8	0.94	0.89	9	19	3	1.4	3
Decanes, ppmv	30	1	21	16	12.77	12.16	29	19	5	7.7	3
Undecanes, ppmv	17	13	17	16	1.89	1.78	17	19	3	2.7	3
Dodecanes, ppmv	1	1	1	1	0.00	0.00	1	19	3	0.2	2
Tridecanes, ppmv	NA	NA	NA	NA	NA	NA	NA	19	0	0	0
Tetradecanes, ppmv	NA	NA	NA	NA	NA	NA	NA	19	0	0	0
Pentadecanes, ppmv	NA	NA	NA	NA	NA	NA	NA	19	0	0	0
Hexadecanes, ppmv	NA	NA	NA	NA	NA	NA	NA	19	0	0	0
Heptadecanes, ppmv	NA	NA	NA	NA	NA	NA	NA	19	0	0	0

Table 24. Chemical Compositions of the Processed Biogas from Landfill (Continued)

Component	Max	Min	Median	Avg	Std Dev	Ave Dev	90% Mode	# of Samples Analyzed	# of Samples with Hits	Result	Rank
Octadecanes, ppmv	NA	NA	NA	NA	NA	NA	NA	19	0	0	0
Nonadecanes, ppmv	NA	NA	NA	NA	NA	NA	NA	19	0	0	0
Eicosanes +, ppmv	NA	NA	NA	NA	NA	NA	NA	19	0	0	0
Hydrogen Sulfide, ppmv	0.53	0.30	0.48	0.45	0.09	0.08	0.53	16	4	0.1	2
Sulfur Dioxide, ppmv	0.08	0.06	0.07	0.07	0.01	0.01	0.08	16	3	0.01	1
Carbonyl Sulfide, ppmv	0.88	0.08	0.18	0.30	0.29	0.23	0.87	16	10	0.5	2
Carbon Disulfide, ppmv	NA	NA	NA	NA	NA	NA	NA	16	0	0	0
Methyl Mercaptan, ppmv	NA	NA	NA	NA	NA	NA	NA	16	0	0	0
Ethyl Mercaptan, ppmv	NA	NA	NA	NA	NA	NA	NA	16	0	0	0
i-Propyl Mercaptan, ppmv	NA	NA	NA	NA	NA	NA	NA	16	0	0	0
n-Propyl Mercaptan, ppmv	NA	NA	NA	NA	NA	NA	NA	16	0	0	0
t-Butyl Mercaptan, ppmv	NA	NA	NA	NA	NA	NA	NA	16	0	0	0
Dimethyl Sulfide, ppmv	1.88	0.06	1.11	1.03	0.64	0.54	1.78	16	8	0.9	2
Methyl Ethyl Sulfide, ppmv	NA	NA	NA	NA	NA	NA	NA	16	0	0	0
Diethyl Sulfide, ppmv	NA	NA	NA	NA	NA	NA	NA	16	0	0	0
Di-t-Butyl Sulfide, ppmv	NA	NA	NA	NA	NA	NA	NA	16	0	0	0
Dimethyl Disulfide, ppmv	0.17	0.05	0.09	0.10	0.05	0.05	0.16	16	4	0.04	1
Methyl Ethyl Disulfide, ppmv	NA	NA	NA	NA	NA	NA	NA	16	0	0	0
Methyl i-Propyl Disulfide, ppmv	NA	NA	NA	NA	NA	NA	NA	16	0	0	0
Diethyl Disulfide, ppmv	NA	NA	NA	NA	NA	NA	NA	16	0	0	0
Methyl n-Propyl Disulfide, ppmv	NA	NA	NA	NA	NA	NA	NA	16	0	0	0
Methyl t-Butyl Disulfide, ppmv	NA	NA	NA	NA	NA	NA	NA	16	0	0	0
Ethyl i-Propyl Disulfide, ppmv	NA	NA	NA	NA	NA	NA	NA	16	0	0	0
Ethyl n-Propyl Disulfide, ppmv	NA	NA	NA	NA	NA	NA	NA	16	0	0	0
Ethyl t-Butyl Disulfide, ppmv	NA	NA	NA	NA	NA	NA	NA	16	0	0	0
Di-i-Propyl Disulfide, ppmv	NA	NA	NA	NA	NA	NA	NA	16	0	0	0

Table 24. Chemical Compositions of the Processed Biogas from Landfill (Continued)

Component	Max	Min	Med	Avg	Std Dev	Ave Dev	90% Mode	# of Samples	# of Hits	Result	Rank
i-Propyl n-Propyl Disulfide, ppmv	NA	NA	NA	NA	NA	NA	NA	16	0	0	0
Di-n-Propyl Disulfide, ppmv	NA	NA	NA	NA	NA	NA	NA	16	0	0	0
i-Propyl t-Butyl Disulfide, ppmv	NA	NA	NA	NA	NA	NA	NA	16	0	0	0
n-Propyl t-Butyl Disulfide, ppmv	NA	NA	NA	NA	NA	NA	NA	16	0	0	0
Di-t-Butyl Disulfide, ppmv	NA	NA	NA	NA	NA	NA	NA	16	0	0	0
Dimethyl Trisulfide, ppmv	NA	NA	NA	NA	NA	NA	NA	16	0	0	0
Diethyl Trisulfide, ppmv	NA	NA	NA	NA	NA	NA	NA	16	0	0	0
Di-t-Butyl Trisulfide, ppmv	NA	NA	NA	NA	NA	NA	NA	16	0	0	0
Thiophene, ppmv	NA	NA	NA	NA	NA	NA	NA	16	0	0	0
C1-Thiophenes, ppmv	NA	NA	NA	NA	NA	NA	NA	16	0	0	0
C2-Thiophenes, ppmv	NA	NA	NA	NA	NA	NA	NA	16	0	0	0
C3-Thiophenes, ppmv	NA	NA	NA	NA	NA	NA	NA	16	0	0	0
Benzothiophene, ppmv	NA	NA	NA	NA	NA	NA	NA	16	0	0	0
C1-Benzothiophenes, ppmv	NA	NA	NA	NA	NA	NA	NA	16	0	0	0
C2-Benzothiophenes, ppmv	NA	NA	NA	NA	NA	NA	NA	16	0	0	0
Thiophane, ppmv	NA	NA	NA	NA	NA	NA	NA	16	0	0	0
Thiophenol, ppmv	NA	NA	NA	NA	NA	NA	NA	16	0	0	0
Individual Unidentified, ppmv as S	NA	NA	NA	NA	NA	NA	NA	16	0	0	0
Dichlorodifluoromethane, ppmv	3.60	1.35	2.56	2.61	0.69	0.54	3.48	12	12	3.5	3
1,2-Dichlorotetrafluoroethane, ppmv	0.17	0.11	0.13	0.14	0.02	0.02	0.17	12	6	0.08	1
1,1,2-Trichloro-1,2,2-trifluoroethane, ppmv	NA	NA	NA	NA	NA	NA	NA	12	0	0	0
Trichlorofluoromethane, ppmv	0.24	0.13	0.16	0.18	0.04	0.04	0.23	12	6	0.1	2
Chloromethane, ppmv	NA	NA	NA	NA	NA	NA	NA	12	0	0	0
Dichloromethane, ppmv	NA	NA	NA	NA	NA	NA	NA	12	0	0	0
Chloroform, ppmv	NA	NA	NA	NA	NA	NA	NA	12	0	0	0
Carbon Tetrachloride, ppmv	NA	NA	NA	NA	NA	NA	NA	12	0	0	0

Table 24. Chemical Compositions of the Processed Biogas from Landfill (Continued)

Component	Max	Min	Med	Avg	Std Dev	Ave Dev	90% Mode	# of Samples	# of Hits	Result	Rank
Chloroethane, ppmv	0.66	0.41	0.59	0.56	0.09	0.07	0.65	12	8	0.4	2
1,1-Dichloroethane, ppmv	NA	NA	NA	NA	NA	NA	NA	12	0	0	0
1,2-Dichloroethane, ppmv	NA	NA	NA	NA	NA	NA	NA	12	0	0	0
1,1,1-Trichloroethane, ppmv	NA	NA	NA	NA	NA	NA	NA	12	0	0	0
1,1,2-Trichloroethane, ppmv	NA	NA	NA	NA	NA	NA	NA	12	0	0	0
1,1,2,2-Tetrachloroethane, ppmv	NA	NA	NA	NA	NA	NA	NA	12	0	0	0
Chloroethene (Vinyl Chloride), ppmv	0.33	0.13	0.25	0.24	0.07	0.05	0.33	12	8	0.2	2
1,1-Dichloroethene, ppmv	NA	NA	NA	NA	NA	NA	NA	12	0	0	0
cis-1,2-Dichloroethene, ppmv	NA	NA	NA	NA	NA	NA	NA	12	0	0	0
Trichloroethene, ppmv	NA	NA	NA	NA	NA	NA	NA	12	0	0	0
Tetrachloroethene, ppmv	NA	NA	NA	NA	NA	NA	NA	12	0	0	0
1,2-Dichloropropane, ppmv	NA	NA	NA	NA	NA	NA	NA	12	0	0	0
3-Chloropropene, ppmv	NA	NA	NA	NA	NA	NA	NA	12	0	0	0
cis-1,3-Dichloropropene, ppmv	NA	NA	NA	NA	NA	NA	NA	12	0	0	0
trans-1,3-Dichloropropene, ppmv	NA	NA	NA	NA	NA	NA	NA	12	0	0	0
Bromomethane, ppmv	NA	NA	NA	NA	NA	NA	NA	12	0	0	0
1,2-Dibromoethane, ppmv	NA	NA	NA	NA	NA	NA	NA	12	0	0	0
Chlorobenzene, ppmv	NA	NA	NA	NA	NA	NA	NA	12	0	0	0
1,2-Dichlorobenzene, ppmv	NA	NA	NA	NA	NA	NA	NA	12	0	0	0
1,3-Dichlorobenzene, ppmv	NA	NA	NA	NA	NA	NA	NA	12	0	0	0
1,4-Dichlorobenzene, ppmv	NA	NA	NA	NA	NA	NA	NA	12	0	0	0
1,2,4-Trichlorobenzene, ppmv	NA	NA	NA	NA	NA	NA	NA	12	0	0	0
Hexachloro-1,3-butadiene, ppmv	NA	NA	NA	NA	NA	NA	NA	12	0	0	0
Mercury, µg/M^3	0.28	0.14	0.21	0.21	0.07	0.07	0.27	16	2	0.03	1
Arsenic, µg/M^3	NA	NA	NA	NA	NA	NA	NA	15	0	0	0

Table 24. Chemical Compositions of the Processed Biogas from Landfill (Continued)

Component	Max	Min	Med	Avg	Std Dev	Ave Dev	90% Mode	# of Samples	# of Hits	Result	Rank
Barium, µg/M^3	NA	NA	NA	NA	NA	NA	NA	15	0	0	0
Beryllium, µg/M^3	NA	NA	NA	NA	NA	NA	NA	15	0	0	0
Cadmium, µg/M^3	NA	NA	NA	NA	NA	NA	NA	15	0	0	0
Cobalt, µg/M^3	NA	NA	NA	NA	NA	NA	NA	15	0	0	0
Chromium, µg/M^3	NA	NA	NA	NA	NA	NA	NA	15	0	0	0
Copper, µg/M^3	250.00	148.00	206.00	201.33	41.77	35.56	241.20	15	3	48.24	4
Manganese, µg/M^3	NA	NA	NA	NA	NA	NA	NA	15	0	0	0
Molybdenum, µg/M^3	NA	NA	NA	NA	NA	NA	NA	15	0	0	0
Nickel, µg/M^3	NA	NA	NA	NA	NA	NA	NA	15	0	0	0
Lead, µg/M^3	NA	NA	NA	NA	NA	NA	NA	15	0	0	0
Antimony, µg/M^3	NA	NA	NA	NA	NA	NA	NA	15	0	0	0
Selenium, µg/M^3	NA	NA	NA	NA	NA	NA	NA	15	0	0	0
Strontium, µg/M^3	NA	NA	NA	NA	NA	NA	NA	15	0	0	0
Thallium, µg/M^3	NA	NA	NA	NA	NA	NA	NA	15	0	0	0
Zinc, µg/M^3	111.00	28.00	54.50	62.00	30.34	24.50	94.80	15	4	25.28	4
1,1,3,3-Tetramethyldisiloxane, ppmv as Si	NA	NA	NA	NA	NA	NA	NA	16	0	0	0
Pentamethyldisiloxane, ppmv as Si	NA	NA	NA	NA	NA	NA	NA	16	0	0	0
Hexamethyldisilane, ppmv as Si	NA	NA	NA	NA	NA	NA	NA	16	0	0	0
Hexamethyldisiloxane (L2), ppmv as Si	NA	NA	NA	NA	NA	NA	NA	16	0	0	0
Octamethyltrisiloxane (L3), ppmv as Si	NA	NA	NA	NA	NA	NA	NA	16	0	0	0
Octamethylcyclotetrasiloxane , ppmv as Si	4.90	0.30	2.50	2.55	2.16	2.15	4.78	16	4	1.2	3
Decamethyltetrasiloxane (L4), ppmv as Si	NA	NA	NA	NA	NA	NA	NA	16	0	0	0
Decamethylcyclopentasiloxane, ppmv as Si	NA	NA	NA	NA	NA	NA	NA	16	0	0	0
Dodecamethylpentasiloxane , ppmv as Si	NA	NA	NA	NA	NA	NA	NA	16	0	0	0
Unidentified Si	NA	NA	NA	NA	NA	NA	NA	16	0	0	0

Table 25. Chemical Compositions of Raw Biogas from Dairy Farms

Component	Max	Min	Med	Avg	Std Dev	Ave Dev	90% Mode	# of Samples	# of Hits	Result	Rank
Helium, mol%	NA	NA	NA	NA	NA	NA	NA	62	0	0	0
Hydrogen, mol%	NA	NA	0.07	NA	NA	NA	NA	62	1	0	0
Carbon Dioxide, mol%	44.00	15.64	39.31	37.46	5.43	4.12	42.15	68	68	42.1	5
Oxygen/Argon, mol%	8.45	0.03	0.34	1.51	2.29	1.66	5.06	62	35	2.9	3
Nitrogen, mol%	200.00	0.06	0.46	6.62	25.57	9.62	12.32	63	63	12.3	4
Carbon Monoxide, mol%	NA	NA	NA	NA	NA	NA	NA	62	0	0	0
Methane, mol%	70.00	33.50	58.75	58.27	5.93	3.45	63.41	68	68	63.4	5
Ethane, ppmv	NA	NA	NA	NA	NA	NA	NA	62	0	0	0
Ethene, ppmv	NA	NA	NA	NA	NA	NA	NA	62	0	0	0
Ethyne, ppmv	NA	NA	NA	NA	NA	NA	NA	62	0	0	0
Propane, ppmv	NA	NA	18	NA	NA	NA	NA	62	1	0	0
Propene, ppmv	NA	NA	NA	NA	NA	NA	NA	62	0	0	0
Propadiene, ppmv	NA	NA	NA	NA	NA	NA	NA	62	0	0	0
Propyne, ppmv	NA	NA	NA	NA	NA	NA	NA	62	0	0	0
i-Butane, ppmv	NA	NA	NA	NA	NA	NA	NA	62	0	0	0
n-Butane, ppmv	NA	NA	NA	NA	NA	NA	NA	62	0	0	0
1-Butene, ppmv	NA	NA	NA	NA	NA	NA	NA	62	0	0	0
i-Butene, ppmv	NA	NA	NA	NA	NA	NA	NA	62	0	0	0
trans-2-Butene, ppmv	NA	NA	NA	NA	NA	NA	NA	62	0	0	0
cis-2-Butene, ppmv	NA	NA	NA	NA	NA	NA	NA	62	0	0	0
1,3-Butadiene, ppmv	NA	NA	NA	NA	NA	NA	NA	62	0	0	0
i-Pentane, ppmv	NA	NA	NA	NA	NA	NA	NA	62	0	0	0
n-Pentane, ppmv	NA	NA	NA	NA	NA	NA	NA	62	0	0	0
neo-Pentane, ppmv	NA	NA	NA	NA	NA	NA	NA	62	0	0	0
Pentenes, ppmv	NA	NA	NA	NA	NA	NA	NA	62	0	0	0
Hexane Plus, ppmv	118	1	3	23	34	26	73	62	18	21.2	4
Ammonia, ppmv	450	43	247	247	204	204	409	62	2	13.2	4

Table 25. Chemical Compositions of Raw Biogas from Dairy Farms (Continued)

Component	Max	Min	Med	Avg	Std Dev	Ave Dev	90% Mode	# of Samples	# of Hits	Result	Rank
Cyclopentane, ppmv	1.00	1.00	1	1.00	0.00	0.00	1	20	2	0.1	2
Methylcyclopentane, ppmv	NA	NA	NA	NA	NA	NA	NA	20	0	0	0
Cyclohexane, ppmv	NA	NA	NA	NA	NA	NA	NA	20	0	0	0
Methylcyclohexane, ppmv	NA	NA	NA	NA	NA	NA	NA	20	0	0	0
Benzene, ppmv	0.50	0.06	0.10	0.22	0.20	0.19	0.4	23	3	0.05	1
Toluene, ppmv	8.70	0.01	0.52	2.44	3.64	3.13	6.4	23	4	1.1	3
Ethylbenzene, ppmv	NA	NA	5.1	NA	NA	NA	NA	21	1	0	0
m,p-Xylene, ppmv	NA	NA	10.3	NA	NA	NA	NA	21	1	0	0
Styrene, ppmv	NA	NA	3.2	NA	NA	NA	NA	21	1	0	0
o-Xylene, ppmv	NA	NA	3.8	NA	NA	NA	NA	21	1	0	0
C3 Benzenes, ppmv	1.00	1.00	1.0	NA	NA	0.00	1.0	20	2	0.1	2
Naphthalene, ppmv	NA	NA	NA	NA	NA	NA	NA	20	0	0	0
C1 Naphthalenes, ppmv	NA	NA	NA	NA	NA	NA	NA	20	0	0	0
C2 Naphthalenes, ppmv	NA	NA	NA	NA	NA	NA	NA	20	0	0	0
hexane, ppmv	3.0	1.0	1.0	1.5	0.66	0.58	2.0	20	11	1.1	3
Heptanes, ppmv	NA	NA	1.0	NA	NA	0.00	1.0	20	3	0.2	2
2,2,4-Trimethylpentane, ppmv	NA	NA	NA	NA	NA	NA	NA	20	0	0	0
Octanes, ppmv	NA	NA	NA	NA	NA	NA	NA	20	0	0	0
Nonanes, ppmv	NA	NA	NA	NA	NA	NA	NA	20	0	0	0
Decanes, ppmv	NA	NA	NA	NA	NA	NA	NA	20	0	0	0
Undecanes, ppmv	NA	NA	1.0	NA	NA	NA	NA	20	1	0	0
Dodecanes, ppmv	NA	NA	NA	NA	NA	NA	NA	20	0	0	0
Tridecanes, ppmv	NA	NA	NA	NA	NA	NA	NA	20	0	0	0
Tetradecanes, ppmv	NA	NA	NA	NA	NA	NA	NA	20	0	0	0
Pentadecanes, ppmv	NA	NA	NA	NA	NA	NA	NA	20	0	0	0
Hexadecanes, ppmv	NA	NA	NA	NA	NA	NA	NA	20	0	0	0
Heptadecanes, ppmv	NA	NA	NA	NA	NA	NA	NA	20	0	0	0

Table 25. Chemical Compositions of Raw Biogas from Dairy Farms (Continued)

Component	Max	Min	Med	Avg	Std Dev	Ave Dev	90% Mode	# of Samples	# of Hits	Result	Rank
Octadecanes, ppmv	NA	NA	NA	NA	NA	NA	NA	20	0	0	0
Nonadecanes, ppmv	NA	NA	NA	NA	NA	NA	NA	20	0	0	0
Eicosanes +, ppmv	NA	NA	NA	NA	NA	NA	NA	20	0	0	0
Hydrogen Sulfide, ppmv	6570	0.05	1755	2008	1731	1470	4090	32	26	3323	5
Sulfur Dioxide, ppmv	7.73	0.07	0.40	1.09	1.79	1.09	2.19	25	17	1.5	3
Carbonyl Sulfide, ppmv	26.35	0.09	1.11	2.28	5.02	2.28	3.64	25	25	3.6	3
Carbon Disulfide, ppmv	0.77	0.03	0.10	0.15	0.19	0.11	0.20	25	12	0.09	1
Methyl Mercaptan, ppmv	7.88	0.10	0.67	1.66	2.12	1.58	5.29	25	21	4.4	3
Ethyl Mercaptan, ppmv	0.38	0.05	0.20	0.18	0.09	0.07	0.27	25	19	0.2	2
i-Propyl Mercaptan, ppmv	2.67	0.08	0.37	0.55	0.60	0.43	1.00	25	20	0.8	2
n-Propyl Mercaptan, ppmv	0.10	0.06	0.08	0.08	0.01	0.01	0.10	25	5	0.02	1
t-Butyl Mercaptan, ppmv	0.60	0.05	0.15	0.21	0.19	0.15	0.44	25	6	0.1	2
Dimethyl Sulfide, ppmv	1.09	0.08	0.21	0.36	0.31	0.25	0.79	25	16	0.5	2
Methyl Ethyl Sulfide, ppmv	NA	NA	NA	NA	NA	NA	NA	25	0	0	0
Diethyl Sulfide, ppmv	NA	NA	NA	NA	NA	NA	NA	25	0	0	0
Di-t-Butyl Sulfide, ppmv	NA	NA	NA	NA	NA	NA	NA	25	0	0	0
Dimethyl Disulfide, ppmv	0.32	0.13	0.20	0.22	0.08	0.07	0.30	25	3	0.04	1
Methyl Ethyl Disulfide, ppmv	NA	NA	NA	NA	NA	NA	NA	25	0	0	0
Methyl i-Propyl Disulfide, ppmv	NA	NA	NA	NA	NA	NA	NA	25	0	0	0
Diethyl Disulfide, ppmv	NA	NA	0.15	NA	NA	NA	NA	25	1	0	0
Methyl n-Propyl Disulfide, ppmv	NA	NA	NA	NA	NA	NA	NA	25	0	0	0
Methyl t-Butyl Disulfide, ppmv	NA	NA	NA	NA	NA	NA	NA	25	0	0	0
Ethyl i-Propyl Disulfide, ppmv	NA	NA	NA	NA	NA	NA	NA	25	0	0	0
Ethyl n-Propyl Disulfide, ppmv	NA	NA	NA	NA	NA	NA	NA	25	0	0	0
Ethyl t-Butyl Disulfide, ppmv	NA	NA	NA	NA	NA	NA	NA	25	0	0	0
Di-i-Propyl Disulfide, ppmv	NA	NA	NA	NA	NA	NA	NA	25	0	0	0

Table 25. Chemical Compositions of Raw Biogas from Dairy Farms (Continued)

Component	Max	Min	Med	Avg	Std Dev	Ave Dev	90% Mode	# of Samples	# of Hits	Result	Rank
i-Propyl n-Propyl Disulfide, ppmv	NA	NA	NA	NA	NA	NA	NA	25	0	0	0
Di-n-Propyl Disulfide, ppmv	NA	NA	NA	NA	NA	NA	NA	25	0	0	0
i-Propyl t-Butyl Disulfide, ppmv	NA	NA	NA	NA	NA	NA	NA	25	0	0	0
n-Propyl t-Butyl Disulfide, ppmv	NA	NA	NA	NA	NA	NA	NA	25	0	0	0
Di-t-Butyl Disulfide, ppmv	NA	NA	NA	NA	NA	NA	NA	25	0	0	0
Dimethyl Trisulfide, ppmv	NA	NA	NA	NA	NA	NA	NA	25	0	0	0
Diethyl Trisulfide, ppmv	NA	NA	NA	NA	NA	NA	NA	25	0	0	0
Di-t-Butyl Trisulfide, ppmv	NA	NA	NA	NA	NA	NA	NA	25	0	0	0
Thiophene, ppmv	0.26	0.06	0.13	0.15	0.07	0.06	0.25	25	9	0.09	1
C1-Thiophenes, ppmv	NA	NA	NA	NA	NA	NA	NA	25	0	0	0
C2-Thiophenes, ppmv	NA	NA	0.05	NA	NA	NA	NA	25	1	0	0
C3-Thiophenes, ppmv	NA	NA	NA	NA	NA	NA	NA	25	0	0	0
Benzothiophene, ppmv	NA	NA	NA	NA	NA	NA	NA	25	0	0	0
C1-Benzothiophenes, ppmv	NA	NA	NA	NA	NA	NA	NA	25	0	0	0
C2-Benzothiophenes, ppmv	NA	NA	NA	NA	NA	NA	NA	25	0	0	0
Thiophane, ppmv	NA	NA	NA	NA	NA	NA	NA	25	0	0	0
Thiophenol, ppmv	NA	NA	NA	NA	NA	NA	NA	25	0	0	0
Individual Unidentified, ppmv as S	2.04	0.10	1.07	1.07	0.97	0.97	1.85	25	2	0.1	2
Dichlorodifluoromethane, ppmv	NA	NA	0.35	NA	NA	NA	NA	21	1	0	0
1,2-Dichlorotetrafluoroethane, ppmv	NA	NA	NA	NA	NA	NA	NA	21	0	0	0
1,1,2-Trichloro-1,2,2-trifluoroethane, ppmv	NA	NA	NA	NA	NA	NA	21	0	0	0	0
Trichlorofluoromethane, ppmv	NA	NA	NA	NA	NA	NA	NA	21	0	0	0
Chloromethane, ppmv	NA	NA	NA	NA	NA	NA	NA	21	0	0	0
Dichloromethane, ppmv	NA	NA	NA	NA	NA	NA	NA	21	0	0	0
Chloroform, ppmv	NA	NA	NA	NA	NA	NA	NA	21	0	0	0
Carbon Tetrachloride, ppmv	NA	NA	NA	NA	NA	NA	NA	21	0	0	0

Table 25. Chemical Compositions of Raw Biogas from Dairy Farms (Continued)

Component	Max	Min	Med	Avg	Std Dev	Ave Dev	90% Mode	# of Samples	# of Hits	Result	Rank
Chloroethane, ppmv	NA	NA	NA	NA	NA	NA	NA	21	0	0	0
1,1-Dichloroethane, ppmv	NA	NA	NA	NA	NA	NA	NA	21	0	0	0
1,2-Dichloroethane, ppmv	NA	NA	NA	NA	NA	NA	NA	21	0	0	0
1,1,1-Trichloroethane, ppmv	NA	NA	NA	NA	NA	NA	NA	21	0	0	0
1,1,2-Trichloroethane, ppmv	NA	NA	NA	NA	NA	NA	NA	21	0	0	0
1,1,2,2-Tetrachloroethane, ppmv	NA	NA	NA	NA	NA	NA	NA	21	0	0	0
Chloroethene (Vinyl Chloride), ppmv	NA	NA	0.38	NA	NA	NA	NA	21	1	0	0
1,1-Dichloroethene, ppmv	NA	NA	NA	NA	NA	NA	NA	21	0	0	0
cis-1,2-Dichloroethene, ppmv	NA	NA	NA	NA	NA	NA	NA	21	0	0	0
Trichloroethene, ppmv	NA	NA	NA	NA	NA	NA	NA	21	0	0	0
Tetrachloroethene, ppmv	NA	NA	NA	NA	NA	NA	NA	21	0	0	0
1,2-Dichloropropane, ppmv	NA	NA	NA	NA	NA	NA	NA	21	0	0	0
3-Chloropropene, ppmv	NA	NA	NA	NA	NA	NA	NA	21	0	0	0
cis-1,3-Dichloropropene, ppmv	NA	NA	NA	NA	NA	NA	NA	21	0	0	0
trans-1,3-Dichloropropene, ppmv	NA	NA	NA	NA	NA	NA	NA	21	0	0	0
Bromomethane, ppmv	NA	NA	NA	NA	NA	NA	NA	21	0	0	0
1,2-Dibromoethane, ppmv	NA	NA	NA	NA	NA	NA	NA	0	0	0	0
Chlorobenzene, ppmv	NA	NA	NA	NA	NA	NA	NA	21	0	0	0
1,2-Dichlorobenzene, ppmv	NA	NA	NA	NA	NA	NA	NA	21	0	0	0
1,3-Dichlorobenzene, ppmv	NA	NA	NA	NA	NA	NA	NA	21	0	0	0
1,4-Dichlorobenzene, ppmv	NA	NA	0.17	NA	NA	NA	NA	21	1	0	0
1,2,4-Trichlorobenzene, ppmv	NA	NA	NA	NA	NA	NA	NA	21	0	0	0
Hexachloro-1,3-butadiene, ppmv	NA	NA	NA	NA	NA	NA	NA	21	0	0	0
Mercury, µg/M^3	0.06	0.02	0.02	0.03	0.02	0.02	0.02	19	4	0.004	1
Arsenic, µg/M^3	NA	NA	NA	NA	NA	NA	NA	9	0	0	0

Table 25. Chemical Compositions of Raw Biogas from Dairy Farms (Continued)

Component	Max	Min	Med	Avg	Std Dev	Ave Dev	90% Mode	# of Samples	# of Hits	Result	Rank
Cadmium, µg/M^3	NA	NA	NA	NA	NA	NA	NA	9	0	0	0
Copper, µg/M^3	NA	NA	60	NA	NA	NA	NA	9	1	0	0
Lead, µg/M^3	NA	NA	NA	NA	NA	NA	NA	9	0	0	0
Molybdenum, µg/M^3	NA	NA	2	NA	NA	NA	NA	9	1	0	0
Selenium, µg/M^3	NA	NA	NA	NA	NA	NA	NA	9	0	0	0
1,1,3,3-Tetramethyldisiloxane, ppmv as Si	NA	NA	NA	NA	NA	NA	NA	19	0	0	0
Pentamethyldisiloxane, ppmv as Si	NA	NA	NA	NA	NA	NA	NA	19	0	0	0
Hexamethyldisilane, ppmv as Si	NA	NA	0.84	NA	NA	NA	NA	19	1	0	0
Hexamethyldisiloxane (L2), ppmv as Si	NA	NA	NA	NA	NA	NA	NA	19	0	0	0
Octamethyltrisiloxane (L3), ppmv as Si	NA	NA	NA	NA	NA	NA	NA	19	0	0	0
Octamethylcyclotetrasiloxane , ppmv as Si	NA	NA	11.57	NA	NA	NA	NA	19	1	0	0
Decamethyltetrasiloxane, ppmv as Si	NA	NA	NA	NA	NA	NA	NA	19	0	0	0
Decamethylcyclopentasiloxane , ppmv as Si	NA	NA	4.68	NA	NA	NA	NA	19	1	0	0
Dodecamethylpentasiloxane , ppmv as Si	NA	NA	NA	NA	NA	NA	NA	19	0	0	0
Trimethyl silanol, ppmv as Si	NA	NA	NA	NA	NA	NA	NA	12	0	0	0
Hexamathylcyclotrisiloxane (D3), ppmv as Si	NA	NA	NA	NA	NA	NA	NA	12	0	0	0
Unidentified organic silicon compound ppmv as Si	NA	1.30	NA	NA	NA	NA	12	1	0	0	0

Table 26. Chemical Compositions of Processed Biogas from Dairy Farms

Component	Max	Min	Med	Avg	Std Dev	Ave Dev	90% Mode	# of Samples	# of Hits	Result	Rank
Helium, mol%	NA	NA	NA	NA	NA	NA	NA	23	0	0	0
Hydrogen, mol%	NA	NA	NA	NA	NA	NA	NA	23	0	0	0
Carbon Dioxide, mol%	0.95	0.06	0.35	0.54	0.34	0.33	0.94	23	23	0.9	2
Oxygen/Argon, mol%	1.99	0.39	0.85	0.91	0.48	0.39	1.44	23	10	0.6	2
Nitrogen, mol%	7.81	0.20	0.38	1.80	2.04	1.70	3.96	23	23	4.0	3
Carbon Monoxide, mol%	NA	NA	NA	NA	NA	NA	NA	23	0	0	0
Methane, mol%	99.63	89.35	99.27	97.26	2.83	2.44	99.61	23	23	99.6	5
Ethane, ppmv	NA	NA	1109	NA	NA	NA	NA	23	1	0	0
Ethene, ppmv	NA	NA	NA	NA	NA	NA	NA	23	0	0	0
Ethyne, ppmv	NA	NA	NA	NA	NA	NA	NA	23	0	0	0
Propane, ppmv	NA	NA	284	NA	NA	NA	NA	23	1	0	0
Propene, ppmv	NA	NA	NA	NA	NA	NA	NA	23	0	0	0
Propadiene, ppmv	NA	NA	NA	NA	NA	NA	NA	23	0	0	0
Propyne, ppmv	NA	NA	NA	NA	NA	NA	NA	23	0	0	0
i-Butane, ppmv	NA	NA	53	NA	NA	NA	NA	23	1	0	0
n-Butane, ppmv	NA	NA	53	NA	NA	NA	NA	23	1	0	0
1-Butene, ppmv	NA	NA	NA	NA	NA	NA	NA	23	0	0	0
i-Butene, ppmv	NA	NA	NA	NA	NA	NA	NA	23	0	0	0
trans-2-Butene, ppmv	NA	NA	NA	NA	NA	NA	NA	23	0	0	0
cis-2-Butene, ppmv	NA	NA	NA	NA	NA	NA	NA	23	0	0	0
1,3-Butadiene, ppmv	NA	NA	NA	NA	NA	NA	NA	23	0	0	0
i-Pentane, ppmv	NA	NA	17	NA	NA	NA	NA	23	1	0	0
n-Pentane, ppmv	NA	NA	NA	NA	NA	NA	NA	23	0	0	0
neo-Pentane, ppmv	NA	NA	NA	NA	NA	NA	NA	23	0	0	0
Pentenes, ppmv	NA	NA	NA	NA	NA	NA	NA	23	0	0	0
Hexane Plus, ppmv	NA	NA	21	NA	NA	NA	NA	23	1	0	0
Ammonia, ppmv	NA	NA	NA	NA	NA	NA	NA	23	0	0	0

Table 26. Chemical Compositions of Processed Biogas from Dairy Farms (Continued)

Component	Max	Min	Med	Avg	Std Dev	Ave Dev	90% Mode	# of Samples	# of Hits	Result	Rank
Cyclopentane, ppmv	NA	NA	4	NA	NA	NA	NA	23	1	0	0
Methylcyclopentane, ppmv	NA	NA	2	NA	NA	NA	NA	23	1	0	0
Cyclohexane, ppmv	NA	NA	3	NA	NA	NA	NA	23	1	0	0
Methylcyclohexane, ppmv	NA	NA	2	NA	NA	NA	NA	23	1	0	0
Benzene, ppmv	NA	NA	1	NA	NA	NA	NA	23	1	0	0
Toluene, ppmv	NA	NA	1	NA	NA	NA	NA	23	1	0	0
Ethylbenzene, ppmv	NA	NA	NA	NA	NA	NA	NA	23	0	0	0
m,p-Xylene, ppmv	NA	NA	NA	NA	NA	NA	NA	23	0	0	0
Styrene, ppmv	NA	NA	NA	NA	NA	NA	NA	23	0	0	0
o-Xylene, ppmv	NA	NA	NA	NA	NA	NA	NA	23	0	0	0
C3 Benzenes, ppmv	NA	NA	NA	NA	NA	NA	NA	23	0	0	0
Naphthalene, ppmv	NA	NA	NA	NA	NA	NA	NA	23	0	0	0
C1 Naphthalenes, ppmv	NA	NA	NA	NA	NA	NA	NA	23	0	0	0
C2 Naphthalenes, ppmv	NA	NA	NA	NA	NA	NA	NA	23	0	0	0
hexane, ppmv	NA	NA	6	NA	NA	NA	NA	23	1	0	0
Heptanes, ppmv	NA	NA	1	NA	NA	NA	NA	23	1	0	0
2,2,4-Trimethylpentane, ppmv	NA	NA	NA	NA	NA	NA	NA	23	0	0	0
Octanes, ppmv	NA	NA	1	NA	NA	NA	NA	23	1	0	0
Nonanes, ppmv	NA	NA	NA	NA	NA	NA	NA	23	0	0	0
Decanes, ppmv	NA	NA	NA	NA	NA	NA	NA	23	0	0	0
Undecanes, ppmv	NA	NA	NA	NA	NA	NA	NA	23	0	0	0
Dodecanes, ppmv	NA	NA	NA	NA	NA	NA	NA	23	0	0	0
Tridecanes, ppmv	NA	NA	NA	NA	NA	NA	NA	23	0	0	0
Tetradecanes, ppmv	NA	NA	NA	NA	NA	NA	NA	23	0	0	0
Pentadecanes, ppmv	NA	NA	NA	NA	NA	NA	NA	23	0	0	0
Hexadecanes, ppmv	NA	NA	NA	NA	NA	NA	NA	23	0	0	0
Heptadecanes, ppmv	NA	NA	NA	NA	NA	NA	NA	23	0	0	0

Table 26. Chemical Compositions of Processed Biogas from Dairy Farms (Continued)

Component	Max	Min	Med	Avg	Std Dev	Ave Dev	90% Mode	# of Samples	# of Hits	Result	Rank
Octadecanes, ppmv	NA	NA	NA	NA	NA	NA	NA	23	0	0	0
Nonadecanes, ppmv	NA	NA	NA	NA	NA	NA	NA	23	0	0	0
Eicosanes +, ppmv	NA	NA	NA	NA	NA	NA	NA	23	0	0	0
Hydrogen Sulfide, ppmv	NA	NA	NA	NA	NA	NA	NA	23	0	0	0
Sulfur Dioxide, ppmv	NA	NA	NA	NA	NA	NA	NA	23	0	0	0
Carbonyl Sulfide, ppmv	5.28	0.05	0.14	0.71	1.36	0.83	1.41	23	20	0	0
Carbon Disulfide, ppmv	NA	NA	NA	NA	NA	NA	NA	23	0	0	0
Methyl Mercaptan, ppmv	NA	NA	NA	NA	NA	NA	NA	23	0	0	0
Ethyl Mercaptan, ppmv	NA	NA	NA	NA	NA	NA	NA	23	0	0	0
i-Propyl Mercaptan, ppmv	NA	NA	NA	NA	NA	NA	NA	23	0	0	0
n-Propyl Mercaptan, ppmv	NA	NA	NA	NA	NA	NA	NA	23	0	0	0
t-Butyl Mercaptan, ppmv	NA	NA	NA	NA	NA	NA	NA	23	0	0	0
Dimethyl Sulfide, ppmv	NA	NA	NA	NA	NA	NA	NA	23	0	0	0
Methyl Ethyl Sulfide, ppmv	NA	NA	NA	NA	NA	NA	NA	23	0	0	0
Diethyl Sulfide, ppmv	NA	NA	NA	NA	NA	NA	NA	23	0	0	0
Di-t-Butyl Sulfide, ppmv	NA	NA	NA	NA	NA	NA	NA	23	0	0	0
Dimethyl Disulfide, ppmv	NA	NA	NA	NA	NA	NA	NA	23	0	0	0
Methyl Ethyl Disulfide, ppmv	NA	NA	NA	NA	NA	NA	NA	23	0	0	0
Methyl i-Propyl Disulfide, ppmv	NA	NA	NA	NA	NA	NA	NA	23	0	0	0
Diethyl Disulfide, ppmv	NA	NA	NA	NA	NA	NA	NA	23	0	0	0
Methyl n-Propyl Disulfide, ppmv	NA	NA	NA	NA	NA	NA	NA	23	0	0	0
Methyl t-Butyl Disulfide, ppmv	NA	NA	NA	NA	NA	NA	NA	23	0	0	0
Ethyl i-Propyl Disulfide, ppmv	NA	NA	NA	NA	NA	NA	NA	23	0	0	0
Ethyl n-Propyl Disulfide, ppmv	NA	NA	NA	NA	NA	NA	NA	23	0	0	0
Ethyl t-Butyl Disulfide, ppmv	NA	NA	NA	NA	NA	NA	NA	23	0	0	0
Di-i-Propyl Disulfide, ppmv	NA	NA	NA	NA	NA	NA	NA	23	0	0	0

Table 26. Chemical Compositions of Processed Biogas from Dairy Farms (Continued)

Component	Max	Min	Med	Avg	Std Dev	Ave Dev	90% Mode	# of Samples	# of Hits	Result	Rank
i-Propyl n-Propyl Disulfide, ppmv	NA	NA	NA	NA	NA	NA	NA	23	0	0	0
Di-n-Propyl Disulfide, ppmv	NA	NA	NA	NA	NA	NA	NA	23	0	0	0
i-Propyl t-Butyl Disulfide, ppmv	NA	NA	NA	NA	NA	NA	NA	23	0	0	0
n-Propyl t-Butyl Disulfide, ppmv	NA	NA	NA	NA	NA	NA	NA	23	0	0	0
Di-t-Butyl Disulfide, ppmv	NA	NA	NA	NA	NA	NA	NA	23	0	0	0
Dimethyl Trisulfide, ppmv	NA	NA	NA	NA	NA	NA	NA	23	0	0	0
Diethyl Trisulfide, ppmv	NA	NA	NA	NA	NA	NA	NA	23	0	0	0
Di-t-Butyl Trisulfide, ppmv	NA	NA	NA	NA	NA	NA	NA	23	0	0	0
Thiophene, ppmv	NA	NA	NA	NA	NA	NA	NA	23	0	0	0
C1-Thiophenes, ppmv	NA	NA	NA	NA	NA	NA	NA	23	0	0	0
C2-Thiophenes, ppmv	NA	NA	NA	NA	NA	NA	NA	23	0	0	0
C3-Thiophenes, ppmv	NA	NA	NA	NA	NA	NA	NA	23	0	0	0
Benzothiophene, ppmv	NA	NA	NA	NA	NA	NA	NA	23	0	0	0
C1-Benzothiophenes, ppmv	NA	NA	NA	NA	NA	NA	NA	23	0	0	0
C2-Benzothiophenes, ppmv	NA	NA	NA	NA	NA	NA	NA	23	0	0	0
Thiophane, ppmv	NA	NA	NA	NA	NA	NA	NA	23	0	0	0
Thiophenol, ppmv	NA	NA	NA	NA	NA	NA	NA	23	0	0	0
Individual Unidentified, ppmv as S	NA	NA	NA	NA	NA	NA	NA	23	0	0	0
Dichlorodifluoromethane, ppmv	NA	NA	NA	NA	NA	NA	NA	16	0	0	0
1,2-Dichlorotetrafluoroethane, ppmv	NA	NA	NA	NA	NA	NA	NA	16	0	0	0
1,1,2-Trichloro-1,2,2-trifluoroethane, ppmv	NA	NA	NA	NA	NA	NA	NA	16	0	0	0
Trichlorofluoromethane, ppmv	NA	NA	NA	NA	NA	NA	NA	16	0	0	0
Chloromethane, ppmv	NA	NA	NA	NA	NA	NA	NA	16	0	0	0
Dichloromethane, ppmv	NA	NA	NA	NA	NA	NA	NA	16	0	0	0
Chloroform, ppmv	NA	NA	NA	NA	NA	NA	NA	16	0	0	0
Carbon Tetrachloride, ppmv	NA	NA	NA	NA	NA	NA	NA	16	0	0	0

Table 26. Chemical Compositions of Processed Biogas from Dairy Farms (Continued)

Component	Max	Min	Med	Avg	Std Dev	Ave Dev	90% Mode	# of Samples	# of Hits	Result	Rank
Chloroethane, ppmv	NA	NA	NA	NA	NA	NA	NA	16	0	0	0
1,1-Dichloroethane, ppmv	NA	NA	NA	NA	NA	NA	NA	16	0	0	0
1,2-Dichloroethane, ppmv	NA	NA	NA	NA	NA	NA	NA	16	0	0	0
1,1,1-Trichloroethane, ppmv	NA	NA	NA	NA	NA	NA	NA	16	0	0	0
1,1,2-Trichloroethane, ppmv	NA	NA	NA	NA	NA	NA	NA	16	0	0	0
1,1,2,2-Tetrachloroethane, ppmv	NA	NA	NA	NA	NA	NA	NA	16	0	0	0
Chloroethene (Vinyl Chloride), ppmv	NA	NA	NA	NA	NA	NA	NA	16	0	0	0
1,1-Dichloroethene, ppmv	NA	NA	NA	NA	NA	NA	NA	16	0	0	0
cis-1,2-Dichloroethene, ppmv	NA	NA	NA	NA	NA	NA	NA	16	0	0	0
Trichloroethene, ppmv	NA	NA	NA	NA	NA	NA	NA	16	0	0	0
Tetrachloroethene, ppmv	NA	NA	NA	NA	NA	NA	NA	16	0	0	0
1,2-Dichloropropane, ppmv	NA	NA	NA	NA	NA	NA	NA	16	0	0	0
3-Chloropropene, ppmv	NA	NA	NA	NA	NA	NA	NA	16	0	0	0
cis-1,3-Dichloropropene, ppmv	NA	NA	NA	NA	NA	NA	NA	16	0	0	0
trans-1,3-Dichloropropene, ppmv	NA	NA	NA	NA	NA	NA	NA	16	0	0	0
Bromomethane, ppmv	NA	NA	NA	NA	NA	NA	NA	16	0	0	0
1,2-Dibromoethane, ppmv	NA	NA	NA	NA	NA	NA	NA	16	0	0	0
Chlorobenzene, ppmv	NA	NA	NA	NA	NA	NA	NA	16	0	0	0
1,2-Dichlorobenzene, ppmv	NA	NA	NA	NA	NA	NA	NA	16	0	0	0
1,3-Dichlorobenzene, ppmv	NA	NA	NA	NA	NA	NA	NA	16	0	0	0
1,4-Dichlorobenzene, ppmv	NA	NA	NA	NA	NA	NA	NA	16	0	0	0
1,2,4-Trichlorobenzene, ppmv	NA	NA	NA	NA	NA	NA	NA	16	0	0	0
Hexachloro-1,3-butadiene, ppmv	NA	NA	NA	NA	NA	NA	NA	16	0	0	0
Mercury, µg/M^3	NA	NA	NA	NA	NA	NA	NA	21	0	0	0
Arsenic, µg/M^3	NA	NA	NA	NA	NA	NA	NA	20	0	0	0

Table 26. Chemical Compositions of Processed Biogas from Dairy Farms (Continued)

Component	Max	Min	Med	Avg	Std Dev	Ave Dev	90% Mode	# of Samples	# of Hits	Result	Rank
Cadmium, µg/M^3	NA	NA	NA	NA	NA	NA	NA	20	0	0	0
Copper, µg/M^3	NA	NA	NA	NA	NA	NA	NA	20	0	0	0
Lead, µg/M^3	NA	NA	NA	NA	NA	NA	NA	20	0	0	0
Molybdenum, µg/M^3	NA	NA	NA	NA	NA	NA	NA	20	0	0	0
Selenium, µg/M^3	NA	NA	NA	NA	NA	NA	NA	20	0	0	0
1,1,3,3-Tetramethyldisiloxane, ppmv as Si	NA	NA	NA	NA	NA	NA	NA	18	0	0	0
Pentamethyldisiloxane, ppmv as Si	NA	NA	NA	NA	NA	NA	NA	18	0	0	0
Hexamethyldisilane, ppmv as Si	NA	NA	NA	NA	NA	NA	NA	18	0	0	0
Hexamethyldisiloxane (L2), ppmv as Si	NA	NA	NA	NA	NA	NA	NA	18	0	0	0
Octamethyltrisiloxane (L3), ppmv as Si	NA	NA	NA	NA	NA	NA	NA	18	0	0	0
Octamethylcyclotetrasiloxane , ppmv as Si	NA	NA	NA	NA	NA	NA	NA	18	0	0	0
Decamethyltetrasiloxane, ppmv as Si	NA	NA	NA	NA	NA	NA	NA	18	0	0	0
Decamethylcyclopentasiloxane , ppmv as Si	NA	NA	NA	NA	NA	NA	NA	18	0	0	0
Dodecamethylpentasiloxane , ppmv as Si	NA	NA	NA	NA	NA	NA	NA	18	0	0	0

Table 27. Scoring Scheme for Biogas Constituents

	Low Concentration	High Concentration	Assigned Rank
Mol% Level Scoring	40	100	5
	10	40	4
	1	10	3
	0.1	1	2
	< 0.1	NA	1
ppm Level Scoring	> 100	NA	5
	10	100	4
	1	10	3
	0.1	1	2
	< 0.1	NA	1

Table 28. CO_2 partial pressure, pH and the Compositions of Carbonic Acid Solutions*

P_{CO_2} (atm)	pH	$[CO_2]$ (mol/L)	$[H_2CO_3]$ (mol/L)	$[HCO_3^-]$ (mol/L)	$[CO_3^{2-}]$ (mol/L)
10^{-8}	7.00	3.36×10^{-10}	5.71×10^{-13}	1.42×10^{-9}	7.90×10^{-13}
10^{-6}	6.81	3.36×10^{-8}	5.71×10^{-11}	9.16×10^{-8}	3.30×10^{-11}
10^{-4}	5.92	3.36×10^{-6}	5.71×10^{-9}	1.19×10^{-6}	5.57×10^{-11}
3.5×10^{-4}	5.65	1.18×10^{-5}	2.00×10^{-8}	2.23×10^{-6}	5.60×10^{-11}
10^{-3}	5.42	3.36×10^{-5}	5.71×10^{-8}	3.78×10^{-6}	5.61×10^{-11}
10^{-2}	4.92	3.36×10^{-4}	5.71×10^{-7}	1.19×10^{-5}	5.61×10^{-11}
10^{-1}	4.42	3.36×10^{-3}	5.71×10^{-6}	3.78×10^{-5}	5.61×10^{-11}
1	3.92	3.36×10^{-2}	5.71×10^{-5}	1.20×10^{-4}	5.61×10^{-11}
2.5	3.72	8.40×10^{-2}	1.43×10^{-4}	1.89×10^{-4}	5.61×10^{-11}
10	3.42	0.336	5.71×10^{-4}	3.78×10^{-4}	5.61×10^{-11}

* Data from Wikipedia: http://en.wikipedia.org/wiki/Carbonic_acid

Table 29. General Physical Properties of the Hydrocarbons Present in Biogas*

Chemical	Formula	Boiling point (°F)	Melting point (°F)	Density ($g \cdot cm^{-3}$)
Methane	CH_4	-259.60	-297.40	gas
Ethane	C_2H_6	-128.20	-295.17	gas
Propane	C_3H_8	-43.60	-306.40	gas
Butane	C_4H_{10}	31.10	-211.00	gas
Pentane	C_5H_{12}	96.80	-202.00	0.626
Hexane	C_6H_{14}	156.20	-139.00	0.659
Heptane	C_7H_{16}	208.40	-131.80	0.684
Octane	C_8H_{18}	258.80	-70.60	0.703
Nonane	C_9H_{20}	303.80	-65.20	0.718
Decane	$C_{10}H_{22}$	345.20	-22.00	0.73
Undecane	$C_{11}H_{24}$	384.80	-14.80	0.74
Dodecane	$C_{12}H_{26}$	420.80	14.00	0.749
Tridecane	$C_{13}H_{28}$	453.20	23.00	0.756
Cyclopentane	C_5H_{10}	120.20	-137.20	0.751
Cyclohexane	C_6H_{12}	177.33	43.70	0.779
Ethylene	C_2H_4	-154.66	-272.56	1.178
Propylene	C_3H_6	-53.68	-301.36	1.81
Benzene	C_6H_6	176.18	41.90	0.8765
Toluene	C_7H_8	231.08	-135.40	0.8669
Xylene	C_8H_{10}	281.30	-53.32	0.864
Ethylbenzene	C_8H_{10}	276.80	-139.00	0.8665
Styrene	C_8H_8	293.00	-23.08	0.91
C3-benzene	C_9H_{12}	318.20	-146.20	0.862

* Data from:

1. Wikipedia: http://en.wikipedia.org
2. National Institute of Standards and Technology (NIST) Chemistry WebBook: http://webbook.nist.gov/cgi/cbook.cgi?ID=C74828&Units=SI
3. International Programme on Chemical Safety (IPCS) webpage: http://www.inchem.org/

Table 30. General Physical Properties of the Organosulfur Compounds Present in Biogas*

Chemicals	Formula	Boiling point (°F)	Melting point (°F)	Density ($g \cdot cm^{-3}$)
Carbonyl Sulfide	OCS	-58.36	-217.84	Gas
Carbon Disulfide	CS_2	115.34	-167.44	1.261
Methyl Mercaptan	CH_4S	42.71	-189.40	0.9
Ethyl Mercaptan	C_2H_6S	95.00	-234.40	0.8617
i-Propyl Mercaptan	C_3H_8S	130.73	-204.07	0.814
n-Propyl Mercaptan	C_3H_8S	153.95	-171.67	0.84
t-Butyl Mercaptan	$C_4H_{10}S$	146.93	33.53	0.8
Dimethyl Sulfide	C_2H_6S	98.60	-144.40	0.84
Methyl Ethyl Sulfide	C_3H_8S	152.33	-159.07	0.827
Diethyl Sulfide	$C_4H_{10}S$	197.60	-154.84	0.837
Dimethyl Disulfide	$C_2H_6S_2$	229.73	-120.37	1.06
Diethyl Disulfide	$C_4H_{10}S_2$	308.93	-150.07	0.993
Methyl Ethyl Disulfide	$C_3H_8S_2$	276.80	NA	1.017
Thiophene	C_4H_4S	183.20	-36.40	1.051
C1-Thiophenes	$C_5H_{11}S$	NA	NA	NA
Thiophane	C_4H_8S	246.20	-140.80	1

* Data from:

1. Wikipedia: http://en.wikipedia.org
2. National Institute of Standards and Technology (NIST) Chemistry WebBook: http://webbook.nist.gov/cgi/cbook.cgi?ID=C74828&Units=SI
3. International Programme on Chemical Safety (IPCS) webpage: http://www.inchem.org/

Table 31. General Physical Properties of the Halocarbons Present in Biogas*

Chemicals	Formula	Boiling point (°F)	Melting point (°F)	Density ($g \cdot cm^{-3}$)
Dichlorodifluoromethane	CCl_2F_2	-21.64	-251.86	1.486 @ -21.6°F
1,2-Dichlorotetrafluoroethane	$C_2Cl_2F_4$	38.30	-137.20	1.455
1,1,2-Trichloro-1,2,2-trifluoroethane	$C_2Cl_3F_3$	117.86	-31.00	1.56
Trichlorofluoroethane	CCl_3F	74.79	-166.86	1.494
Chloromethane	CH_3Cl	-11.56	-143.86	0.002 @ 32°F
Vinylchloride	C_2H_3Cl	8.60	-245.20	0.91
1,1-Dichloroethane	$C_2H_4Cl_2$	134.96	-142.60	1.2
1,1-Dichloroethene	$C_2H_2Cl_2$	89.60	-187.60	1.213
1,4-Dichlorobenzene	$C_6H_4Cl_2$	345.20	128.30	1.25 (solid)

* Data from:

1. Wikipedia: http://en.wikipedia.org
2. National Institute of Standards and Technology (NIST) Chemistry WebBook: http://webbook.nist.gov/cgi/cbook.cgi?ID=C74828&Units=SI
3. International Programme on Chemical Safety (IPCS) webpage: http://www.inchem.org/

Table 32. General Physical Properties of the Organosilicon Compounds Present in Biogas*

Chemicals	Formula	Boiling point (°F)	Melting point (°F)	Density ($g \cdot cm^{-3}$)
Hexamethyldisilane	$C_6H1_8Si_2$	235.13	57.11	0.715
Octamethylcyclotetrasiloxane	$C_8H_{24}O_4Si_4$	346.73	62.33	0.956
Decamethylcyclopentasiloxane	$C_{10}H_{30}O_5Si_5$	194.00	-459.67	0.958
Decamethyltetrasiloxane	$C_{10}H_{30}O_3Si_4$	381.20	-90.40	0.854

* Data from:

1. Wikipedia: http://en.wikipedia.org
2. National Institute of Standards and Technology (NIST) Chemistry WebBook: http://webbook.nist.gov/cgi/cbook.cgi?ID=C74828&Units=SI
3. International Programme on Chemical Safety (IPCS) webpage: http://www.inchem.org/

Table 33. Solubility Parameters of the Compounds Presented in Biogas*

Group #	Gas Constituents	δ (Mpa)$^{1/2}$	H-Bonding Group
3	Methane	11.0	Poor
	Ethane	12.3	Poor
	Propane	13.1	Poor
	n-Butane	13.9	Poor
	i-Butane	14.5	Poor
	n-Pentane	14.3	Poor
	i-Pentane	13.8	Poor
	2,2,4-Trimethylpentane	14.0	Poor
	n-Hexane	14.9	Poor
	Heptanes	15.1	Poor
	Octanes	15.6	Poor
	Nonanes	15.8	Poor
	Decanes	15.8	Poor
	Undecanes	15.9	Poor
	Dodecanes	16.0	Poor
	Tridecanes	16.2	Poor
4	Cyclopentane	16.9	Poor
	Methylcyclopentane	16.1	Poor
	Cyclohexane	16.8	Poor
	Methylcyclohexane	16.1	Poor
5	Ethene	NA	NA
	Propene	NA	NA
	Pentenes	NA	NA
6	Benzene	18.8	Poor
	Toluene	18.2	Poor
	Ethylbenzene	18.0	Poor
	m,p-Xylene	18.0	Poor
	o-Xylene	17.8	Poor
	Styrene	19.0	Poor
	C3 benzene	17.6	Poor
7	Carbonyl Sulfide	NA	NA
	Carbon Disulfide	20.5	NA
	Methyl Mercaptan	NA	NA
	Ethyl Mercaptan	18.4	NA
	i-Propyl Mercaptan	17.1	NA
	n-Propyl Mercaptan	18.1	NA
	t-Butyl Mercaptan	15.9	NA
	Dimethyl Sulfide	18.6	NA
	Methyl Ethyl Sulfide	17.9	NA
	Diethyl Sulfide	17.4	NA

* Data from *Polymer Handbook* (Brandrup 1999)

Table 33. Solubility Parameters of the Compounds Presented in Biogas (Continued)*

Group #	Gas Constituents	Δ (Mpa)$^{1/2}$	H-Bonding Group
7	Dimethyl Disulfide	20.2	NA
	Diethyl Disulfide	NA	NA
	Methyl Ethyl Disulfide	NA	NA
	Methyl n-Propyl Disulfide	NA	NA
	Methyl t-Butyl Disulfide	NA	NA
	i-Propyl t-Butyl Disulfide	NA	NA
	Dimethyl Trisulfide	NA	NA
	Thiophene	20.1	NA
	C1-Thiophenes	NA	NA
	C2-Thiophenes	NA	NA
	Thiophane	20.4	NA
	Thiophneol	20.2	NA
8	Dichlorodifluoromethane (CFC-12)	12.5	NA
	1,2-Dichlorotetrafluoroethane (CFC-114)	12.9	NA
	1,1,2-Trichloro-1,2,2-trifluoroethane (CFC-113)	14.7	NA
	Trichlorofluoroethane (CFC-11)	15.5	NA
	Chloromethane	NA	NA
	Dichloromethane (Methylene Chloride)	17.7	NA
	Vinylchloride	16.0	Moderate
	1,1-Chloroethane	18.8	NA
	1,1-Dichloroethane	16.9	NA
	1,2-Dichloroethane	18.2	NA
	1,1,1-Trichloroethane	17.2	NA
	1,1-dichloroethene	17.3	NA
	cis-1,2-dichloroethene	NA	NA
	Trichloroethene	NA	NA
	Tetrachloroethene	NA	NA
	Chlorobenzene	19.4	NA
	1,2-Dichlorobenzene	20.5	NA
	1,3-Dichlorobenzene	NA	NA
	1,4-Dichlorobenzene	NA	NA
9	Hexamethyldisilane	NA	NA
	Hexamethyldisiloxane (L2)	NA	NA
	Octamethyltrisiloxane	NA	NA
	Octamethylcyclotetrasiloxane	NA	NA
	Decamethyltetrasiloxane	NA	NA
	Decamethylcyclopentasiloxane	NA	NA
	Trimethyl silanol	NA	NA
	Hexamethylcyclotrisiloxane	NA	NA

* Data from *Polymer Handbook* (Brandrup 1999)

Table 34. Solubility Parameters of the Selected Plastics and Elastomers*

Polymers			δ (Mpa)$^{1/2}$	
			Range	Average
Elastomers	SBR	BUNA S 94/6	16.6-16.5	17.3
		BUNA S 90/10	17.1	
		BUNA S 87.5/12.5	16.4-17.6	
		BUNA S 85/15	17.2-17.5	
		BUNA S 75/25	16.5-17.6	
		BUNA S 71.5/28.5	16.6-17.5	
		BUNA S 70/30	17.4	
		BUNA S 60/40	17.5-17.8	
		Polysar 5630	18.1	
	NBR	BUNA N 82/18	17.9-17.7	19.5
		BUNA N 82/20	18.4-19.4	
		BUNA N 82/18	17.7-17.9	
		BUNA N 80/20	18.4-19.4	
		BUNA N 75/25	18.2-19.4	
		BUNA N 70/30	19.2-20.3	
		BUNA N 61/39	20.5-21.4	
		Hycar (BFGoodrich)	21.0	
	CR		15.2-19.2	17.7
	SI		14.9-19.7	16.9
Plastics	PE		16.0-18.4	16.8
	PA11		19.2	
	PA12		19.0	

* Data from *Polymer Handbook* (Brandrup 1999)

Table 35. Vaporization Heat (ΔHvap), Molar Volumes (Vm) and the Calculated Solubility Parameters (δ)*

Gas Constituents	ΔHvap (kJ)	Vm (cm^3)	δ $(Mpa)^{1/2}$
i-Pentane (2-Methyl Butane)	24.85	117.46	13.8
n-Pentane	26.70	115.26	14.5
Undecane	56.40	210.81	16.0
Tridecane	66.43	243.39	16.2
Methylcyclopentane	31.63	112.38	16.1
Methylcyclohexane	35.36	127.27	16.1
o-Xylene (1,2-Dimethylbenzene)	41.00	106.00	19.1
m-Xylene (1,3-Dimethylbenzene)	41.00	106.00	19.1
p-Xylene (1,3-Dimethylbenzene)	41.00	106.00	19.1
Ethyl Mercaptan	27.30	72.11	18.6
i-Propyl Mercaptan	29.63	93.37	17.1
n-Propyl Mercaptan	32.00	90.48	18.1
t-Butyl Mercaptan	30.90	112.50	15.9
Dimethyl Sulfide	27.90	73.81	18.6
Methyl Ethyl Sulfide	32.00	91.90	17.9
Diethyl Sulfide	35.90	107.53	17.6
Dimethyl Disulfide	38.50	88.68	20.2
Thiophene	34.70	79.92	20.1
Thiophane	39.20	88.00	20.4
Thiophenol	47.56	110.00	20.2
1,1-dichloroethene	26.48	79.97	17.3
2,2,4-Trimethylpentane	35.14	165.70	14.0
Dichloromethane	29.00	85.00	17.7
1,1-Dichloroethane	30.80	99.00	16.9
1,2-Dichloroethane	35.20	99.00	18.2
1,1,1-trichloroethane	32.50	101.06	17.2
Chlorobenzene	41.00	101.40	19.5

* Data from:

1. National Institute of Standards and Technology (NIST) Chemistry WebBook: http://webbook.nist.gov/cgi/cbook.cgi?ID=C74828&Units=SI

Table 36. PE and PA12 Compatibility with the Organic Constituents in Biogas

Group #	Gas Constituents	δ (Mpa)$^{1/2}$	PE (Δδ) & Impact					PA12 (Δδ) & Impact	
			δ_{min}=16	δ_{max}=18.4	δ_{ave}=16.8	Min Δδ	Rating	δ=19	Rating
3	Methane	11	5	7.4	5.75	5	1	8	1
	Ethane	12.3	3.7	6.1	4.45	3.7	1	6.7	1
	Propane	13.1	2.9	5.3	3.65	2.9	2	5.9	1
	n-Butane	13.9	2.1	4.5	2.85	2.1	2	5.1	1
	i-Butane	14.5	1.5	3.9	2.25	1.5	3	4.5	1
	n-Pentane	14.3	1.7	4.1	2.45	1.7	3	4.7	1
	i-Pentane	13.8	2.2	4.6	2.95	2.2	2	5.2	1
	2,2,4-Trimethylpentane	14.0	2.0	4.4	2.7	2.0	3	5.0	1
	n-Hexane	14.9	1.1	3.5	1.85	1.1	3	4.1	1
	Heptanes	15.1	0.9	3.3	1.65	0.9	4	3.9	1
	Octanes	15.6	0.4	2.8	1.15	0.4	5	3.4	1
	Nonanes	15.8	0.2	2.6	0.95	0.2	5	3.2	1
	Decanes	15.8	0.2	2.6	0.95	0.2	5	3.2	1
	Undecanes	15.9	0.1	2.5	0.85	0.1	5	3.1	1
	Dodecanes	16	0	2.4	0.75	0	5	3	2
	Tridecanes	16.2	0.2	2.2	0.55	0.2	5	2.8	2
4	Cyclopentane	16.9	0.9	1.5	0.15	0.15	5	2.1	2
	Methylcyclopentane	16.1	0.1	2.3	0.65	0.1	5	2.9	2
	Cyclohexane	16.8	0.8	1.6	0.05	0.05	5	2.2	2
	Methylcyclohexane	16.1	0.07	2.33	0.68	0.07	5	2.93	2
5	Ethene	NA	NA	NA	NA	NA	**5**	NA	**5**
	Propene	NA	NA	NA	NA	NA	**5**	NA	**5**
	Pentenes	NA	NA	NA	NA	NA	**5**	NA	**5**

Table 36. PE and PA12 Compatibility with the Organic Constituents in Biogas (Continued)

Group #	Gas Constituents	δ (Mpa)$^{1/2}$	PE (Δδ) & Impact					PA12 (Δδ) & Impact	
			δ_{min}=16	δ_{max}=18.4	δ_{ave}=16.8	Min Δδ	Rating	δ=19	Rating
6	Benzene	18.8	2.8	0.4	2.1	0.4	5	0.2	5
	Toluene	18.2	2.2	0.2	1.5	0.2	5	0.8	4
	Ethylbenzene	18.0	2.0	0.4	1.3	0.4	5	1	4
	m,p-Xylene	18.0	2.0	0.4	1.3	0.4	5	1	4
	o-Xylene	17.8	1.8	0.6	1.1	0.6	4	1.2	3
	Styrene	19.0	3.0	0.6	2.3	0.6	4	0	5
	C3 benzene	17.6	1.6	0.8	0.9	0.8	4	1.4	3
7	Carbonyl Sulfide	NA	NA	NA	NA	NA	5	NA	5
	Carbon Disulfide	20.5	4.5	2.1	3.8	2.1	2	1.5	3
	Methyl Mercaptan	NA	NA	NA	NA	NA	5	NA	5
	Ethyl Mercaptan	18.4	2.4	0.0	1.7	0.0	5	0.6	4
	i-Propyl Mercaptan	17.1	1.1	1.4	0.3	0.3	5	2.0	3
	n-Propyl Mercaptan	18.1	2.1	0.3	1.3	0.3	5	0.9	4
	t-Butyl Mercaptan	15.9	0.1	2.5	0.9	0.1	5	3.1	1
	Dimethyl Sulfide	18.6	2.6	0.2	1.8	0.2	5	0.44	5
	Methyl Ethyl Sulfide	17.9	1.9	0.5	1.2	0.5	5	1.1	3
	Diethyl Sulfide	17.4	1.4	1.0	0.6	0.6	4	1.6	3
	Dimethyl Disulfide	20.2	4.2	1.8	3.4	1.8	3	1.2	3
	Diethyl Disulfide	NA	NA	NA	NA	NA	5	NA	5
	Methyl Ethyl Disulfide	NA	NA	NA	NA	NA	5	NA	5
	Methyl n-Propyl Disulfide	NA	NA	NA	NA	NA	5	NA	5
	Methyl t-Butyl Disulfide	NA	NA	NA	NA	NA	5	NA	5
	i-Propyl t-Butyl Disulfide	NA	NA	NA	NA	NA	5	NA	5
	Dimethyl Trisulfide	NA	NA	NA	NA	NA	5	NA	5
	Thiophene	20.1	4.1	1.7	3.3	1.7	3	1.1	3
	C1-Thiophenes	NA	NA	NA	NA	NA	5	NA	5
	C2-Thiophenes	NA	NA	NA	NA	NA	5	NA	5
	Thiophane	20.4	4.4	2.0	3.7	2.0	2	1.4	3
	Thiophneol	20.2	4.2	1.8	3.5	1.8	3	1.2	3

Table 36. PE and PA12 Compatibility with the Organic Constituents in Biogas (Continued)

Group #	Gas Constituents	δ (Mpa)$^{1/2}$	PE (Δδ) & Impact					PA12 Δδ & Impact	
			δ_{min}=16	δ_{max}=18.4	δ_{ave}=16.8	Min Δδ	Rating	δ=19	Rating
8	Dichlorodifluoromethane (CFC-12)	12.5	3.5	5.9	4.3	3.5	1	6.5	1
	1,2-Dichlorotetrafluoroethane (CFC-114)	12.9	3.1	5.5	3.9	3.1	1	6.1	1
	1,1,2-Trichloro-1,2,2-trifluoroethane (CFC-113)	14.7	1.3	3.7	2.1	1.3	3	4.3	1
	Trichlorofluoroethane (CFC-11)	15.5	0.5	2.9	1.3	0.5	5	3.5	1
	Chloromethane	NA	NA	NA	NA	NA	5	NA	5
	Dichloromethane (Methylene Chloride)	17.7	1.7	0.7	0.9	0.7	4	1.3	3
	Vinylchloride	16.0	0.0	2.4	0.8	0.0	5	3	2
	1,1-Chloroethane	18.8	2.8	0.4	2.1	0.4	5	0.2	5
	1,1-Dichloroethane	16.9	0.9	1.5	0.2	0.2	5	2.1	2
	1,2-Dichloroethane	18.2	2.2	0.2	1.4	0.2	5	0.8	4
	1,1,1-Trichloroethane	17.2	1.2	1.2	0.5	0.5	5	1.8	3
	1,1-dichloroethene	17.3	1.3	1.1	0.6	0.6	4	1.7	3
	cis-1,2-dichloroethene	NA	NA	NA	NA	NA	5	NA	5
	Trichloroethene	NA	NA	NA	NA	NA	5	NA	5
	Tetrachloroethene	NA	NA	NA	NA	NA	5	NA	5
	Chlorobenzene	19.4	3.4	1.0	2.7	1.0	4	0.4	5
	1,2-Dichlorobenzene	20.5	4.5	2.1	3.8	2.1	2	1.5	3
	1,3-Dichlorobenzene	NA	NA	NA	NA	NA	5	NA	5
	1,4-Dichlorobenzene	NA	NA	NA	NA	NA	5	NA	5
9	Hexamethyldisilane	NA	NA	NA	NA	NA	5	NA	5
	Hexamethyldisiloxane (L2)	NA	NA	NA	NA	NA	5	NA	5
	Octamethyltrisiloxane	NA	NA	NA	NA	NA	5	NA	5
	Octamethylcyclotetrasiloxane	NA	NA	NA	NA	NA	5	NA	5
	Decamethyltetrasiloxane	NA	NA	NA	NA	NA	5	NA	5
	Decamethylcyclopentasiloxane	NA	NA	NA	NA	NA	5	NA	5
	Trimethyl silanol	NA	NA	NA	NA	NA	5	NA	5
	Hexamethylcyclotrisiloxane	NA	NA	NA	NA	NA	5	NA	5

Table 37. SBR Compatibility with the Organic Constituents in Biogas

Group #	Gas Constituents	δ (Mpa)$^{1/2}$	SBR ($\Delta\delta$) & Impact				
			δ_{min}=16.4	δ_{max}=18.1	δ_{ave}=17.3	Min $\Delta\delta$	Rating
3	Methane	11	5.4	7.1	6.3	5.4	1
	Ethane	12.3	4.1	5.8	5.0	4.1	1
	Propane	13.1	3.3	5.0	4.2	3.3	1
	n-Butane	13.9	2.5	4.2	3.4	2.5	2
	i-Butane	14.5	1.9	3.6	2.8	1.9	3
	n-Pentane	14.3	2.1	3.8	3.0	2.1	2
	i-Pentane	13.8	2.6	4.3	3.5	2.6	2
	2,2,4-Trimethylpentane	14.0	2.4	4.1	3.3	2.4	2
	n-Hexane	14.9	1.5	3.2	2.4	1.5	3
	Heptanes	15.1	1.3	3.0	2.2	1.3	3
	Octanes	15.6	0.8	2.5	1.7	0.8	4
	Nonanes	15.8	0.6	2.3	1.5	0.6	4
	Decanes	15.8	0.6	2.3	1.5	0.6	4
	Undecanes	15.9	0.5	2.2	1.4	0.5	5
	Dodecanes	16	0.4	2.1	1.3	0.4	5
	Tridecanes	16.2	0.2	1.9	1.1	0.2	5
4	Cyclopentane	16.9	0.5	1.2	0.4	0.4	5
	Methylcyclopentane	16.1	0.3	2.0	1.2	0.3	5
	Cyclohexane	16.8	0.4	1.3	0.5	0.4	5
	Methylcyclohexane	16.1	0.3	2.0	1.2	0.3	5
5	Ethene	NA	NA	NA	NA	NA	**5**
	Propene	NA	NA	NA	NA	NA	**5**
	Pentenes	NA	NA	NA	NA	NA	**5**

Table 37. SBR Compatibility with the Organic Constituents in Biogas (Continued)

Group #	Gas Constituents	δ (Mpa)$^{1/2}$	SBR (Δδ) & Impact				
			δ_{min}=16.4	δ_{max}=18.1	δ_{ave}=17.3	Min Δδ	Rating
6	Benzene	18.8	2.4	0.7	1.5	0.7	4
	Toluene	18.2	1.8	0.1	0.9	0.1	5
	Ethylbenzene	18.0	1.6	0.1	0.7	0.1	5
	m,p-Xylene	18.0	1.6	0.1	0.7	0.1	5
	o-Xylene	17.8	1.4	0.3	0.6	0.3	5
	Styrene	19.0	2.6	0.9	1.7	0.9	4
	C3 benzene	17.6	1.2	0.5	0.3	0.3	5
7	Carbonyl Sulfide	NA	NA	NA	NA	NA	**5**
	Carbon Disulfide	20.5	4.1	2.4	3.2	2.4	2
	Methyl Mercaptan	NA	NA	NA	NA	NA	**5**
	Ethyl Mercaptan	18.4	2.0	0.3	1.1	0.3	5
	i-Propyl Mercaptan	17.1	0.7	1.1	0.2	0.2	5
	n-Propyl Mercaptan	18.1	1.7	0.0	0.8	0.0	5
	t-Butyl Mercaptan	15.9	0.5	2.2	1.4	0.5	4
	Dimethyl Sulfide	18.6	2.2	0.5	1.3	0.5	5
	Methyl Ethyl Sulfide	17.9	1.5	0.2	0.6	0.2	5
	Diethyl Sulfide	17.4	1.0	0.7	0.1	0.1	5
	Dimethyl Disulfide	20.2	3.8	2.1	2.9	2.1	2
	Diethyl Disulfide	NA	NA	NA	NA	NA	**5**
	Methyl Ethyl Disulfide	NA	NA	NA	NA	NA	**5**
	Methyl n-Propyl Disulfide	NA	NA	NA	NA	NA	**5**
	Methyl t-Butyl Disulfide	NA	NA	NA	NA	NA	**5**
	i-Propyl t-Butyl Disulfide	NA	NA	NA	NA	NA	**5**
	Dimethyl Trisulfide	NA	NA	NA	NA	NA	**5**
	Thiophene	20.1	3.7	2.0	2.8	2.0	3
	C1-Thiophenes	NA	NA	NA	NA	NA	5
	C2-Thiophenes	NA	NA	NA	NA	NA	**5**
	Thiophane	20.4	4.0	2.3	3.1	2.3	2
	Thiophneol	20.2	3.8	2.1	3.0	2.1	2

Table 37. SBR Compatibility with the Organic Constituents in Biogas (Continued)

Group #	Gas Constituents	δ (Mpa)$^{1/2}$	SBR (Δδ) & Impact				
			δ_{min}=16.4	δ_{max}=18.1	δ_{ave}=17.3	Min Δδ	Rating
8	Dichlorodifluoromethane (CFC-12)	12.5	3.9	5.6	4.8	3.9	1
	1,2-Dichlorotetrafluoroethane (CFC-114)	12.9	3.5	5.2	4.4	3.5	1
	1,1,2-Trichloro-1,2,2-trifluoroethane (CFC-113)	14.7	1.7	3.4	2.6	1.7	3
	Trichlorofluoroethane (CFC-11)	15.5	0.9	2.6	1.8	0.9	4
	Chloromethane	NA	NA	NA	NA	NA	**5**
	Dichloromethane (Methylene Chloride)	17.7	1.3	0.4	0.4	0.4	5
	Vinylchloride	16.0	0.4	2.1	1.3	0.4	5
	1,1-Chloroethane	18.8	2.4	0.7	1.5	0.7	4
	1,1-Dichloroethane	16.9	0.5	1.2	0.4	0.4	5
	1,2-Dichloroethane	18.2	1.8	0.1	0.9	0.1	5
	1,1,1-Trichloroethane	17.2	0.8	0.9	0.1	0.1	5
	1,1-dichloroethene	17.3	0.9	0.8	0.0	0.0	5
	cis-1,2-dichloroethene	NA	NA	NA	NA	NA	**5**
	Trichloroethene	NA	NA	NA	NA	NA	**5**
	Tetrachloroethene	NA	NA	NA	NA	NA	**5**
	Chlorobenzene	19.4	3.0	1.3	2.1	1.3	3
	1,2-Dichlorobenzene	20.5	4.1	2.4	3.2	2.4	2
	1,3-Dichlorobenzene	NA	NA	NA	NA	NA	**5**
	1,4-Dichlorobenzene	NA	NA	NA	NA	NA	**5**
9	Hexamethyldisilane	NA	NA	NA	NA	NA	**5**
	Hexamethyldisiloxane (L2)	NA	NA	NA	NA	NA	**5**
	Octamethyltrisiloxane	NA	NA	NA	NA	NA	**5**
	Octamethylcyclotetrasiloxane	NA	NA	NA	NA	NA	**5**
	Decamethyltetrasiloxane	NA	NA	NA	NA	NA	**5**
	Decamethylcyclopentasiloxane	NA	NA	NA	NA	NA	**5**
	Trimethyl silanol	NA	NA	NA	NA	NA	**5**
	Hexamethylcyclotrisiloxane	NA	NA	NA	NA	NA	**5**

Table 38. NBR Compatibility with the Organic Constituents in Biogas

Group #	Gas Constituents	δ (Mpa)$^{1/2}$	NBR (Δδ) & Impact				
			δ_{min}=17.7	δ_{max}=21	δ_{ave}=19.5	Min Δδ	Rating
3	Methane	11	6.7	10.0	8.5	6.7	1
	Ethane	12.3	5.4	8.7	7.2	5.4	1
	Propane	13.1	4.6	7.9	6.4	4.6	1
	n-Butane	13.9	3.8	7.1	5.6	3.8	1
	i-Butane	14.5	3.2	6.5	5.0	3.2	1
	n-Pentane	14.3	3.4	6.7	5.2	3.4	1
	i-Pentane	13.8	3.9	7.2	5.7	3.9	1
	2,2,4-Trimethylpentane	14.0	3.7	7.0	5.4	3.7	1
	n-Hexane	14.9	2.8	6.1	4.6	2.8	2
	Heptanes	15.1	2.6	5.9	4.4	2.6	2
	Octanes	15.6	2.1	5.4	3.9	2.1	2
	Nonanes	15.8	1.9	5.2	3.7	1.9	3
	Decanes	15.8	1.9	5.2	3.7	1.9	3
	Undecanes	15.9	1.8	5.1	3.6	1.8	3
	Dodecanes	16	1.7	5.0	3.5	1.7	3
	Tridecanes	16.2	1.5	4.8	3.3	1.5	3
4	Cyclopentane	16.9	0.8	4.1	2.6	0.8	4
	Methylcyclopentane	16.1	1.6	4.9	3.4	1.6	3
	Cyclohexane	16.8	0.9	4.2	2.7	0.9	4
	Methylcyclohexane	16.1	1.6	4.9	3.4	1.6	3
5	Ethene	NA	NA	NA	NA	NA	**5**
	Propene	NA	NA	NA	NA	NA	**5**
	Pentenes	NA	NA	NA	NA	NA	**5**

Table 38. NBR Compatibility with the Organic Constituents in Biogas (Continued)

Group #	Gas Constituents	δ (Mpa)$^{1/2}$	NBR (Δδ) & Impact				
			δ_{min}=17.7	δ_{max}=21	δ_{ave}=19.5	Min Δδ	Rating
6	Benzene	18.8	1.1	2.2	0.7	0.7	4
	Toluene	18.2	0.5	2.8	1.3	0.5	5
	Ethylbenzene	18.0	0.3	3.0	1.5	0.3	5
	m,p-Xylene	18.0	0.3	3.0	1.5	0.3	5
	o-Xylene	17.8	0.1	3.2	1.6	0.1	5
	Styrene	19.0	1.3	2.0	0.5	0.5	5
	C3 benzene	17.6	0.1	3.4	1.9	0.1	5
7	Carbonyl Sulfide	NA	NA	NA	NA	NA	**5**
	Carbon Disulfide	20.5	2.8	0.5	1.0	0.5	5
	Methyl Mercaptan	NA	NA	NA	NA	NA	**5**
	Ethyl Mercaptan	18.4	0.7	2.6	1.1	0.7	4
	i-Propyl Mercaptan	17.1	0.6	4.0	2.4	0.6	4
	n-Propyl Mercaptan	18.1	0.4	2.9	1.4	0.4	5
	t-Butyl Mercaptan	15.9	1.8	5.1	3.6	1.8	3
	Dimethyl Sulfide	18.6	0.9	2.4	0.9	0.9	4
	Methyl Ethyl Sulfide	17.9	0.2	3.1	1.5	0.2	5
	Diethyl Sulfide	17.4	0.3	3.6	2.1	0.3	5
	Dimethyl Disulfide	20.2	2.5	0.9	0.7	0.7	4
	Diethyl Disulfide	NA	NA	NA	NA	NA	**5**
	Methyl Ethyl Disulfide	NA	NA	NA	NA	NA	**5**
	Methyl n-Propyl Disulfide	NA	NA	NA	NA	NA	**5**
	Methyl t-Butyl Disulfide	NA	NA	NA	NA	NA	**5**
	i-Propyl t-Butyl Disulfide	NA	NA	NA	NA	NA	**5**
	Dimethyl Trisulfide	NA	NA	NA	NA	NA	**5**
	Thiophene	20.1	2.4	0.9	0.6	0.6	4
	C1-Thiophenes	NA	NA	NA	NA	NA	**5**
	C2-Thiophenes	NA	NA	NA	NA	NA	**5**
	Thiophane	20.4	2.7	0.6	1.0	0.6	4
	Thiophneol	20.2	2.5	0.8	0.8	0.8	4

Table 38. NBR Compatibility with the Organic Constituents in Biogas (Continued)

Group #	Gas Constituents	δ (Mpa)$^{1/2}$	NBR (Δδ) & Impact				
			δ_{min}=17.7	δ_{max}=21	δ_{ave}=19.5	Min Δδ	Rating
8	Dichlorodifluoromethane (CFC-12)	12.5	5.2	8.5	7.0	5.2	1
	1,2-Dichlorotetrafluoroethane (CFC-114)	12.9	4.8	8.1	6.6	4.8	1
	1,1,2-Trichloro-1,2,2-trifluoroethane (CFC-113)	14.7	3.0	6.3	4.8	3.0	2
	Trichlorofluoroethane (CFC-11)	15.5	2.2	5.5	4.0	2.2	2
	Chloromethane	NA	NA	NA	NA	NA	**5**
	Dichloromethane (Methylene Chloride)	17.7	0.0	3.3	1.8	0.0	5
	Vinylchloride	16.0	1.7	5.0	3.5	1.7	3
	1,1-Chloroethane	18.8	1.1	2.2	0.7	0.7	4
	1,1-Dichloroethane	16.9	0.8	4.1	2.6	0.8	4
	1,2-Dichloroethane	18.2	0.5	2.8	1.3	0.5	5
	1,1,1-Trichloroethane	17.2	0.5	3.8	2.2	0.5	5
	1,1-dichloroethene	17.3	0.4	3.7	2.2	0.4	5
	cis-1,2-dichloroethene	NA	NA	NA	NA	NA	**5**
	Trichloroethene	NA	NA	NA	NA	NA	**5**
	Tetrachloroethene	NA	NA	NA	NA	NA	**5**
	Chlorobenzene	19.4	1.7	1.6	0.1	0.1	5
	1,2-Dichlorobenzene	20.5	2.8	0.5	1.0	0.5	5
	1,3-Dichlorobenzene	NA	NA	NA	NA	NA	**5**
	1,4-Dichlorobenzene	NA	NA	NA	NA	NA	**5**
9	Hexamethyldisilane	NA	NA	NA	NA	NA	**5**
	Hexamethyldisiloxane (L2)	NA	NA	NA	NA	NA	**5**
	Octamethyltrisiloxane	NA	NA	NA	NA	NA	**5**
	Octamethylcyclotetrasiloxane	NA	NA	NA	NA	NA	**5**
	Decamethyltetrasiloxane	NA	NA	NA	NA	NA	**5**
	Decamethylcyclopentasiloxane	NA	NA	NA	NA	NA	**5**
	Trimethyl silanol	NA	NA	NA	NA	NA	**5**
	Hexamethylcyclotrisiloxane	NA	NA	NA	NA	NA	**5**

Table 39. CR Compatibility with the Organic Constituents in Biogas

Group #	Gas Constituents	δ (Mpa)$^{1/2}$	CR ($\Delta\delta$) & Impact				
			δ_{min}=15.2	δ_{max}=19.2	δ_{ave}=17.7	Min $\Delta\delta$	Rating
3	Methane	11	4.2	8.2	6.7	4.2	1
	Ethane	12.3	2.9	6.9	5.4	2.9	2
	Propane	13.1	2.1	6.1	4.6	2.1	2
	n-Butane	13.9	1.3	5.3	3.8	1.3	3
	i-Butane	14.5	0.7	4.7	3.2	0.7	4
	n-Pentane	14.3	0.9	4.9	3.4	0.9	4
	i-Pentane	13.8	1.4	5.4	3.9	1.4	3
	2,2,4-Trimethylpentane	14.0	1.2	5.2	3.7	1.2	3
	n-Hexane	14.9	0.3	4.3	2.8	0.3	5
	Heptanes	15.1	0.1	4.1	2.6	0.1	5
	Octanes	15.6	0.4	3.6	2.1	0.4	5
	Nonanes	15.8	0.6	3.4	1.9	0.6	4
	Decanes	15.8	0.6	3.4	1.9	0.6	4
	Undecanes	15.9	0.7	3.3	1.8	0.7	4
	Dodecanes	16	0.8	3.2	1.7	0.8	4
	Tridecanes	16.2	1.0	3.0	1.5	1.0	4
4	Cyclopentane	16.9	1.7	2.3	0.8	0.8	4
	Methylcyclopentane	16.1	0.9	3.1	1.6	0.9	4
	Cyclohexane	16.8	1.6	2.4	0.9	0.9	4
	Methylcyclohexane	16.1	0.9	3.1	1.7	0.9	4
5	Ethene	NA	NA	NA	NA	NA	**5**
	Propene	NA	NA	NA	NA	NA	**5**
	Pentenes	NA	NA	NA	NA	NA	**5**

Table 39. CR Compatibility with the Organic Constituents in Biogas (Continued)

Group #	Gas Constituents	δ (Mpa)$^{1/2}$	CR (Δδ) & Impact				
			δ_{min}=15.2	δ_{max}=19.2	δ_{ave}=17.7	Min Δδ	Rating
6	Benzene	18.8	3.6	0.4	1.1	0.4	5
	Toluene	18.2	3.0	1.0	0.5	0.5	5
	Ethylbenzene	18.0	2.8	1.2	0.3	0.3	5
	m,p-Xylene	18.0	2.8	1.2	0.3	0.3	5
	o-Xylene	17.8	2.6	1.4	0.1	0.1	5
	Styrene	19.0	3.8	0.2	1.3	0.2	5
	C3 benzene	17.6	2.4	1.6	0.1	0.1	5
7	Carbonyl Sulfide	NA	NA	NA	NA	NA	**5**
	Carbon Disulfide	20.5	5.3	1.3	2.8	1.3	3
	Methyl Mercaptan	NA	NA	NA	NA	NA	**5**
	Ethyl Mercaptan	18.4	3.2	0.8	0.7	0.7	4
	i-Propyl Mercaptan	17.1	1.9	2.2	0.7	0.7	4
	n-Propyl Mercaptan	18.1	2.9	1.1	0.3	0.3	5
	t-Butyl Mercaptan	15.9	0.7	3.3	1.8	0.7	4
	Dimethyl Sulfide	18.6	3.4	0.6	0.8	0.6	4
	Methyl Ethyl Sulfide	17.9	2.7	1.3	0.2	0.2	5
	Diethyl Sulfide	17.4	2.2	1.8	0.3	0.3	5
	Dimethyl Disulfide	20.2	5.0	0.9	2.4	0.9	4
	Diethyl Disulfide	NA	NA	NA	NA	NA	**5**
	Methyl Ethyl Disulfide	NA	NA	NA	NA	NA	**5**
	Methyl n-Propyl Disulfide	NA	NA	NA	NA	NA	**5**
	Methyl t-Butyl Disulfide	NA	NA	NA	NA	NA	**5**
	i-Propyl t-Butyl Disulfide	NA	NA	NA	NA	NA	**5**
	Dimethyl Trisulfide	NA	NA	NA	NA	NA	**5**
	Thiophene	20.1	4.9	0.9	2.4	0.9	4
	C1-Thiophenes	NA	NA	NA	NA	NA	**5**
	C2-Thiophenes	NA	NA	NA	NA	NA	**5**
	Thiophane	20.4	5.2	1.2	2.7	1.2	3
	Thiophneol	20.2	5.0	1.0	2.5	1.0	3

Table 39. CR Compatibility with the Organic Constituents in Biogas (Continued)

Group #	Gas Constituents	δ (Mpa)$^{1/2}$	CR (Δδ) & Impact				
			δ_{min}=15.2	δ_{max}=19.2	δ_{ave}=17.7	Min Δδ	Rating
8	Dichlorodifluoromethane (CFC-12)	12.5	2.7	6.7	5.2	2.7	2
	1,2-Dichlorotetrafluoroethane (CFC-114)	12.9	2.3	6.3	4.8	2.3	2
	1,1,2-Trichloro-1,2,2-trifluoroethane (CFC-113)	14.7	0.5	4.5	3.0	0.5	5
	Trichlorofluoroethane (CFC-11)	15.5	0.3	3.7	2.2	0.3	5
	Chloromethane	NA	NA	NA	NA	NA	**5**
	Dichloromethane (Methylene Chloride)	17.7	2.5	1.5	0.1	0.1	5
	Vinylchloride	16.0	0.8	3.2	1.7	0.8	4
	1,1-Chloroethane	18.8	3.6	0.4	1.1	0.4	5
	1,1-Dichloroethane	16.9	1.7	2.3	0.8	0.8	4
	1,2-Dichloroethane	18.2	3.0	1.0	0.5	0.5	5
	1,1,1-Trichloroethane	17.2	2.0	2.0	0.5	0.5	5
	1,1-dichloroethene	17.3	2.1	1.9	0.4	0.4	5
	cis-1,2-dichloroethene	NA	NA	NA	NA	NA	**5**
	Trichloroethene	NA	NA	NA	NA	NA	**5**
	Tetrachloroethene	NA	NA	NA	NA	NA	**5**
	Chlorobenzene	19.4	4.2	0.2	1.7	0.2	5
	1,2-Dichlorobenzene	20.5	5.3	1.3	2.8	1.3	3
	1,3-Dichlorobenzene	NA	NA	NA	NA	NA	**5**
	1,4-Dichlorobenzene	NA	NA	NA	NA	NA	**5**
9	Hexamethyldisilane	NA	NA	NA	NA	NA	**5**
	Hexamethyldisiloxane (L2)	NA	NA	NA	NA	NA	**5**
	Octamethyltrisiloxane	NA	NA	NA	NA	NA	**5**
	Octamethylcyclotetrasiloxane	NA	NA	NA	NA	NA	**5**
	Decamethyltetrasiloxane	NA	NA	NA	NA	NA	**5**
	Decamethylcyclopentasiloxane	NA	NA	NA	NA	NA	**5**
	Trimethyl silanol	NA	NA	NA	NA	NA	**5**
	Hexamethylcyclotrisiloxane	NA	NA	NA	NA	NA	**5**

Table 40. Silicon Rubber Compatibility with the Organic Constituents in Biogas

Group #	Gas Constituents	δ (Mpa)$^{1/2}$	SI ($\Delta\delta$) & Impact				
			δ_{min}=14.9	δ_{max}=19.7	δ_{ave}=16.9	Min $\Delta\delta$	Rating
3	Methane	11	3.9	8.7	5.9	3.9	1
	Ethane	12.3	2.6	7.4	4.6	2.6	2
	Propane	13.1	1.8	6.6	3.8	1.8	3
	n-Butane	13.9	1.0	5.8	3.0	1.0	4
	i-Butane	14.5	0.4	5.2	2.4	0.4	5
	n-Pentane	14.3	0.6	5.4	2.6	0.6	4
	i-Pentane	13.8	1.1	5.9	3.1	1.1	3
	2,2,4-Trimethylpentane	14.0	0.9	5.7	2.9	0.9	4
	n-Hexane	14.9	0.0	4.8	2.0	0.0	5
	Heptanes	15.1	0.2	4.6	1.8	0.2	5
	Octanes	15.6	0.7	4.1	1.3	0.7	4
	Nonanes	15.8	0.9	3.9	1.1	0.9	4
	Decanes	15.8	0.9	3.9	1.1	0.9	4
	Undecanes	15.9	1.0	3.8	1.0	1.0	4
	Dodecanes	16	1.1	3.7	0.9	0.9	4
	Tridecanes	16.2	1.3	3.5	0.7	0.7	4
4	Cyclopentane	16.9	2.0	2.8	0.0	0.0	5
	Methylcyclopentane	16.1	1.2	3.6	0.8	0.8	4
	Cyclohexane	16.8	1.9	2.9	0.1	0.1	5
	Methylcyclohexane	16.1	1.2	3.6	0.9	0.9	4
5	Ethene	NA	NA	NA	NA	NA	**5**
	Propene	NA	NA	NA	NA	NA	**5**
	Pentenes	NA	NA	NA	NA	NA	**5**

Table 40. Silicon Rubber Compatibility with the Organic Constituents in Biogas (Continued)

Group #	Gas Constituents	δ (Mpa)$^{1/2}$	SI (Δδ) & Impact				
			δ_{min}=14.9	δ_{max}=19.7	δ_{ave}=16.9	Min Δδ	Rating
6	Benzene	18.8	3.9	0.9	1.9	0.9	4
	Toluene	18.2	3.3	1.5	1.3	1.3	3
	Ethylbenzene	18.0	3.1	1.7	1.1	1.1	3
	m,p-Xylene	18.0	3.1	1.7	1.1	1.1	3
	o-Xylene	17.8	2.9	1.9	0.9	0.9	4
	Styrene	19.0	4.1	0.7	2.1	0.7	4
	C3 benzene	17.6	2.7	2.1	0.7	0.7	4
7	Carbonyl Sulfide	NA	NA	NA	NA	NA	**5**
	Carbon Disulfide	20.5	5.6	0.8	3.6	0.8	4
	Methyl Mercaptan	NA	NA	NA	NA	NA	**5**
	Ethyl Mercaptan	18.4	3.5	1.3	1.5	1.3	3
	i-Propyl Mercaptan	17.1	2.2	2.7	0.1	0.1	5
	n-Propyl Mercaptan	18.1	3.2	1.6	1.1	1.1	3
	t-Butyl Mercaptan	15.9	1.0	3.8	1.1	1.0	4
	Dimethyl Sulfide	18.6	3.7	1.1	1.6	1.1	3
	Methyl Ethyl Sulfide	17.9	3.0	1.8	1.0	1.0	4
	Diethyl Sulfide	17.4	2.5	2.3	0.5	0.5	5
	Dimethyl Disulfide	20.2	5.3	0.4	3.2	0.4	5
	Diethyl Disulfide	NA	NA	NA	NA	NA	**5**
	Methyl Ethyl Disulfide	NA	NA	NA	NA	NA	**5**
	Methyl n-Propyl Disulfide	NA	NA	NA	NA	NA	**5**
	Methyl t-Butyl Disulfide	NA	NA	NA	NA	NA	**5**
	i-Propyl t-Butyl Disulfide	NA	NA	NA	NA	NA	**5**
	Dimethyl Trisulfide	NA	NA	NA	NA	NA	**5**
	Thiophene	20.1	5.2	0.4	3.1	0.4	5
	C1-Thiophenes	NA	NA	NA	NA	NA	**5**
	C2-Thiophenes	NA	NA	NA	NA	NA	**5**
	Thiophane	20.4	5.5	0.7	3.5	0.7	4
	Thiophneol	20.2	5.3	0.5	3.3	0.5	4

Table 40. Silicon Rubber Compatibility with the Organic Constituents in Biogas (Continued)

Group #	Gas Constituents	δ (Mpa)$^{1/2}$	SI ($\Delta\delta$) & Impact				
			δ_{min}=14.9	δ_{max}=19.7	δ_{ave}=16.9	Min $\Delta\delta$	Rating
8	Dichlorodifluoromethane (CFC-12)	12.5	2.4	7.2	4.4	2.4	2
	1,2-Dichlorotetrafluoroethane (CFC-114)	12.9	2.0	6.8	4.0	2.0	3
	1,1,2-Trichloro-1,2,2-trifluoroethane (CFC-113)	14.7	0.2	5.0	2.2	0.2	5
	Trichlorofluoroethane (CFC-11)	15.5	0.6	4.2	1.4	0.6	4
	Chloromethane	NA	NA	NA	NA	NA	5
	Dichloromethane (Methylene Chloride)	17.7	2.8	2.0	0.7	0.7	4
	Vinylchloride	16.0	1.1	3.7	0.9	0.9	4
	1,1-Chloroethane	18.8	3.9	0.9	1.9	0.9	4
	1,1-Dichloroethane	16.9	2.0	2.8	0.0	0.0	5
	1,2-Dichloroethane	18.2	3.3	1.5	1.2	1.2	3
	1,1,1-Trichloroethane	17.2	2.3	2.5	0.3	0.3	5
	1,1-dichloroethene	17.3	2.4	2.4	0.4	0.4	5
	cis-1,2-dichloroethene	NA	NA	NA	NA	NA	5
	Trichloroethene	NA	NA	NA	NA	NA	5
	Tetrachloroethene	NA	NA	NA	NA	NA	5
	Chlorobenzene	19.4	4.5	0.3	2.5	0.3	5
	1,2-Dichlorobenzene	20.5	5.6	0.8	3.6	0.8	4
	1,3-Dichlorobenzene	NA	NA	NA	NA	NA	5
	1,4-Dichlorobenzene	NA	NA	NA	NA	NA	5
9	Hexamethyldisilane	NA	NA	NA	NA	NA	5
	Hexamethyldisiloxane (L2)	NA	NA	NA	NA	NA	5
	Octamethyltrisiloxane	NA	NA	NA	NA	NA	5
	Octamethylcyclotetrasiloxane	NA	NA	NA	NA	NA	5
	Decamethyltetrasiloxane	NA	NA	NA	NA	NA	5
	Decamethylcyclopentasiloxane	NA	NA	NA	NA	NA	5
	Trimethyl silanol	NA	NA	NA	NA	NA	5
	Hexamethylcyclotrisiloxane	NA	NA	NA	NA	NA	5

Table 41. Compatibility Analysis for PE and PA12 in Raw Landfill Biogas

Group #	Landfill Biogas		PE		PA12	
	Constituent	Weight	Impact	Score	Impact	Score
1	He	1	0	0	0	0
	H2	3	0	0	0	0
	N2	4	0	0	0	0
2	CO_2	5	0	0	1	5
	O_2	3	0	0	1	3
	CO	0	0	0	0	0
	H_2S	5	0	0	3	15
	SO_2	2	2	4	5	10
3	Methane	5	1	5	1	5
	Ethane	3	1	3	1	3
	Propane	4	2	8	1	4
	n-Butane	1	2	2	1	1
	i-Butane	3	3	9	1	3
	n-Pentane	2	3	6	1	2
	i-Pentane	3	2	6	1	3
	2,2,4-Trimethylpentane	2	3	6	1	2
	Hexane	4	3	12	1	4
	Heptanes	4	4	16	1	4
	Octanes	4	5	20	1	4
	Nonanes	4	5	20	1	4
	Decanes	4	5	20	1	4
	Undecanes	4	5	20	1	4
	Dodecanes	3	5	15	2	6
	Tridecanes	2	5	10	2	4
4	Cyclopentane	3	5	15	2	6
	Methylcyclopentane	3	5	15	2	6
	Cyclohexane	3	5	15	2	6
	Methylcyclohexane	3	5	15	2	6
5	Ethene	2	5	10	5	10
	Propene	3	5	15	5	15
	Pentenes	2	5	10	5	10
6	Benzene	3	5	15	5	15
	Toluene	4	5	20	4	16
	Ethylbenzene	3	5	15	4	12
	m,p-Xylene	4	5	20	4	16
	o-Xylene	3	4	12	3	9
	Styrene	3	4	12	5	15
	C3 benzene	4	4	16	3	12

Table 41. Compatibility Analysis for PE and PA12 in Raw Landfill Biogas (Continued)

Group #	Landfill Biogas		PE		PA12	
	Constituent	Weight	Impact	Score	Impact	Score
7	Carbonyl Sulfide	3	5	15	5	15
	Carbon Disulfide	2	2	4	3	6
	Methyl Mercaptan	3	5	15	5	15
	Ethyl Mercaptan	2	5	10	4	8
	i-Propyl Mercaptan	3	5	15	3	9
	n-Propyl Mercaptan	2	5	10	4	8
	t-Butyl Mercaptan	2	5	10	1	2
	Dimethyl Sulfide	4	5	20	5	20
	Methyl Ethyl Sulfide	2	5	10	3	6
	Diethyl Sulfide	1	4	4	3	3
	Dimethyl Disulfide	2	3	6	3	6
	Diethyl Disulfide	0	5	0	5	0
	Methyl Ethyl Disulfide	1	5	5	5	5
	Methyl n-Propyl Disulfide	1	5	5	5	5
	Methyl t-Butyl Disulfide	0	5	0	5	0
	i-Propyl t-Butyl Disulfide	1	5	5	5	5
	Dimethyl Trisulfide	1	5	5	5	5
	Thiophene	2	3	6	3	6
	C1-Thiophenes	2	5	10	5	10
	C2-Thiophenes	1	5	5	5	5
	Thiophane	2	2	4	3	6
	Thiophenol	1	3	3	3	3
8	Dichlorodifluoromethane (CFC-12)	4	1	4	1	4
	1,2-Dichlorotetrafluoroethane (CFC-114)	2	1	2	1	2
	1,1,2-Trichloro-1,2,2-trifluoroethane (CFC-113)	1	3	3	1	1
	Trichlorofluoroethane (CFC-11)	3	5	15	1	3
	Chloromethane	1	5	5	5	5
	Dichloromethane (Methylene Chloride)	4	4	16	3	12
	Vinylchloride	3	5	15	2	6
	Chloroethane	2	5	10	5	10
	1,1-Dichloroethane	2	5	10	2	4
	1,2-Dichloroethane	1	5	5	4	4
	1,1,1-Trichloroethane	2	5	10	3	6
	1,1-Dichloroethene	2	4	8	3	6
	cis-1,2-Dichloroethene	3	5	15	5	15
	Trichloroethene	3	5	15	5	15
	Tetrachloroethene	3	5	15	5	15
	Chlorobenzene	2	4	8	5	10
	1,2-Dichlorobenzene	1	2	2	3	3
	1,3-Dichlorobenzene	1	5	5	5	5
	1,4-Dichlorobenzene	1	5	5	5	5

Table 41. Compatibility Analysis for PE and PA12 in Raw Landfill Biogas (Continued)

Group #	Landfill Biogas		PE		PA12	
	Constituent	Weight	Impact	Score	Impact	Score
9	Hexamethyldisilane	3	5	15	5	15
	Hexamethyldisiloxane (L2)	2	5	10	5	10
	Octamethyltrisiloxane (L3)	1	5	5	5	5
	Octamethylcyclotetrasiloxane (D4)	3	5	15	5	15
	Decamethyltetrasiloxane (L4)	1	5	5	5	5
	Decamethylcyclopentasiloxane (D5)	3	5	15	5	15
	Trimethyl Silanol	3	5	15	5	15
	Hexamethylcyclotrisiloxane (D3)	2	5	10	5	10
10	Antimony	5	0	0	0	0
	Zinc	4	0	0	0	0
	Arsenic	5	0	0	0	0
	Mercury	3	0	0	0	0
Total				**862**		**663**

Table 42. Compatibility Analysis for PE and PA12 in Processed Landfill Biogas

Group #	Landfill Biogas		PE		PA12	
	Constituent	Weight	Impact	Score	Impact	Score
1	He	0	0	0	0	0
	H_2	2	0	0	0	0
	N_2	4	0	0	0	0
2	CO_2	3	0	0	1	3
	O_2	3	0	0	1	3
	CO	0	0	0	0	0
	H_2S	2	0	0	3	6
	SO_2	1	2	2	5	5
3	Methane	5	1	5	1	5
	Ethane	0	1	0	1	0
	Propane	4	2	8	1	4
	n-Butane	0	2	0	1	0
	i-Butane	3	3	9	1	3
	n-Pentane	0	3	0	1	0
	i-Pentane	0	2	0	1	0
	2,2,4-Trimethylpentane	0	3	0	1	0
	Hexane	3	3	9	1	3
	Heptanes	3	4	12	1	3
	Octanes	3	5	15	1	3
	Nonanes	3	5	15	1	3
	Decanes	3	5	15	1	3
	Undecanes	3	5	15	1	3
	Dodecanes	2	5	10	2	4
	Tridecanes		5	0	2	0
4	Cyclopentane	2	5	10	2	4
	Methylcyclopentane	2	5	10	2	4
	Cyclohexane	2	5	10	2	4
	Methylcyclohexane	2	5	10	2	4
5	Ethene	0	**5**	0	**5**	0
	Propene	3	**5**	15	**5**	15
	Pentenes	0	**5**	0	**5**	0
6	Benzene	2	5	10	5	10
	Toluene	3	5	15	4	12
	Ethylbenzene	2	5	10	4	8
	m,p-Xylene	2	5	10	4	8
	o-Xylene	2	4	8	3	6
	Styrene	0	4	0	5	0
	C3 benzene	2	4	8	3	6

Table 42. Compatibility Analysis for PE and PA12 in Processed Landfill Biogas (Continued)

Group #	Landfill Biogas		PE		PA12	
	Constituent	Weight	Impact	Score	Impact	Score
7	Carbonyl Sulfide	2	5	10	5	10
	Carbon Disulfide	0	2	0	3	0
	Methyl Mercaptan	0	5	0	5	0
	Ethyl Mercaptan	0	5	0	4	0
	i-Propyl Mercaptan	0	5	0	3	0
	n-Propyl Mercaptan	0	5	0	4	0
	t-Butyl Mercaptan	0	5	0	1	0
	Dimethyl Sulfide	2	5	10	5	10
	Methyl Ethyl Sulfide	0	5	0	3	0
	Diethyl Sulfide	0	4	0	3	0
	Dimethyl Disulfide	1	3	3	3	3
	Diethyl Disulfide	0	5	0	5	0
	Methyl Ethyl Disulfide	0	5	0	5	0
	Methyl n-Propyl Disulfide	0	5	0	5	0
	Methyl t-Butyl Disulfide	0	5	0	5	0
	i-Propyl t-Butyl Disulfide	0	5	0	5	0
	Dimethyl Trisulfide	0	5	0	5	0
	Thiophene	0	3	0	3	0
	C1-Thiophenes	0	5	0	5	0
	C2-Thiophenes	0	5	0	5	0
	Thiophane	0	2	0	3	0
	Thiophenol	0	3	0	3	0
8	Dichlorodifluoromethane (CFC-12)	3	1	3	1	3
	1,2-Dichlorotetrafluoroethane (CFC-114)	1	1	1	1	1
	1,1,2-Trichloro-1,2,2-trifluoroethane (CFC-113)	0	3	0	1	0
	Trichlorofluoroethane (CFC-11)	2	5	10	1	2
	Chloromethane	0	5	0	5	0
	Dichloromethane (Methylene Chloride)	0	4	0	3	0
	Vinylchloride	2	5	10	2	4
	Chloroethane	2	5	10	5	10
	1,1-Dichloroethane	0	5	0	2	0
	1,2-Dichloroethane	0	5	0	4	0
	1,1,1-Trichloroethane	0	5	0	3	0
	1,1-Dichloroethene	0	4	0	3	0
	cis-1,2-Dichloroethene	0	5	0	5	0
	Trichloroethene	0	5	0	5	0
	Tetrachloroethene	0	5	0	5	0
	Chlorobenzene	0	4	0	5	0
	1,2-Dichlorobenzene	0	2	0	3	0
	1,3-Dichlorobenzene	0	5	0	5	0
	1,4-Dichlorobenzene	0	5	0	5	0

Table 42. Compatibility Analysis for PE and PA12 in Processed Landfill Biogas (Continued)

Group #	Landfill Biogas		PE		PA12	
	Constituent	Weight	Impact	Score	Impact	Score
9	Hexamethyldisilane	0	5	0	5	0
	Hexamethyldisiloxane (L2)	0	5	0	5	0
	Octamethyltrisiloxane (L3)	0	5	0	5	0
	Octamethylcyclotetrasiloxane (D4)	3	5	15	5	15
	Decamethyltetrasiloxane (L4)	0	5	0	5	0
	Decamethylcyclopentasiloxane (D5)	0	5	0	5	0
	Trimethyl Silanol	0	5	0	5	0
	Hexamethylcyclotrisiloxane (D3)	0	5	0	5	0
10	Antimony	0	0	0	0	0
	Zinc	4	0	0	0	0
	Arsenic	0	0	0	0	0
	Mercury	1	0	0	0	0
Total				**323**		**210**

Table 43. Compatibility Analysis for SBR, NBR, CR and SI in Raw Landfill Biogas

Group #	Landfill Biogas		SBR		NBR		CR		SI	
	Gas Constituents	Weight	Impact	Score	Impact	Score	Impact	Score	Impact	Score
1	He	1	0	0	0	0	0	0	0	0
	H_2	3	0	0	0	0	0	0	0	0
	N_2	4	0	0	0	0	0	0	0	0
2	CO_2	5	3	15	3	15	0	0	0	0
	O_2	3	3	9	3	9	3	9	1	3
	CO	0	0	0	0	0	5	0	0	0
	H_2S	5	5	25	5	25	5	25	4	20
	SO_2	2	5	10	2	4	3	6	2	4
3	Methane	5	1	5	1	5	1	5	1	5
	Ethane	3	1	3	1	3	2	6	2	6
	Propane	4	1	4	1	4	2	8	3	12
	n-Butane	1	2	2	1	1	3	3	4	4
	i-Butane	3	3	9	1	3	4	12	5	15
	n-Pentane	2	2	4	1	2	4	8	4	8
	i-Pentane	3	2	6	1	3	3	9	3	9
	2,2,4-Trimethylpentane	2	2	4	1	2	3	6	4	8
	Hexane	4	3	12	2	8	5	20	5	20
	Heptanes	4	3	12	2	8	5	20	5	20
	Octanes	4	4	16	2	8	5	20	4	16
	Nonanes	4	4	16	3	12	4	16	4	16
	Decanes	4	4	16	3	12	4	16	4	16
	Undecanes	4	5	20	3	12	4	16	4	16
	Dodecanes	3	5	15	3	9	4	12	4	12
	Tridecanes	2	5	10	3	6	4	8	4	8
4	Cyclopentane	3	5	15	4	12	4	12	5	15
	Methylcyclopentane	3	5	15	3	9	4	12	4	12
	Cyclohexane	3	5	15	4	12	4	12	5	15
	Methylcyclohexane	3	5	15	3	9	4	12	4	12
5	Ethene	2	5	10	5	10	5	10	5	10
	Propene	3	5	15	5	15	5	15	5	15
	Pentenes	2	5	10	5	10	5	10	5	10

Table 43. Compatibility Analysis for SBR, NBR, CR and SI in Raw Landfill Biogas (Continued)

Group #	Landfill Biogas		SBR		NBR		CR		SI	
	Gas Constituents	Weight	Impact	Score	Impact	Score	Impact	Score	Impact	Score
6	Benzene	3	4	12	4	12	5	15	4	12
	Toluene	4	5	20	5	20	5	20	3	12
	Ethylbenzene	3	5	15	5	15	5	15	3	9
	m,p-Xylene	4	5	20	5	20	5	20	3	12
	o-Xylene	3	5	15	5	15	5	15	4	12
	Styren	3	4	12	5	15	5	15	4	12
	C3 benzene	4	5	20	5	20	5	20	4	16
7	Carbonyl Sulfide	3	5	15	5	15	5	15	5	15
	Carbon Disulfide	2	2	4	5	10	3	6	4	8
	Methyl Mercaptan	3	5	15	5	15	5	15	5	15
	Ethyl Mercaptan	2	5	10	4	8	4	8	3	6
	i-Propyl Mercaptan	3	5	15	4	12	4	12	5	15
	n-Propyl Mercaptan	2	5	10	5	10	5	10	3	6
	t-Butyl Mercaptan	2	4	8	3	6	4	8	4	8
	Dimethyl Sulfide	4	5	20	4	16	4	16	3	12
	Methyl Ethyl Sulfide	2	5	10	5	10	5	10	4	8
	Diethyl Sulfide	1	5	5	5	5	5	5	5	5
	Dimethyl Disulfide	2	2	4	4	8	4	8	5	10
	Diethyl Disulfide	0	5	0	5	0	5	0	5	0
	Methyl Ethyl Disulfide	1	5	5	5	5	5	5	5	5
	Methyl n-Propyl Disulfide	1	5	5	5	5	5	5	5	5
	Methyl t-Butyl Disulfide	0	5	0	5	0	5	0	5	0
	i-Propyl t-Butyl Disulfide	1	5	5	5	5	5	5	5	5
	Dimethyl Trisulfide	1	5	5	5	5	5	5	5	5
	Thiophene	2	3	6	4	8	4	8	5	10
	C1-Thiophenes	2	5	10	5	10	5	10	5	10
	C2-Thiophenes	1	5	5	5	5	5	5	5	5
	Thiophane	2	2	4	4	8	3	6	4	8
	Thiophneol	1	2	2	4	4	3	3	4	4
8	Dichlorodifluoromethane (CFC-12)	4	1	4	1	4	2	8	2	8
	1,2-Dichlorotetrafluoroethane (CFC-114)	2	1	2	1	2	2	4	3	6

Table 43. Compatibility Analysis for SBR, NBR, CR and SI in Raw Landfill Biogas (Continued)

Group #	Landfill Biogas		SBR		NBR		CR		SI	
	Gas Constituents	Weight	Impact	Score	Impact	Score	Impact	Score	Impact	Score
8	1,1,2-Trichloro-1,2,2-trifluoroethane (CFC-113)	1	3	3	2	2	5	5	5	5
	Trichlorofluoroethane (CFC-11)	3	4	12	2	6	5	15	4	12
	Chloromethane	1	5	5	5	5	5	5	5	5
	Dichloromethane (Methylene Chloride)	4	5	20	5	20	5	20	4	16
	Vinylchloride	3	5	15	3	9	4	12	4	12
	Chloroethane	2	4	8	4	8	5	10	4	8
	1,1-Dichloroethane	2	5	10	4	8	4	8	5	10
	1,2-Dichloroethane	1	5	5	5	5	5	5	3	3
	1,1,1-Trichloroethane	2	5	10	5	10	5	10	5	10
	1,1-dichloroethene	2	5	10	5	10	5	10	5	10
	cis-1,2-dichloroethene	3	5	15	5	15	5	15	5	15
	Trichloroethene	3	5	15	5	15	5	15	5	15
	Tetrachloroethene	3	5	15	5	15	5	15	5	15
	Chlorobenzene	2	3	6	5	10	5	10	5	10
	1,2-Dichlorobenzene	1	2	2	5	5	3	3	4	4
	1,3-Dichlorobenzene	1	5	5	5	5	5	5	5	5
	1,4-Dichlorobenzene	1	5	5	5	5	5	5	5	5
9	Hexamethyldisilane	3	5	15	5	15	5	15	5	15
	Hexamethyldisiloxane (L2)	2	5	10	5	10	5	10	5	10
	Octamethyltrisiloxane	1	5	5	5	5	5	5	5	5
	Octamethylcyclotetrasiloxane	3	5	15	5	15	5	15	5	15
	Decamethyltetrasiloxane	1	5	5	5	5	5	5	5	5
	Decamethylcyclopentasiloxane	3	5	15	5	15	5	15	5	15
	Trimethyl silanol	3	5	15	5	15	5	15	5	15
	Hexamethylcyclotrisiloxane	2	5	10	5	10	5	10	5	10
10	Antimony	5	0	0	0	0	0	0	0	0
	Zinc	4	0	0	0	0	0	0	0	0
	Arsenic	5	0	0	0	0	0	0	0	0
	Mercury	3	0	0	0	0	0	0	0	0
Total				**892**		**814**		**913**		**871**

Table 44. Compatibility Analysis for SBR, NBR, CR and SI in Processed Landfill Biogas

Group #	Landfill Biogas		SBR		NBR		CR		SI	
	Gas Constituents	Weight	Impact	Score	Impact	Score	Impact	Score	Impact	Score
1	He	0	0	0	0	0	0	0	0	0
	H_2	2	0	0	0	0	0	0	0	0
	N_2	4	0	0	0	0	0	0	0	0
2	CO_2	3	3	9	3	9	0	0	0	0
	O_2	3	3	9	3	9	3	9	1	3
	CO	0	0	0	0	0	5	0	0	0
	H_2S	2	5	10	5	10	5	10	4	8
	SO_2	1	5	5	2	2	3	3	2	2
3	Methane	5	1	5	1	5	1	5	1	5
	Ethane	0	1	0	1	0	2	0	2	0
	Propane	4	1	4	1	4	2	8	3	12
	n-Butane	0	2	0	1	0	3	0	4	0
	i-Butane	3	3	9	1	3	4	12	5	15
	n-Pentane	0	2	0	1	0	4	0	4	0
	i-Pentane	0	2	0	1	0	3	0	3	0
	2,2,4-Trimethylpentane	0	2	0	1	0	3	0	4	0
	Hexane	3	3	9	2	6	5	15	5	15
	Heptanes	3	3	9	2	6	5	15	5	15
	Octanes	3	4	12	2	6	5	15	4	12
	Nonanes	3	4	12	3	9	4	12	4	12
	Decanes	3	4	12	3	9	4	12	4	12
	Undecanes	3	5	15	3	9	4	12	4	12
	Dodecanes	2	5	10	3	6	4	8	4	8
	Tridecanes	0	5	0	3	0	4	0	4	0
4	Cyclopentane	2	5	10	4	8	4	8	5	10
	Methylcyclopentane	2	5	10	3	6	4	8	4	8
	Cyclohexane	2	5	10	4	8	4	8	5	10
	Methylcyclohexane	2	5	10	3	6	4	8	4	8
5	Ethene	0	**5**	0	**5**	0	**5**	0	**5**	0
	Propene	3	**5**	15	**5**	15	**5**	15	**5**	15
	Pentenes	0	**5**	0	**5**	0	**5**	0	**5**	0

Table 44. Compatibility Analysis for SBR, NBR, CR and SI in Processed Landfill Biogas (Continued)

Group #	Landfill Biogas		SBR		NBR		CR		SI	
	Gas Constituents	Weight	Impact	Score	Impact	Score	Impact	Score	Impact	Score
6	Benzene	2	4	8	4	8	5	10	4	8
	Toluene	3	5	15	5	15	5	15	3	9
	Ethylbenzene	2	5	10	5	10	5	10	3	6
	m,p-Xylene	2	5	10	5	10	5	10	3	6
	o-Xylene	2	5	10	5	10	5	10	4	8
	Styrene		4	0	5	0	5	0	4	0
	C3 benzene	2	5	10	5	10	5	10	4	8
7	Carbonyl Sulfide	2	5	10	5	10	5	10	5	10
	Carbon Disulfide		2	0	5	0	3	0	4	0
	Methyl Mercaptan		5	0	5	0	5	0	5	0
	Ethyl Mercaptan		5	0	4	0	4	0	3	0
	i-Propyl Mercaptan		5	0	4	0	4	0	5	0
	n-Propyl Mercaptan		5	0	5	0	5	0	3	0
	t-Butyl Mercaptan		4	0	3	0	4	0	4	0
	Dimethyl Sulfide	2	5	10	4	8	4	8	3	6
	Methyl Ethyl Sulfide		5	0	5	0	5	0	4	0
	Diethyl Sulfide		5	0	5	0	5	0	5	0
	Dimethyl Disulfide	1	2	2	4	4	4	4	5	5
	Diethyl Disulfide		5	0	5	0	5	0	5	0
	Methyl Ethyl Disulfide		5	0	5	0	5	0	5	0
	Methyl n-Propyl Disulfide		5	0	5	0	5	0	5	0
	Methyl t-Butyl Disulfide		5	0	5	0	5	0	5	0
	i-Propyl t-Butyl Disulfide		5	0	5	0	5	0	5	0
	Dimethyl Trisulfide		5	0	5	0	5	0	5	0
	Thiophene		3	0	4	0	4	0	5	0
	C1-Thiophenes		5	0	5	0	5	0	5	0
	C2-Thiophenes		5	0	5	0	5	0	5	0
	Thiophane		2	0	4	0	3	0	4	0
	Thiophneol		2	0	4	0	3	0	4	0
8	Dichlorodifluoromethane (CFC-12)	3	1	3	1	3	2	6	2	6
	1,2-Dichlorotetrafluoroethane (CFC-114)	1	1	1	1	1	2	2	3	3

Table 44. Compatibility Analysis for SBR, NBR, CR and SI in Processed Landfill Biogas (Continued)

Group #	Landfill Biogas		SBR		NBR		CR		SI	
	Gas Constituents	Weight	Impact	Score	Impact	Score	Impact	Score	Impact	Score
8	1,1,2-Trichloro-1,2,2-trifluoroethane (CFC-113)	0	3	0	2	0	5	0	5	0
	Trichlorofluoroethane (CFC-11)	2	4	8	2	4	5	10	4	8
	Chloromethane	0	5	0	5	0	5	0	5	0
	Dichloromethane (Methylene Chloride)	0	5	0	5	0	5	0	4	0
	Vinylchloride	0	5	0	3	0	4	0	4	0
	Chloroethane	2	4	8	4	8	5	10	4	8
	1,1-Dichloroethane	0	5	0	4	0	4	0	5	0
	1,2-Dichloroethane	0	5	0	5	0	5	0	3	0
	1,1,1-Trichloroethane	0	5	0	5	0	5	0	5	0
	1,1-dichloroethene	0	5	0	5	0	5	0	5	0
	cis-1,2-dichloroethene	0	5	0	5	0	5	0	5	0
	Trichloroethene	0	5	0	5	0	5	0	5	0
	Tetrachloroethene	0	5	0	5	0	5	0	5	0
	Chlorobenzene	0	3	0	5	0	5	0	5	0
	1,2-Dichlorobenzene	0	2	0	5	0	3	0	4	0
	1,3-Dichlorobenzene	0	5	0	5	0	5	0	5	0
	1,4-Dichlorobenzene	0	5	0	5	0	5	0	5	0
9	Hexamethyldisilane	0	5	0	5	0	5	0	5	0
	Hexamethyldisiloxane (L2)	0	5	0	5	0	5	0	5	0
	Octamethyltrisiloxane	0	5	0	5	0	5	0	5	0
	Octamethylcyclotetrasiloxane	3	5	15	5	15	5	15	5	15
	Decamethyltetrasiloxane	0	5	0	5	0	5	0	5	0
	Decamethylcyclopentasiloxane	0	5	0	5	0	5	0	5	0
	Trimethyl silanol	0	5	0	5	0	5	0	5	0
	Hexamethylcyclotrisiloxane	0	5	0	5	0	5	0	5	0
10	Antimony	0	0	0	0	0	0	0	0	0
	Zinc	4	0	0	0	0	0	0	0	0
	Arsenic	0	0	0	0	0	0	0	0	0
	Mercury	1	0	0	0	0	0	0	0	0
Total		0		**325**		**272**		**333**		**308**

Table 45. Compatibility Analysis for PE and PA12 in Raw Dairy Biogas

Group #	Dairy Farm Biogas		PE		PA12	
	Gas Constituents	Weight	Impact	Score	Impact	Score
1	H_2	0	0	0	0	0
	N_2	4	0	0	0	0
2	CO_2	5	0	0	1	5
	O_2	3	0	0	1	3
	H_2S	5	0	0	3	15
	SO_2	3	2	6	5	15
	Ammonia	4	0	0	0	0
3	Methane	5	1	5	1	5
	Propane	0	2	0	1	0
	Hexane	3	3	9	1	3
	Heptanes	2	4	8	1	2
	Undecanes	0	5	0	1	0
4	Cyclopentane	2	4	8	3	6
6	Benzene	1	5	5	5	5
	Toluene	3	5	15	4	12
	Ethylbenzene	0	5	0	4	0
	m,p-Xylene	0	5	0	4	0
	o-Xylene	0	5	0	4	0
	Styrene	0	4	0	5	0
	C3 benzene	2	4	8	3	6
7	Carbonyl Sulfide	3	**5**	15	**5**	15
	Carbon Disulfide	1	2	2	3	3
	Methyl Mercaptan	3	**5**	15	**5**	15
	Ethyl Mercaptan	2	5	10	5	10
	i-Propyl Mercaptan	2	5	10	3	6
	n-Propyl Mercaptan	1	5	5	4	4
	t-Butyl Mercaptan	2	5	10	1	2
	Dimethyl Sulfide	2	5	10	5	10
	Dimethyl Disulfide	1	3	3	3	3
	Diethyl Disulfide	0	**5**	0	**5**	0
	Thiophene	1	3	3	3	3
8	Dichlorodifluoromethane	0	1	0	1	0
	Vinylchloride	0	5	0	2	0
	1,4-dichlorobenzene	0	2	0	3	0
9	Hexamethyldisilane	0	**5**	0	**5**	
	Octamethylcyclotetrasiloxane (D4)	0	**5**	0	**5**	0
	Decamethylcyclopentasiloxane (D5)	0	**5**	0	**5**	0
10	Mercury	1	0	0	0	0
	Copper	0	0	0	0	0
	Molybdenum	0	0	0	0	0
Total				**177**		**178**

Table 46. Compatibility Analysis for PE and PA12 in Processed Dairy Biogas

Group #	Dairy Farm Biogas		PE		PA12	
	Gas Constituents	Weight	Impact	Score	Impact	Score
1	H_2	0	0	0	0	0
	N_2	3	0	0	0	0
2	CO_2	2	0	0	1	2
	O_2	2	0	0	1	2
	H_2S	0	0	0	3	0
	SO_2	0	2	0	5	0
	Ammonia	0	0	0	0	0
3	Methane	5	1	5	1	5
	Propane	0	2	0	1	0
	Hexane	0	3	0	1	0
	Heptanes	0	4	0	1	0
	Undecanes	0	5	0	1	0
4	Cyclopentane	0	4	0	3	0
6	Benzene	0	5	0	5	0
	Toluene	0	5	0	4	0
	Ethylbenzene	0	5	0	4	0
	m,p-Xylene	0	5	0	4	0
	o-Xylene	0	5	0	4	0
	Styrene	0	4	0	5	0
	C3 benzene	0	4	0	3	0
7	Carbonyl Sulfide	3	**5**	15	**5**	15
	Carbon Disulfide	0	2	0	3	0
	Methyl Mercaptan	0	**5**	0	**5**	0
	Ethyl Mercaptan	0	5	0	5	0
	i-Propyl Mercaptan	0	5	0	3	0
	n-Propyl Mercaptan	0	5	0	4	0
	t-Butyl Mercaptan	0	5	0	1	0
	Dimethyl Sulfide	0	5	0	5	0
	Dimethyl Disulfide	0	3	0	3	0
	Diethyl Disulfide	0	**5**	0	**5**	0
	Thiophene	0	3	0	3	0
8	Dichlorodifluoromethane	0	1	0	1	0
	Vinylchloride	0	5	0	2	0
	1,4-dichlorobenzene	0	2	0	3	0
9	Hexamethyldisilane	0	**5**		**5**	
	Octamethylcyclotetrasiloxane (D4)	0	**5**	0	**5**	0
	Decamethylcyclopentasiloxane (D5)	0	**5**	0	**5**	0
10	Mercury	0	0	0	0	0
	Copper	0	0	0	0	0
	Molybdenum	0	0	0	0	0
Total				**20**		**24**

Table 47. Compatibility Analysis for SBR, NBR, CR and SI in Raw Dairy Biogas

Group #	Dairy Farm Biogas		SBR		NBR		CR		SI	
	Gas Constituents	Weight	Impact	Score	Impact	Score	Impact	Score	Impact	Score
1	H_2	0	0	0	0	0	0	0	0	0
	N_2	4	0	0	0	0	0	0	0	0
2	CO_2	5	3	15	3	15	0	0	0	0
	O_2	3	3	9	3	9	3	9	1	3
	H2S	5	5	25	5	25	5	25	4	20
	SO_2	3	5	15	2	6	3	9	2	6
	Ammonia	4	5	20	0	0	0	0	0	0
3	Methane	5	1	5	1	5	1	5	1	5
	Propane	0	1	0	1	0	2	0	3	0
	Hexane	3	3	9	2	6	5	15	5	15
	Heptanes	2	3	6	2	4	5	10	5	10
	Undecanes	0	5	0	3	0	4	0	4	0
4	Cyclopentanes	2	5	10	5	10	5	10	4	8
6	Benzene	1	4	4	4	4	5	5	4	4
	Toluene	3	5	15	5	15	5	15	3	9
	Ethylbenzene	0	5	0	5	0	5	0	3	0
	m,p-Xylene	0	5	0	5	0	5	0	3	0
	o-Xylene	0	5	0	5	0	5	0	3	0
	Styrene	0	4	0	5	0	5	0	4	0
	C3 benzene	2	5	10	5	10	5	10	4	8

Table 47. Compatibility Analysis for SBR, NBR, CR and SI in Raw Dairy Biogas (Continued)

Group #	Dairy Farm Biogas		SBR		NBR		CR		SI	
	Gas Constituents	Weight	Impact	Score	Impact	Score	Impact	Score	Impact	Score
7	Carbonyl Sulfide	3	5	15	5	15	5	15	5	15
	Carbon Disulfide	1	2	2	5	5	3	3	4	4
	Methyl Mercaptan	3	5	15	5	15	5	15	5	15
	Ethyl Mercaptan	2	5	10	4	8	4	8	3	6
	i-Propyl Mercaptan	2	5	10	4	8	4	8	5	10
	n-Propyl Mercaptan	1	5	5	5	5	5	5	3	3
	t-Butyl Mercaptan	2	4	8	3	6	4	8	4	8
	Dimethyl Sulfide	2	5	10	4	8	4	8	3	6
	Dimethyl Disulfide	1	2	2	4	4	4	4	5	5
	Diethyl Disulfide	0	5	0	5	0	5	0	5	0
	Thiophene	1	3	3	4	4	4	4	5	5
8	Dichlorodifluoromethane	0	1	0	1	0	2	0	2	0
	Vinylchloride	0	5	0	3	0	4	0	4	0
	1,4-dichlorobenzene	0	2	0	5	0	3	0	4	0
9	Hexamethydisilane	0	5	0	5	0	5	0	5	0
	Octamethylcyclotetrasiloxane (D4)	0	5	0	5	0	5	0	5	0
	Decamethylcyclopentasiloxane (D5)	0	5	0	5	0	5	0	5	0
10	Mercury	1	0	0	0	0	0	0	0	0
	Copper	0	0	0	0	0	0	0	0	0
	Molybdenum	0	0	0	0	0	0	0	0	0
Total				**253**		**217**		**246**		**195**

Table 48. Compatibility Analysis for SBR, NBR, CR and SI in Processed Dairy Biogas

Group #	Dairy Farm Biogas		SBR		NBR		CR		SI	
	Gas Constituents	Weight	Impact	Score	Impact	Score	Impact	Score	Impact	Score
1	H_2	0	0	0	0	0	0	0	0	0
	N_2	3	0	0	0	0	0	0	0	0
2	CO_2	2	3	6	3	6	0	0	0	0
	O_2	2	3	6	3	6	3	6	1	2
	H_2S	0	4	0	4	0	5	0	4	0
	SO_2	0	5	0	2	0	3	0	2	0
	Ammonia	0	5	0	0	0	0	0	0	0
3	Methane	5	1	5	1	5	1	5	1	5
	Propane	0	1	0	1	0	2	0	3	0
	Hexane	0	3	0	2	0	5	0	5	0
	Heptanes	0	3	0	2	0	5	0	5	0
	Undecanes	0	5	0	3	0	4	0	4	0
4	Cyclopentanes	0	5	0	5	0	5	0	4	0
6	Benzene	0	4	0	4	0	5	0	4	0
	Toluene	0	5	0	5	0	5	0	3	0
	Ethylbenzene	0	5	0	5	0	5	0	3	0
	m,p-Xylene	0	5	0	5	0	5	0	3	0
	o-Xylene	0	5	0	5	0	5	0	3	0
	Styrene	0	4	0	5	0	5	0	4	0
	C3 benzene	0	5	0	5	0	5	0	4	0

Table 48. Compatibility Analysis for SBR, NBR, CR and SI in Processed Dairy Biogas (Continued)

Group #	Dairy Farm Biogas		SBR		NBR		CR		SI	
	Gas Constituents	Weight	Impact	Score	Impact	Score	Impact	Score	Impact	Score
7	Carbonyl Sulfide	3	5	15	5	15	5	15	5	15
	Carbon Disulfide	0	2	0	5	0	3	0	4	0
	Methyl Mercaptan	0	5	0	5	0	5	0	5	0
	Ethyl Mercaptan	0	5	0	4	0	4	0	3	0
	i-Propyl Mercaptan	0	5	0	4	0	4	0	5	0
	n-Propyl Mercaptan	0	5	0	5	0	5	0	3	0
	t-Butyl Mercaptan	0	4	0	3	0	4	0	4	0
	Dimethyl Sulfide	0	5	0	4	0	4	0	3	0
	Dimethyl Disulfide	0	2	0	4	0	4	0	5	0
	Diethyl Disulfide	0	5	0	5	0	5	0	5	0
	Thiophene	0	3	0	4	0	4	0	5	0
8	Dichlorodifluoromethane	0	1	0	1	0	2	0	2	0
	Vinylchloride	0	5	0	3	0	4	0	4	0
	1,4-dichlorobenzene	0	2	0	5	0	3	0	4	0
9	Hexamethydisilane	0	5	0	5	0	5	0	5	0
	Octamethylcyclotetrasiloxane (D4)	0	5	0	5	0	5	0	5	0
	Decamethylcyclopentasiloxane (D5)	0	5	0	5	0	5	0	5	0
10	Mercury	0	0	0	0	0	0	0	0	0
	Copper	0	0	0	0	0	0	0	0	0
	Molybdenum	0	0	0	0	0	0	0	0	0
Total				**32**		**32**		**26**		**22**

Table 49. Baseline and Comparative Testing Methods

Test	Property	Test Method/Procedure	Material	
			Plastics	Elastomers
Baseline	Density	Helium Pycnometer/PP300	X	X
	Glass Transition Temperature	DSC/ASTM D 3418	X	X
	Chemical Makeup	FTIR/ASTM D3677	X	X
	Extractable Content	ASTM D 297	NA	X
Comparative	Compression	ASTM D 575	NA	X
	Dimensional Change	TMA/ASTM E831 (modified)	X	X
	Hardness	ASTM D2240	X	X
	Tensile Strength	ASTM D638	X	NA
		ASTM D412	NA	X
	Slow Crack Growth	ASTM F1473	X	NA
	SEM-EDX Analysis	ASTM E986	X	X

Table 50. Baseline Testing Matrix

Baseline Test	# of Test Specimen			
	PE	NBR	SBR	Total #
Density	3	3	3	9
Glass Transition Temperature	3	3	3	9
Chemical Makeup	1	1	1	3
Extractable Content	NA	1	1	2
Total	7	8	8	23

Table 51. Comparative Test Matrix

Saturation Test (Gas Sample)	Property Test	# of Specimens			
		PE	NBR	SBR	Total
No Gas Exposure	Compression	6	6	6	18
	Dimensional Change*	0	0	0	0
	Hardness	5	5	5	15
	Tensile Strength	6	6	6	18
	Slow Crack Growth Resistance	3	NA	NA	3
Raw Landfill	Compression	6	6	6	18
	Dimensional Change	3	3	3	9
	Hardness	5	5	5	15
	Tensile Strength	6	6	6	18
	Slow Crack Growth Resistance	3	NA	NA	3
	SEM Analysis	1	1	1	3
Processed Landfill	Compression	6	6	6	18
	Dimensional Change	3	3	3	9
	Hardness	5	5	5	15
	Tensile Strength	6	6	6	18
	Slow Crack Growth Resistance	3	NA	NA	3
	SEM Analysis	1	1	1	3
Raw Dairy	Compression	6	6	6	18
	Dimensional Change	3	3	3	9
	Hardness	5	5	5	15
	Tensile Strength	6	6	6	18
	Slow Crack Growth Resistance	3	NA	NA	3
	SEM Analysis	1	1	1	3
Standard Natural Gas	Compression	6	6	6	18
	Dimensional Change	3	3	3	9
	Hardness	5	5	5	15
	Tensile Strength	6	6	6	18
	Slow Crack Growth Resistance	3	NA	NA	3
	SEM Analysis	1	1	1	3
Total		**116**	**101**	**101**	**318**

*: Specimen dimension will be measured before and after saturation test on the same specimen. No additional specimen is required.

Table 52. Comparative Test Specimens

Property Test	Test Method	Dimension (inch)			
		Diameter	Length	Width	Thickness
Compression	ASTM D 575	1.129	NA	NA	0.51
Dimensional Change	TMA/ASTM E831 (modified)	NA	0.25	0.25	0.25
Hardness	ASTM D2240	NA	2	2	0.25
Tensile Strength	ASTM D638	NA	2.25	0.75	0.25
	ASTM D412	NA	4.5	1	0.08
Slow Crack Growth Resistance	ASTM F1473	NA	2	1	0.25

Table 53. FuelMaker FM4 Compressor Specifications

Specification	Rating
Minimum Gas Inlet Pressure	7 in. WC
Maximum Gas Inlet Pressure	2 psig
Minimum Gas Flow Rate	1.6 SCFM @ 104°F and 7 in. WC gas inlet pressure
Maximum Gas Flow Rate	2.7 SCFM @ -40°F and 2 psig gas inlet pressure
Nominal Gas Flow Rate	1.8 SCFM @ 68°F and 7 in. WC gas inlet pressure
Dimensions (L x W x H)	21 in. x 20 in. x 39 in.
Weight	145 lbs.
Noise	45 dBA @ 16.5 ft., hemispherical field
Ambient Temperature Rating	-40°F to 104°F

Rank		PA12 (363)	PE (562)	SBR (592)	NBR (514)	CR (613)	SI (571)
Severe (20 & 25)	25			H2S			
	20		Octanes			Hexane	
			Nonanes			Heptanes	
			Decanes			Octanes	
			Undecanes				
			Toluene, m, p-Xylene				
				C3 Benzene			
		Dimethyl Sulfide					
				Methylene Chloride			
Moderate to Severe (15 & 16)	16	Toluene	Heptanes	Octanes	Dimethyl Sulfide		Octanes
		m, p-Xylene	C3 Benzene	Nonanes			Nonanes
			Methylene Chloride	Decanes			Decanes
				Undecanes			Undecanes
							C3 Benzene
							Methylene Chloride
	15	H2S		CO2			
			Dodecanes				i-Butane
			Cyclopentane				Cyclopentane
			Methylcyclopentane				
			Cyclohexane				Cyclohexane
			Methylcyclohexane				
		Benzene			Benzene		
			o-Xylene				
			Ethylbenzene				
		Styrene	i-Propyl Mercaptan		Styrene		i-Propyl Mercaptan
			CFC-11			CFC-11	
			Vinylchloride				

G1 G2 G3 G4 G5 G6 G7 G8 G9 G10

Figure 14. The Compatibility Map for PA, PE12, SBR, NBR, CR and SI in Landfill Gas

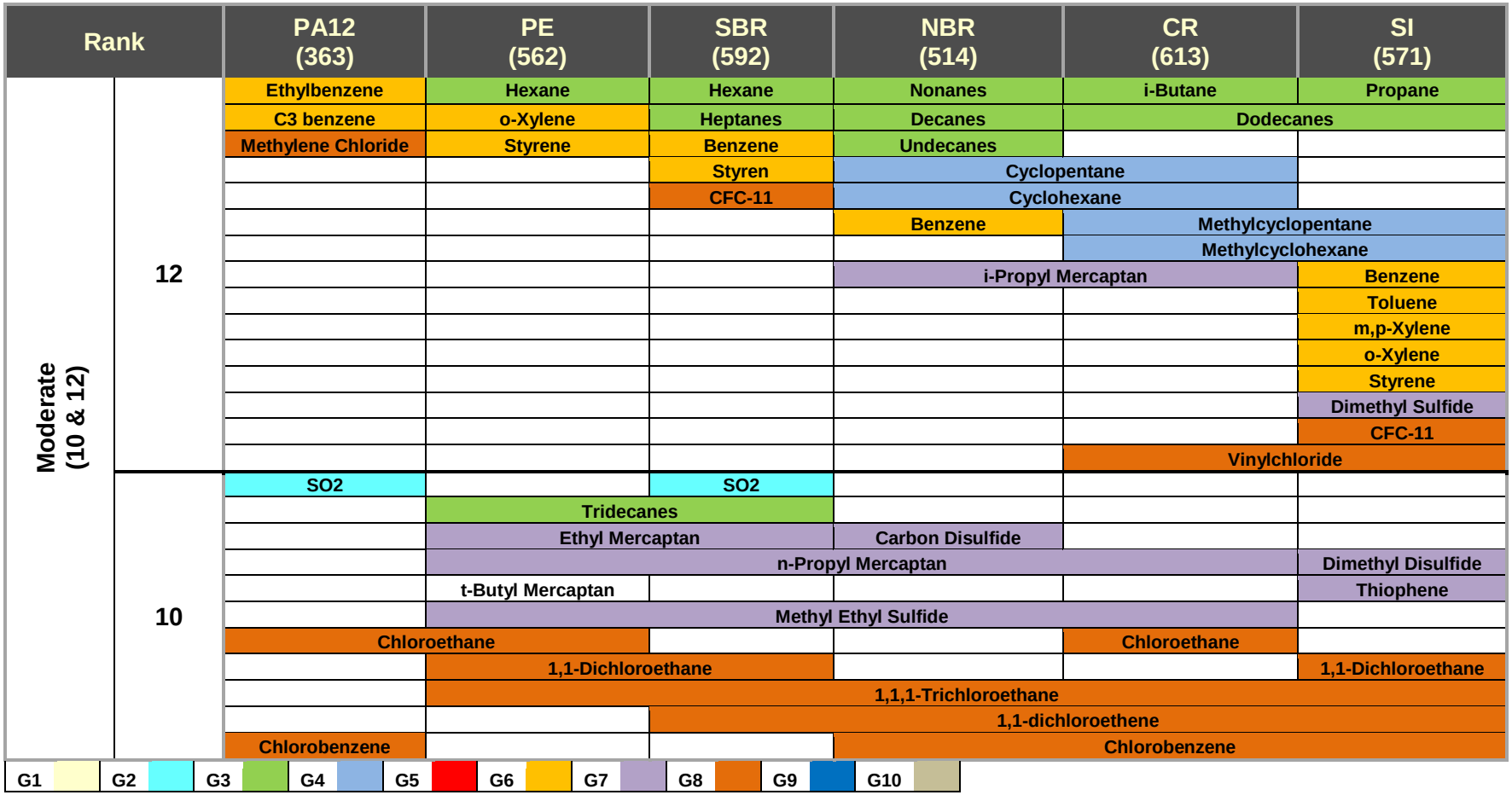

Figure 14. The Compatibility Map for PA, PE12, SBR, NBR, CR and SI in Landfill Gas (Continued)

Rank		PA12 (363)	PE (562)	SBR (592)	NBR (514)	CR (613)	SI (571)
Minor to Moderate (5, 6, 8 & 9)				O2			
	9		i-Butane		Dodecanes	i-Pentane	
		o-Xylene			Methylcyclopentane		Ethylbenzene
		i-Propyl Mercaptan			Methylcyclohexane		
					Vonylchloride		
	8	Ethyl Mercaptan	Propane	t-Butyl Mercaptan	Dimethyl Disulfide	t-Butyl Mercaptan	
		n-Propyl Mercaptan	Chlorobenzene			Dimethyl Disulfide	
					Thiophene		Methyl Ethyl Sulfide
					Thiophane		Thiophane
				Chloroethane		CFC-12	
			1,1-Dichloroethene		1,1-Dichloroethane		Chloroethane
	6	Dodecanes	n-Pentane		Tridecanes	SO2	
		Cyclopentane	i-Pentane		t-Butyl Mercaptan	Ethane	
		Methylcyclopentane	2,2,4-Trimethylpentane		CFC-11	2,2,4-Trimethylpentane	Ethyl Mercaptan
		Cyclohexane	Dimethyl Disulfide			Carbon Disulfide	n-Propyl Mercaptan
		Methylcyclohexane	Thiophene	Thiophene		Thiophane	CFC-114
		Carbon Disulfide		Chlorobenzene			
		Methyl Ethyl Sulfide					
		Dimethyl Disulfide					
		Thiophene					
		Thiophane					
		Vinylchloride					
		1,1,1-					
		1,1-Dichloroethene					
	5	CO2					
		Methane					
				Diethyl Sulfide			
			1,2-Dichloroethane				
					1,2-Dichlorobenzene	CFC-113	

G1 G2 G3 G4 G5 G6 G7 G8 G9 G10

Figure 14. The Compatibility Map for PA, PE12, SBR, NBR, CR and SI in Landfill Gas (Continued)

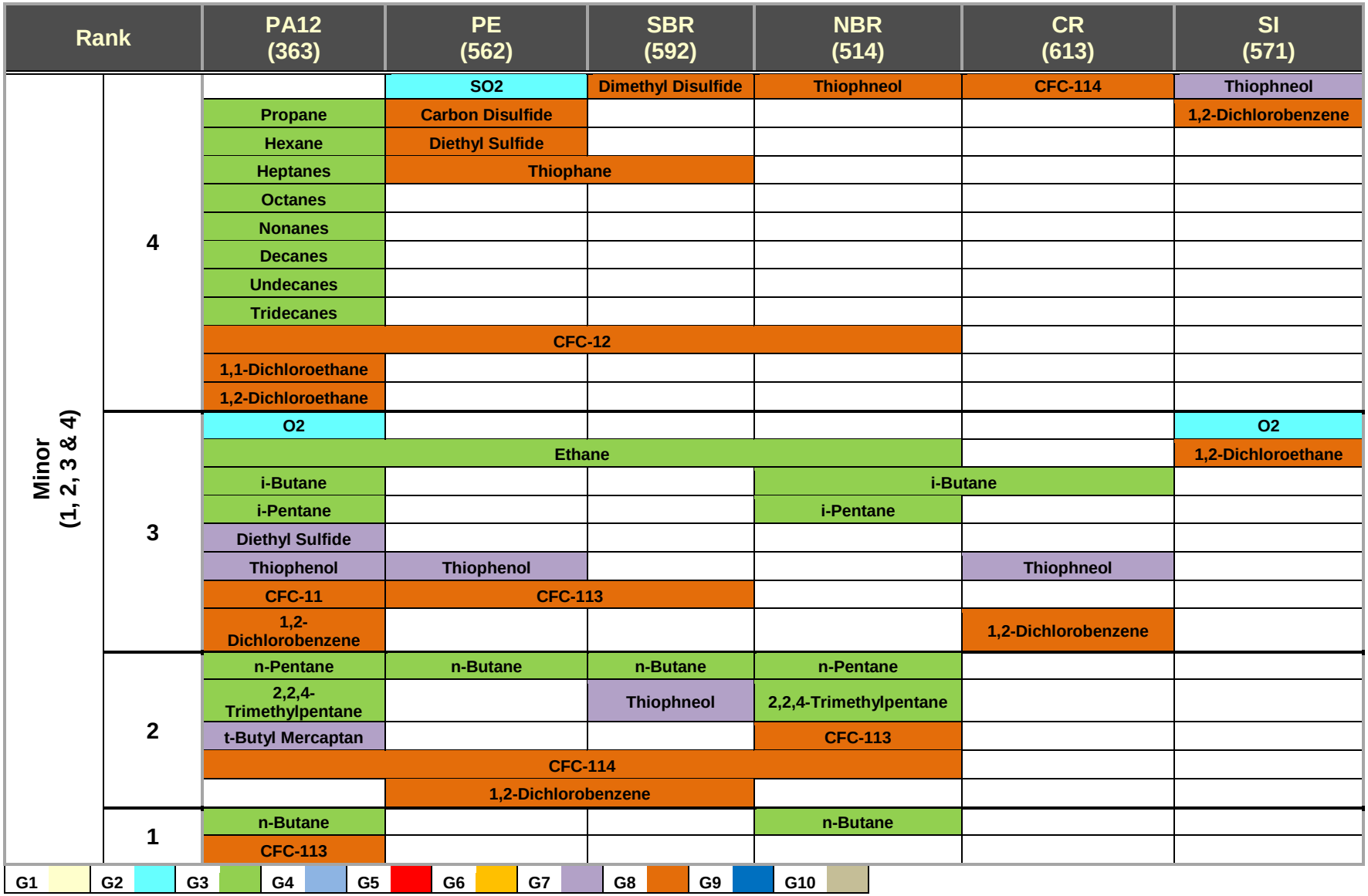

Figure 14. The Compatibility Map for PA, PE12, SBR, NBR, CR and SI in Landfill Gas (Continued)

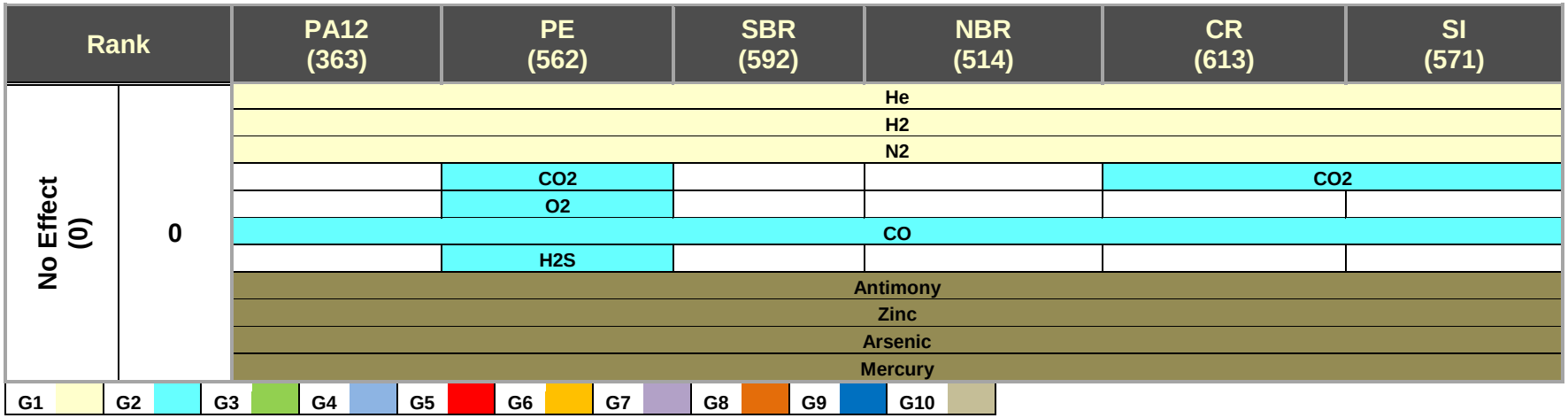

Figure 14. The Compatibility Map for PA, PE12, SBR, NBR, CR and SI in Landfill Gas (Continued)

Rank		PA (117)	PE (118)	SBR (193)	NBR (157)	CR (161)	SI (135)
Severe (20 & 25)	25			H2S			
	20			Ammonia			H2S
Moderate to Severe (15 & 16)	15	H2S		CO2		Hexane	
		SO2		SO2			
			Toluene				
Moderate (10 & 12)	10					Heptanes	
				Cyclopentanes			
				C3 benzene			
		Ethyl Mercaptan					
			i-Propyl Mercaptan				i-Propyl Mercaptan
			t-Butyl				
		Dimethyl Sulfide					
Minor to Moderate (5, 6, 8 & 9)	9			O2			
			Hexane			SO2	
							Toluene
	8		Heptanes	t-Butyl Mercaptan	Ethyl Mercaptan		Cyclopentane
			Cyclopentane		i-Propyl Mercaptan		C3 benzene
			C3 benzene			t-Butyl Mercaptan	
					Dimethyl Sulfide		
	6	Cyclopentane	SO2	Heptanes	SO2		SO2
		C3 benzene			Hexane		Ethyl Mercaptan
		i-Propyl Mercaptan			t-Butyl Mercaptan		Dimethyl Sulfide
	5	CO2					
		Methane					
		Benzene			Carbon Disulfide	Benzene	Dimethyl Disulfide
			n-Propyl Mercaptan				Thiophene

G1 G2 G3 G4 G5 G6 G7 G8 G9 G10

Figure 15. The Compatibility Map for PA, PE12, SBR, NBR, CR and SI in Dairy Gas (Continued)

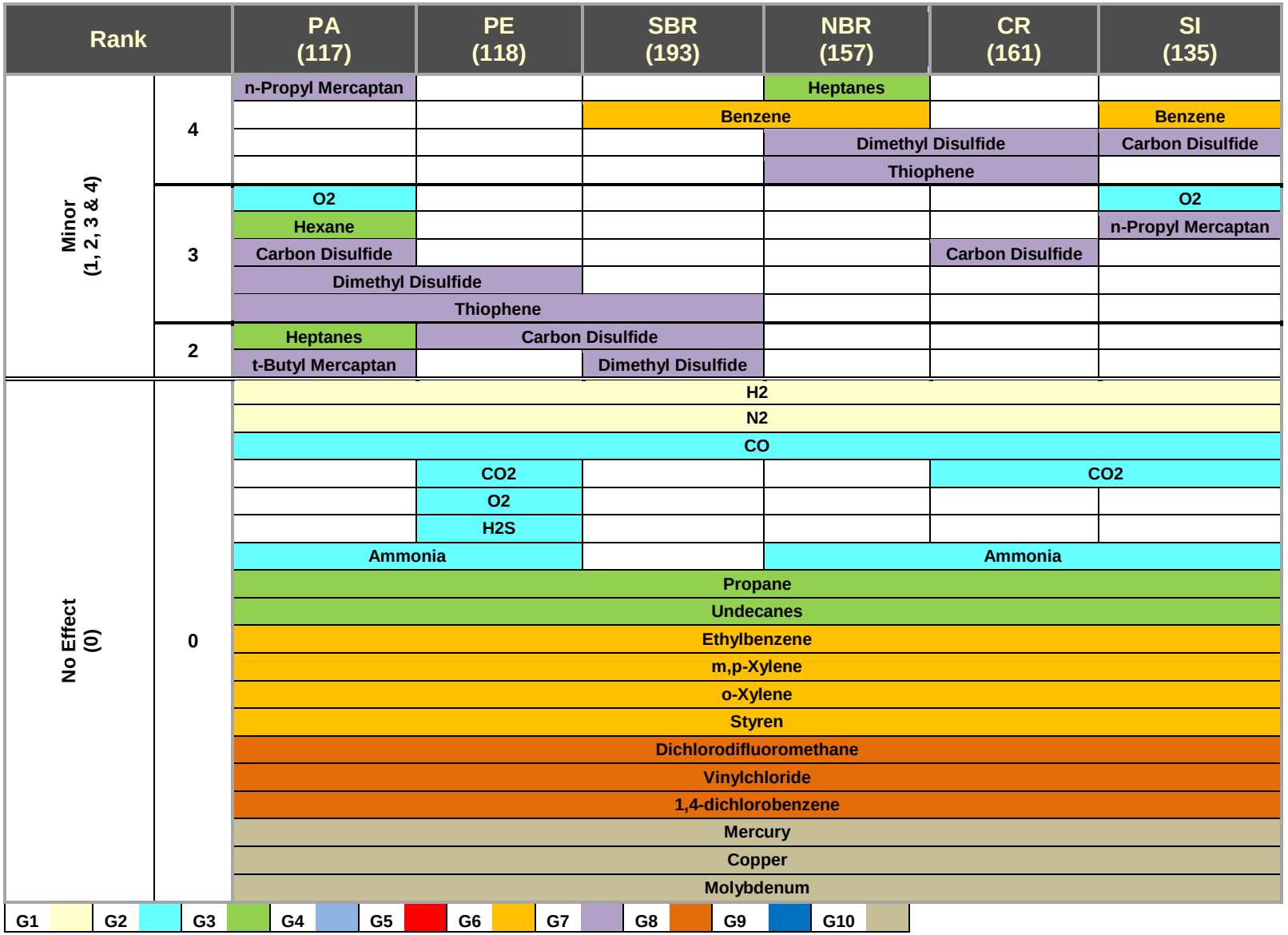

Figure 15. The Compatibility Map for PA, PE12, SBR, NBR, CR and SI in Dairy Gas (Continued)

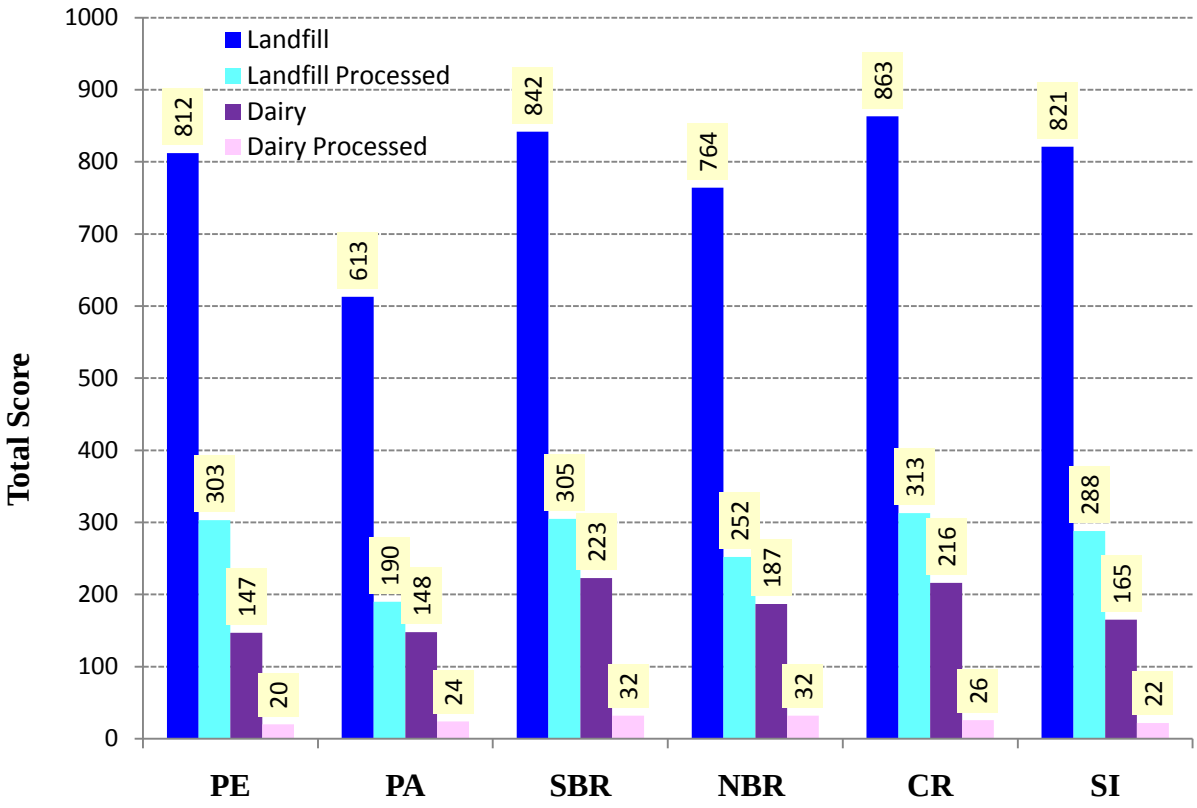

Figure 16. Total Score of PE, PA12, SBR, NBR, CR and SI in Landfill and Dairy Gases

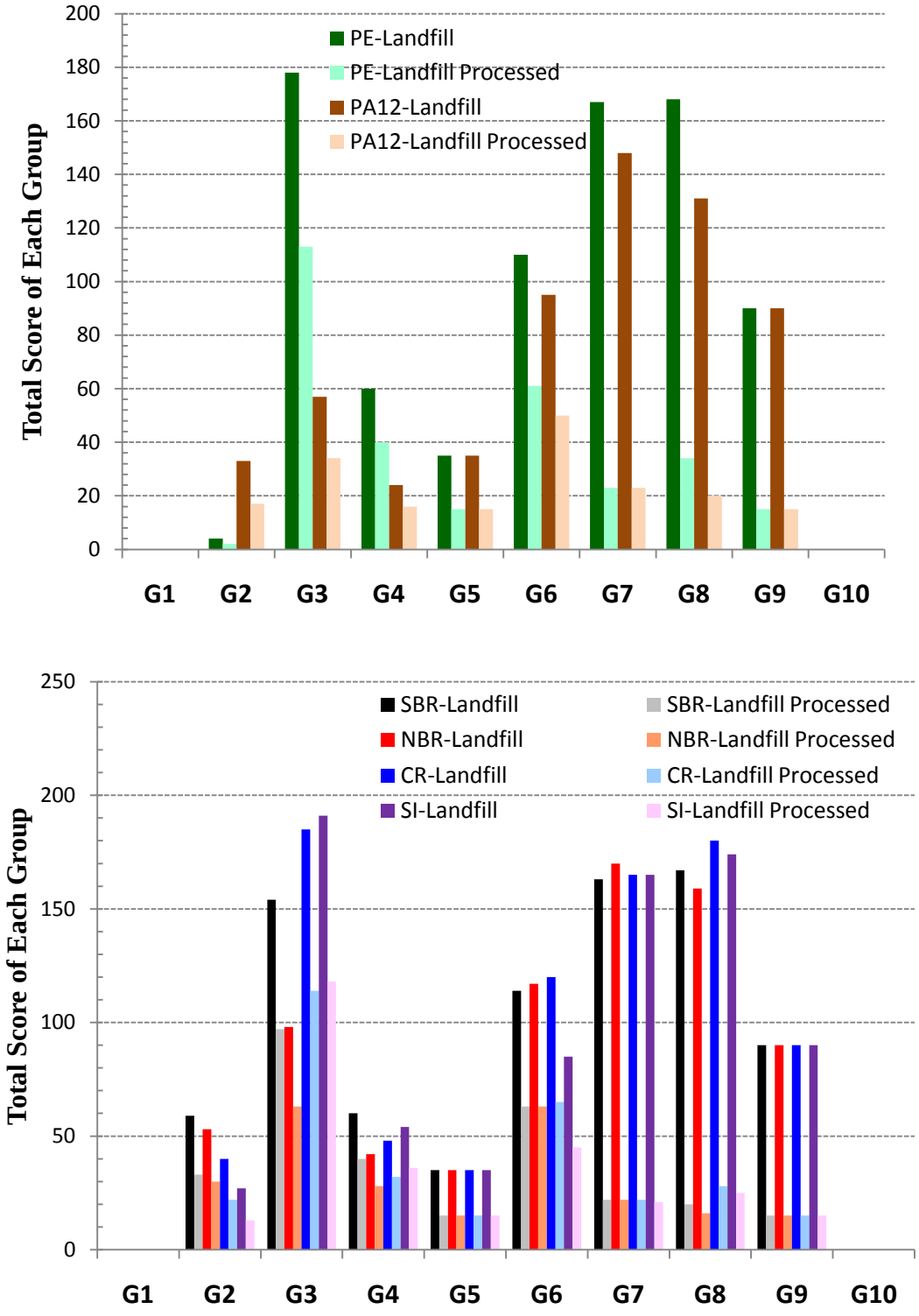

Figure 17. The Risk Score of PE, PA12, SBR, NBR, CR and SI in Raw and Processed Landfill Gas

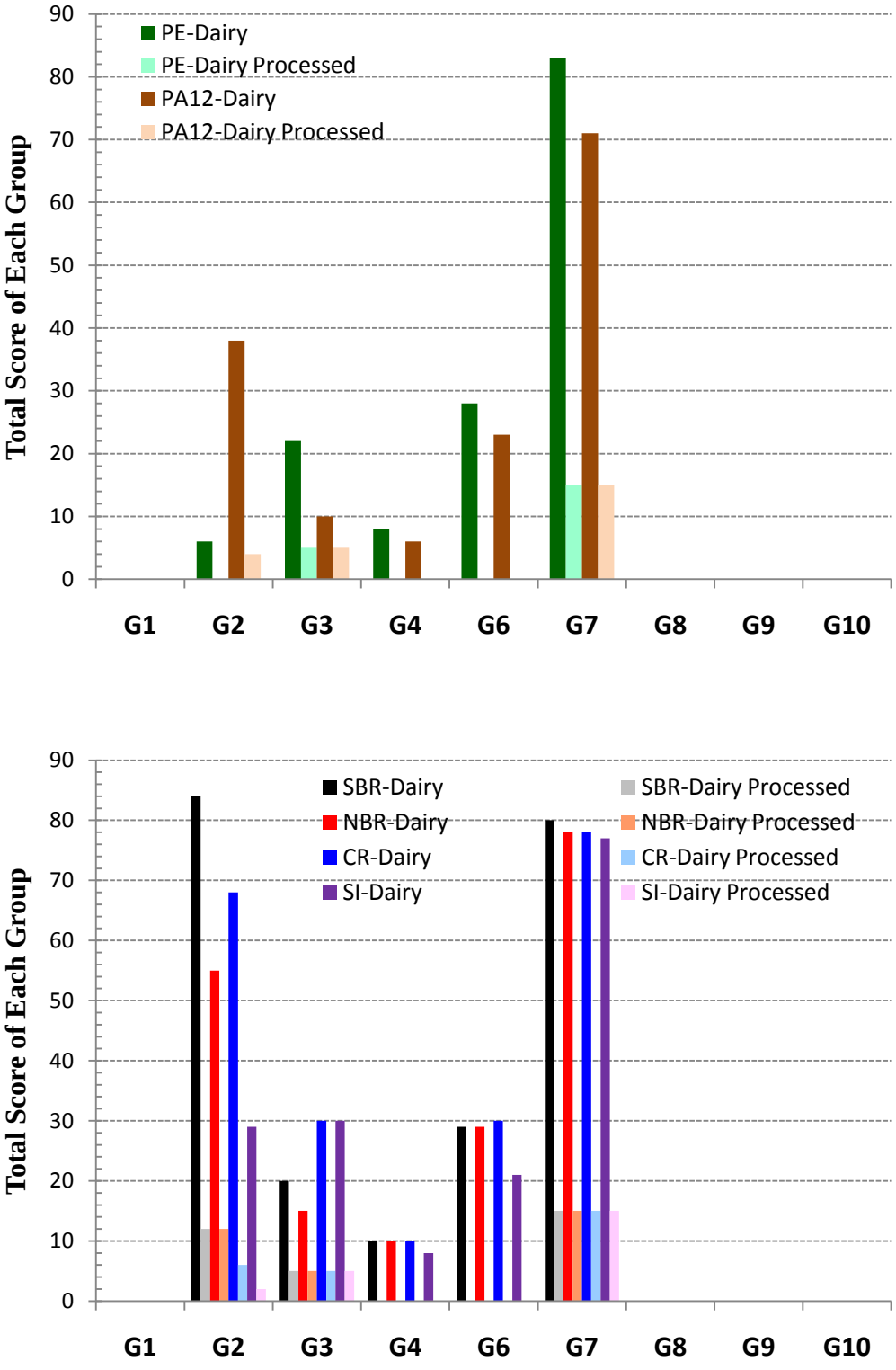

Figure 18. The Risk Score of PE, PA12, SBR, NBR, CR and SI in Raw and Processed Dairy Gas

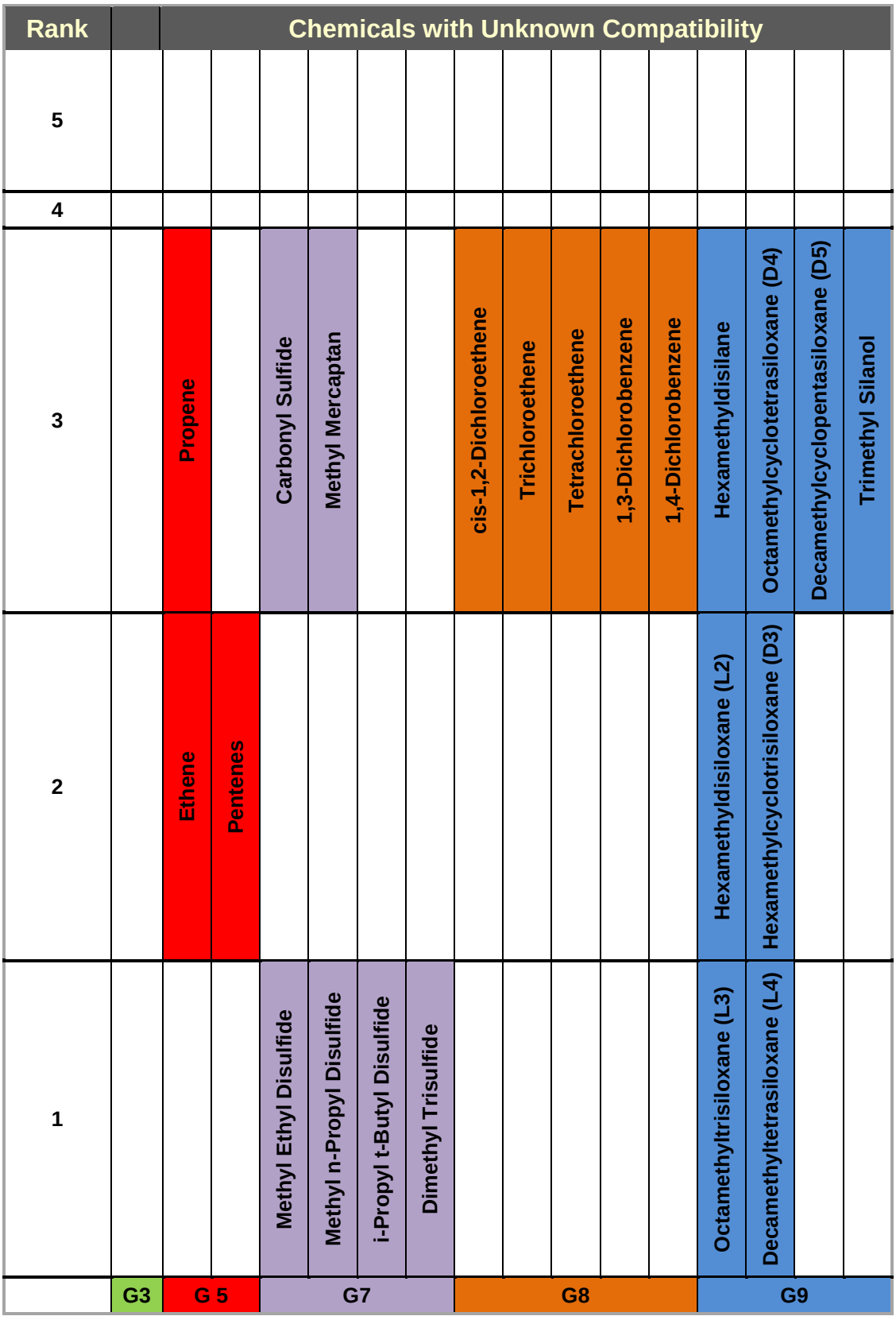

Figure 19. The Rank of the Chemicals in Biogas with Unknown Compatibility

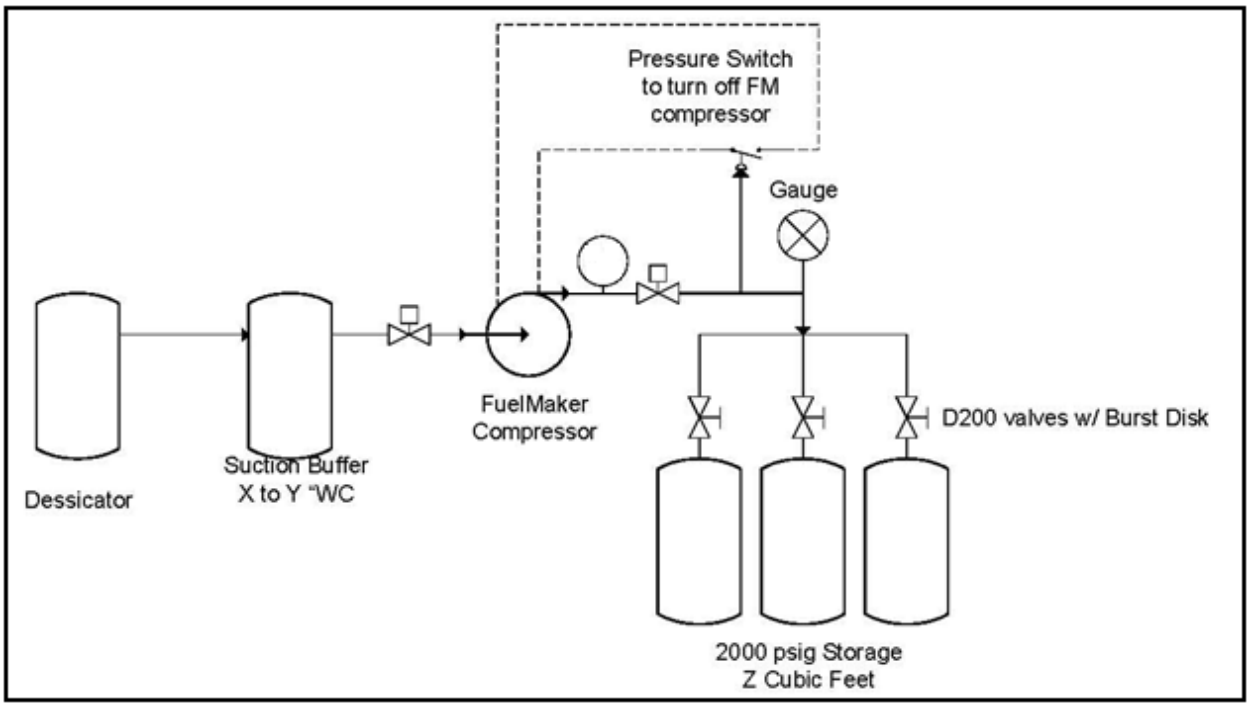

Note:
The circle downstream of the FuelMaker FM4 Compressor is a cooling coil for the gas coming out at 2000 psi.

Figure 20. Biogas Collection Schematic

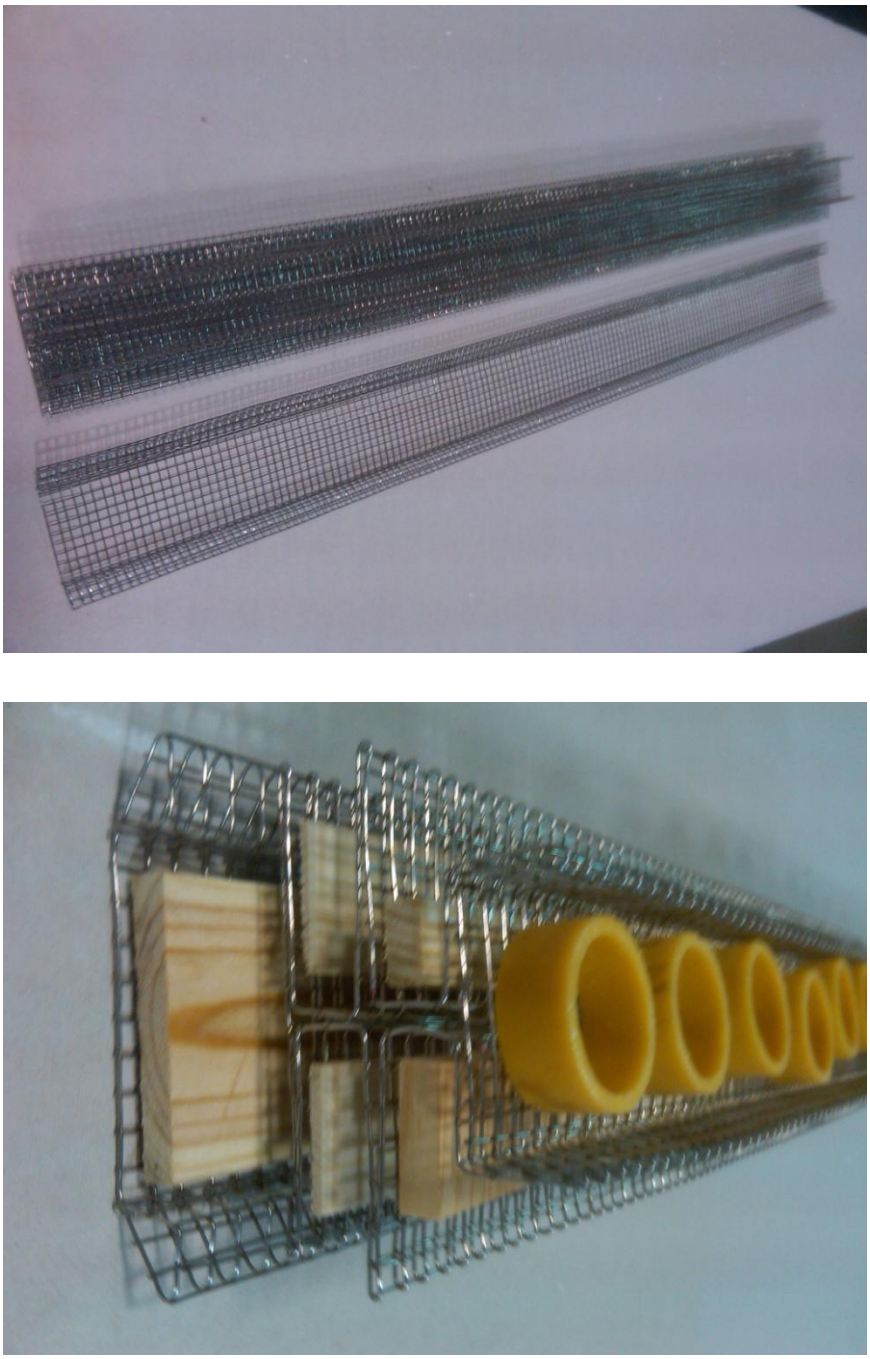

Figure 21. Test Sample Cage

References for Tasks 1 - 4

1. Angostini, R.A. and R.D. Young, *A case history: Investigations of microbially influenced corrosion in a west Texas waterflood. NACE paper no. 119.* 1990.
2. Farthing, S., *Company combats MIC with aggressive control program.* Pipeline and Gas Industry, 1997. **Oct '97**: p. 43-47.
3. Pope, D.H. and R.M. Pope, *Guide for the Monitoring and Treatment of Microbiologically Influenced Corrosion in the Natural Gas Industry*. 1998, Gas Research Institute.
4. Pope, D.H., et al., *Mitigation strategies for microbially influenced corrosion in gas industry facilities.* Corrosion '89, 1989: p. NACE paper 192.
5. Strickland, L.N., R. T. Fortnum, B. W. DuBose, *A case history of microbiologically influenced corrosion in the Lost Hills oilfield, Kern county California.* Corrosion '96, 1996: p. NACE paper 297.
6. Emde, K.M.E., D. W. Smith, and R. Facey, *Initial investigation of microbially influenced corrosion (MIC) in a low temperature water distribution system.* Water Research, 1992. **26**: p. 169-175.
7. Angell, P., *Understanding microbially influenced corrosion as biofilm-mediated changes in surface chemistry.* Curr. Opin. Biotechnol., 1999. **10**(3): p. 269-72.
8. Dzierzewicz, Z., B. Cwalina, L. Weglarz, S. Glab, *Isolation and evaluation of corrosive aggressivity of wild strains of sulfate reducing bacteria.* Acta Microbiologica Polonica, 1992. **41**: p. 211-221.
9. Dzierzewicz, Z., et al., *The relationship between microbial metabolic activity and biocorrosion of carbon steel.* Res. Microbiol., 1997. **148**(9): p. 785-93.
10. Hamilton, W.A., *Sulphate-reducing bacteria and anaerobic corrosion.* Annu. Rev. Microbiol., 1985. **39**: p. 195-217.
11. Horn, J. and D. Jones, *Microbiologically influenced corrosion: Perspectives and approaches,* in *Manual of environmental microbiology*, C.J. Hurst, Crawford, R. L., Knudsen, G. R., McInerney, M. J., Stetzenbach, L. D., Editor. 2002, ASM Press: Washinton, DC. p. 1072-1083.
12. Zhu, X.Y., *"Detection and Mitigation of Microbiologically-Influenced Corrosion (MIC) in Natural Gas Pipelines". GTI Project 20153, completed in March 2007.* 2007.
13. Zhu, X.Y., H. Modi, and J.J. Kilbane II, *Efficacy and risks of nitrate application for the mitigation of SRB-induced corrosion.* In Proceedings of the NACE International Annual Conference, Corrosion/2006, Paper #06524. San Diego, CA., 2006: p. 1-41.
14. Li, S.Y., et al., *Microbiologically Influenced Corrosion of Carbon Steel Exposed to Anaerobic Soil.* Corrosion, 2001. **57**(9): p. 815-828.
15. Kane, R.D. and S. Campbell, *Real-Time Corrosion Monitoring of Steel Influenced by Microbial Activity (SRB) in Simulated Seawater Injection Environments.* CORROSION NACExpo'04, 2004: p. NACE Paper 04579.
16. King, R.A. and D.S. Wakerley, *Corrosion of Mild Steel by Ferrous Sulphide.* Br Corros J, 1973. **8**(1): p. 41-45.
17. King, R.A., J.D.A. Miller, and D.S. Wakerley, *Corrosion of Mild Steel in Cultures of Sulphate-Reducing Bacteria: Effect of changing the soluble iron concentration during growth.* Br Corros J, 1973. **8**(2): p. 89-93.

18. Jack, T.R., et al., *Corrosion Consequences of Secondary Oxidation of Microbial Corrosion.* Corrosion, 1998. **54**(3): p. 246-252.

19. Zhu, X.Y., *"Bioreactor/Chemostat System for Rapid Biodemilitarization of Munitions" for DOD/DARPA, subcontracted from SRI. Subcontract No. 41-000810. GTI project No. 20569. Completed in Angust 2008.*

20. de Franca, F.P. and M.T.S. Lutterbach, *Variation in sessile microflora during biofilm formation on AISI-304 stainless steel coupons.* Journal of industrial microbiology, 1996. **17**(1): p. 6-10.

21. Pope, D.H. and R.M. Pope, *Microbiologically Influenced Corrosion in Fire Protection Sprinkler Systems*, in *A Practical Manual on Microbiologically Influenced Corrosion*, J.G.S. II, Editor. 2001, NACE International: Houston, TX. p. 5.1-5.7.

22. NACE, *Detection, Testing, and Evaluation of Microbiologically Influenced Corrosion (MIC) on External Surfaces of Buried Pipelines.* NACE Standard TM0106-2006, 2006.

23. Batista, J.F., R. F. Pereira, J. M. Lopes, M. F. Carvalho, M. J. Feio, M. A. Reis,, *In situ corrosion control in industrial water systems.* Biodegradation, 2000. **11**(6): p. 441-8.

24. Kasahara, K. and F. Kajiyama, *Role of Sulfate Reducing Bacteria in the Localized Corrosion of Buried Pipes.* Biologically Induced Corrosion; Proceedings of the International Conference on Biologically Induced Corrosion. June 10-12, 1985, Gaithersburg, Maryland. Houston, TX, NACE., 1986: p. 171-183.

25. Shi, X., R. Avci, and Z. Lewandowski, *Microbially deposited manganese and iron oxides on passive metals—their chemistry and consequences for material performance.* Corrosion, 2002. **58**: p. 728.

26. Waters, M.S., et al., *Simultaneous interferometric measurement of corrosive or demineralizing bacteria and their mineral interfaces.* Appl Environ Microbiol., 2009. **75**(5): p. 1445-1449.

27. Little, B.J., P.A. Wagner, and Z. Lewandowski, *The role of biomineralization in microbiologically influenced corrosion, p. 294/1–294/18. In Proceedings of the CORROSION/98 Research Topical Symposia. NACE International, Houston, TX.* 1998.

28. Pope, D.H., *Microbiologically Influenced Corrosion of Internal Aspects of Natural Gas Industry Pipelines and Associated Equipment: Mechniasms, Diagnosis, and Mitigation*, in *A Practical Manual on Microbiologically Influenced Corrosion*, J.G.S. II, Editor. 2001, NACE International: Houston, TX. p. 6.13-6.25.

29. Pope, D.H., et al., *Organic Acid Corrosion of Carbon Steel: A Mechanism of Microbiologically Influenced Corrosion.* In Proceedings of the NACE International Annual Conference, Corrosion/1988, Paper #79. Houston, TX., 1988.

30. Graves, J.W., E. H. Sullivan, *Internal corrosion in gas gathering systems and transmission lines.* Materials Protection, 1996. **5**: p. 33-37.

31. Kholodenko, V.P., S. K. Jigletsova, V. A. Chugnov, V. B. Rodin, V. S. Kobelev, S. V. Karpov, *Chemicomicrobiological diagnostics of stress corrosion cracking of trunk pipelines.* Appl. Biochem. Microbiol., 2000. **36**: p. 594-601.

32. Pope, D.H., T. P. Zintel, B. A. Cookingham, R. G. Morris, D. Howard, R. A. Day, J. R. Frank, and G. E. Pogemiller, *Mitigation strategies for microbially influenced corrosion in gas industry facilities.* Corrosion '89, 1989: p. NACE paper 192.

33. Pope, D.H., R. M. Pope, *Guide for the monitoring and treatment of microbiologically influenced corrosion in the natural gas industry.* 1998, Gas Research Institute.

34. Scott, P.J.B., *Expert Consensus on MIC: Prevention and Monitoring.* Materials Performance, 2004(3): p. 2-6.

35. Jack, T.R., et al., *Microbiologically Influenced Corrosion Testing*, in *The Characterization of Sulfate-Reducing Bacteria in Heavy Oil Waterflood Operations*, J.R. Kearns and B.J. Little, Editors. 1994, Philadelphia, PA: ASTM. p. 108.

36. von Wolzogen Kuhr, C.A.H. and L.S. van der Vlugt, *The graphitization of cast iron as an electrochemical process in anaerobic soils.* Water Research, 1934. **18**: p. 147-165.

37. McNeil, M.B. and B.J. Little, *Mackinawite Formation During Microbial Corrosion,.* Corrosion, 1990. **46**: p. 599-600.

38. Tributsch, H., et al., *Role of Transient Iron Sulfide Films in Microbial Corrosion of Steel.* Corrosion, 1998. **54**(3): p. 216-227.

39. Hardy, J.A. and J.L. Brown, *The Corrosion of Mild Steel By Biogenic Sulfide Films Exposed to Air.* Corrosion, 1984. **40**(12): p. 650.

40. Jack, T.R. and M.J. Wilmott, *Indicator Minerals Formed During External Corrosion of Line Pipe.* MP, 1995. **34**: p. 19.

41. Pope, D.H. and E.A.M. III, *Some Experiences With Microbiologically Influenced Corrosion of Pipelines.* MP, 1995. **34**(5): p. 23.

42. Gibson, G.R. and X. Wang, *Regulatory effects of bifidobacteria on the growth of other colonic bacteria.* J. Appl. Bacteriol., 1994. **77**(4): p. 412-20.

43. Zellner, G., et al., *Anaerofilum pentosovorans gen. nov., sp. nov., and Anaerofilum agile sp. nov., two new, strictly anaerobic, mesophilic, acidogenic bacteria from anaerobic bioreactors.* Int. J. Syst. Bacteriol., 1996. **46**(4): p. 871-5.

44. Kanauchi, O., et al., *Increased growth of Bifidobacterium and Eubacterium by germinated barley foodstuff, accompanied by enhanced butyrate production in healthy volunteers.* Int. J. Mol. Med., 1999. **3**(2): p. 175-9.

45. Broda, D.M., et al., *Clostridium algidixylanolyticum sp. nov., a psychrotolerant, xylan- degrading, spore-forming bacterium.* Int. J. Syst. Evol. Microbiol., 2000. **50 Pt 2**: p. 623-31.

46. Vetting, M.W., et al., *Structure of Acinetobacter strain ADP1 protocatechuate 3, 4-dioxygenase at 2.2 A resolution: implications for the mechanism of an intradiol dioxygenase.* Biochemistry, 2000. **39**(27): p. 7943-55.

47. Zhu, X.Y., J. Lubeck, and J.J. Kilbane, 2nd, *Characterization of microbial communities in gas industry pipelines.* Appl Environ Microbiol, 2003. **69**(9): p. 5354-63.

48. Little, B.J. and P. Wagner, *Microbiologically Influenced Corrosion*, in *Peabody's Control of Pipeline Corrosion*, R.L. Bianchetti, Editor. 2001, Houston, TX: NACE, 2001.

49. Towers, R., *Accelerated Corrosion in Cargo Tanks of Large, Double-Hull Ships, Causes and Countermeasures.* Protective Coatings Europe, 2000(3): p. 30-42.

50. Hines, M.E., P.T. Visscher, and R. Devereux, *Sulfur cycling*, in *Manual of Environmental Microbiology*, L.D. Stetzenbach, Editor. 2002, ASM Press: Washington, DC. p. 427-438.

51. Mudryk, Z.J., et al., *The occurrence and activity of sulphate-reducing bacteria in the bottom sediments of the Gulf of Gdañsk.* OCEANOLOGIA, 2000. **42**(1): p. 105-117.

52. Caumette, P., *Ecology and physiology of phototrophic bacteria and sulphate-reducing bacteria in marine salterns.* Experientia, 1993. **49**: p. 473-481.

53. Bak, F. and P. N., *Sulfate-reducing bacteria in littoral sediment of Lake Constance.* FEMS Microbiol. Ecol., 1991. **85**: p. 43–52.

54. Le Borgne, S., et al., *Detecting and Monitoring Bacteria in Seawater Injection Systems.* Materials Performance, 2007. **46**(11): p. 52-56.

55. Jack, T.R., *MIC in Underground Environments: External Corrosion in the Gas pipeline Industry*, in *A Practical Manual on Microbiologically Influenced Corrosion*, J.G.S. II, Editor. 2001, NACE International: Houston, TX. p. 6.1-6.42.

56. Campaignolle, X., et al., *Stabilization of Localized Corrosion of Carbon Steel by Sulfate-Reducing Bacteria.* Nace International Corrosion 93, Paper no. 302, 1993: p. 1-7.

57. Daumas, S., M. Magot, and J.L. Crolet, *Measurement of the net production of acidity by a sulphate-reducing bacterium: experimental checking of theoretical models of microbially influenced corrosion.* Res. Microbiol., 1993. **144**(4): p. 327-332.

58. Hemmingsen, T., H. Vangdal, and T. Våland, *Formation of Ferrous Sulfide Film from Sulfite on Steel Under Anaerobic Conditions.* Corrosion, 1992. **48**(6): p. 475-481.

59. Campaignolle, X. and J.-L. Crolet, *Method for Studying Stabilization of Localized Corrosion on Carbon Steel by Sulfate-Reducing Bacteria.* Corrosion, 1997. **53**(6).

60. Tanji, Y., et al., *Chemical Analysis of an Artificial Biofilm that Enhances or Inhibits Carbon Steel Corrosion.* Corrosion, 2002. **58**(3): p. 232-239.

61. King, L.D. and J.D.A. Miller, *Corrosion by the sulfate reducing bacteria.* Nature, 1971. **233**: p. 491-492.

62. King, R.A., J.D.A. Miller, and J.S. Smith, *Corrosion of mild steel by iron sulfides.* Brit Corrosion J, 1973. **8**: p. 137-142.

63. Angeles-Ch, C., et al., *Microbiologically Influenced Corrosion by Citrobacter in Sour Gas Pipelines.* Materials Performance, 2002. **41**(8): p. 50-55.

64. Little, B.J., R.I. Ray, and R.K. Pope, *Relationship Between Corrosion and the Biological Sulfur Cycle: A Review.* Corrosion, 2000. **56**(4): p. 433.

65. Gonzalez, J.L., et al., *A damage model for assessing pipeline safety in corrosion environments.* Corrosion, 1997. **53**: p. 935-943.

66. Zhu, X.Y., *Rapid Quantification of Butyric Acid-Producing Bacteria Using Real-Time PCR*. 2007, Gas Technology Institute: USA.

67. Zhu, X.Y., *Rapid Quantification of Acetic Acid-Producing Bacteria Using Real-Time PCR*. 2008, Gas Technology Institute: USA.

68. Emerson, D. and W.C. Ghiorse *Isolation, Cultural Maintenance, and Taxonomy of a Sheath-Forming Strain of Leptothrix discophora and Characterization of Manganese-Oxidizing Activity Associated with the Sheath.* Appl. Environ. Microbiol., 1992. **58**: p. 4001-4010.

69. Hanert, H.H., *The genus Siderocapsa (and other iron- or manganese-oxidizing eubacteria,* in *The Prokaryotes, a Handbook on Habitats, Isolation and Identification of Bacteria,* M. Starr, et al., Editors. 1981, Springer-Verlag: New York. p. 1049-1059.

70. Dickinson, W.H. and Z. Lewandowski, *Manganese Biofouling and the Corrosion Behavior of Stainless Steel.* Biofouling, 1996. **10**: p. 79-93.

71. Hamilton, W.A., *Sulphate-reducing bacteria and anaerobic corrosion.* Ann. Rev. Microbiol., 1985. **39**: p. 195-217.

72. Zhu, X.Y., et al., *Rapid detection and quantification of microbes related to microbiologically influenced corrosion using quantitative polymerase chain reaction.* Corrosion, 2006. **62**: p. 950-955.

73. Zhu, X.Y., et al., *Application of Quantitative, Real-Time PCR in Monitoring Microbiologically-Influenced Corrosion (MIC) in Gas Pipelines.* In Proceedings of the NACE International Annual Conference, Corrosion/2005, Paper #05493. Houston, TX., 2005: p. 1-20.

74. Myers, C. and K.H. Nealson, *Bacterial Manganese Reduction and Growth with Manganese Oxide as the Sole Electron Acceptor.* Science, 1988. **240**: p. 1319.

75. Dubey, R.S. and Upadhyay, *Microbial Corrosion Monitoring by an Amperometric Microbial Biosensor Developed using Whole Cell of Pseudomonas sp.* Biosensors and Bioelectronics, 2001. **16**: p. 995-1000.

76. Nordstrom, D.K. and G. Southam, *Geomicrobiology of Sulfide Mineral Oxidation*, in *Reviews in Mineralogy Geomicrobiology: Interactions Between Microbes and Minerals*, J.F. Banfield and K.H. Nealson, Editors. 1997, Washington, DC: Mineralogical Society of America. p. 361-390.

77. Boivin, J., et al., *The Influence of Enzyme Systems on MIC.* CORROSION/90, paper no. 128 (Houston, TX: NACE, 1990). 1990.

78. Braker, G., A. Fesefeldt, and K.-P. Witzel, *Development of PCR Primer Systems for Amplification of Nitrite Reductase Genes (nirK and nirS) To Detect Denitrifying Bacteria in Environmental Samples.* Appl. Environ. Microbiol., 1998. **64**(10): p. 3769-3775.

79. Nemati, M., G.E. Jenneman, and G. Voordouw, *Impact of nitrate-mediated microbial control of souring in oil reservoirs on the extent of corrosion.* Biotechnol. Prog., 2001. **17**(5): p. 852-9.

80. Zintel, T.P., G.J. Licina, and T.R. Jack, *Techniques for MIC Monitoring*, in *A Practical Manual on Microbiologically Influenced Corrosion*, J.G.S. II, Editor. 2001, NACE International: Houston, TX. p. 10.1-10.19.

81. NACE, *Field Monitoring of Bacterial Growth in Oilfield and Gas Systems.* NACE Standard TM0194-2004.

82. Little, B., P. Wager, and F. Mansfeld, *Microbiologically Influenced Corrosion of Metals and Alloys.* Int. Mat. Rev., 1991. **36**(6): p. 253-272.

83. Hernández-Gayosso, M.J., et al., *Microbial consortium influence upon steel corrosion rate, using the electrochemical impedance spectroscopy technique.* Materials and Corrosion, 2004. **55**(9): p. 676-683.

84. API, *Recommended Practice for Biological Analysis of Subsurface Injection Waters, American Petroleum Institute, Washington, D.C.,*. 1982.

85. Williams, W.A., J.H. Lobos, and W.E. Cheetham, *A phylogenetic analysis of aerobic polychlorinated biphenyl-degrading bacteria.* Int. J. Syst. Bacteriol., 1997. **47**(1): p. 207-10.

86. Maidak, B.L., et al., *The RDP-II (Ribosomal Database Project).* Nucleic Acids Res, 2001. **29**(1): p. 173-4.

87. Muyzer, G., E.C. de Waal, and A.G. Uitterlinden, *Profiling of complex microbial populations by denaturing gradient gel electrophoresis analysis of polymerase chain reaction-amplified genes coding for 16S rRNA.* Appl Environ Microbiol, 1993. **59**(3): p. 695-700.

88. Zhu, X.Y., T. Zhong, Y. Pandya, R. D. Joerger, *16S rRNA-based analysis of microbiota from the cecum of broiler chickens.* Appl. Environ. Microbiol., 2002. **68**(1): p. 124-37.

89. Osburne, M.S., T. H. Griossman, P. R. August, I. A. MacNeil, *Tapping into microbial diversity for natural products drug discovery.* ASM News, 2000. **66**: p. 411-417.

90. Torsvik, V., J. Goksoyr, and F.L. Daae, *High diversity in DNA of soil bacteria.* Appl Environ Microbiol, 1990. **56**(3): p. 782-7.

91. Harmsen, H.J., et al., *Population dynamics of propionate-oxidizing bacteria under methanogenic and sulfidogenic conditions in anaerobic granular sludge.* Appl. Environ. Microbiol., 1996. **62**(6): p. 2163-8.

92. Zhu, X.Y. and R.D. Joerger, *Composition of microbiota in content and mucus from cecae of broiler chickens as measured by fluorescent in situ hybridization with group-specific, 16S rRNA-targeted oligonucleotide probes.* Poult Sci, 2003. **82**(8): p. 1242-9.

93. Voordouw, G., *Reverse Sample Genome Probing of Microbial Community Dynamics.* ASM News, 1998. **64**: p. 627-633.

94. Voordouw, G., et al., *Application of Reverse Sample Genoma Probing to the Identification of Sulfate-Reducing Bacteria*, in *Microbiologically Influenced Corrosion Testing, ASTM STP 1232*, J.R. Kearns and B.J. Little, Editors. 1994, Philadelphia, PA: ASTM. p. 188-199.

95. Telang, A.J., S. Ebert, J. M. Foght, D. W. S. Westlake, G. E. Jenneman, D. Gevertz, G. Voordouw, *Effect of nitrate injection on the microbial community in an oil field as monitored by reverse sample genome probing.* Appl. Environ. Microbiol., 1997. **63**(5): p. 1785-1793.

96. Skovhus, T.L., et al., *Real-Time Quantitative PCR for Assessment of Abundance of Pseudoalteromonas Species in Marine Samples.* Appl. Environ. Microbiol., 2004. **70**(4): p. 2373-2382.

97. Stults, J.R., O. Snoeyenbos-West, B. Methe, D. R. Lovley, D. P. Chandler, *Application of the 5' fluorogenic exonuclease assay (TaqMan) for quantitative ribosomal DNA and rRNA analysis in sediments.* Appl. Environ. Microbiol., 2001. **67**(6): p. 2781-2789.

98. Suzuki, M.T., L.T. Taylor, and E.F. DeLong, *Quantitative Analysis of Small-Subunit rRNA Genes in Mixed Microbial Populations via 5'-Nuclease Assays.* Appl. Environ. Microbiol., 2000. **66**(11): p. 4605-4614.

99. Brinkman, N.E., et al., *Evaluation of a Rapid, Quantitative Real-Time PCR Method for Enumeration of Pathogenic Candida Cells in Water.* Appl. Environ. Microbiol., 2003. **69**(3): p. 1775-1782.

100. Guy, R.A., et al., *Real-Time PCR for Quantification of Giardia and Cryptosporidium in Environmental Water Samples and Sewage.* Appl. Environ. Microbiol., 2003. **69**(9): p. 5178-5185.

101. Ibekwe, A.M., et al., *Multiplex Fluorogenic Real-Time PCR for Detection and Quantification of Escherichia coli O157:H7 in Dairy Wastewater Wetlands.* Appl. Environ. Microbiol., 2002. **68**(10): p. 4853-4862.

102. Blackburn, F.E., *Non-Bioassay Techniques for Monitoring SRB.* CORROSION/2004 (Houston, TX: NACE, 2004).

103. Dorsey, M.H., et al., *Monitoring for Corrosion and Microbiological Activity in a Cooling Water System.* Plant Power Chemistry, 2002. **4**(12): p. 721-731.

104. Royer, R.A. and R.F. Unz, *Use of Electrical Resistance Probes for Studying Microbiologically Influenced Corrosion.* Corrosion, 2002. **58**(10): p. 863-870.

105. Pope, D.H., *State-of-the-Art Report on Monitoring, Prevention and Mitigation of Microbiolwically lnfluenced Corrosion in the Natural Gas Industrv.* Topical Report, GRI-9210382. Gas Research Institute, Chicago, IL, 1992.

106. Lockwood, S.F., et al., *Microbiologically lnfluenced Corrosion in the Natural Gas Industry.* Topical Report (Unpublished) to Gas Research Institute, February 1993., 1993.

107. Lutey, R.W., *Treatment for the Mitigation of MIC*, in *A Practical Manual on Microbiologically Influenced Corrosion*, J.G. Stoecker, Editor. 1993, Houston, TX: NACE. p. 9.1-9.9.30.

108. Nichols, W.W., et al., *The penetration of antibiotics into aggregates of mucoid and non-mucoid Pseudomonas aeruginose.* J. Gen. Microbiol., 1989. **35**(35): p. 1219-1303.

109. Kajdasz, R.E., R.V. Einstman, and L. Young-Bandala, *Biocidal Efficacy with Respect to Sessile and Planktonic.* IWV, 1984: p. 85-93.

110. McCoy, W.F., *Strategies for the treatment of biological biofouling.*, in *Biological fouling of industrial water systems - A problem solving approach*, M.W. Mittelman and G.G. Geysey, Editors. 1987, Water Micro. Associates: San Diego, CA. p. 247-268.

111. Pope, D.H. and R. Skultety, *Microbiologically lnfluenced Corrosion in Natural Gas Storage Fields: Diagnosis, Monitoring and Control.* NACE International Conference on Microbiologically lnfluenced Corrosion, Paper No. 57. New Orleans, LA., 1995.

112. Webster, B.J. and R.C. Newman, *ASTM STP 1232: Producing Rapid Sulfate-Reducing Bacteria-Influenced Corrosion in the Laboratory*, in *Microbiologically Influenced Corrosion Testing*, J. Kearns and B.J. Little, Editors. 1994, ASTM: West Conshohocken, PA. p. 28-41.

113. Little, B. and R. Ray, *A Perspective on Corrosion Inhibition by Biofilms.* Corrosion, 2002. **58**(5): p. 424-428.

114. Jayaraman, A., et al., *Axenic aerobic biofilms inhibit corrosion of copper and aluminum.* Appl Microbiol Biotechnol., 1999. **52**(6): p. 787-790.

115. Jayaraman, A., et al., *Inhibiting sulfate-reducing bacteria in biofilms on steel with antimicrobial peptides generated in situ.* Appl Microbiol Biotechnol., 1999. **52**(2): p. 267-275.

116. Zuo, R., *Biofilms: strategies for metal corrosion inhibition employing microorganisms.* Appl Microbiol Biotechnol., 2007. **76**(6): p. 1245.

117. Zuo, R. and T.K. Wood, *Inhibiting mild steel corrosion from sulfate-reducing and iron-oxidizing bacteria using gramicidin-S-producing biofilms.* Appl Microbiol Biotechnol., 2004. **65**(6): p. 747-753.

118. Zuo, R., et al., *Inhibiting mild steel corrosion from sulfate-reducing bacteria using antimicrobial-producing biofilms in Three-Mile-Island process water.* Appl Microbiol Biotechnol., 2004. **64**(2): p. 275-283.

119. Chan, K.Y., L.C. Xu, and H.H. Fang, *Anaerobic electrochemical corrosion of mild steel in the presence of extracellular polymeric substances produced by a culture enriched in sulfate-reducing bacteria.* Environ Sci Technol., 2002. **36**(8): p. 1720-1727.

120. Hernandez, G., et al., *Corrosion Inhibition of Steel by Bacteria*. Corrosion, 1994. **50**(08): p. 603-608.

121. Jayaraman, A., et al., *Axenic Aerobic Biofilms Inhibit Corrosion of SAE 1018 Steel through Oxygen Depletion.* Applied Microbiology and Biotechnology, 1997. **48**: p. 11-17.

122. McCafferty, E. and J.V. McArdle. *Corrosion Inhibition by Biological Siderophore*. in *182nd Society Meeting (Toronto, Canada: The Electrochemical Society)*. 1992.

123. Eashwar, M. and S. Maruthamuthu, *Mechanism of biologically produced ennoblement: Ecological perspectives and a hypothetical model.* Biofouling, 1995. **8**(3): p. 203-213.

124. Little, B., P. Wagner, and F. Mansfeld, *Microbiologically Influenced Corrosion of Metals and Alloys.* Int. Mat. Rev., 1991. **36**(6): p. 253-272.

125. Geesey, G.G., in *Biofouling and biocorrosion in industrial water systems*, H.-C. Flemming and G.G. Geesey, Editors. 1991, Springer-Verlag: Berlin.

126. Heitz, E., in *Microbially influenced corrosion of materials*, E. Heitz, H.-C. Flemming, and W. Sand, Editors. 1996, Springer-Verlag: Berlin, New York.

127. AGA, *American Gas Association. Transmission Measurement Committee. AGA Report No. 4A, Natural Gas Contract Measurement and Quality Clauses – 2008 DRAFT. Washington, DC: American Gas Association, 2008*. 2008.

128. Alexander, B. and F.G. Priest, *Bacillus glucanolyticus, a new species that degrades a variety of beta-glucans.* Int. J. Syst. Bacteriol., 1989. **39**: p. 112-115.

129. Pridal, A., *Microorganisms in Dead Bumble Bee Larvae (Bombus spp.) from Laboratory-Reared Colonies.* ACTA Universitatis Agriculturae et Silviculturae Mendelianae Brunensis, 2001(5): p. 41-48.

130. http://en.wikipedia.org/wiki/Bacillus_licheniformis.

131. Scheldeman, P., et al., *Incidence and Diversity of Potentially Highly Heat-Resistant Spores Isolated at Dairy Farms 10.1128/AEM.71.3.1480-1494.2005.* Appl. Environ. Microbiol., 2005. **71**(3): p. 1480-1494.

132. Little, B.J., J.S. Lee, and R.I. Ray, *Diagnosing Microbiologically Influenced Corrosion: A State-of-the-Art Review.* Corrosion, 2006(62): p. 1006.

133. Pots, B.F.M. and S.D. Kapusta, *Prediction of Corrosion Rates of the Main Corrosion Mechanisms in Upstream Applications.* Nace International Corrosion 2005. Paper No. 05550., 2005: p. 1-21.

134. Crolet, J.-L., *Observation of Non-SRB Sulfidogenic Bacteria from Oilfield Production Facilities.* CORROSION/95, paper no. 188 (Houston TX, NACE, 1995). 1995.

135. Crolet, J.-L., *From the General Mechanism to Specific Mechanisms of Localized Corrosion*, in *Localized Corrosion*, F. Dabosi, G. Beranger, and B. Baroux, Editors. 1994, Les Editions de Physique: Les Ulis, France.

136. Crolet, J.-L., S. Daumas, and M. Magot, *pH Regulation by Sulfate-Reducing Bacteria.* CORROSION/93, paper no. 303 (Houston TX: NACE), 1993.

137. Lee, W., et al., *Role of Sulfate-Reducing Bacteria in Corrosion of Mild Steel: A Review.* Biofouling, 1995. **8**: p. 165-194.

138. Newman, R.C., B.J. Webster, and R.G. Kelly, *The electro- chemistry of SRB corrosion and related inorganic phenomena.* ISIJ Int, 1991. **31**: p. 201-209.

139. Yang, B., *Localized Corrosion Monitoring in Cooling Water Systems.* CORROSION/95, paper no. 541 (Houston, TX: NACE, 1995). 1995.

140. Walt, D.R., et al., *The effect of gravity on initial microbial adhesion.* J. Colloidal Interface Sci, 1985. **107**(2): p. 334-336.

141. Marmur, A. and E. Ruckenstein, *Gravity and cell adhesion.* Journal of Colloid and Interface Science, 1986. **114**(1): p. 261-266.

142. Picioreanu, C. and M.C.M.v. Loosdrecht, *A Mathematical Model for Initiation of Microbiologically Influenced Corrosion by Differential Aeration.* J. Electrochemical Society, 2002. **149**(6): p. B211-B223.

143. Sooknah, R., S. Papavinasam, and R.W. Revie, *Validation of a Predictive Model for Microbiologically Influenced Corrosion, NACE/2008, Paper 08503.*

144. King, F., *Microbiologically Influenced Corrosion of Nuclear Waste Containers.* Corrosion, 2009. **65**(4): p. 233-251.

145. Zhao, K., J. Wen, and T. Gu, *Mechanistic Modeling of Anaerobic THPS Degradation in Seawater Under Various Conditions, NACE/08, Paper 08512.*

146. Gu, T., K. Zhao, and S. Nesic, *A New Mechanistic Model for MIC Based on a Biocatalytic Cathodic Sulfate Reduction Theory, NACE/09, Paper 09390.* 2009.

147. Song, F.M. and N. Sridhar, *Modeling Pipeline Crevice Corrosion under a Disbonded Coating with or without Cathodic Protection under Transient and Steady-State Conditions.* Corrosion Science, 2008. **50**(1): p. 70-83.

148. Song, F.M. and N. Sridhar, *Modeling Pipeline Corrosion under a Disbonded Coating under the Influence of Underneath Flow.* Corrosion, 2008. **64**(1): p. 40-50.

149. Song, F.M. and N. Sridhar, *A Two-Dimensional Model for Steel Corrosion under a Disbonded Coating due to Oxygen with or without Cathodic Protection-Part 1: Full Numerical Solution.* Corrosion, 2006. **62**(8): p. 676-686.

150. Song, F.M., D.A. Jones, and D.W. Kirk, *Corrosion and Current Flow within a Pipeline Disc Crevice.* Corrosion, 2005. **62**(2): p. 145-154.

151. Song, M., et al., *CO2 Corrosion of Bare Steel under an Aqueous Boundary Layer with Oxygen and Cathodic Protection.* Corrosion, 2004. **60**(9): p. 845-851.

152. Song, F.M., et al., *CO2 Corrosion of Bare Steel under an Aqueous Boundary Layer with Oxygen.* Journal of The Electrochemical Society, 2002. **149**(11): p. B479-B486.

153. Song, F.M., et al., *CO2 Corrosion of Bare Steel under an Aqueous Boundary Layer.* Corrosion, 2004. **60**(8): p. 736-748.

154. Song, F.M., *Exploring to Predict Pipeline High-pH SCC Crack Growth Rate, Sept. 29-Oct. 3, 2008, ASME IPC 2008, Paper 64671 (A Best Conference Paper).* 2008.

155. Song, F.M., *Overall Mechanisms of High pH and Near-Neutral pH SCC, Models for Forecasting SCC Susceptible Locations, and Simple Algorithms for Predicting High pH SCC Crack Growth Rates. March 16-20, 2008 (Houston, TX: NACE, 2008) Paper: 08129.* 2008.

References for Task 6, 7 and 8

1. AGA, Plastic Pipe Manual for Gas Service, 8th edition, Washington DC: American Gas Association (AGA), 2006, pp. 1-30.
2. An Engineering Guide to Elastomer and Manufacturing Standards, Bloomfield: Minor Rubber Company Inc., 2001, pp. 1-30.
3. ASME B31.8-2007, Gas Transmission and Distribution Piping Systems, New York, NY: The American Society of Mechanical Engineers, 2007.
4. ASTM D 297, Standard Test Methods for Rubber Products-Chemical Analysis, West Conshhohocken, PA: ASTM.
5. ASTM D 575, Standard Test Method for Rubber Properties in Compression, West Conshhohocken, PA: ASTM.
6. ASTM D638, Standard Test Method for Tensile Properties of Plastics, West Conshhohocken, PA: ASTM.
7. ASTM D 1418, Standard Practice for Rubber and Rubber Latices-Nomenclature, West Conshhohocken, PA: ASTM.
8. ASTM D1598, Standard Test Method for Time-to-Failure of Plastic Pipe under Constant Internal Pressure, West Conshhohocken, PA: ASTM.
9. ASTM D2240, Standard Test Method for Rubber Property-Durometer Hardness, West Conshhohocken, PA: ASTM.
10. ASTM D2513, Standard Specification for Thermoplastic Gas Pressure Pipe, Tubing and Fittings, West Conshhohocken, PA: ASTM.
11. ASTM D 3418, Standard Test Method for Transition of Polymers by Differential Scanning Calorimetry, West Conshhohocken, PA: ASTM.
12. ASTM D3350, Standard Specification for Polyethylene Plastics Pipe and Fittings MaterialsPPI, West Conshhohocken, PA: ASTM.
13. ASTM D 3677, Standard Test Methods for Rubber Identification by Infrared Spectrophotometry, West Conshhohocken, PA: ASTM.
14. ASTM E831, Standard Test Method for Linear Thermal Expansion of Solid Materials by Thermomechanical Analysis, West Conshhohocken, PA: ASTM.
15. ASTM F876, Standard Specification for Crosslinked Polyethylene (PEX) Tubing, West Conshhohocken, PA: ASTM.
16. Bradey, G. S., et al., Materials Handbook, New York: McGraw-Hill Co., 1997, pp. 303-311.
17. Brandrup, J. et al., Polymer Handbook, 4th edition, Vol. 1 and 2, New York: John Wiley & Sons, 1999.
18. Brömstrup, Heiner, ed., PE 100 Pipe Systems, 2nd ed., Essen, Germany: Vulkan-Verlag GmbH, 2004.
19. Dick, John S., ed., Rubber Technology Compouding and Testing for Performance. Cincinnati: HanserGardner Publications, 2001, pp. 1-69.
20. Gent, Alan N., ed. Engineering with Rubber, How to Design Rubber Components, Cincinnati: HanserGardner Publications, 2001.

21. GRI Report: 99/0039, Technical Reference on the Physical, Mechanical, and Chemial Properties of PA11 Pipe Materials for Use in Gas Distribution Systems Operating at High Pressures and Temperatures, Des Plains, IL: Gas Technology Institute, 1999.
22. Harper, Charles A., Handbook of Plastics, Elastomers, and Composites, 4th ed., New York, NY: The McGraw-Hill Companies, Inc., 2004, pp. 1-16.
23. International Programme on Chemical Safety (IPCS) webpage: http://www.inchem.org/
24. Johnson, Peter S., Rubber Processing an Introduction, Cincinnati: HanserGardner Publications, 2001, pp. 137-140.
25. Mantell, C. L., ed., Engineering Materials Handbook, New York: McGraw-Hill Co., 1958, pp. 32-132.
26. Mark, J. E., Polymer Data Handbook, New York, NY: Oxford University Press, Inc, 1999, pp. 221-230.
27. Mason, Jim, et al., Technical Review of Rilsan® Polyamide-11 High Pressure Natural Gas Pipe Field Installations, Coiling Studies and Pipe Durability Testing, Plastics Pipes XII, Milan, Italy, April. 19-22, 2004.
28. McKetta, John J. ed., Encyclopedia of Chemical Processing and Design, New York: 1985, pp. 369-372.
29. National Institute of Standards and Technology (NIST) Chemistry WebBook: http://webbook.nist.gov/chemistry/
30. Ohm, Robert F., ed, The Vanderfilt Rubber Handbook, Norwalk: R. T. Vanderbilt Company Inc., 1990.
31. Online Database of Plastic Materials: http://www.polymerweb.com/
32. Osswald, T. A., and Menges, G., Materials Science of Polymers for Engineers, Cincinnati: HanserGardner Publications, 2003.
33. Pankow, V.R., Dredging Applications of High Density Polyethylene Pipe, Vicksburg, MS: Hydraulic Laboratory, US Army Engineer Waterways Experiment Station, 1987.
34. PDL, Handbook of Plastic Joining (A Practical Guide), Norwich, NY: Plastics Design Library (PDL), 1997.
35. Peacock, Andrew J., Handbook of Polyethylene: Structures, Properties and Applications, New York: Marcel Dekker, Inc, 2000.
36. Plastics Database: http://www.plasticsusa.com/
37. PPI Report: TN-15/2009, Resistance of Solid Wall Polyethylene Pipe to a Sanitary Sewage Environment, Washington DC: Plastic Pipe Institute (PPI), 2009.
38. PPI Report, TN-17/2008, Crosslinked Polyethylene (PEX) Pipe and Tubing, Washington DC: Plastic Pipe Institute (PPI), 2008.
39. PPI Report, TR-19/2007, Chemical Resistance of Thermoplatics Piping Materials, Washington DC: Plastic Pipe Institute (PPI), 2007
40. PPI Report, TR-11, Resistance of Thermoplastic Piping Materials to Micro- and Macro-Biological Attack, Washington DC: Plastic Pipe Institute (PPI), 2006.
41. PPI, Design Guide for Residential PEX Water Supply Plumbing Systems, Washington DC: Plastic Pipe Institute (PPI), 2006.

42. PPI, Handbook of Polyethylene Pipe, Washington DC: Plastic Pipe Institute (PPI), 2006, pp. 5-103.
43. PPI Report, TR-18, Weatherability of Thermoplastics Piping, Washington DC: Plastic Pipe Institute (PPI), 2005.
44. Rodgers, Brendan, ed., Rubber Compounding Chemistry and Applications, New York: Marcel Dekker, Inc, 2001.
45. Rosen, S. L., Fundamental Principles of Polymeric Mateirals, New York: John Wiley & Sons, 1982.
46. Scholten, Frans, et al., Polyamide 11, 12 and 6.12 for High-Pressure Gas Pipelines, IGRC 2008, Paris, France, Oct. 8-10, 2008.
47. Schweitzer, P.A., Corroison of Polymers and Elastomers, 2nd ed., Boca Raton, FL: Taylor & Francis Goup, LLC, 2007.
48. Schweitzer, P.A., Corrosion-Resistant Linings and Coatings, New York: Marcel Dekker, Inc, 2001.
49. Schweitzer, P.A., Mechanical and Corrosion-Resistant Properties of Plastics and Elastomers, New York: Marcel Dekker, Inc, 2000.
50. Stafford, T., Plastics in Pressure Pipes, Rapra Review Report, Vol. 9, United Kingdom: Rapra Technology Limited, 1998.
51. Synthetic Rubber: The Story of an Industry, Houston: International Institute of Synthetic Rubber Producers, Inc., pp. 15-20.
52. White, James L., ed., Rubber Processing, Technology-Materials-Principles, Cincinnati: HanserGardner Publications, 1995, pp. 1-57.
53. Wikipedia: http://en.wikipedia.org/wiki/Main_Page
54. Willoughby, David A., Plastic Piping Handbook, New York, NY: The McGraw-Hill Companies, Inc., 2002, pp. 1.1-2.16
55. Wright, D.C., Environmental Stress Cracking of Plastics, Shawbury, United Kingdom: Rapra Technology Limited, 1996.